Modélisation du partage de la lumière dans l'association de cultures blé - pois (Triticum aestivum L. - Pisum sativum L.). Une approche de type plante virtuelle.

Romain Barillot

Romain Barillot. Modélisation du partage de la lumière dans l'association de cultures blé - pois (Triticum aestivum L. - Pisum sativum L.). Une approche de type plante virtuelle.. Agronomie. Université d'Angers, 2012. Français. NNT : . tel-00854575

l'université
nantes
angers
le mans

PÔLE DE RECHERCHE ET D'ENSEIGNEMENT SUPÉRIEUR

université
angers

Thèse de Doctorat

Romain Barillot

Mémoire présenté en vue de l'obtention
du grade de Docteur de l'Université d'Angers
Sous le label de l'Université Nantes Angers Le Mans

Discipline : DS10
Spécialité : Sciences agronomiques
Laboratoire : Groupe ESA, Laboratoire d'Écophysiologie Végétale et Agroécologie

Soutenue le 05 décembre 2012

École doctorale : VENAM

Modélisation du partage de la lumière dans l'association de cultures blé - pois

(*Triticum aestivum* L. - *Pisum sativum* L.).

Une approche de type plante virtuelle.

JURY

Rapporteurs :	**M. Christophe GODIN**, Directeur de recherche, INRIA de Montpellier **M. Bertrand NEY**, Professeur d'Université, SIAFFE, AgroParisTech
Examinateurs :	**Mme Guénaëlle CORRE-HELLOU**, Enseignant-Chercheur Groupe ESA, ANGERS **M. Olivier TURC,** Chargé de recherche, INRA de Montpellier **M. Alain VIAN**, Professeur d'Université, Université d'Angers
Directeur de Thèse :	**M. Abraham J. ESCOBAR-GUTIÉRREZ**, Chargé de recherche, INRA de Lusignan
Co-encadrants de Thèse :	**M. Mario CANNAVACCIUOLO**, Enseignant chercheur, Groupe ESA, Angers **M. Didier COMBES**, Ingénieur de recherche, INRA de Lusignan

Thèse de Doctorat

Romain Barillot

Mémoire présenté en vue de l'obtention
du grade de Docteur de l'Université d'Angers
Sous le label de l'Université Nantes Angers Le Mans

Discipline : Sciences agronomiques et écologiques
Spécialité : Sciences agronomiques
Laboratoire : Groupe ESA, Laboratoire d'Écophysiologie Végétale et Agroécologie

Soutenue le 05 décembre 2012

École doctorale : VENAM

Modélisation du partage de la lumière dans l'association de cultures blé - pois

(*Triticum aestivum* L. - *Pisum sativum* L.).

Une approche de type plante virtuelle.

JURY

Rapporteurs :	**M. Christophe GODIN**, Directeur de recherche, INRIA de Montpellier **M. Bertrand NEY**, Professeur d'Université, SIAFFE, AgroParisTech
Examinateurs :	**Mme Guénaëlle CORRE-HELLOU**, Enseignant-Chercheur Groupe ESA, ANGERS **M. Olivier TURC,** Chargé de recherche, INRA de Montpellier **M. Alain VIAN**, Professeur d'Université, Université d'Angers
Directeur de Thèse :	**M. Abraham J. ESCOBAR-GUTIÉRREZ**, Chargé de recherche, INRA de Lusignan
Co-encadrants de Thèse :	**M. Mario CANNAVACCIUOLO**, Enseignant chercheur, Groupe ESA, Angers **M. Didier COMBES**, Ingénieur de recherche, INRA de Lusignan

« L'esprit scientifique doit se former contre la Nature, contre ce qui est, en nous et hors de nous, l'impulsion et l'instruction de la Nature, contre l'entraînement naturel, contre le fait coloré et divers. »

« Rendre géométrique la représentation, c'est-à-dire dessiner les phénomènes et ordonner en série les évènements décisifs d'une expérience, voilà la tâche première où s'affirme l'esprit scientifique. »

Gaston Bachelard. La formation de l'esprit scientifique, 2004.

Remerciements

Je souhaite, au terme de ma thèse, exprimer ma reconnaissance aux personnes qui ont participé à la réalisation de ce long projet et qui m'ont soutenu tout au long de ces trois années.

Naturellement, une première pensée pour Abraham Escobar-Gutiérrez pour m'avoir proposé et encouragé à m'engager dans la thèse. *Abraham, j'ai apprécié pouvoir partager ta philosophie de la modélisation.*

Je pense à toutes les personnes du LEVA, pour m'avoir soutenu tout au long de ces trois années : Mario Cannavacciuolo, Guénaëlle Corre-Hellou, Joëlle Fustec, Frédérique Pellet, Vincent Oury et Solange Renaud.

J'ai eu aussi beaucoup de plaisir à échanger et discuter de nos projets respectifs avec Benoit Fayaud. Une pensée également pour *Valérie Chevalier et le travail que tu as accompli au cours de ton stage.*

Merci tout spécialement à Sylvain Pineau, *merci pour ton soutien technique et amical sans faille. J'ai vraiment apprécié ta participation et ta capacité d'adaptation à un type d'expérimentation qui était nouveau pour toi.*

Ma reconnaissance s'adresse également à toutes les personnes de l'équipe d'Ecophysiologie des plantes de Lusignan. Notamment Gaëtan Louarn, *pour nos discussions et tes réflexions toujours pertinentes. Jean-Louis Durand qui a su m'initier au raisonnement scientifique dès mes débuts dans les laboratoires de recherche, grâce à ton raisonnement extrêmement rigoureux et tes connaissances étendues.*

Enfin, je tiens à nommer les membres de mon comité de pilotage qui ont su m'orienter et me conseiller au cours de ces trois années : Bruno Andrieu, Guénaëlle Corre-Hellou, Vincent Guérin et Jérémie Lecoeur ainsi que les personnes qui ont su m'assister dans la prise en main des différents modèles et plateformes informatiques : Frédérique Boudon, Michaël Chelle, Nicolas Donès, Christian Fournier et Christophe Pradal.

Lors de mes déplacements à Lusignan, j'ai eu l'occasion de rencontrer un autre doctorant. Au terme de réflexions approfondies sur sa thématique ainsi que sur le concept de thèse, il considérait que les remerciements n'avaient pas leur place dans le document de thèse puisque les personnes étaient *in fine* impliquées dans le cadre de leurs missions.

Sur la base de cette distinction, je tiens donc à *remercier* très chaleureusement deux personnes qui ont fait bien plus que leur simple travail au cours de ces 3 ans.

Tout d'abord Pierre Huynh, qui a eu la patience de m'enseigner rigoureusement les fondements de la programmation et sa passion de l'algorithmique. *Merci pour ta gentillesse, ton soutien en toutes circonstances, ton ouverture d’esprit et tout ce que tu m'as transmis. Nos échanges entre points de vue biologique et informatique ont été extrêmement fructueux et passionnants. Il en restera une méthode de travail et d'échange interdisciplinaire qui me seront utiles pour la suite et que j'essaierais de reproduire.*

Enfin, un merci tout particulier à Didier Combes, avec qui j’ai pris un véritable plaisir à travailler. Merci pour ton investissement permanent et sans faille tout au long de cette thèse. *Tes compétences, ta bonne humeur, ton soutien amical et les connaissances que tu m'as transmises au niveau scientifique et méthodologique ont été le ciment indispensable à la construction de cette thèse. J’espère sincèrement avoir de nouveau l’occasion de travailler avec toi.*

Avant-propos

Cette thèse a été financée par la région Pays de la Loire ainsi que le Groupe ESA. Les travaux se sont déroulés au sein de l'Unité de Recherche en écophysiologie végétale et agroécologie (LEVA) du Groupe ESA, Angers, et de l'unité INRA UR 4P3F Ecophysiologie des plantes fourragères, Lusignan. Les expérimentations en conditions non-contrôlées ont été effectuées sur une parcelle mise à disposition par la FNAMS Pays de Loire Bretagne.

Travaux publiés lors de la thèse

ARTICLES DANS DES REVUES INTERNATIONALES OU NATIONALE AVEC COMITE DE LECTURE (ACL)

Barillot R, Combes D, Chevalier V, Fournier C, Escobar-Gutiérrez AJ. 2012a. How does pea architecture influence light sharing in virtual wheat - pea mixtures? A simulation study based on pea genotypes with contrasting architectures. *AoB PLANTS*.

Barillot R, Combes D, Pineau S, Huynh P, Escobar-Gutiérrez AJ. 2012b. Comparison of the morphogenesis of three genotypes of pea (*Pisum sativum*) grown in pure stands and wheat-based intercropping systems. *Agronomy for Sustainable Development*: UNDER REVIEW.

Barillot R, Louarn G, Escobar-Gutiérrez AJ, Huynh P, Combes D. 2011. How good is the turbid medium-based approach for accounting for light partitioning in contrasted grass-legume intercropping systems? *Annals of Botany,* **108**: 1013-1024.

COMMUNICATIONS AVEC ACTES DANS UN CONGRES INTERNATIONAL (ACTI)

Barillot R, Combes D, Chevalier V, Louarn G, Escobar-Gutiérrez AJ. 2012a. Variability of Pea Morphogenesis. An Exploratory Study Based on Six Pea Genotypes with Contrasting Architectures. In IEEE 4th International Symposium on Plant Growth Modeling, Simulation, Visualization and Applications, 31 October -3 November, 2012. ShangHai, China.

Barillot R, Combes D, Huynh P, Escobar-Gutiérrez AJ. 2010. Analysing light sharing in cereal/legume intercropping systems through Functional Structural Plant Models. In 6th International Workshop on Functional-Structural Plant Models, University of Davis, CA.

Barillot R, Combes D, Huynh P, Escobar-Gutiérrez AJ. 2012b. Ideotype construction using an architectural model of pea (*Pisum sativum* L.). In Plant and Canopy Architecture Impact on Disease Epidemiology and Pest Development, July 1-5, 2012. Rennes, France.

Corre-Hellou G, Naudin C, Coste F, Malagoli P, Fayaud B, Barillot R, Escobar-Gutiérrez AJ. 2010. Functioning and Agro Ecological Roles of Legumes in Intercropping Systems to Combine High Productivity, High Quality and Reduction of External N Inputs. In Legumes for global health, April 26-30, 2010. Antalya, Turkey.

TABLE DES MATIERES

Introduction générale

Figure 1 : Exemples de légumineuses cultivées en Europe. A gauche, le pois (*Pisum sativum* L.) appartenant à la tribu des *Vicieae.* A droite, la luzerne (*Medicago sativa* L.), tribu des *Trifolieae*.

1 Défis agricoles du XXI$^{\text{ème}}$ siècle

Au cours des soixante dernières années, les systèmes de production agricoles des pays industrialisés ont principalement été destinés à assurer **l'autosuffisance alimentaire**. Cette volonté politique a ainsi nécessité *de facto* le recours à des **pratiques agricoles intensives** permettant d'obtenir d'importants niveaux de production de la part des agrosystèmes. Outre l'importante technicité requise de la part de l'ensemble de la filière agricole (instituts de recherche, instituts techniques, coopératives, agriculteurs…), l'obtention de tels niveaux de rendement a nécessité la conjugaison de nombreux moyens tels que la sélection variétale, les intrants chimiques de synthèse (pesticides, apports azotés…) ainsi que la mécanisation de la plupart des travaux agricoles consommateurs d'énergie fossile.

Toutefois, ces systèmes de production fortement anthropisés, de plus en plus intensifs et spécialisés, ont conduit à l'apparition **d'impacts sur l'environnement jugés négatifs** par les sociétés humaines *e.g.* lixiviation de l'azote et eutrophisation des eaux, érosion des sols, diminution de la biodiversité, rejet de gaz à effet de serre (Giller *et al.*, 1997, Tilman *et al.*, 2002). La prise de conscience environnementale actuelle qui s'opère au niveau sociétal et politique nécessite donc désormais de **repenser les modes de production agricole**. D'importants et nombreux défis restent néanmoins à relever puisqu'il s'agira d'assurer une production agricole de qualité, et suffisante pour faire face à l'augmentation de la population humaine à venir (Pisani et Lebiez, 2007). Il s'agira également de diminuer l'impact environnemental des activités agricoles, tout en maintenant un niveau de rentabilité économique suffisant pour le maintien d'une agriculture compétitive (Griffon, 1999, Parmentier, 2007, Chevassus-au-Louis *et al.*, 2009). De nombreux efforts de recherche ont été ainsi entrepris afin d'explorer des **systèmes de culture alternatifs** capables de substituer une partie des technologies agricoles actuelles par l'utilisation de régulations biologiques (interactions entre agents biologiques et leurs impacts sur les dynamiques de population) et la production de services écosystémiques (services intrants, service de production et services produits hors revenu agricole direct) (Le Roux *et al.*, 2008). Il s'agit donc de mettre en place une nouvelle technologie fondée sur **l'écologie scientifique** (Pisani et Lebiez, 2007).

2 Importance agro-écologique et économique des légumineuses

Compte tenu de ce contexte, les **légumineuses** présentent des propriétés biologiques spécifiques leur conférant des atouts majeurs dans la conception d'une agriculture capable de répondre aux enjeux définis ci-dessus. Historiquement, ces espèces sont présentes dans de nombreuses agricultures ainsi les légumineuses rencontrées dans la zone tempérée européenne (*e.g.* Figure 1) appartiennent principalement à deux tribus, relativement proches au niveau évolutif (Duc *et al.*, 2010), les *Vicieae* (pois, fèves et féveroles, vesces) et les *Trifolieae* (luzernes, trèfles).

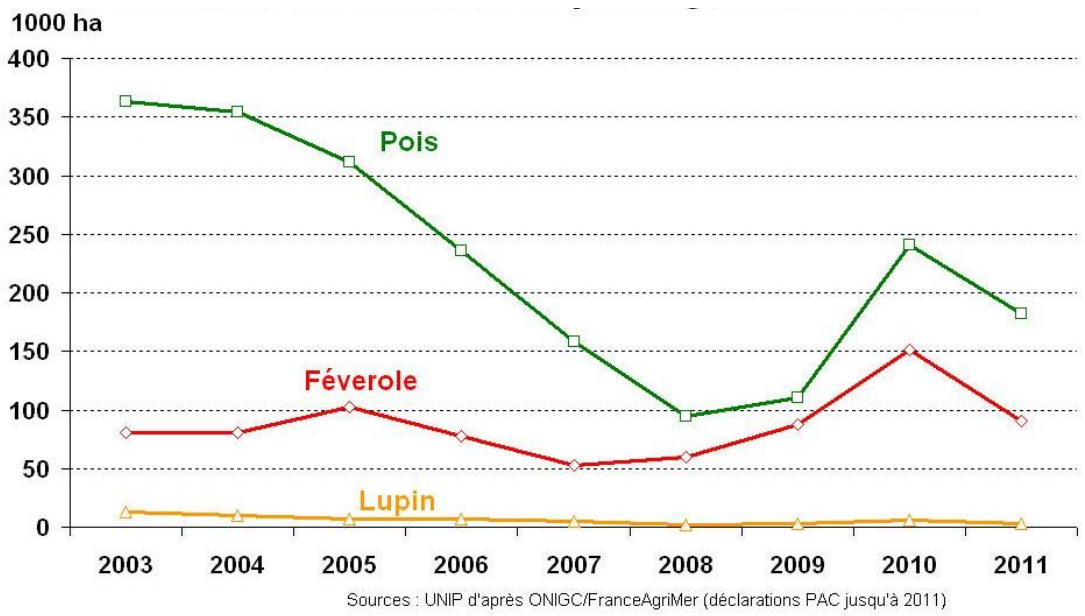

Figure 2 : Evolution des surfaces de trois protéagineux en France : le pois, la féverole et le lupin. D'après UNIP 2011.

Ces espèces présentent la capacité unique de **fixer l'azote atmosphérique** (N_2) au niveau de structures anatomiques spécifiques - les nodosités - formées au niveau racinaire avec des bactéries du genre *Rhizobium* à la suite d'une symbiose.

L'introduction de légumineuses dans les assolements agricoles permet donc d'améliorer de façon significative **l'autonomie en azote des agrosystèmes** et ainsi leur impact environnemental. En France, on estime la fixation symbiotique des légumineuses à 520 000 t d'azote pour l'année 2010 (Duc *et al.*, 2010). Une partie de l'azote fixé peut également être restituée au sol à l'issue du cycle de croissance des légumineuses *via* la minéralisation des pailles et rhizodépôts. Les légumineuses constituent donc un précédent cultural stratégique dans l'élaboration des rotations de cultures. Lorsqu'il n'est pas soumis aux processus de lixiviation, l'azote déposé par les légumineuses peut en effet être absorbé par le système racinaire des cultures suivantes (*e.g.* céréales, colza). L'introduction des légumineuses dans les rotations semble également augmenter l'efficience de ces cultures vis-à-vis de l'azote (Duc *et al.*, 2010). Un avantage supplémentaire des légumineuses (fourragères ou destinées à la production de graines) réside dans le fait qu'elles constituent une source importante de protéines végétales à caractère nutritionnel élevé, un domaine où l'Europe est majoritairement déficitaire (Duc *et al.*, 2010).

Paradoxalement, il apparait que **moins de 5 % des surfaces arables françaises étaient allouées aux légumineuses à graines** en 2005, alors que l'Europe est la première zone du monde en terme de consommation de matières riches en protéines, notamment dans le cadre de la production animale (source : programme UE-GL-Pro 2006). De plus, il semble que l'évolution des assolements français observée depuis 2003 ne fournisse pas d'indications présageant d'une augmentation des surfaces allouées aux légumineuses (Figure 2). Cet état de fait implique donc au niveau européen un recours important aux **importations de protéines végétales** (soja), principalement en provenance du continent américain (*e.g.* Anil *et al.*, 1998). Au-delà de l'impact économique, la réduction des surfaces agricoles allouées aux légumineuses semblent également impliquée dans la stagnation des rendements de blé en Europe (Brisson *et al.*, 2010). Malgré des progrès très sensibles en matière de sélection variétale, le recul de l'utilisation des légumineuses en Europe semble être notamment lié à la sensibilité de ces espèces à certains facteurs abiotiques, et plus particulièrement à la verse, mais également biotiques, tels que le champignon *Mycosphaerella pinodes*, responsable d'une maladie fongique très préjudiciable chez le pois : l'ascochytose.

Dans un tel contexte agro-écologique et économique, la **compréhension et la maitrise du fonctionnement biologique des légumineuses**, en interaction avec leur environnement, font donc partie intégrante du processus de réintroduction de ces espèces dans les agrosystèmes européens. Des axes de recherche ont ainsi été mis en place afin de progresser sur la compréhension des déterminants physiologiques et écologiques du fonctionnement des légumineuses, ainsi que sur l'identification de **systèmes de cultures durables intégrant des légumineuses**.

Figure 3 : diversité des associations de cultures. A gauche, un exemple d'agroforesterie : paulownia-blé. Au centre, un mélange de trois espèces annuelles : maïs, haricot et tournesol. A droite, une association céréales-légumineuses d'espèces pérennes : dactyle-luzerne.

3 Association céréales – légumineuses : intérêts et finalités

Les travaux de recherche évoqués ci-dessus ont notamment conduit à un regain d'intérêt pour le concept plurimillénaire **d'association de cultures**, pratique quasiment disparue des régions tempérées devant l'intensification de l'agriculture et son degré de mécanisation. L'association de cultures se définit comme le mélange d'au moins deux espèces différentes sur une même surface, pendant une période significative de leur développement (Willey, 1979). De nombreux travaux ont montré que ces cultures présentaient des intérêts agronomiques et économiques importants : niveaux de productivité élevés et stables (en terme de quantité et de qualité), diminution du recours aux pesticides, préservation de la biodiversité, diminution de l'érosion du sol, pour revue voir Malézieux *et al.* (2009). Les associations de cultures se déclinent ainsi sous plusieurs formes : association de végétaux ligneux et herbacés (agroforesterie), association de cultures annuelles et/ou pérennes *etc.*, chacune d'entre elles pouvant être composée de peuplements bi- ou plurispécifiques, mono- ou pluri-variétaux (Figure 3).

Parmi les nombreuses combinaisons d'espèces explorées, **les associations céréales - légumineuses** se sont révélées comme étant des agrosystèmes particulièrement performants, présentant des niveaux de rendements équivalents ou supérieurs à ceux observés en culture pure (Ofori et Stern, 1987). D'autres travaux ont également montré que les teneurs en protéines des grains de la céréale sont plus élevées qu'en culture pure (Jensen, 1996b, Corre-Hellou *et al.*, 2006). L'implantation des légumineuses en association avec une céréale permet également de réduire les risques de verse (rôle de tuteur joué par la céréale), de développement des adventices (Hauggaard-Nielsen *et al.*, 2001, Corre-Hellou *et al.*, 2011) et également de maladies sous certaines conditions (Trenbath, 1993). Les associations céréales – légumineuses constituent donc une solution pertinente à la **réintroduction des légumineuses dans les assolements agricoles** alliant ainsi **productivité** et **autonomie vis-à-vis des intrants d'azotés**. Ces associations se destinent ainsi à des **finalités multiples**. Dans les secteurs où l'élevage domine, les associations sont principalement cultivées pour la production de fourrage ou de grains pour l'autoconsommation à la ferme. Dans les zones céréalières, elles sont majoritairement destinées à la production des grains de céréales ou de protéagineux (ITAB, 2011).

Malgré les nombreux bénéfices et finalités mis en évidence, la **pratique de l'association céréale - légumineuse reste marginale** dans la plupart des pays industrialisés, et les filières économiques situées en aval de la production ne semblent pas être en place. En 2009, la superficie du territoire français occupée par les associations céréales - légumineuses s'élevait à 50 000 ha soit 0.18 % de la surface agricole utile. De plus, la production est principalement issue de l'agriculture biologique et destinée à l'autoconsommation dans les élevages (Guichard, 2009). Afin de promouvoir le recours aux associations céréale – légumineuse, il est nécessaire d'en identifier les facteurs limitants tant au niveau de la filière qu'au niveau technique.

Figure 4 : Illustration du développement d’une association blé-pois (photographies verticales du couvert).

S. Pineau & R. Barillot (2011).

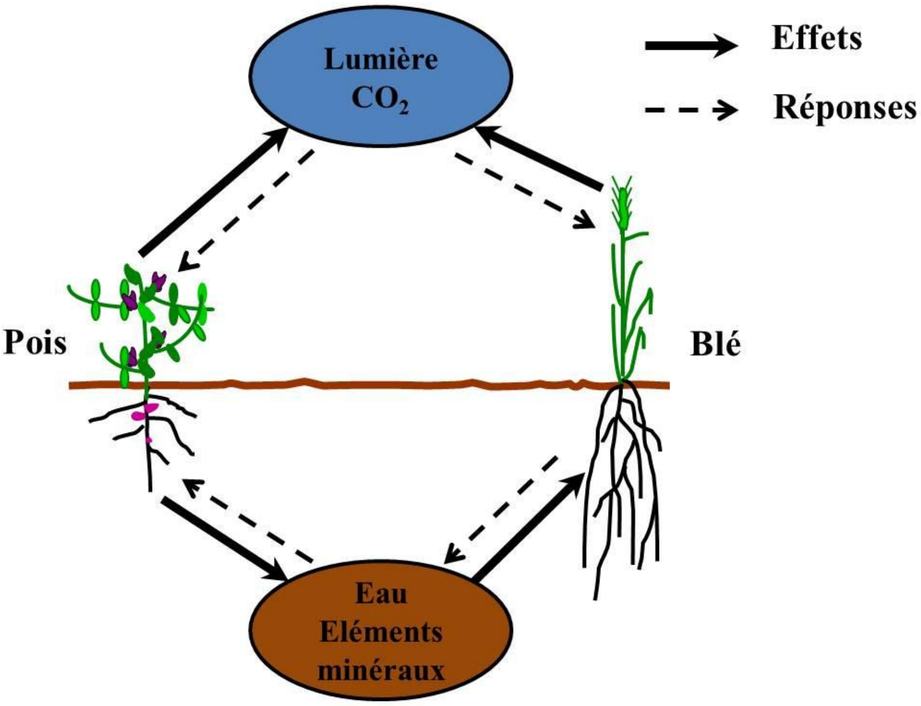

Figure 5 : Schéma des interactions entre plantes de pois et de blé au sein d’une association. Ces interactions résultent de l’effet de chacune des espèces sur les ressources du milieu mais aussi des réponses induites par la modification des ressources. D’après Louarn *et al.* (2010).

D'un point de vue purement agronomique, une des contraintes fortes réside dans l'incertitude, pour l'agriculteur, de prévoir la proportion de chaque espèce à la récolte. En effet, si les doses semées sont contrôlées, ce n'est pas le cas de la dynamique de mise en place de chacune des espèces. Il apparait donc d'ores et déjà que les **caractéristiques structurales et fonctionnelles des espèces associées** sont des déterminants majeurs de l'équilibre entre les processus de **compétition** (lumière, eau, azote) **et de complémentarité** (*e.g.* profils racinaires et aériens complémentaires) qui s'opèrent entre ces espèces. Cet équilibre est d'autant plus complexe à appréhender qu'il est multidimensionnel (accès à la lumière, l'eau, les ressources minérales…) et sous la dépendance des facteurs environnementaux.

4 L'association céréales - légumineuses : un système complexe

La **morphogénèse** de chacune des espèces associées, *i.e.* l'ensemble des processus conduisant à l'acquisition de leur structure physique, conduit à de nombreuses **interactions** intra- et **interspécifiques** permanentes et dynamiques (Figure 4), évoluant à la fois au niveau temporel (période du cycle de développement) et spatial (aérien ou souterrain). Ces interactions (Figure 5) sont perçues par l'un et l'autre des partenaires *via* les modifications d'environnement qu'elles engendrent, et notamment à travers leurs effets sur les ressources du milieu (Haynes, 1980, Ofori et Stern, 1987, Vandermeer, 1989, Sinoquet et Cruz, 1995). En effet, le développement de chacune des espèces entraine une modification du **phylloclimat**, c'est-à-dire des conditions perçues au niveau des organes (Chelle, 2005), pouvant ainsi aboutir à une modification du microclimat à l'échelle du couvert (température, humidité relative, rayonnement). Ces interactions modifient également **l'accès et la quantité des ressources** du milieu, les principales étant la lumière, l'eau et l'azote.

L'association d'une céréale et d'une légumineuse peut ainsi déboucher sur des situations écologiques contrastées où l'on peut distinguer des processus : i) de **facilitation :** interactions positives, augmentation de la taille des niches écologiques (Bruno *et al.*, 2003), ii) de **complémentarité :** les espèces n'accèdent pas à des ressources situées dans les mêmes zones et/ou à des moments différents, augmentation de l'efficience d'utilisation des ressources (Huyghe et Litrico, 2008) et iii) de **compétition** (réponse négative chez au moins une des espèces associées)**. Le gain de productivité et la stabilité** des associations de cultures reposent donc sur la capacité des espèces associées à être **complémentaires dans l'exploitation de leur milieu** (Louarn *et al.*, 2010).

L'objectif des travaux de recherche menés sur les associations céréales – légumineuses consiste donc à identifier et à mettre en place des leviers capables de **maximiser les processus de facilitation et de complémentarité** entre espèces associées, et ainsi à minimiser la compétition interspécifique de façon à ce qu'elle soit *in fine* plus faible que la compétition intraspécifique rencontrée en culture pure. La **compétition pour la lumière** et les **modalités de son partage** au sein des espèces présentes dans le couvert constituent, de fait, un axe d'étude nécessaire à la compréhension du fonctionnement des associations de cultures et du raisonnement de leur pilotage. Le travail de thèse décrit dans ce document s'inscrit dans cette thématique, et a pour objectif général :

D'analyser le partage du rayonnement dans les associations blé - pois

L'objet d'étude utilisé au cours de ce travail pour appréhender le fonctionnement des associations céréales - légumineuses a été effectivement défini par **l'association blé (*Triticum aestivum* L.) – pois (*Pisum sativum* L.).** Parmi les associations céréales - légumineuses, le mélange du blé et du pois est en effet fréquemment étudié et utilisé en France, le pois étant la légumineuse la plus cultivée (Ney et Carrouée, 2005, Duc *et al.*, 2010). Concernant ces deux espèces, un important *corpus* de données, génétiques, (éco-)physiologiques et agronomiques, est de plus disponible dans la littérature, y compris en situation d'association (Ghaley *et al.*, 2005, Naudin, 2009, Naudin *et al.*, 2010).

Problématique et objectifs de l’étude

1 Partage des ressources et interactions dans les associations blé - pois

L'accès aux ressources du milieu peut être symétriquement lié à la taille relative des espèces, définie par la distribution spatiale des organes aériens et souterrains (Schwinning et Weiner, 1998, Louarn *et al.*, 2010). Le degré de symétrie entre la taille de l'individu et sa capacité à préempter une ressource est de plus, dépendant de la nature de celle cette dernière. On peut ainsi observer des compétitions, dites *asymétriques*, dans le cas de ressources peu mobiles du sol ou encore pour la lumière. Dans ces situations, la ressource est principalement captée par l'individu dominant du couvert. Nous détaillons ci-dessous deux ressources majeures influençant le développement et la proportion de chaque espèce dans le couvert ainsi que sa productivité potentielle : **l'azote et la lumière**.

1.1 Azote

De nombreux travaux concernant les associations se sont intéressés à la complémentarité spatiale et temporelle pour l'azote qui s'opère entre la céréale et la légumineuse (Fujita *et al.*, 1992, Jensen, 1996a, Jensen, 1996b, Hauggaard-Nielsen *et al.*, 2001, Adam *et al.*, 2002, Corre-Hellou *et al.*, 2006, Fustec *et al.*, 2010). En effet, la forte compétitivité de la céréale pour l'azote du sol conduit la légumineuse à se reposer quasi-exclusivement sur la fixation symbiotique. Ces caractéristiques physiologiques conduisent ainsi chaque espèce à utiliser des sources d'azote relativement séparées (Louarn *et al.*, 2010) constituant *de facto* une forte complémentarité pour l'azote entre céréales et légumineuses (**séparation de niche**). L'équilibre entre espèces reste toutefois fortement dépendant de la disponibilité de l'azote présent dans le sol ainsi que des modalités des éventuels apports externes d'azote (Naudin, 2009, Naudin *et al.*, 2010).

1.2 Lumière

Ces différentes stratégies d'acquisition de l'azote sont également fortement dépendantes de **l'accès de chacune des espèces à la ressource lumineuse**. La lumière est en effet impliquée dans les mécanismes d'assimilation ainsi que dans la fourniture de **squelettes carbonés,** nécessaires au fonctionnement des nodosités développées par les légumineuses. Le rayonnement fournit en effet la source d'énergie nécessaire à l'accumulation et l'allocation de la biomasse, et ce, dès les stades de développement les plus précoces. Au-delà de cet aspect trophique pour le carbone, la lumière constitue également un ensemble de signaux, dits ***photomorphogénétiques***, impliqués dans la morphogénèse aérienne et souterraine des plantes (Smith, 1982, Varlet-Grancher *et al.*, 1993b, Ballare et Casal, 2000, Barillot *et al.*, 2010).

La **compétition pour la lumière et son partage entre les espèces associées** constituent un point clé de la compréhension du fonctionnement des associations. Il est donc primordial **d'élucider les mécanismes sous-jacents** à la détermination du partage de la lumière dans les couverts plurispécifiques tels que les associations blé – pois.

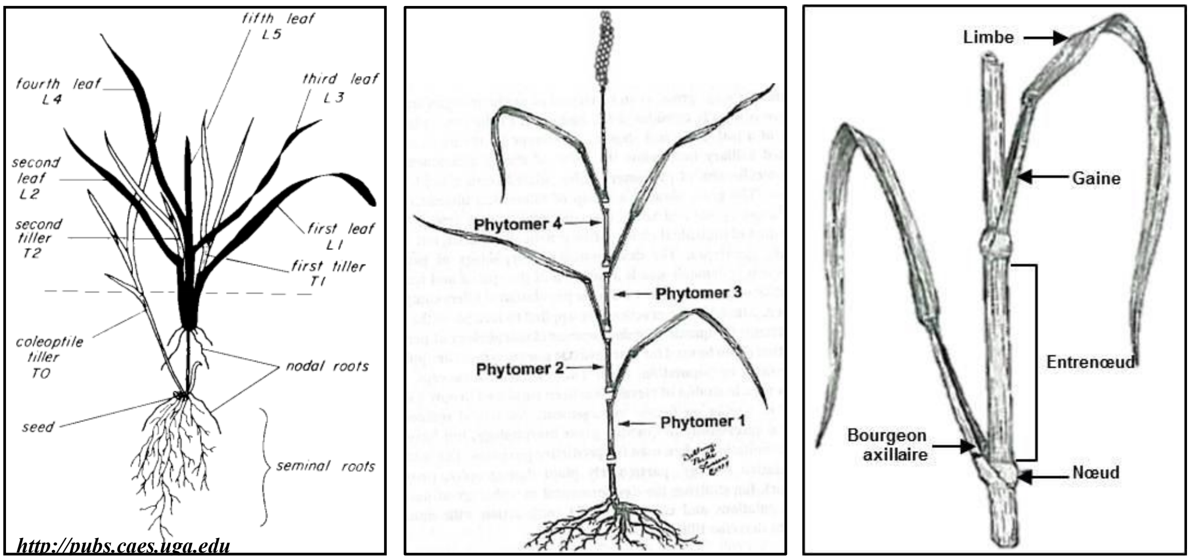

Figure 6 : Anatomie du blé. A : description des différents axes feuillés. B : définition des phytomères du blé. C : description d'un phytomère de blé et de ses composants (Moore et Moser, 1995).

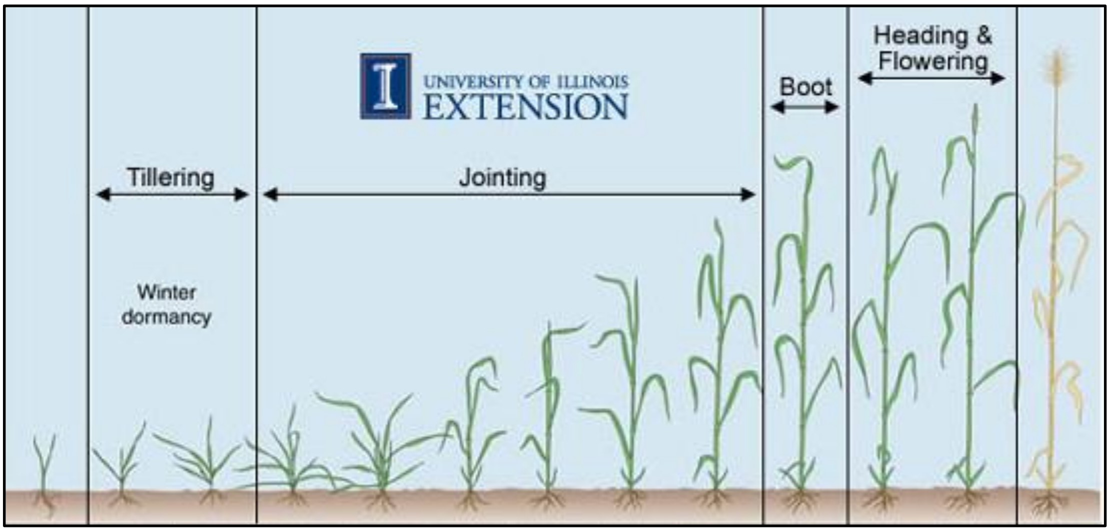

Figure 7 : Principales étapes du cycle de développement du blé (source : Université de l'Illinois, USA)

2 Architecture des plantes et partage de la lumière dans les associations

L’interception du rayonnement de l’ensemble du couvert végétal, ainsi que son partage entre espèces associées, sont fortement reliés à la **structure physique** de la canopée (Ross, 1981b, Sinoquet et Caldwell, 1995) qui émerge du déploiement de **l’architecture des individus** constituant le couvert (Moulia *et al.*, 1998). Cette **description multi-échelle** de la structure de la canopée révèle l’importance de l’architecture des plantes en tant que déterminant de l’interception du couvert ainsi que le partage entre individus. Ce concept central d’architecture a été notamment initié dans le domaine de la botanique par les travaux de Hallé *et al.* (1978). Chez les végétaux on définira l’architecture des plantes comme **l’organisation tridimensionnelle de leur structure physique** (Reinhardt et Kuhlemeier, 2002). D’un point de vue évolutif, l’architecture de l’appareil végétatif des plantes (organismes fixés) reflète ainsi la nécessité trophique d’établir une **surface d’échange avec l’environnement**. Ainsi, d’après Bournérias et Bock (2006) :

> *« Développer de grandes surfaces de contact avec le milieu environnant permet de pallier la dilution de toutes ces sources de matière et d’énergie [e.g. la lumière] indispensables [à la croissance des végétaux]. »*

Afin de réguler la quantité de rayonnement absorbée, les plantes vont ainsi présenter une très grande variété d’architectures, en fonction des espèces et des environnements dans lesquels elles se développent. Trois composantes majeures de l’architecture des plantes vont intervenir dans le partage du rayonnement dans un couvert végétal : i) la quantité et la distribution spatiale de la **surface foliaire** développée par chaque espèce, ii) la **hauteur** atteinte par les plantes dans le couvert et iii) **l’orientation spatiale** des organes végétatifs aériens qui définit l’efficacité intrinsèque de ces surfaces à intercepter le rayonnement incident (Sinoquet *et al.*, 1990, Sinoquet et Caldwell, 1995, Louarn *et al.*, 2010).

Puisque nous avons montré que l’architecture des espèces est un déterminant majeur du partage du rayonnement, il convient à présent de caractériser la morphologie aérienne du blé et du pois.

2.1 Morphogénèse et anatomie de l’appareil végétatif aérien du blé et du pois

2.1.1 Le blé (*Triticum aestivum L.*)

Le blé fait partie de la famille des Poacées. Il s’agit d’une plante monocotylédone autogame. Une plante de blé (Figure 6) est composée d’un ensemble d’axes (**brin maitre** et **talles**) comprenant une partie végétative (pseudo-tiges), une partie reproductrice (l’épi) et un système racinaire fasciculé (Gate, 1995). Le blé n’élabore pas de véritables tiges, au sens histologique du terme, mais plutôt une « pseudo-tige » constituée de la gaine de la feuille adjacente.

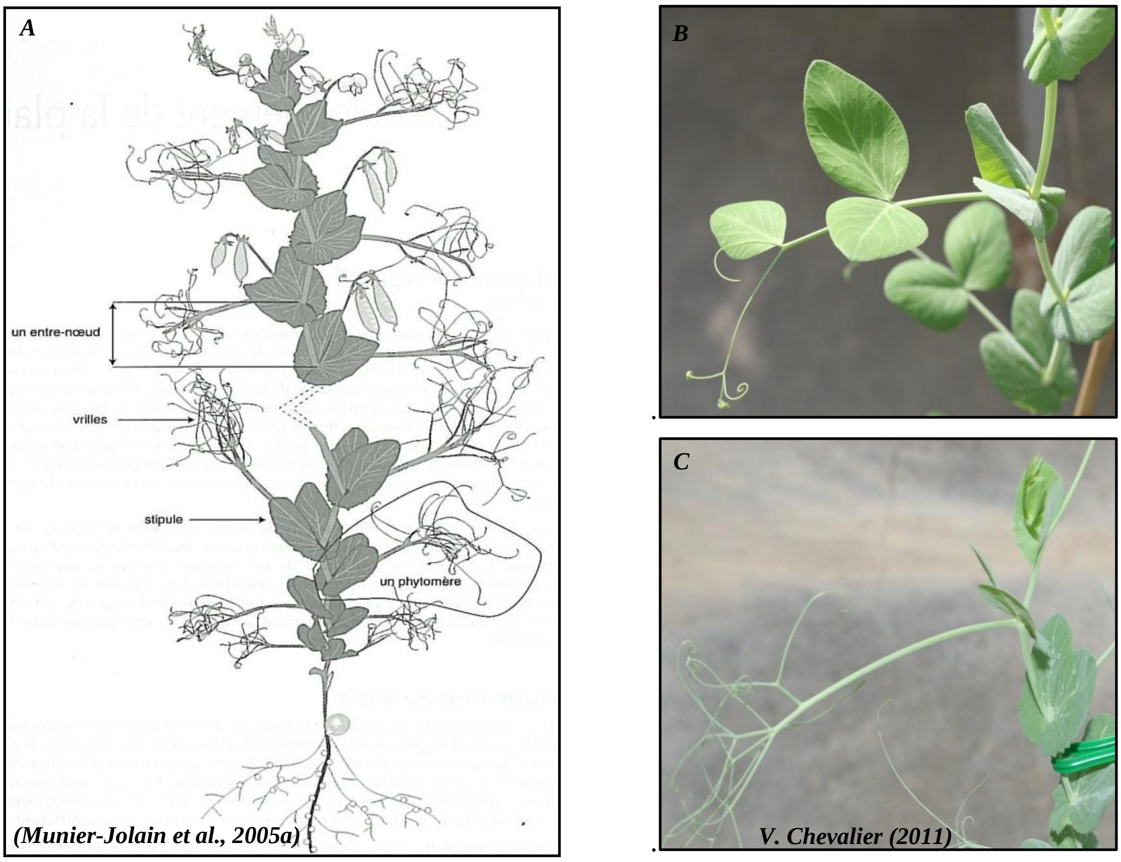

(Munier-Jolain et al., 2005a)

V. Chevalier (2011)

Figure 8 : Anatomie du pois. A : Anatomie d'une variété *afila* et description d'un phytomère. B : une variété de pois *feuillue*, comportant stipules, folioles et vrilles. C : une variété de pois *afila* comportant uniquement des stipules et vrilles.

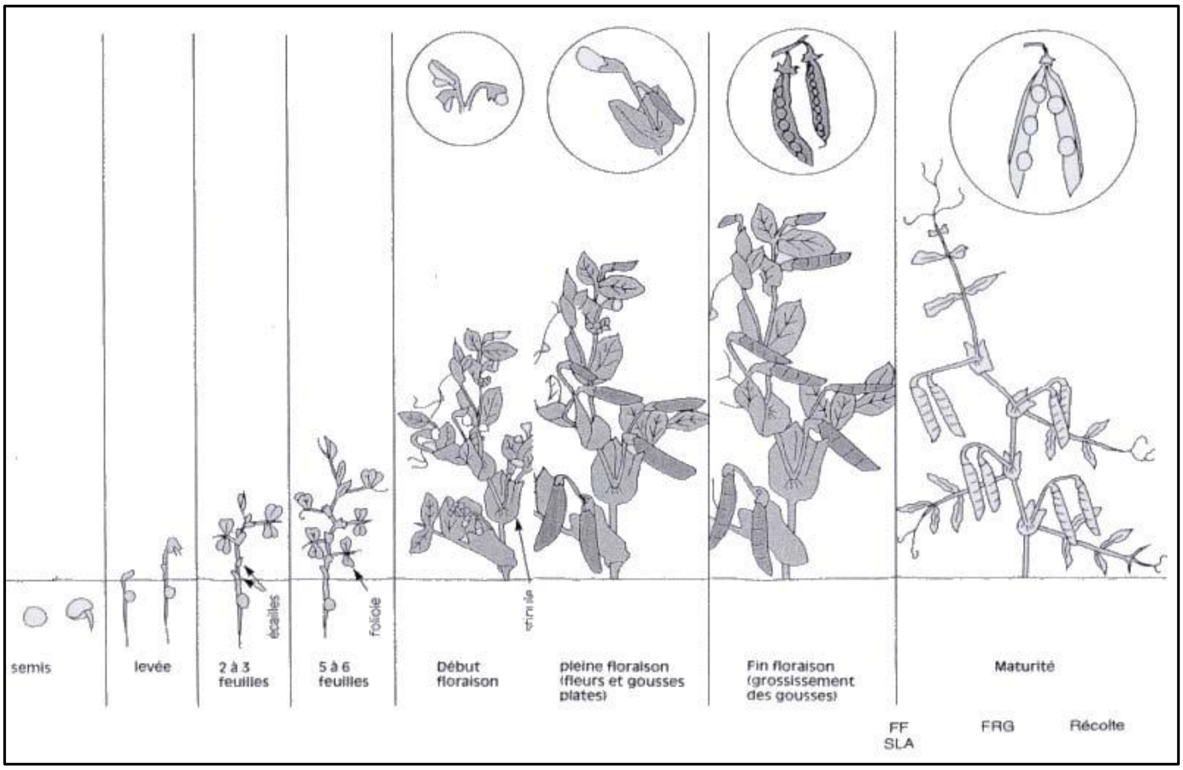

Figure 9 : Principales étapes du cycle de développement du pois (Boyeldieu, 1991)

Les feuilles sont émises par un méristème caulinaire, situé à la base des axes, et croissent successivement dans la pseudo-tige avant d'émerger au sommet de la plante. Chaque axe présente une structure modulaire, issue de l'activité itérative des méristèmes, formant ainsi un ensemble d'unités morphologiques répétées : *les phytomères* (Gray, 1849, White, 1979). Les phytomères de l'appareil aérien du blé sont ainsi constitués d'un nœud, d'un entrenœud, d'un bourgeon axillaire capable d'initier la croissance de talles supplémentaires, et d'une feuille (gaine plus limbe, délimités par une ligule).

Quatre phases majeures (Figure 7) peuvent être distinguées au cours du développement du blé (Gate, 1995). La première phase correspond aux stades d'émergence du blé et du déploiement des premières feuilles sur le brin maitre. Dans un second temps, lorsque 3 à 4 feuilles sont étalées, le processus de tallage se met en place à partir des bourgeons situés à l'aisselle des feuilles. La troisième phase majeure du développement du blé consiste ensuite en une forte croissance verticale des tiges induite par l'allongement des entrenœuds. Au cours de cette phase, l'inflorescence, initialement située à la base de la plante, progresse à travers les gaines avant d'émerger au sommet de la plante, initiant ainsi la floraison. La dernière étape du développement comprend les phases de formation et de maturation des graines situées dans l'épi.

2.1.2 Le pois (*Pisum sativum L.*)

Le pois appartient à la famille des Fabacées. C'est une plante dicotylédone principalement autogame. Une plante de pois (Figure 8) se compose d'un ou plusieurs axes (**tige principale** et **ramifications**) comprenant une partie végétative (les tiges), une partie reproductrice (les gousses) et un système racinaire pivotant (Munier-Jolain *et al.*, 2005a). Contrairement au blé, l'appareil végétatif du pois est mis en place par le fonctionnement de méristèmes caulinaires situés à l'*extrémité* des tiges. Le pois présente également une architecture modulaire relativement bien définie. La tige de pois peut donc être appréhendée comme un empilement de phytomères comprenant un entrenœud, un méristème axillaire capable d'initier la croissance de ramifications supplémentaires, et d'une feuille composée. Chez le pois, la feuille a une organisation complexe (Figure 8B et C). Les variétés dites *feuillues* présentent en effet des feuilles constituées d'une paire de stipules, d'une ou plusieurs paire(s) de folioles et de vrilles. En revanche, chez les variétés dites *afila*, les folioles sont remplacées par des vrilles.

A l'instar du blé, quelques phases majeures du développement de l'appareil végétatif du pois (Figure 9) peuvent être identifiées (pour une revue voir Munier-Jolain *et al.*, 2005a). La première phase correspond à l'émergence du pois et au déploiement des premiers phytomères pré-initiés dans la graine, les deux premiers étant communément qualifiés d'*écailles* (feuilles vestigiales). La phase suivante correspond aux stades foliaires : émergence des ramifications et croissance verticale des tiges jusqu'au début de la floraison. Contrairement au blé, le pois présente une croissance indéterminée *i.e.* la floraison ne met pas fin au développement végétatif.

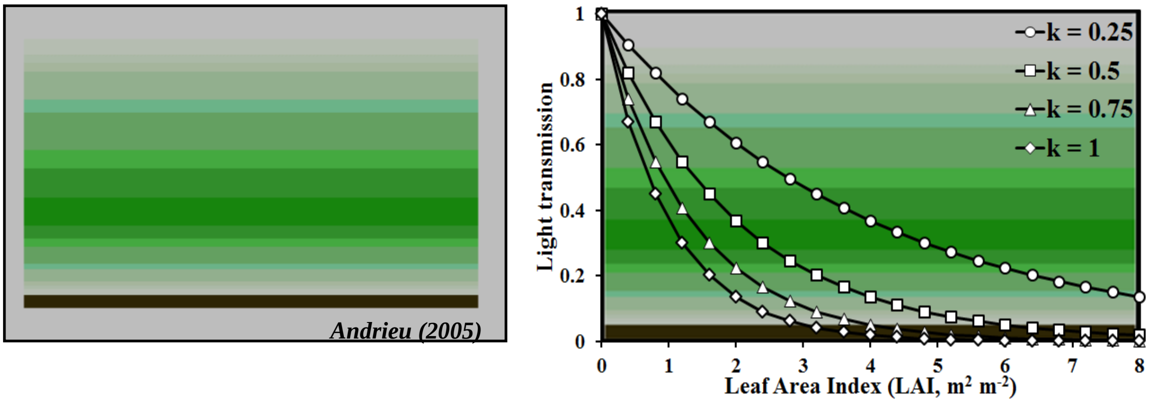
Andrieu (2005)

Figure 10 : Gauche : l'approche turbid medium permet de représenter la canopée comme un milieu turbide homogène. Droite : la lumière se transmet aux couches inférieures du couvert en appliquant la loi de Beer-Lambert, fonction du LAI et du coefficient d'extinction (k).

Ainsi, avec la progression de la floraison, des organes de nature et d'âge différents coexistent sur la plante de pois. Enfin, les dernières étapes du cycle consistent en la formation et la maturation des graines situées à l'intérieur des gousses.

2.2 Modélisation du partage du rayonnement dans l'association

Nous avons montré que l'architecture aérienne des espèces, caractérisée ci-dessus, est un paramètre majeur du partage de la lumière dans les associations de cultures. Il est donc maintenant nécessaire d'identifier une approche pertinente capable de tenir compte i) de l'architecture du pois et du blé et ii) du partage de la lumière à l'intérieur de ce type de peuplement.

Bien que le partage du rayonnement dans les associations céréales – légumineuses soit un déterminant majeur de leur fonctionnement, ce paramètre reste toutefois difficilement accessible aux mesures directes (positionnement des capteurs, nombre de capteurs, perturbations de l'architecture des plantes dues aux capteurs…). Ces contraintes ont ainsi conduit au développement de **modèles** permettant d'estimer le partage du rayonnement dans des couverts plurispécifiques. Plusieurs approches ont émergé de ces problématiques, les deux principales sont présentées ci-dessous.

2.2.1 Approche turbid medium

La majorité des travaux concernant le partage du rayonnement est basée sur une approche statistique dite *turbid medium* (milieu turbide) (Sinoquet *et al.*, 1990, Sinoquet et Caldwell, 1995, Tsubo et Walker, 2002, Tsubo *et al.*, 2005, Awal *et al.*, 2006). Cette approche considère l'ensemble de la canopée comme un **gaz homogène** constitué d'éléments de dispersion de très petite taille et dans lequel la lumière se propage (Figure 10). Les éléments de dispersion représentent les parties aériennes des plantes qui sont réparties de façon **homogène** dans le volume de la canopée. Cette représentation du couvert permet ensuite de calculer la quantité de lumière transmise vers les couches inférieures, en appliquant la loi de **Beer-Lambert**, décrite comme une exponentielle décroissante fonction de la surface foliaire cumulée par mètre-carré de sol (LAI).

Le développement de cette approche analytique reste toutefois basé sur l'approche turbid medium qui nécessite de travailler sur un milieu pouvant être considéré comme homogène et continu, et dans lequel les phytoéléments de petite taille sont répartis aléatoirement dans l'espace. Or, la validité de cette hypothèse peut être remise en question dans le cas des cultures associées. En effet, les associations céréales - légumineuses peuvent constituer des canopées **hétérogènes** (*e.g.* répartition verticale et horizontale de la surface foliaire non uniforme). Ainsi, l'estimation du partage du rayonnement à l'aide de modèles basés sur l'approche turbid medium devient plus complexe dans ces situations, notamment lorsque les deux espèces présentent des propriétés architecturales différentes pouvant de surcroît varier selon dans le temps et l'espace.

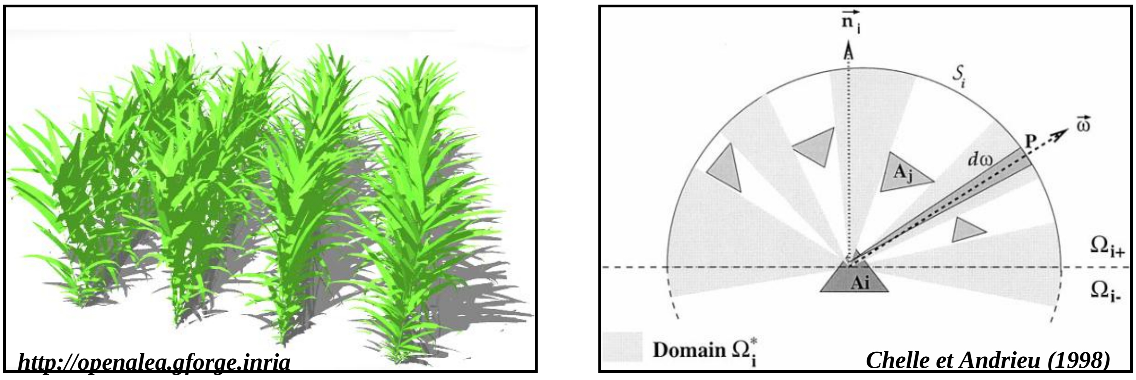

http://openalea.gforge.inria

Chelle et Andrieu (1998)

Figure 11 : L'approche plante virtuelle permet de décrire explicitement l'architecture de chaque individu du couvert (gauche) et de calculer leur interception en utilisant notamment des modèles de radiosité (droite).

2.2.2 Approche plante virtuelle

En parallèle se développent depuis plusieurs années des approches de modélisation dites *individu-centré* dont le principe consiste à représenter le peuplement comme une **collection de plantes individuelles**, plutôt que comme la duplication d'une plante moyenne. De plus, d'autres démarches de modélisation, appelée *plante virtuelle*, permettent également de représenter les individus à travers la **description explicite de leur architecture**. Un des intérêts majeurs de cette approche réside dans la possibilité de tenir compte de l'hétérogénéité spatiale des ressources et de la considérer comme élément structurant de la mise en place de l'architecture des plantes (Godin, 2000, Verdenal, 2009). Ainsi, l'interception du rayonnement peut être évaluée à l'échelle de la plante voire de l'organe *via* par exemple, des **modèles de radiosité** (Figure 11).

Nous avons défini précédemment l'architecture des plantes comme la description tridimensionnelle de leur structure physique. Toutefois, la modélisation de l'architecture pose la question des **modes de représentation** possibles (Verdenal, 2009), à la fois :

- Conceptuels : définir les propriétés pertinentes pour décrire la structure physique des plantes et,
- Formels : définir les modes de représentation de l'information (mathématique, graphique, numérique)

Ainsi, les modes de représentation sur lesquels reposent l'approche plante virtuelle sont basés sur des concepts proches de la description botanique des plantes, et notamment de leur **modularité** (concept du phytomères). L'approche plante virtuelle repose sur le paradigme selon lequel l'architecture peut être décrite par (Godin, 2000) :

- L'inventaire des composants constituant l'architecture aérienne des plantes (**décomposition**)
- Les connexions entre ces composants : la **topologie**
- Les propriétés **géométriques** des composants (position spatiale et orientation).

Les formalismes utilisés pour représenter et mettre en relation (topologie) les constituants architecturaux reposent principalement sur l'analogie avec la structure d'arbres multiples en mathématique, au sens de la **théorie des graphes** (Godin et Caraglio, 1998). La dynamique de ces arbres est ensuite gérée par des grammaires formelles (*e.g.* les L-Systems, Prusinkiewicz et Lindenmayer, 1990) qui définissent les règles d'évolution des composants de l'architecture aboutissant ainsi à la simulation de la morphogénèse des plantes, ou comme cela a été proposé récemment, de la dynamique des paysages fragmentés (Gaucherel *et al.*, 2012). Le couplage avec des méthodes d'**interprétation graphique** a ensuite permis de bénéficier de représentations tridimensionnelles réalistes de la structure physique des plantes.

D'autres travaux ont par la suite permis de mettre en relation ces modèles architecturés avec le fonctionnement physiologique des plantes, donnant ainsi naissance aux modèles dits *structure – fonction* ou *Functional Structural Plant Model* en anglais (**FSPM** ; Godin et Sinoquet, 2005, Vos *et al.*, 2010, DeJong *et al.*, 2011). Ces modèles sont notamment issus de l'introduction de formalismes et de concepts capables de véhiculer et d'intégrer l'information issue de l'interaction « facteurs du milieu - structure de la plante » et de la mettre en relation avec des modèles de fonctionnement (photosynthèse, transpiration, morphogénèse…) qui peuvent également, par rétroaction, affecter la structure des plantes (Fournier et Andrieu, 1998, Prusinkiewicz, 2004a, Prusinkiewicz, 2004b, Verdenal *et al.*, 2008).

De par la prise en compte explicite de l'architecture des plantes, les modèles structure-fonction fournissent ainsi un **cadre conceptuel** permettant l'analyse du partage du rayonnement dans les associations blé – pois. Bien que cette approche paraisse adaptée à l'étude de la compétition pour la lumière et de son partage, peu de travaux l'ont utilisée afin de modéliser l'interception du rayonnement dans les associations de cultures, *e.g.* Lamanda *et al.* (2008) en agroforesterie, Cici *et al.* (2008) dans un système légumineuse-adventice, ou encore Sonohat *et al.* (2002) dans le cas d'une association de plantes pérennes (Fétuque élevée – Trèfle blanc).

3 Objectifs de l'étude

Nous avons montré que l'architecture des plantes est un élément déterminant du partage du rayonnement dans les associations blé - pois et que plusieurs approches de modélisation permettraient d'étudier ces relations entre architecture et interception de la lumière. Le travail de thèse présenté ici se propose donc de contribuer à i) élucider le **déterminisme architectural du partage de la lumière** dans les associations blé – pois et ii) à **évaluer** et **concevoir une approche de modélisation** permettant de caractériser et d'étudier le partage de la lumière dans ces couverts. Au vue de ces objectifs, les hypothèses suivantes ont été émises au cours de la thèse:

- Des **caractères architecturaux décrits à l'échelle de la plante**, voire de l'organe, sont des paramètres déterminants dans le partage du rayonnement à l'échelle du couvert.
- La **description de la structure physique** des plantes, *i.e.* sans intégrer de façon explicite leurs réponses et interactions écophysiologiques, fournit un cadre d'analyse pertinent des modalités du partage de la lumière.
- Un **simulateur de la morphogénèse aérienne du pois et du blé** constitue un cadre conceptuel adapté à l'étude du partage du rayonnement au sein du couvert.
- Le simulateur est un outil heuristique capable de faire émerger des éléments liés à la **construction d'idéotypes** de plantes adaptées aux cultures plurispécifiques.

Sur la base de ces hypothèses, nous tenterons d'apporter des éléments de réponses aux questionnements suivants :

- Quelle **approche pertinente** pour **évaluer** et **introspecter** le déterminisme architectural du partage de rayonnement dans les associations blé – pois. ?
- Quels sont les **paramètres architecturaux** du blé et du pois susceptibles d'affecter le partage du rayonnement ? Comment les affectent-ils ?
- L'impact des paramètres architecturaux est-il constant au cours de la **dynamique** du développement de l'association ?
- Ces paramètres architecturaux sont-ils **variables** entre **génotypes** ? Entre **conditions environnementales**?

Ces éléments illustrent ainsi la **dualité** du travail proposé ici qui a nécessité d'aborder la problématique à travers deux approches distinctes mais complémentaires : i) une approche **écophysiologique** voire agronomique, permettant d'identifier les problématiques et objectifs en rapport avec les modalités du partage de la lumière dans les associations blé – pois, et ii) une seconde démarche destinée à concevoir et mettre en place un cadre d'analyse, basé sur la modélisation, capable de répondre aux objectifs fixés.

La structure de ce document tient donc compte de l'ensemble des éléments évoqués ci-dessus et retrace également le raisonnement suivi au cours du travail de thèse.

- Le premier chapitre est dédié à **l'analyse des approches de modélisation** utilisées pour évaluer le partage du rayonnement dans les associations blé – pois.
- Le second chapitre est consacré à l'**acquisition et à la caractérisation** de l'architecture de divers **génotypes de pois**. Le travail de thèse s'est en effet plus particulièrement focalisé sur le pois, pour lequel peu de travaux et d'outils sont disponibles quant à la modélisation de son architecture aérienne. Ce chapitre a également permis d'identifier des **paramètres de l'architecture aérienne** du pois susceptibles de modifier le partage de la lumière dans l'association.
- L'objectif du troisième chapitre était ensuite de i) caractériser la **morphogénèse aérienne du pois** en conditions non contrôlées et ii) à en évaluer la **plasticité** entre des conditions de culture pure et d'association avec du blé. Cette expérimentation a notamment inclus trois génotypes de pois présentant des caractères morphologiques contrastés.
- Enfin, le quatrième chapitre est dédié à la construction d'un **modèle architecturé de pois, L-Pea**. Le modèle L-pea a par la suite été associé à un **modèle architecturé de blé** (Fournier *et al.*, 2003) afin de reproduire la dynamique de croissance de l'association. Ce **simulateur** a été utilisé afin d'étudier la **sensibilité du partage de la lumière** dans les associations blé – pois en réponse à des **variations d'architecture** appliquées chez le pois et lez blé.
- Enfin, la **discussion générale** synthétise les **conclusions** et **perspectives** développées au cours de ces différents travaux.

Les chapitres I à IV sont rédigés sous formes d'articles scientifiques en anglais, certains étant acceptés, d'autres en révision ou en cours de soumission. De plus, un court paragraphe est également présent à la fin de chaque chapitre afin de synthétiser les principaux résultats et d'expliciter la façon dont ils sont articulés avec la suite du document.

Bibliographie

Adam B, Donès N, Sinoquet H. 2002. VegeSTAR - software to compute light interception and canopy photosynthesis from images of 3D digitised plants. 3.0 ed. Clermont-Ferrand, UMR PIAF INRA-UBP.

Andrieu B. 2005. Approche plante virtuelle pour la modélisation des plantes et peuplements cultives.

Anil, Park, Phipps, Miller. 1998. Temperate intercropping of cereals for forage: a review of the potential for growth and utilization with particular reference to the UK. *Grass & Forage Science,* **53**: 301-317.

Awal MA, Koshi H, Ikeda T. 2006. Radiation interception and use by maize/peanut intercrop canopy. *Agricultural and Forest Meteorology,* **139**: 74-83.

Ballare CL, Casal JJ. 2000. Light signals perceived by crop and weed plants. *Field Crops Research,* **67**: 149-160.

Barillot R, Frak E, Combes D, Durand J-L, Escobar-Gutiérrez AJ. 2010. What determines the complex kinetics of stomatal conductance under blueless PAR in *Festuca arundinacea*? Subsequent effects on leaf transpiration. *Journal of Experimental Botany,* **61**: 2795-2806.

Bournérias M, Bock C. 2006. *Le génie des végétaux.* Belin. Pour la science: Paris, France.

Boyeldieu J. 1991. *Produire des grains oléagineux et protéagineux.* Lavoisier Tec&Doc: Paris, France.

Brisson N, Gate P, Gouache D, Charmet G, Oury F-X, Huard F. 2010. Why are wheat yields stagnating in Europe? A comprehensive data analysis for France. *Field Crops Research,* **119**: 201-212.

Bruno JF, Stachowicz JJ, Bertness MD. 2003. Inclusion of facilitation into ecological theory. *Trends in Ecology & Evolution,* **18**: 119-125.

Chelle M. 2005. Phylloclimate or the climate perceived by individual plant organs: What is it? How to model it? What for? *New Phytologist,* **166**: 781-790.

Chelle M, Andrieu B. 1998. The nested radiosity model for the distribution of light within plant canopies. *Ecological Modelling,* **111**: 75-91.

Chevassus-au-Louis B, Ferone G, Griffon M, Kahn A, Pisani E. 2009. *Les défis de l'agricultures mondiale au XXI siècle.* Angers, France.

Cici SZ-H, Adkins S, Hanan J. 2008. A Canopy Architectural Model to Study the Competitive Ability of Chickpea with Sowthistle. *Annals of Botany,* **101**: 1311-1318.

Corre-Hellou G, Dibet A, Hauggaard-Nielsen H, Crozat Y, Gooding M, Ambus P, Dahlmann C, von Fragstein P, Pristeri A, Monti M, Jensen ES. 2011. The competitive ability of pea–barley intercrops against weeds and the interactions with crop productivity and soil N availability. *Field Crops Research,* **122**: 264-272.

Corre-Hellou G, Fustec J, Crozat Y. 2006. Interspecific competition for soil N and its interaction with N_2 fixation, leaf expansion and crop growth in pea–barley intercrops. *Plant and Soil,* **282**: 195-208.

DeJong TM, Da Silva D, Vos J, Escobar-Gutiérrez AJ. 2011. Using functional–structural plant models to study, understand and integrate plant development and ecophysiology. *Annals Of Botany,* **108**: 987-989.

Duc G, Mignolet C, Carrouée B, Huyghe C. 2010. Importance économique passée et présente des légumineuses : Rôle historique dans les assolements et les facteurs d'évolution. *Innovations Agronomiques,* **11**: 1-24.

Fournier C, Andrieu B. 1998. A 3D Architectural and Process-based Model of Maize Development. *Annals Of Botany,* **81**: 233-250.

Fournier C, Andrieu B, Ljutovac S, Saint-Jean S. 2003. ADEL-wheat: A 3D architectural model of wheat development. *Proceedings of the 2003 Plant Growth Modeling, Simulation, Visualization, and Applications.* Beijing, China, IEEE Computer Society.

Fujita K, Ofosu-Budu KG, Ogata S. 1992. Biological nitrogen fixation in mixed legume-cereal cropping systems. *Plant And Soil,* **141**: 155-175.

Fustec J, Lesuffleur F, Mahieu S, Cliquet J-B. 2010. Nitrogen rhizodeposition of legumes. A review. *Agron. Sustain. Dev.,* **30**: 57-66.

Gate P. 1995. *Ecophysiologie du blé.* Lavoisier.

Gaucherel C, Boudon F, Houet T, Castets M, Godin C. 2012. Understanding Patchy Landscape Dynamics: Towards a Landscape Language. *PLoS ONE,* **7**: e46064.

Ghaley B, Hauggaard-Nielsen H, Høgh-Jensen H, Jensen E. 2005. Intercropping of Wheat and Pea as Influenced by Nitrogen Fertilization. *Nutrient Cycling In Agroecosystems,* **73**: 201-212.

Giller KE, Beare MH, Lavelle P, Izac AMN, Swift MJ. 1997. Agricultural intensification, soil biodiversity and agroecosystem function. *Applied Soil Ecology,* **6**: 3-16.

Godin C. 2000. Representing and encoding plant architecture: A review. *Annals of Forest Science,* **57**: 413-438.

Godin C, Caraglio Y. 1998. A Multiscale Model of Plant Topological Structures. *Journal of Theoretical Biology,* **191**: 1-46.

Godin C, Sinoquet H. 2005. Functional-structural plant modelling. *New Phytologist,* **166**: 705-708.

Gray A. 1849. On the composition of the plant by phytons, and some applications of phyllotaxis. In 438-444.

Griffon M. 1999. Développement durable et agriculture : la révolution doublement verte. *Cahiers Agricultures* **8**: 259-267.

Guichard L. 2009. Réduire les intrants azotés : intérêt des associations céréale-légumineuse. *Service Presse INRA.* Versailles-Grignon.

Hallé F, Oldeman RAA, Tomlinson PB. 1978. *Tropical trees and forests. An architectural analysis.* Springer-Verlag: Berlin.

Hauggaard-Nielsen H, Ambus P, Jensen ES. 2001. Interspecific competition, N use and interference with weeds in pea-barley intercropping. *Field Crops Research,* **70**: 101-109.

Haynes RJ. 1980. Competitive aspects of the grass-legume association. In: Brady NC ed. *Advances in agronomy.* Academic Press.

Huyghe C, Litrico I. 2008. Analyse de la relation entre la diversité spécifique des prairies et leur valeur agronomique (bibliographie). *Fourrages,* **194**: 147-160.

ITAB. 2011. La culture des associations céréales/protéagineux en AB.

Jensen ES. 1996a. Compared cycling in a soil-plant system of pea and barley residue nitrogen. *Plant And Soil,* **182**: 13-23.

Jensen ES. 1996b. Grain yield, symbiotic N2 fixation and interspecific competition for inorganic N in pea-barley intercrops. *Plant and Soil,* **182**: 25-38.

Lamanda N, Dauzat J, Jourdan C, Martin P, Malézieux E. 2008. Using 3D architectural models to assess light availability and root bulkiness in coconut agroforestry systems. *Agroforestry Systems,* **72**: 63-74.

Le Roux X, Barbault R, Baudry J, Burel F, Doussan I, Garnier E, Herzog F, Lavorel

S, Lifran R, Roger-Estrade J, Sarthou JP, Trommetter M. 2008. Agriculture et biodiversité. Valoriser les synergies. Expertise scientifique collective, synthèse du rapport. France, INRA.

Louarn G, Corre-Hellou G, Fustec J, Lô-Pelzer E, Julier B, Litrico I, Hinsinger P, Lecomte C. 2010. Déterminants écologiques et physiologiques de la productivité et de la stabilité des associations graminées-légumineuses. *Innovations Agronomiques,* **11**: 79-99.

Malézieux E, Crozat Y, Dupraz C, Laurans M, Makowski D, Ozier-Lafontaine H, Rapidel B, de Tourdonnet S, Valantin-Morison M. 2009. Mixing plant species in cropping systems: concepts, tools and models. A review. *Agron. Sustain. Dev.,* **29**: 43-62.

Moore KJ, Moser LE. 1995. Quantifying Developmental Morphology of Perennial Grasses. *Crop Sci.,* **35**: 37-43.

Moulia B, Edelin C, Jeuffroy MH, Allirand JM, Loup C, Chartier M. 1998. Premiers éléments d'analyse du développement architectural des herbacées cultivées. In: Maillard P, Bonhomme R eds. *Fonctionnement des peuplements végétaux sous contraintes environnementales.* Paris, France, INRA editions.

Munier-Jolain N, Biarnès V, Chaillet I, Lecoeur J, Jeuffroy M-H, Carrouée B, Crozat Y, Guilioni L, Lejeune I, Tivoli B. 2005. *Agrophysiologie du pois protéagineux.* INRA: Paris, FRANCE.

Naudin C. 2009. *Nutrition azotée des associations Pois-Blé d'hiver (Pisum sativum L. – Triticum aestivum L.) : Analyse, modélisation et propositions de stratégies de gestion*, Angers.

Naudin C, Corre-Hellou G, Pineau S, Crozat Y, Jeuffroy M-H. 2010. The effect of various dynamics of N availability on winter pea-wheat intercrops: Crop growth, N partitioning and symbiotic N2 fixation. *Field Crops Research,* **119**: 2-11.

Ney B, Carrouée B. 2005. Préface. In: Munier-Jolain N, Biarnes V, Chaillet I, Lecoeur J, Jeuffroy M-H eds. *Agrophysiologie du pois protéagineux.* Paris, Inra-Quae.

Ofori F, Stern WR. 1987. Cereal-legume intercropping systems. *Advances in agronomy,* **41**: 41-90.

Parmentier B. 2007. *Nourrir l'humanité, les grands problèmes de l'agriculture mondiale au XXIe siècle.* Paris, France.

Pisani E, Lebiez M. 2007. *Une politique mondiale pour nourrir le monde.* Springer: Paris, France.

Prusinkiewicz P. 2004a. Art and science for life: Designing and growing virtual plants with L-systems. *Nursery Crops Development, Evaluation, Production And Use*: 15-28.

Prusinkiewicz P. 2004b. Modeling plant growth and development. *Current Opinion in Plant Biology,* **7**: 79-83.

Prusinkiewicz P, Lindenmayer A. 1990. *The algorithmic beauty of plants.* Springer-Verlag: New-York.

Reinhardt D, Kuhlemeier C. 2002. Plant architecture. *EMBO Rep,* **3**: 846-851.

Ross J. 1981. Role of phytometric investigations in the studies of plant stand architecture and radiation regime. In: Ross J ed. *The radiation regime and architecture of plant stands.* The Hague, The Netherlands, Junk, W.

Schwinning S, Weiner J. 1998. Mechanisms determining the degree of size asymmetry in competition among plants. *Oecologia,* **113**: 447-455.

Sinoquet H, Caldwell MM. 1995. Estimation of light capture and partitioning in intercropping systems. In: Sinoquet H, Cruz P eds. *Ecophysiology of tropical intercropping.* Paris, INRA Editions.

Sinoquet H, Cruz P. 1995. *Ecophysiology of tropical intercropping.* INRA Editions: Paris, France.

Sinoquet H, Moulia B, Gastal F, Bonhomme R, Varlet -Grancher C. 1990. Modeling the radiative balance of the components of a well-mixed canopy: application to a white clover-tall fescue mixture. *Acta Oecologica-International Journal of Ecology,* **11**: 469-486.

Smith H. 1982. Light quality, photoperception, and plant strategy. *Annual Review of Plant Physiology,* **33**: 481-518.

Sonohat G, Sinoquet H, Varlet-Grancher C, Rakocevic M, Jacquet A, Simon JC, Adam B. 2002. Leaf dispersion and light partitioning in three-dimensionally digitized tall fescue-white clover mixtures. *Plant, Cell and Environment,* **25**: 529-538.

Tilman D, Cassman KG, Matson PA, Naylor R, Polasky S. 2002. Agricultural sustainability and intensive production practices. *Nature,* **418**: 671-677.

Trenbath BR. 1993. Intercropping for the management of pests and diseases. *Field Crops Research,* **34**: 381-405.

Tsubo M, Walker S. 2002. A model of radiation interception and use by a maize-bean intercrop canopy. *Agricultural and Forest Meteorology,* **110**: 203-215.

Tsubo M, Walker S, Ogindo HO. 2005. A simulation model of cereal-legume intercropping systems for semi-arid regions: I. Model development. *Field Crops Research,* **93**: 10-22.

Vandermeer J. 1989. *The ecology of intercropping.* Cambridge University Press: Cambridge, UK.

Varlet-Grancher C, Moulia B, Sinoquet H, Russell G. 1993. Spectral Modification Of Light Within Plant Canopies - How To Quantify Its Effects On The Architecture Of The Plant Stand. In: Varlet-Grancher C, Moulia B, Sinoquet H eds. *Crop Structure And Light Microclimate. Characterization and applications.* Versailles, INRA.

Verdenal A. 2009. *De la simulation de la morphogénèse de l'appareil aérien du ray-grass anglais (Lolium perenne L.).*

Exploration d'un schéma cybernétique inspiré du concept d'auto-organisation et applications., UNIVERSITE DE POITIERS, Poitiers.

Verdenal A, Combes D, Escobar-Gutiérrez AJ. 2008. A study of ryegrass architecture as a self-regulated system, using functional-structural plant modelling. *Functional Plant Biology,* **35**: 911-924.

Vos J, Evers JB, Buck-Sorlin GH, Andrieu B, Chelle M, de Visser PHB. 2010. Functional-structural plant modelling: a new versatile tool in crop science. *Journal of Experimental Botany,* **61**: 2101-2115.

White J. 1979. The Plant as a Metapopulation. *Annual Review of Ecology and Systematics,* **10**: 109-145.

Willey RW. 1979. Intercropping-its importance and research needs. Part 1. Competition and yield advantages. *Field Crop Abstracts,* **32**: 1-10.

Chapitre I

How good is the turbid medium-based approach for accounting for light partitioning in contrasted grass–legume intercropping systems?

Romain Barillot, Gaëtan Louarn, Abraham J. Escobar-Gutiérrez, Pierre Huynh and Didier Combes

Publié dans le journal Annals of Botany 108: 1013–1024, 2011

Annals of Botany 108: 1013–1024, 2011
doi:10.1093/aob/mcr199, available online at www.aob.oxfordjournals.org

ANNALS OF BOTANY Founded 1887

PART OF A SPECIAL ISSUE ON FUNCTIONAL–STRUCTURAL PLANT MODELLING

How good is the turbid medium-based approach for accounting for light partitioning in contrasted grass–legume intercropping systems?

Romain Barillot[1], Gaëtan Louarn[2], Abraham J. Escobar-Gutiérrez[1,2,*], Pierre Huynh[1] and Didier Combes[2]

[1]*LUNAM Université, Groupe Ecole Supérieure d'Agriculture, UPSP Laboratoire d'Ecophysiologie Végétale & Agroécologie, 55 rue Rabelais, BP 30748, F-49007 Angers cedex 01, France and* [2]*INRA, UR4 P3F, Equipe Ecophysiologie des plantes fourragères, Le Chêne – RD 150, BP 6, F-86600 Lusignan, France*
** For correspondence. E-mail abraham.escobar@lusignan.inra.fr*

Received: 11 April 2011 Revision requested: 23 May 2011 Accepted: 28 June 2011 Published electronically: 23 August 2011

- *Background and Aims* Most studies dealing with light partitioning in intercropping systems have used statistical models based on the turbid medium approach, thus assuming homogeneous canopies. However, these models could not be directly validated although spatial heterogeneities could arise in such canopies. The aim of the present study was to assess the ability of the turbid medium approach to accurately estimate light partitioning within grass–legume mixed canopies.
- *Methods* Three contrasted mixtures of wheat–pea, tall fescue–alfalfa and tall fescue–clover were sown according to various patterns and densities. Three-dimensional plant mock-ups were derived from magnetic digitizations carried out at different stages of development. The benchmarks for light interception efficiency (LIE) estimates were provided by the combination of a light projective model and plant mock-ups, which also provided the inputs of a turbid medium model (SIRASCA), i.e. leaf area index and inclination. SIRASCA was set to gradually account for vertical heterogeneity of the foliage, i.e. the canopy was described as one, two or ten horizontal layers of leaves.
- *Key Results* Mixtures exhibited various and heterogeneous profiles of foliar distribution, leaf inclination and component species height. Nevertheless, most of the LIE was satisfactorily predicted by SIRASCA. Biased estimations were, however, observed for (1) grass species and (2) tall fescue–alfalfa mixtures grown at high density. Most of the discrepancies were due to vertical heterogeneities and were corrected by increasing the vertical description of canopies although, in practice, this would require time-consuming measurements.
- *Conclusions* The turbid medium analogy could be successfully used in a wide range of canopies. However, a more detailed description of the canopy is required for mixtures exhibiting vertical stratifications and inter-/intra-species foliage overlapping. Architectural models remain a relevant tool for studying light partitioning in intercropping systems that exhibit strong vertical heterogeneities. Moreover, these models offer the possibility to integrate the effects of microclimate variations on plant growth.

Key words: Turbid medium-based models, functional–structural plant models, light interception efficiency, light partitioning, intercropping systems, grass–legume mixtures, canopy structure, *Festuca arundinacea*, *Medicago sativa*, *Pisum sativum*, *Trifolium repens*, *Triticum aestivum*.

INTRODUCTION

The intensive and specialized agricultural systems put in place during the last 60 years are widely criticized today because of their negative environmental impacts such as nitrogen leaching, soil erosion, loss of biodiversity and high consumption of fossil-derived energy (Giller *et al.*, 1997; Griffon, 1999; Tilman *et al.*, 2002). Against this backcloth, research efforts have been requested to propose systems aimed to ensure sustainable agriculture. In this regard, alternative cropping systems have been explored, leading to renewed interest in crop mixtures, referred to as intercropping (Willey, 1979). Growing two or more crops simultaneously in the same area is assumed to provide high and stabilized yields in terms of quantity and quality (Ofori and Stern, 1987), to reduce the use of fertilizers and pesticides, and to enhance biodiversity conservation (for a review, see Malézieux *et al.*, 2009). Intercropping benefits result from a trade-off between complementarity (e.g. separate root and canopy areas) and competition processes (for light, water and nitrogen) that occur between the component crops. Among the contested resources, light, and in particular its partitioning between the components, appeared to be a key factor, determining the respective proportion of each species in the stand as well as their potential yield.

In the present state of the science and the technology, and due to experimental and cost constraints, light interception of each component within an intercrop cannot be directly measured with radiation sensors (Sonohat *et al.*, 2002), in particular for studies devoted to characterize the phylloclimate (Chelle, 2005). Thus, the only current and feasible alternative is the modelling approach. To our knowledge, most studies dealing with intercropping systems are based on statistical models founded on the turbid medium analogy (Faurie *et al.*, 1996; Lantinga *et al.*, 1999; Tsubo and Walker, 2002; Tsubo *et al.*, 2005; Awal *et al.*, 2006). In this paradigm, light

transmission within a canopy is assumed to follow Beer–Lambert's law (Monsi and Saeki, 1953), i.e. an exponential decrease as a function of the downward cumulative leaf area, LAI, and leaf geometrical properties, namely the extinction coefficient k. In the case of sole crops, light interception efficiency, LIE, can be written as follows:

$$\mathrm{LIE} = 1 - e^{-k\,\mathrm{LAI}}. \tag{1}$$

As Beer–Lambert's law deals with light transmission, i.e. non-interception probability, it cannot be directly used to compute light partitioning amongst mixed species. However, Rimmington (1984) and then Sinoquet and Bonhomme (1991) demonstrated that light interception efficiency LIE_i of species i in a mixture of n components depends on the interception of the whole canopy (right-hand side in eqn 1) weighted by its extinction coefficient, k_i, and its contribution to total LAI, LAI_i (Sinoquet *et al.*, 2000), such that:

$$\mathrm{LIE}_i = \frac{k_i \mathrm{LAI}_i}{\sum_{j=1}^{N} k_j \mathrm{LAI}_j}\left[1 - e^{\left(-\sum_{j=1}^{N} k_j \mathrm{LAI}_j\right)}\right] \tag{2}$$

One of the major assumptions underlying the turbid medium approach is that the canopy can be considered as a homogeneous and continuous medium where leaves are small and randomly distributed. Such a hypothesis could be questioned in intercropping systems which generally build up non-homogeneous canopies (Sinoquet, 1993). Indeed, these systems present several planting patterns such as mixed cropping, row intercropping, and understorey or alley intercropping, thus leading to various spatial heterogeneities. Heterogeneities may be continuous or discontinuous (foliage overlapping or empty space between species, respectively), structured or unstructured (row crops or well-mixed canopies respectively). Moreover, intercropping systems generally include various species having their own (1) morphogenesis and phenology, and (2) radiation interception ability, given by the spatial distribution of LAI and leaf geometrical features. These contrasts might lead to various inter- and intra-species patterns of leaf dispersion, either random, regular or clumped (Nilson, 1971). Light partitioning among component crops would also evolve during the growing cycle due to various dynamics of LAI establishment, thus leading to contrasted situations at canopy closure. Although the turbid medium approach has been widely used and assessed in the case of sole crops (Andrieu and Sinoquet, 1993) or trees (Chen *et al.*, 1993; Combes *et al.*, 2008), a major difficulty arises for the validation of such an approach applied to multispecies stands (Sinoquet and Caldwell, 1995). Indeed, due to the impossibility of carrying out direct measurements of light partitioning in mixed canopies, turbid medium-based estimations are rarely validated or only partially so through the total amount of transmitted radiation reaching the soil (Faurie *et al.*, 1996).

Such limitations could be tackled by using surface-based approaches (Chelle and Andrieu, 1999) which model the canopy structure through realistic three-dimensional (3-D) representations in which individual plant architecture is explicitly described as a collection of interconnected phytoelements, including their geometry and optical properties (Godin, 2000). Thus, canopy heterogeneities are explicitly taken into account when simulating radiative exchanges on these architectural models. Magnetic 3-D digitizing appeared to be the most suitable technique for collecting information on plant architecture prior to *in silico* reconstruction (Moulia and Sinoquet, 1993). Herbaceous mixtures therefore appeared to be a relevant case for study as they are accessible to these kinds of measurements; this is particularly so for grass–legume intercrops, which are widely used because of their strong agronomical interests (Ofori and Stern, 1987; Tsubo and Walker, 2004).

The aim of the present study was to assess the ability of the turbid medium approach to accurately estimate light partitioning within mixed canopies. The turbid medium assessment was conducted on a contrasted range of grass–legume intercropping systems, which display various LAI and height ratios, at different stages of the growing cycle and with contrasted row structures. For this purpose, we considered three kinds of mixtures: (1) an annual mixture of wheat and pea (WP), and two perennial mixtures of (2) tall fescue and alfalfa (FA), and (3) tall fescue and white clover (FC). For each mixture, mini-stands were digitized to provide accurate 3-D descriptions of the canopy structure. Benchmark estimates of mixture light interception efficiencies were obtained from a radiation model based on the projective method applied on the 3-D reconstructed canopies. These reference results were then compared against the computations derived from a turbid medium model.

MATERIALS AND METHODS

Plant material and growing conditions

Some descriptors of the mixed canopies used for this study are presented in Table 1. Detailed descriptions are given below.

Wheat–pea mixtures. Intercropped wheat (*Triticum aestivum* L. 'Apache') and pea (*Pisum sativum* L. 'Lucy'; aphylla type) were grown in 80 × 60 × 30-cm containers in a greenhouse experiment from 1 February 2010 to 15 April 2010 in Angers, France (47°27′N, 00°32′W). Containers were filled with a soil layer of 25 cm, providing 3 g m^{-2} of $\mathrm{NO_3^-}$. The soil was then enriched with 3·5 g m^{-2} $\mathrm{NH_4NO_3}$ at the sowing date and at 850 degree days (DD) from emergence to avoid any N-limitation for plant development. To ensure pea nodulation, each container was inoculated with a solution of *Rhizobium leguminosarum* P221 at 2×10^7 bacteria per plant. Plants were sown at (1) three relative densities, i.e. the percentage of each species varied so that each treatment had the same absolute density, and (2) at two different row arrangements. Each sowing pattern was repeated twice, hereafter denoted '_1' and '_2' as in Table 1. The first three treatments consisted of four alternative rows of wheat and pea sown at different proportions of their optimal density practised in pure stands: (1) 50 % wheat and 50 % pea (W50–P50 Alternate Row), (2) W30–P70 and iii) W70-P30. The fourth treatment also consisted of 50 % wheat and 50 % pea but, in contrast to treatment 1, plants were mixed within each row (W50–P50 Mixed Row). We considered that the optimal density was 250 plants m^{-2} for wheat and 90 plants m^{-2} for pea.

TABLE 1. *Description of the plant mixtures*

Mixture	Digitizing time (degree days, DD; or days after sowing, DAS)	Density	Designation	Leaf area index (m^2 m^{-2}) Grass	Leaf area index (m^2 m^{-2}) Legume	Coefficient of variation of the LAI horizontal distribution Grass	Coefficient of variation of the LAI horizontal distribution Legume	Coefficient of variation of the LAI horizontal distribution Mixture
WP	300 DD	30 % W-70 % P	W30-P70_300DD_1	0·31	0·15	0·99	2·49	0·91
			W30-P70_300DD_2	0·32	0·16	1·35	2·46	1·05
		50 % W-50 % P in alternate rows	W50-P50A_300DD_1	0·48	0·07	0·70	2·46	0·62
			W50-P50A_300DD_2	0·48	0·06	1·14	2·80	0·98
		50 % W-50 % P mixed on the row	W50-P50M_300DD_1	0·43	0·11	0·80	1·13	0·73
			W50-P50M_300DD_2	0·45	0·17	0·63	1·36	0·52
		70 % W-30 % P	W70-P30_300DD_1	0·72	0·03	0·93	2·51	0·87
			W70-P30_300DD_2	0·60	0·03	1·19	2·60	1·14
	685 DD	30 % W-70 % P	W30-P70_685DD_1	0·75	0·54	1·15	1·25	0·62
			W30-P70_685DD_2	0·65	0·56	0·94	0·59	0·59
		50 % W-50 % P in alternate rows	W50-P50A_685DD_1	1·07	0·13	0·57	1·07	0·47
			W50-P50A_685DD_2	0·90	0·22	0·82	1·00	0·71
		50 % W-50 % P mixed on the row	W50-P50M_685DD_1	1·19	0·40	0·62	1·18	0·54
			W50-P50M_685DD_2	1·05	0·60	0·62	0·76	0·44
		70 % W-30 %P	W70–P30_685DD_1	1·54	0·08	0·75	1·41	0·66
			W70–P30_685DD_2	1·51	0·14	1·19	2·60	1·14
	1100 DD	30 % W-70 % P	W30-P70_1100DD_1	1·23	0·98	0·95	0·83	0·50
			W30-P70_1100DD_2	1·12	1·03	0·88	1·19	0·59
		50 % W-50 % P in alternate rows	W50-P50A_1100DD_1	2·05	0·34	0·79	0·71	0·47
			W50-P50A_1100DD_2	1·33	0·48	0·82	0·37	0·60
		50 % W-50 % P mixed on the row	W50–P50M_1100DD_1	2·15	0·54	0·45	0·86	0·41
			W50-P50M_1100DD_2	1·71	0·98	0·33	0·82	0·34
		70 % W-30 % P	W70-P30_1100DD_1	2·56	0·16	0·65	1·06	0·46
			W70-P30_1100D_2	2·56	0·18	0·62	1·18	0·54
FA	670 DD	50 % F-50 % A high density	F50-A50_670DD_HD	3·06	3·83	0·22	0·29	0·08
		50 % F-50 % A low density	F50-A50_670DD_LD	0·75	0·37	0·20	0·28	0·19
	1150 DD	50 % F-50 % A high density	F50-A50_1150DD_HD	2·52	8·06	0·55	1·23	0·34
		50 % F-50 % A low density	F50-A50_1150DD_LD	0·43	1·70	0·86	0·52	0·29
FC	49 DAS	NA	FC_49_1	2·06	0·05	0·19	0·12	0·15
			FC_49_2	1·22	0·24	0·17	0·34	0·11
			FC_49_3	0·60	0·07	0·29	0·19	0·17
	62 DAS	NA	FC_62_1	3·37	0·89	0·43	0·17	0·36
			FC_62_2	0·32	0·36	0·09	2·00	0·09
			FC_62_3	1·62	0·25	0·29	0·45	0·31
	75 DAS	NA	FC_75_1	4·45	0·79	0·38	0·51	0·37
			FC_75_2	3·62	0·97	0·44	0·27	0·39
			FC_75_3	2·31	0·87	0·23	0·28	0·21

Leaf area index and coefficients of variation of its horizontal distribution are given for each species belonging to wheat–pea (WP), tall fescue–alfalfa (FA) and tall fescue–clover (FC) mixtures. Sowing densities of FC mixtures were not available (NA) in the original article of Sonohat *et al.* (2002).

Tall fescue – alfalfa mixtures. A second mixture (FA) consisted of a 50 : 50 alfalfa (*Medicago sativa* L. 'Orcha') and tall fescue (*Festuca arundinacea* Schreb. 'Noria') mixture following an hexagonal lattice for planting, with each individual surrounded by three individuals of its own species and three of the other species (Fig. 1). Such a pattern produces a stand where all plants are equidistant and aggregated by species in rows (Harper, 1961). Two planting densities were studied corresponding respectively in the field to a crowding plant population density shortly after emergence (hereafter HD for high density, 460 plants m^{-2}) and an old stand once self-thinning has occurred and the population density has stabilized (hereafter LD for low density, 50 plants m^{-2}). All plants were grown outdoors at the INRA Lusignan station (46°25′N, 0°7′W, 100 m a.s.l.) from 15 April 2010 to 15 July 2010 in stands of about 1 m^2 at HD and 2 m^2 at LD. Each plant was in an individual pot (5 cm diameter × 40 cm high at HD; 10 cm diameter × 25 cm high at LD) filled with a medium composed of sterile potting mix, sand and brown earth soil (1 : 1 : 1, v/v). All pots were fertirrigated three times a day with a complete nutrient solution so that plants were competing for light only.

Tall fescue–clover mixtures. Data from the tall fescue (*Festuca arundinacea* Schreb. 'Barcel') – white clover (*Trifolium repens* L. 'Huia') mixtures were obtained from a database built up following an experiment conducted and fully described by Sonohat *et al.* (2002). Briefly, FC mixtures were sown on a clay-loam soil near Caen, France (48°55′N, 0°0′E, 60 m a.s.l.) on 18 March 1999. Tall fescue was sown in rows of 0·17 m whereas white clover was broadcast sown.

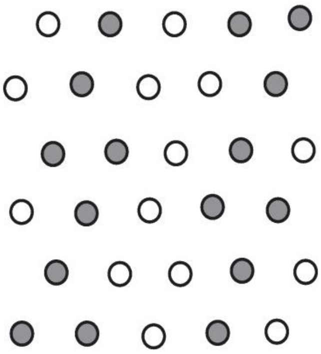

FIG. 1. Illustration of the hexagonal lattice used for the tall fescue (open dots) – alfalfa (closed dots) mixtures. Each individual plant is neighboured by a 50 : 50 proportion of the two species.

Three-dimensional digitizing of canopies and virtual reconstructions

Canopy architecture of each mixture was digitized using a 3-D digitizer (3Space Fastrak, Polhemus Inc., Colchester, VT, USA; Polhemus, 2009). Spatial coordinates as well as each phytoelement orientation were collected with 3A software (Adam *et al.*, 1999) and encoded as Multiscale Tree Graphs (MTG) (Godin and Caraglio, 1998). Data from digitizing were then imported into the Openalea platform (Pradal *et al.*, 2008) where the foliage of each species was reconstructed, thus excluding the other phytoelements in light interception computations, i.e. sheaths, stems and tendrils. These 3-D mock-ups allowed us to provide accurate descriptions of the canopies structure (spatial distribution of LAI) and geometric features (leaf inclination).

Wheat–pea mixtures. Three digitizations were carried out during the growing period at 300, 685 and 1100 DD from emergence (base temperature 0°C). Wheat plants were digitized as a succession of sheaths on which lamina are branched. Then, untouched lamina were described by successive pointing out along the midribs, thus keeping their natural bearing. Pea plants were digitized as a succession of internodes on which the two-stipule orientation and dimension were measured. Wheat leaves were represented as a succession of rectangles whose widths were computed according to the current position on the midrib and the maximal leaf length (Fournier *et al.*, 2003). For pea plants, stipules were reconstructed from a library of about 200 geometric objects stemming from photographs on which we extracted stipule shape. At the reconstruction time, geometric shapes were then (1) attributed according to the relative phytomer number of the considered stipule and (2) resized and reoriented according to the information stored during the digitization.

Tall fescue–alfalfa mixtures. For each FA stand, 3-D magnetic digitizations were performed at two stages of development (670 and 1150 DD after emergence, base temperature 4°C), corresponding to the first two cuts of the mixture at alfalfa early bloom. All plants over soil areas of about 1400 cm^2 (LD) and 900 cm^2 (HD) in the centre of the stand were recorded. For tall fescue, the digitization and reconstruction procedures were the same as for wheat (see above). Alfalfa plant description was also similar to pea, except that main leaf leaflets, instead of stipules, were recorded. Leaflet widths were measured on a sub-sample of phytomers of each plant only. These direct measurements were used to build up plant-specific allometric relationships considering both leaflet length and phytomer position on the stem as predictors of leaflet width.

Tall fescue–clover mixtures. Experimental data were obtained from Sonohat *et al.* (2002) where three plots of the FC mixture ($0{\cdot}17 \times 0{\cdot}10$ m), denoted '_1', '_2' and '_3' in Table 1, were digitized at 49, 62 and 75 d after sowing. The digitizing protocol used by the authors was similar to those described above for WP and FA mixtures; more details are given in Sonohat *et al.* (2002). Tall fescue virtual plants were then reconstructed in the same way as in FA mixtures. Clover leaflets were treated as for alfalfa with an adapted geometric shape.

Estimation of LIE in virtual canopies: reference model

Benchmark estimates of light interception efficiency for each stand were computed on VEGESTAR software (Adam *et al.*, 2002), a radiation model based on the projective method, disregarding multiple scattering and assuming leaves as black bodies. Input files containing information on plant structure, were derived from the stand reconstructions obtained on the Openalea platform. Computations were performed assuming only diffuse radiations, which were approximated by a set of light sources from a sky vault discretized in 46 solid angle sectors (Den Bulk, 1989), including eight zenith angles (9·23, 10·81, 26·57, 31·08, 47·41, 52·62, 69·16 and 90°). LIEs were computed for each direction and then integrated over the sky vault by summing up the 46 directional values. The contribution of each sky sector to the incoming light energy was weighted according to the Standard Overcast sky radiation distribution where sky luminance depends only on elevation (Moon and Spencer, 1942). Thus, the weighting factor, R_a, is given by:

$$R_a = (1 + 2\sin l)(3R_d/7\pi) \tag{3}$$

where l is the sky area altitude and R_d is the diffuse radiation integrated over the sky dome. To avoid border effects, virtual stands were virtually replicated in all directions according to their sowing pattern.

Turbid medium-based model

Light interception efficiencies estimated from the virtual plant models were then compared with the outputs of a turbid medium-based model. Numerous models using the turbid medium analogy are available in the literature, mainly contrasted by their representation of vertical structure of the canopy. In the present work, we used the turbid medium model SIRASCA (Sinoquet *et al.*, 1990), which aims to compute light partitioning in mixed canopies. This model is assumed to provide accurate estimates of light interception and has been validated on a large range of canopies and also

against other models (Sinoquet *et al.*, 2000). This model computes light interception in multispecies canopies from the species LAI and mean leaf inclination angle. Leaf inclinations (α) are used to compute the extinction coefficients (k) by the relationship (Sinoquet *et al.*, 2000):

$$k = 0{\cdot}988[\cos(\alpha/2)]^{2{\cdot}4}. \qquad (4)$$

SIRASCA was set to gradually account for vertical heterogeneity of the foliage, i.e. the canopy was described with either one, two or ten layers, which respectively correspond to the maximal height of the whole canopy, the maximal height of each species and the maximal height of the canopy divided in ten equal layers. SIRASCA inputs such as LAI and mean leaf inclination (eqn 2) for each species were extracted from the 3-D virtual stands.

Statistical analysis

Assessment of the turbid medium approach was based on two criteria: (1) the mean bias of the predictions (MBP) and (2) the root mean squared deviation of the predictions (RMSDP). For each variable, MBP was calculated as the difference between the n pairs of values predicted by (1) the virtual stand-projective method (vpp), taken as a reference, and (2) the turbid medium-based model (tmp), such that:

$$\mathrm{MBP} = \frac{\sum_{i=1}^{n} (\mathrm{tmp} - \mathrm{vpp})}{n} \qquad (5)$$

Significant deviations from zero MBP were assessed based on a t-test by using the UNIVARIATE procedure of SAS 9·2 (SAS Institute, Cary, NC, USA). The RMSDP for each variable was estimated as:

$$\mathrm{RMSDP} = \sqrt{\frac{\sum_{i=1}^{n} (\mathrm{tmp} - \mathrm{vpp})^2}{n}} \qquad (6)$$

RESULTS

Stand mock-ups

Figure 2 shows views of some reconstructed 3-D virtual mixtures presented in the horizontal direction.

Characterization of the mixture structures and light partitioning among component species

Spatial distribution of foliage. LAI ranged from 0·31 to 4·47 $\mathrm{m^2\ m^{-2}}$ for grass and from 0·03 to 8·06 $\mathrm{m^2\ m^{-2}}$ for legume species (Table 1). WP mixtures exhibited the smallest LAI (0·31–2·56 $\mathrm{m^2\ m^{-2}}$ for wheat; 0·03–1·03 $\mathrm{m^2\ m^{-2}}$ for pea). Highest LAI values were observed for alfalfa (maximal LAI of 8·06 $\mathrm{m^2\ m^{-2}}$) and for tall fescue plants in FC stands (maximal LAI of 4·47 $\mathrm{m^2\ m^{-2}}$).

Most of the grass species belonging to the different mixtures showed a triangular vertical distribution of their LAI (Fig. 3). Two cases could be distinguished among these triangular profiles. In the first case, most of the foliage is located in the upper layers of the canopy, such as the vertical profiles of LAI exhibited by tall fescue plants (in FA and FC) where the maximal amount of leaf area is located above the middle of the stand's height. In the second case, most of the foliage is located in the lower layers of the canopy. This was particularly the case for wheat (e.g. W70–P30_1100DD_1, W50–P50A_685DD_1). The LAI of legume species within the FA stands grown at high density and the FC swards (alfalfa and clover, respectively) also followed triangular profiles with variations of LAI between layers ranging from 0·05 to 0·80 $\mathrm{m^2\ m^{-2}}$. In contrast, vertical distributions of alfalfa LAI grown at low density followed a rectangular pattern, as

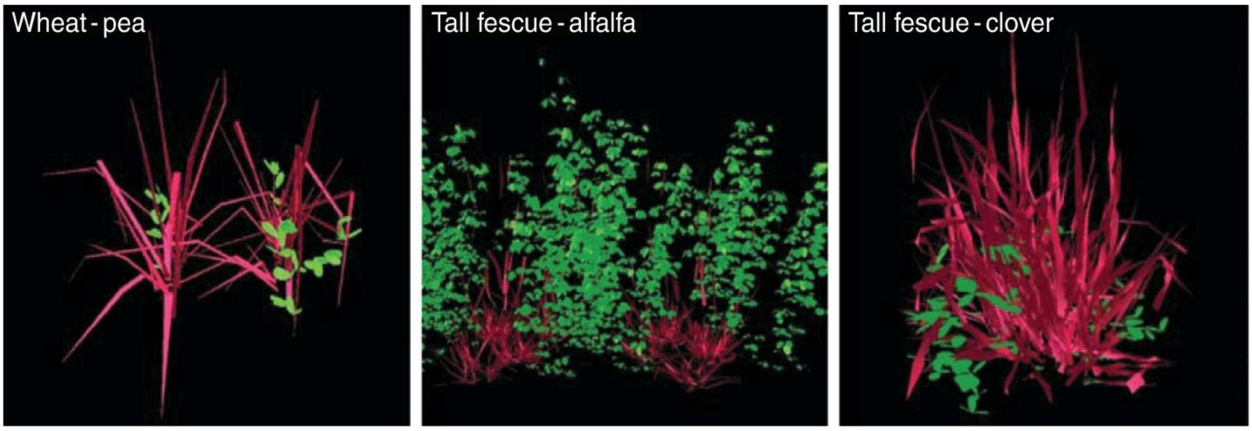

FIG. 2. Horizontal views of some reconstructed 3-D scenes of wheat–pea, tall fescue–alfalfa and tall fescue–clover mixtures. Grass species are showed in red and legumes in green.

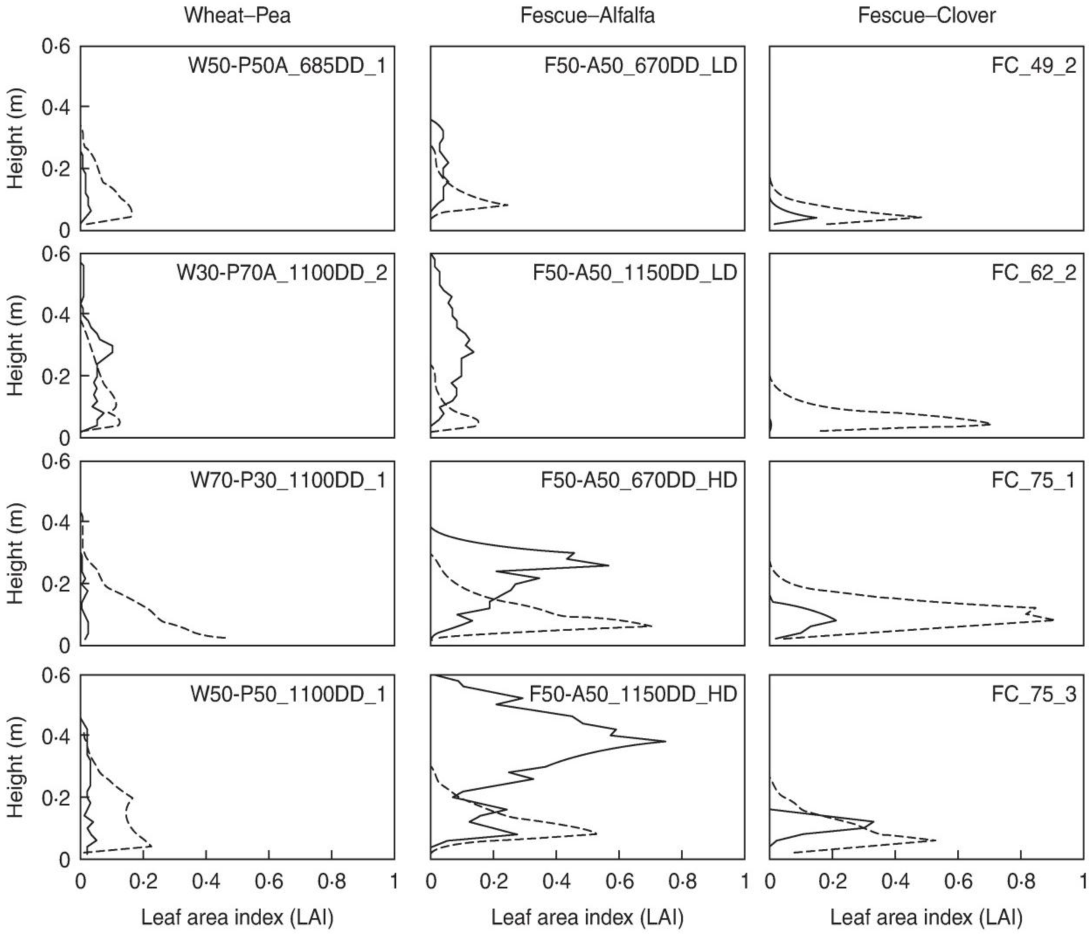

FIG. 3. Typical vertical distribution of leaf area index (LAI) in wheat–pea, tall fescue–alfalfa and tall fescue–clover mixtures. See Table 1 for an explanation of the labels inside the individual graphs. Vertical profiles of LAI are noted for grass (dashed lines) and legume (solid lines) species.

observed for pea plants within WP stands. Differences in component species height were also contrasted according to the mixtures. Height ranged from 100 to 400 mm for grass species and from 70 to 600 mm for legumes. Wheat and pea plants did not show any marked difference in height whereas in FC mixtures tall fescue plants overtopped clover by 50–100 mm. The strongest vertical stratification, however, was observed in the FA swards where (1) alfalfa largely overtopped tall fescue plants by 100–300 mm, and (2) 50–90 % of the alfalfa foliage was located in the upper layer of the canopy.

Figure 4 shows typical horizontal distributions of LAI in different mixtures. Coefficients of variation (CV) of the horizontal distribution of LAI ranged from 0·17 to 1·35 for grasses and from 0·12 to 2·80 for legumes (Table 1). Highest values of CV were observed for wheat (mean ± s.d. 0·79 ± 0·26) and for pea (1·41 ± 0·72). As a result, WP stands exhibited the most marked row arrangement as the CV of the WP mixture was 0·63 ± 0·22 (see typical profiles in Fig. 4). Similar profiles were observed in the FA swards grown at low density (mean CV = 0·70 ± 0·16 for tall fescue and 0·88 ± 0·11 for alfalfa) although their CV was lower than for the WP mixtures (0·32 ± 0·02). In contrast, horizontal heterogeneities were lower in the FA swards grown at high density (0·13 ± 0·06) as well as for the FC stands (0·27 ± 0·10).

Mean leaf inclination. Leaf inclinations of grass species ranged from 37·1 to 58·3° while for legumes it ranged from 27·2 to 42·4°, thus reflecting the more planophile distribution of legume leaves (Table 2). Extinction coefficients (k) were 0·72–0·88 and 0·84–0·93 for grass and legume species, respectively. Within FA stands, component species exhibited distinct leaf inclination as tall fescue foliage was more erect (53·4 ± 2·0°, $k = 0{\cdot}76$) than alfalfa (42·4 ± 6·7°, $k = 0{\cdot}84$) regardless of density and stage of development. The most marked difference in species leaf inclination was found in the FC mixtures where mean leaf inclination was 58·3 ± 4·5° for tall fescue versus 27·2 ± 6·4° for clover, the latter therefore displaying planophile leaves (extinction coefficient reached 0·93). In contrast, the WP mixtures did not show any marked differences between the mean leaf inclination of the two component species, 37·1 ± 5·4° ($k = 0{\cdot}88$) and 36·0 ± 3·1° ($k = 0{\cdot}88$) for wheat and pea, respectively. Moreover, vertical profiles did not show any clear variation in mean leaf inclination as a function of canopy height (data not shown).

Species contribution to canopy LAI and light interception

Mixtures exhibited contrasted ratios of grass/legume LAI as well as light partitioning levels, thus covering a large range of

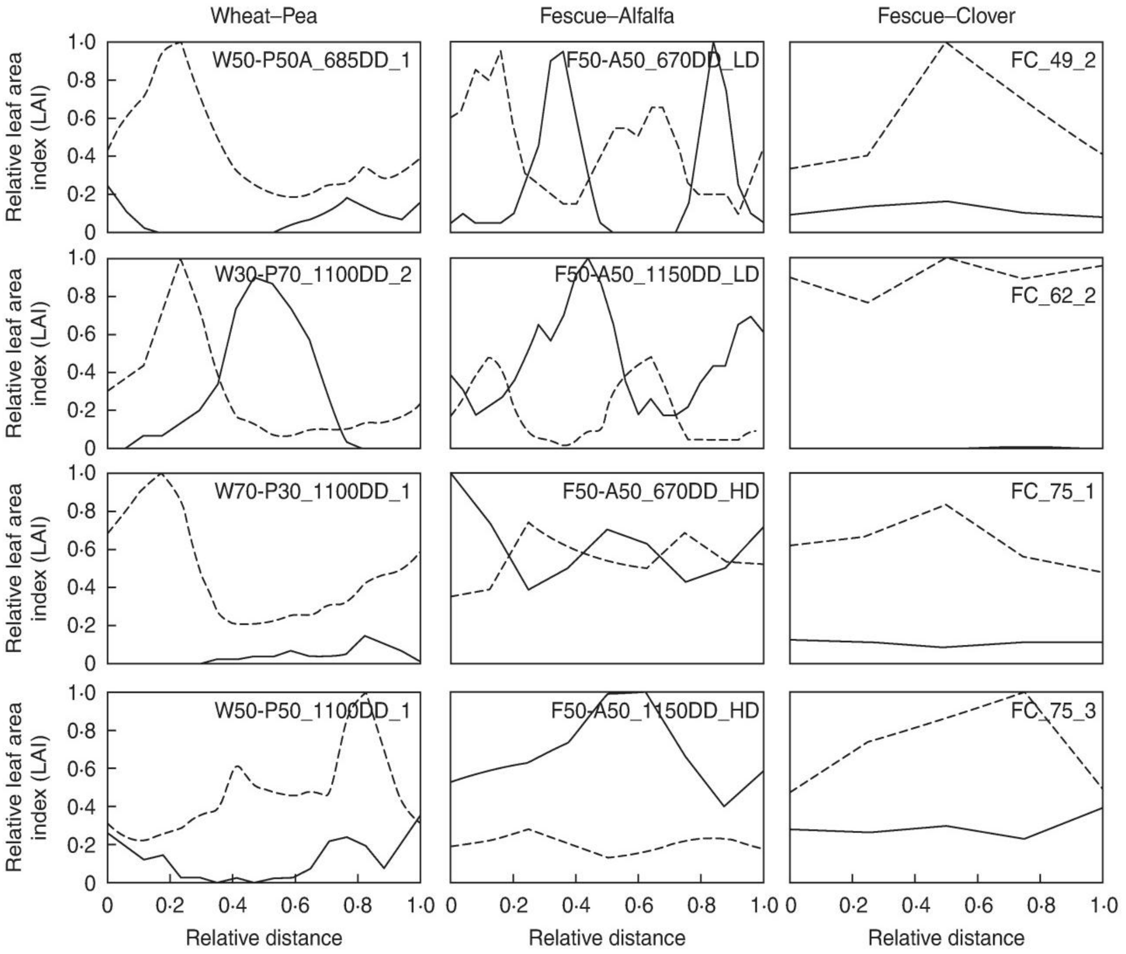

FIG. 4. Typical horizontal distributions of leaf area index (LAI) of the wheat–pea, tall fescue–alfalfa and tall fescue–clover mixtures. See Table 1 for an explanation of the labels inside the individual graphs. Horizontal profiles of LAI are noted for grass (dashed lines) and legume (solid lines) species where each value was normalized according to (1) the distance of the first row and (2) the maximal LAI of the overall mixture.

TABLE 2. *Species mean leaf inclination and extinction coefficients of wheat–pea (WP), tall fescue–alfalfa (FA) and tall fescue–clover (FC) mixtures*

	Grass		Legume	
Mixture	Mean leaf inclination (°)	Extinction coefficient	Mean leaf inclination (°)	Extinction coefficient
WP	37·1 ± 5·4	0·87	36·0 ± 3·1	0·88
FA	53·4 + 2·0	0·75	42·4 ± 6·7	0·84
FC	58·3 ± 4·5	0·71	27·2 ± 6·4	0·92

Extinction coefficients were derived from eqn (4).

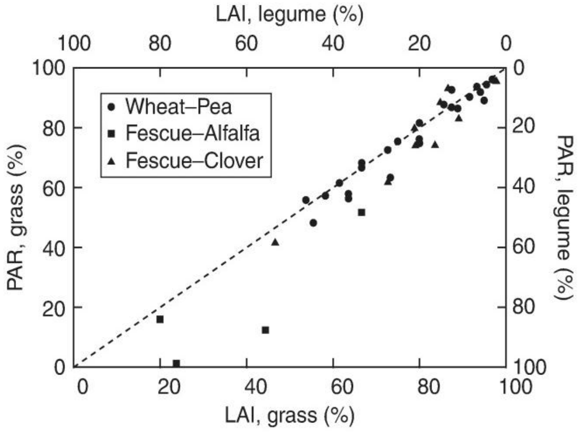

FIG. 5. Species contribution to leaf area index (LAI) and photosynthetically active radiation (PAR) interception. Computations were made on wheat–pea, tall fescue–alfalfa and tall fescue–clover mixtures, as indicated.

possibilities (Fig. 5), i.e. from radiation interception made at 98·69 % by legume species (constituting 76·97 % of the whole canopy) to a situation where grass species represent 96·91 % of the mixture LAI with a interception of incident light of 96·22 %. In most WP and FC stands, canopies were largely constituted by the grass species, respectively wheat and tall fescue plants, which therefore captured most of incident light, ranging from 41·93 to 96·22 % of the overall light interception. WP and FC values were distributed within this interval, depending on the species density and growth stage. In contrast, the FA swards exhibited different levels of interspecific LAI and light interception compared to WP and FC mixtures. Indeed, the contribution of the legume species (alfalfa) to total

LAI ranged from 38·84 to 76·97 %, which therefore intercepted 48·18–98·69 % of incident light. In some cases, similar values of LAI were measured between the two component species. As shown in Table 1, the contribution of each component species to the overall LAI in W30–P70 at 685 and 1100 DD, F50-A50_670DD_HD and FC_62_2, was equivalent, leading to equivalent levels of light interception (grass interception ranged from 46·21 to 63·31 %).

In the case of WP and FC mixtures, points were slightly distributed below the 1 : 1 line whereas most of FA points were markedly located further from this line, in particular for HD mixtures.

Virtual canopies vs. turbid medium approach

The ability of the turbid medium-based approach to estimate LIE of each species was assessed against a 3-D virtual plants-based approach (reference model). The turbid medium approach was set to gradually take into account the vertical distribution of the foliage by considering the canopy as a single layer (Fig. 6A) or by dividing the canopy into two (Fig. 6B) or ten horizontal layers (Fig. 6C). Figure 6 shows that the turbid medium approach was tested on a wide range of LIEs for both grass and legume species, ranging from 0·01 to 0·86 and from 0·01 to 0·99, respectively. The overall estimation of legume LIE by the turbid medium approach was unbiased whereas those for grass species were overestimated (maximal bias reaching −0·05). Predicted LIEs of the soil were significantly underestimated (maximal bias = +0·05).

When using the one-layered option (Fig. 6A), RMSDP was 0·08 and 0·06 for grass and legume components, respectively. For WP and FC mixtures maximal bias (Table 3) reached −0·05 for grass species (RMSDP = 0·06 and 0·07 for wheat and tall fescue, respectively) and −0·01 for legume components (RMSDP = 0·02 and 0·04 for pea and clover, respectively). Strong discrepancies were observed for the FA swards as maximal bias reached −0·16 for tall fescue (RMSDP = 0·18) and +0·14 for alfalfa (RMSDP = 0·14). Maximal deviation was observed for FA stands grown at high density as LIE of tall fescue plants was overestimated by 0·28 and 0·21 for F50-A50_670DD_HD and F50-A50_1150DD_HD, respectively. It could represent up to 17 times the LIE estimated by the reference model. For these two mixtures, alfalfa LIE was underestimated by 0·27 and 0·22, respectively.

Considering the canopy as two layers (Fig. 6B) reduced RMSDP by 0·01. This was particularly the case for the FA swards as bias decreased by 0·04 for tall fescue (RMSDP = 0·15) and 0·05 for alfalfa (RMSDP = 0·14). This improvement in the LIE prediction of FA mixtures was particularly marked for F50-A50_1150DD_HD. In contrast, in some cases, there was no improvement in the LIE prediction compared with the

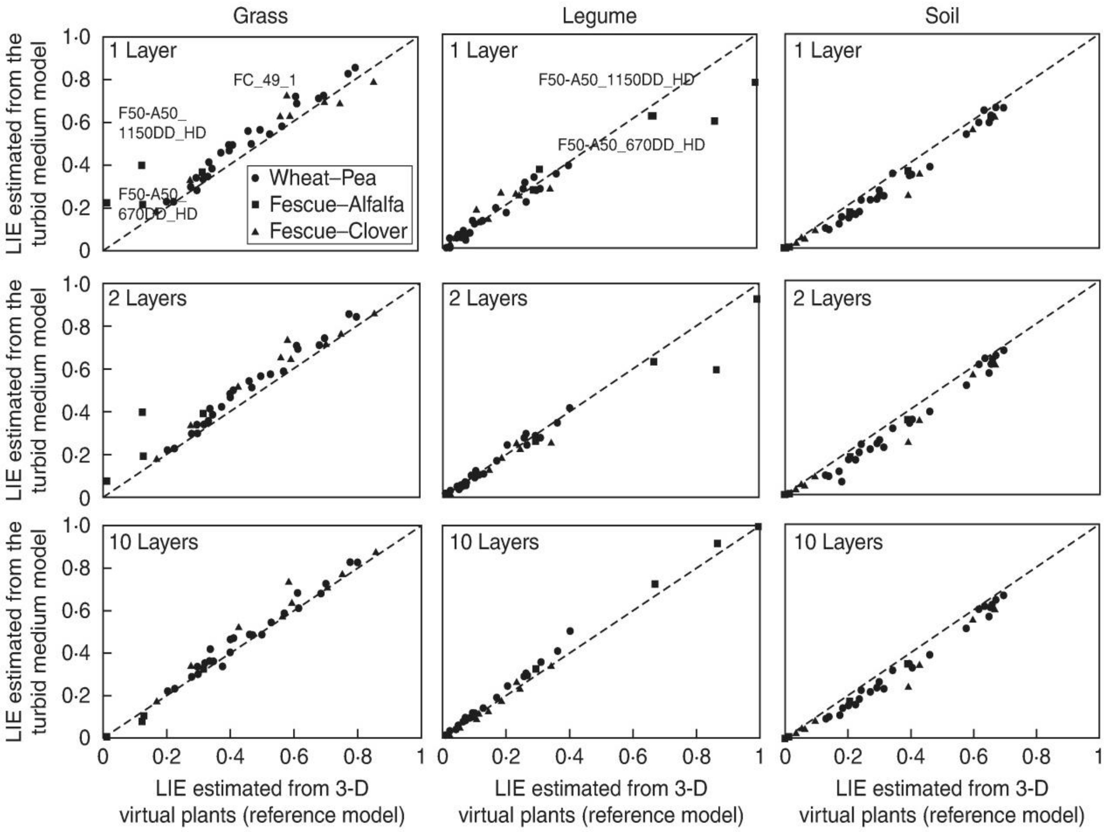

FIG. 6. Comparison between light interception efficiencies (LIE) derived from the turbid medium model and 3-D virtual plants (reference model). Values are presented for grass and legume species as well as for the soil (columns, as indicated). The turbid medium model was assessed by describing the canopy as one, two or ten layers (rows, as indicated). Estimations were made on three mixtures: wheat–pea, tall fescue–alfalfa and tall fescue–clover (as indicated in the first graph) at different densities and stages of development (see Table 1). Five outliers are highlighted.

TABLE 3. *Mean bias of the predictions (MBP) and root mean squared deviation of the predictions (RMSDP) for light interception efficiency estimated by the turbid medium model in wheat–pea (WP), tall fescue–alfalfa (FA) and tall fescue–clover mixtures*

		Grass		Legume		Soil	
No. of layers in SIRASCA	Mixture	MBP	RMSDP	MBP	RMSDP	MBP	RMSDP
1	WP	−0·05***	0·06	0	0·02	+0·05***	0·05
	FA	−0·16*	0·18	+0·14	0·14	+0·02	0·03
	FC	−0·03	0·07	−0·01	0·04	+0·05***	0·06
2	WP	−0·05***	0·06	0	0·02	+0·05***	0·06
	FA	−0·12	0·15	+0·10	0·14	+0·02	0·03
	FC	−0·06***	0·07	+0·01	0·03	+0·05**	0·06
10	WP	−0·02***	0·04	−0·02***	0·03	+0·05***	0·05
	FA	+0·02	0·03	−0·04*	0·04	+0·02	0·03
	FC	−0·05**	0·07	0	0·01	+0·05**	0·06

*$P < 0{\cdot}1$, **$P < 0{\cdot}05$, ***$P < 0{\cdot}01$.

one-layered model (e.g for F50-A50_670DD_HD or FC_49_1). In other cases, description of the canopy in two layers even led to a worse estimation of LIE, in particular for FC mixtures (bias = −0·06, RMSDP = 0·07; bias = +0·01; RMSDP = 0·03; for tall fescue and clover, respectively). Although these discrepancies were slight (mean deviation of $9{\cdot}10 \times 10^{-4} \pm 0{\cdot}001$), they were observed in 42·10 % of the overall mixtures.

Discretization of the canopy into ten small layers (Fig. 6C) produced the best estimation of LIE, very close to the reference model regardless of species, density or mixture stage of development (bias $\leq |0{\cdot}05|$, RMSDP = 0·04). The improvement of LIE estimation was particularly marked for the FA swards as the RMSDP decreased by 80·46 and 75·81 % compared with the one- and two-layered options, respectively. The highest improvement was observed for stand F50-A50_1150DD_HD. In a few cases, however, increasing the vertical description of the canopy to ten layers did not lead to any improvement of LIE estimation, as observed for some tall fescue plants within the FC mixtures (e.g. for FC_49_1).

DISCUSSION

We assessed the turbid medium-based approach for its capacity to accurately estimate LIE of intercropped plants. We studied two different types of species, grasses and legumes, which exhibited contrasted structures and abilities to capture light. Their structural characteristics allowed us to challenge some of the turbid medium assumptions.

Variability in mixture structure, plant architecture and light partitioning among components

As reported by several authors (e.g. Sinoquet and Caldwell, 1995) vertical dominance among components of mixed crops is of upmost importance for light partitioning. In the present study, mixtures exhibited contrasted differences in the height of component species, thus leading to various levels of vertical stratification. We described canopies with equivalent height between component species as well as mixtures where one of the species overtopped the other, either the grass or the legume component. Although these mixtures were grown in controlled conditions, their structures were realistic as they represent several forms of intercropping encountered in agricultural systems. This variability can be understood based on the classification proposed by Malézieux *et al.* (2009) as we described a row mixture of annual crops and two other intercropping systems of perennial species with contrasted levels of row structure and vertical stratification. The FA mixture is close to structures encountered in agroforestry systems (Malézieux *et al.*, 2009).

Variability in mixture structure also results from the vertical distribution of leaf area. Grass species, clover and alfalfa, generally exhibited triangular distributions of their leaf area, as already reported in several monospecific grass canopies (Ross, 1981) and in grass–clover mixtures (Nassiri *et al.*, 1996; Lantinga *et al.*, 1999; Sonohat *et al.*, 2002). These actual vertical profiles of LAI are not in agreement with the assumption of a regular distribution commonly used in studies dealing with light interception. Such disagreements were noted by Schulte and Lantinga (2002). In contrast, regular profiles of vertical LAI distribution were observed for pea and some alfalfa plants.

In addition to the LAI distribution, leaf inclination is the second basic parameter used to characterize a plant's ability to capture light (Sinoquet and Caldwell, 1995). In the intercropping systems described, there were mixtures exhibiting equivalent leaf inclinations between their components as well as species with contrasted leaf inclination. Leaf inclinations for each species were consistent with previous studies on monospecific canopies as reported by Ross (1981), except for wheat leaves for which inclination was lower in the present study. Such differences in leaf inclinations could be the result of species plasticity in response to a multispecific environment compared with monospecific conditions.

As a result of species differences in height, foliage dispersion and inclination, various abilities for light interception and levels of competition for light were observed. Indeed, we described two canopies where the grass was the dominant species and one sward where the legume captured most of the incident light. Whatever the mixture considered, species dominance in terms of light interception was mainly the result of their contribution to overall LAI of the mixture. This was particularly the case for grass species whose lower

ability for light interception, due to erectophile foliage, was counterbalanced by their aptitude to develop a large leaf area and/or by their vertical dominance (Sonohat *et al.*, 2002). Grass–legume mixtures where the grass component is dominant have been widely described and are often considered to be more productive and stable compared with mixtures dominated by the legume component (Haynes and Brady, 1980; Louarn *et al.*, 2010). In contrast, mixtures dominated by a legume lead to strong levels of competition for light as their vertical dominance is enhanced by their structural ability to intercept light (planophile leaves) (Chamblee and Collins, 1988; Louarn *et al.*, 2010). This was particularly the case for the FA swards where the vertical dominance of alfalfa and its high extinction coefficient were combined to give a high stand density, thus leading to a stronger interception of light by alfalfa than its relative contribution to the LAI of the mixture (Fig. 5).

Although all the mixtures used in the present work were a case of study, their structure can highlight light partitioning features in intercropping systems where direct validation with digitizing methods is not possible.

Predicting light partitioning in intercropping systems with a turbid medium-based model

Estimating light partitioning in intercropping systems with the turbid medium approach is based on the assumption that canopies are homogeneous. Here we have shown that the turbid medium approach was in good agreement with the reference model in most of the challenging range of canopy structures. However, these mixtures included structures which could be considered as heterogeneous, such as row mixtures or open-canopies whose LAI was lower than 1 $m^2 m^{-2}$ and where light transmission to the soil was higher than 50 % (early growth stages). Biased estimations of LIE were therefore expected from the turbid medium approach. Similar results were reported by Sinoquet and Bonhomme (1989) in sole crops of maize sown in rows and by Tournebize and Sinoquet (1995) in heterogeneous shrub–grass mixtures whose structure allowed direct measurements of light partitioning. As mentioned by Gutschick (1991), horizontal heterogeneities, i.e. row structures, appeared to be of less importance for estimating light interception with turbid medium-based models, as mixtures with high CV did not show significant discrepancies in regard to their LIE estimates by the turbid medium model.

The two-layered model did not significantly improve LIE estimates of the overall mixtures compared with the one-layered model. In some cases, this even led to more biased estimations of LIE compared with the one-layered model. This result underlines the importance of the definition of plant height. Indeed, layers were defined according to the *maximal* height of each component, which therefore account for single erected laminas with small areas that generally belonged to grass species. Although many studies dealing with light partitioning within intercropping systems were based on a two-layered turbid medium model (Ofori and Stern, 1987; Sinoquet *et al.*, 1990; Sonohat *et al.*, 2002; Tsubo and Walker, 2002; Awal *et al.*, 2006), no details were given on their definition of plant height. We suggest that layer boundaries should rather be delimited by a more ‘functional’ definition of plant height such as the height under which a given proportion of the foliage area may be found (e.g. 90 or 95 %). Thus, when using the turbid medium approach, leaf elements will be dispersed in a layer whose size would be closest to the actual leaf area localization.

The simplest models, with one and two layer(s), were, however, unable to estimate LIE of canopies exhibiting strong vertical stratifications combined with foliage overlapping (e.g. FA stands grown at high density). Horizontal profiles of LAI showed that in these mixtures, species appeared to be well mixed, which therefore led to high levels of inter-species foliage overlapping, referred to as between-species leaf dispersion (Sinoquet and Bonhomme, 1991). Similar conclusions could be drawn from differences of LIE estimations between species as the turbid medium model provided better estimations of legume LIE compared with grass species. Such discrepancies could be the result of contrasted within-species leaf dispersion. Indeed, legumes generally exhibit a quasi-random dispersion of their foliage (Sonohat *et al.*, 2002), but which may vary along the vertical axis (Lantinga *et al.*, 1999). In contrast, grass leaves tended to be more clumped (Lantinga *et al.*, 1999; Sonohat *et al.*, 2002) so, by using the turbid medium analogy, foliar elements of grasses are considered to be randomly dispersed, which therefore ‘artificially’ increases grass LIE. It therefore appears that light partitioning within this kind of canopy structure cannot be satisfactorily simulated by the turbid medium approach, unless a more detailed description of the canopy is provided, which improves the consideration of species height and foliage interpenetration. As a result, the ten-layered model gave predictions very close to the reference model, as the remaining bias was lower than |0·03| for grass and legume species. However, the impact of such small cumulative errors on a predictive model of biomass accumulation remains to be assessed.

Apart from the limitations discussed above, our results show that description of just the vertical stratification is enough to predict light partitioning with a turbid medium-based model in a wide range of intercropping systems and stages of development. However, these conclusions were drawn from results obtained with one of the most complex and detailed turbid medium-based models (SIRASCA) dealing with light partitioning within mixed canopies (Sinoquet *et al.*, 2000). Moreover, increasing the vertical description of canopies (i.e. the number of horizontal layers) would require tedious and time-consuming measurements; for example, the ten-layered model used in the present paper would have required us to measure leaf area and inclination of each species every 1·5–6 cm, depending on mixture height.

Contribution of models based on explicit 3-D description of plant architecture

As reported in most studies using the turbid medium approach, canopies were characterized only by their *leaf* area. To compare the two models on similar canopy structures, stems (or sheaths for grass species) were therefore not taken into account for both SIRASCA and 3-D virtual plant

models although they represent a significant part of the plant area. The use of structural plant models in future works would therefore allow us to quantify the interception of light by stems/sheaths while the cylindrical shape of these organs and their erected bearing require implementation of complex rules in turbid medium-based models. However, as proposed by Da Silva *et al.* (2008), modelling frameworks must be developed to identify a level of plant/organ description that achieves a good compromise between the amount of measurement required to describe the plant architecture (which is also associated with the computation time) and the quality of the resulting light interception model.

Light partitioning within intercropping systems is a crucial issue for studying the dynamics of the system's component species growth. These dynamics result from complex interactions involving the interception of light. In the present study, structural and static plant representations coupled to radiative transfer models were used to characterize light partitioning among component species. Moreover, these spatially explicit representations of plant architecture also offer the possibility to be dynamically coupled with functional models (e.g. photosynthetic functions) thus resulting in functional–structural plant models. As these models could be uses at several scales (stand, plant or organ level), they therefore have the ability to integrate the effects of microclimate variations on plant growth, allowing us to study feedback between plant structure, plant function and microclimate (Godin and Sinoquet, 2005; Vos *et al.*, 2010). Apart from recent studies on a mixture of two perennial species (Sonohat *et al.*, 2002), on an integrated legume–weed system (Cici *et al.*, 2008) and on coconut agroforestry systems (Dauzat and Eroy, 1997; Lamanda *et al.*, 2008), most previous works devoted to estimating light partitioning within intercropping systems used the turbid medium approach by describing the canopy in one or two horizontal layers (Faurie *et al.*, 1996; Lantinga *et al.*, 1999; Tsubo and Walker, 2002; Tsubo *et al.*, 2005; Awal *et al.*, 2006). However, due to experimental constraints inherent to multispecies canopies, these models were not directly validated. As proposed in the present study, 3-D virtual models which explicitly describe plant architecture therefore appeared to be a convenient tool for the assessment of turbid medium models dealing with light partitioning in intercropping systems. Therefore, 3-D structural models, either static or dynamic, remain a complex but efficient tool for studying light partitioning within multispecies stands in order to improve the complementarity between the mixed crops or, by contrast, to analyse/develop more competitive cultivars to improve the management of weeds (Cici *et al.*, 2008). Moreover, such models could also be used to generate virtual experiments suitable for the assessment of the turbid medium approach on other existing intercropping systems or in the framework of theoretical and exploratory studies.

ACKNOWLEDGMENTS

This research is supported by 'La Région Pays de la Loire', France. We thank Arnaud Philipponneau and Cédric Perrot for their great technical assistance.

LITERATURE CITED

Adam B, Sinoquet H, Godin C, Donès N. 1999. *3A – software for the acquisition of plant architecture.* Clermont-Ferrand: UMR PIAF INRA-UBP.

Adam B, Donès N, Sinoquet H. 2002. *VegeSTAR – software to compute light interception and canopy photosynthesis from images of 3D digitised plants.* Clermont-Ferrand: UMR PIAF INRA-UBP.

Andrieu B, Sinoquet H. 1993. Evaluation of structure description requirements for predicting gap fraction of vegetation canopies. *Agricultural and Forest Meteorology* **65**: 207–227.

Awal MA, Koshi H, Ikeda T. 2006. Radiation interception and use by maize/peanut intercrop canopy. *Agricultural and Forest Meteorology* **139**: 74–83.

Chamblee DS, Collins M. 1988. Relationships with other species in a mixture. In: Hanson AA, Barnes DK, Hill RR Jr, eds. *Alfalfa and alfalfa improvement*. Madison, WI: American Society of Agronomy, 439–461.

Chelle M. 2005. Phylloclimate or the climate perceived by individual plant organs: What is it? How to model it? What for? *New Phytologist* **166**: 781–790.

Chelle M, Andrieu B. 1999. Radiative models for architectural modeling. *Agronomie* **19**: 225–240.

Chen SG, Impens I, Ceulemans R, Kockelbergh F. 1993. Measurement of gap fraction of fractal generated canopies using digitalized image analysis. *Agricultural and Forest Meteorology* **65**: 245–259.

Cici SZ-H, Adkins S, Hanan J. 2008. A canopy architectural model to study the competitive ability of chickpea with sowthistle. *Annals of Botany* **101**: 1311–1318.

Combes D, Chelle M, Sinoquet H, Varlet-Grancher C. 2008. Evaluation of a turbid medium model to simulate light interception by walnut trees (hybrid NG38 × RA and *Juglans regia*) and sorghum canopies (*Sorghum bicolor*) at three spatial scales. *Functional Plant Biology* **35**: 823–836.

Da Silva D, Boudon F, Godin C, Sinoquet H. 2008. Multiscale framework for modeling and analyzing light interception by trees. *Multiscale Modeling & Simulation* **7**: 910–933.

Dauzat J, Eroy MN. 1997. Simulating light regime and intercrop yields in coconut based farming systems. *European Journal of Agronomy* **7**: 63–74.

Den Bulk JA. 1989. *The interpretation of remote sensing, a feasibility study.* Thesis, Wageningen.

Faurie O, Soussana JF, Sinoquet H. 1996. Radiation interception, partitioning and use in grass–clover mixtures. *Annals of Botany* **77**: 35–46.

Fournier C, Andrieu B, Ljutovac S, Saint-Jean S. 2003. ADEL-wheat: a 3D architectural model of wheat development. In: Hu BG, ed. *International Symposium on Plant Growth Modeling, Simulation, Visualization, and their Applications*. Beijing: Tsinghua University Press/Springer, 54–63.

Giller KE, Beare MH, Lavelle P, Izac AMN, Swift MJ. 1997. Agricultural intensification, soil biodiversity and agroecosystem function. *Applied Soil Ecology* **6**: 3–16.

Godin C. 2000. Representing and encoding plant architecture: a review. *Annals of Forest Science* **57**: 413–438.

Godin C, Caraglio Y. 1998. A multiscale model of plant topological structures. *Journal of Theoretical Biology* **191**: 1–46.

Godin C, Sinoquet H. 2005. Functional–structural plant modelling. *New Phytologist* **166**: 705–708.

Griffon M. 1999. Développement durable et agriculture: la révolution doublement verte. *Cahiers Agricultures* **8**: 259–267.

Gutschick VP. 1991. Joining leaf photosynthesis models and canopy photon-transport models. In: Myneni RB, Ross J, eds. *Photon–vegetation interactions: applications in optical remote sensing and plant ecology.* Berlin: Springer-Verlag, 501–535.

Harper JL. 1961. Approaches to the study of plant competition. In: Milthorpe FL, ed. *Mechanisms in biological competition*. Cambridge: Symposia of the Society for Experimental Biology, 1–39.

Haynes RJ. 1980. Competitive aspects of the grass–legume association. In Brady NC, ed. *Advances in agronomy.* New York: Academic Press, 227–261.

Lamanda N, Dauzat J, Jourdan C, Martin P, Malézieux E. 2008. Using 3D architectural models to assess light availability and root bulkiness in coconut agroforestry systems. *Agroforestry Systems* **72**: 63–74.

Lantinga EA, Nassiri M, Kropff MJ. 1999. Modelling and measuring vertical light absorption within grass-clover mixtures. *Agricultural and Forest Meteorology* **96**: 71–83.

Louarn G, Corre-Hellou G, Fustec J, *et al*. 2010. Déterminants écologiques et physiologiques de la productivité et de la stabilité des associations graminées-légumineuses. *Innovations Agronomiques* **11**: 79–99.

Malézieux E, Crozat Y, Dupraz C, *et al*. 2009. Mixing plant species in cropping systems: concepts, tools and models. A review. *Agronomy for Sustainable Development* **29**: 43–62.

Monsi M, Saeki T. 1953. Über den Lichtfaktor in den Pflanzengesellschaften und seine Bedeutung für die Stoffproduktion. *Japanese Journal of Botany* **14**: 22–52.

Moon P, Spencer DE. 1942. Illumination from a non-uniform sky. *Illuminating Engineering Society* **37**: 707–726.

Moulia B, Sinoquet H. 1993. Three-dimensional digitizing systems for plant canopy geometrical structure: a review. In: Varlet-Grancher C, Bonhomme R, Sinoquet H, eds. *Crop structure and light microclimate*. Paris: INRA editions, 183–193.

Nassiri M, Elgersma A, Lantinga EA. 1996. Vertical distribution of leaf area, dry matter and radiation in grass-clover mixtures. In: Parente G, Frame J, Orsi S, eds. *Grassland and land use systems. 16th meeting of the European Grassland Federation*. Gorizia, Italy: ERSA, 269–274.

Nilson T. 1971. A theoretical analysis of the frequency of gaps in plant stands. *Agricultural Meteorology* **8**: 25–38.

Ofori F, Stern WR. 1987. Cereal–legume intercropping systems. *Advances in Agronomy* **41**: 41–90.

Polhemus. 2009. *3Space Fastrak user's manual, revision F.* Colchester, VT: Polhemus Inc.

Pradal C, Dufour-Kowalski S, Boudon F, Fournier C, Godin C. 2008. OpenAlea: a visual programming and component-based software platform for plant modelling. *Functional Plant Biology* **35**: 751–760.

Rimmington GM. 1984. A model of the effect of interspecies competition for light on dry-matter production. *Australian Journal of Plant Physiology* **11**: 277–286.

Ross J. 1981. *The radiation regime and architecture of plant stands*. The Hague, The Netherlands: W. Junk, 391 pp.

Schulte RPO, Lantinga EA. 2002. Mechanistic simulation of the vertical structure of mixed swards. *Ecological Modelling* **149**: 229–246.

Sinoquet H. 1993. Modelling radiative transfer in heterogeneous canopies and intercropping systems. In: Varlet-Grancher C, Bonhomme R, Sinoquet H, eds. *Crop structure and light microclimate*. Paris: INRA editions, 229–252.

Sinoquet H, Bonhomme R. 1989. Modelisation de l'interception des rayonnements solaires dans une culture en rangs. II: Structure geometrique du couvert et validation du modele. *Agronomie* **9**: 619–628.

Sinoquet H, Bonhomme R. 1991. A theoretical analysis of radiation interception in a two-species plant canopy. *Mathematical Biosciences* **105**: 23–45.

Sinoquet H, Caldwell MM. 1995. Estimation of light capture and partionning in intercropping systems. In: Sinoquet H, Cruz P, eds. *Ecophysiology of tropical intercropping*. Paris: INRA, 79–97.

Sinoquet H, Moulia B, Gastal F, Bonhomme R, Varlet -Grancher C. 1990. Modeling the radiative balance of the components of a well-mixed canopy: application to a white clover-tall fescue mixture. *Acta Oecologica-International Journal of Ecology* **11**: 469–486.

Sinoquet H, Rakocevic M, Varlet-Grancher C. 2000. Comparison of models for daily light partitioning in multispecies canopies. *Agricultural and Forest Meteorology* **101**: 251–263.

Sonohat G, Sinoquet H, Varlet-Grancher C, *et al*. 2002. Leaf dispersion and light partitioning in three-dimensionally digitized tall fescue-white clover mixtures. *Plant, Cell and Environment* **25**: 529–538.

Tilman D, Cassman KG, Matson PA, Naylor R, Polasky S. 2002. Agricultural sustainability and intensive production practices. *Nature* **418**: 671–677.

Tournebize R, Sinoquet H. 1995. Light interception and partitioning in a shrub/grass mixture. *Agricultural and Forest Meteorology* **72**: 277–294.

Tsubo M, Walker S. 2002. A model of radiation interception and use by a maize–bean intercrop canopy. *Agricultural and Forest Meteorology* **110**: 203–215.

Tsubo M, Walker S. 2004. Shade effects on *Phaseolus vulgaris* L. intercropped with *Zea mays* L. under well-watered conditions. *Journal of Agronomy and Crop Science* **190**: 168–176.

Tsubo M, Walker S, Ogindo HO. 2005. A simulation model of cereal–legume intercropping systems for semi-arid regions: I. Model development. *Field Crops Research* **93**: 10–22.

Vos J, Evers JB, Buck-Sorlin GH, Andrieu B, Chelle M, de Visser PHB. 2010. Functional–structural plant modelling: a new versatile tool in crop science. *Journal of Experimental Botany* **61**: 2101–2115.

Willey RW. 1979. Intercropping – its importance and research needs. Part 1. Competition and yield advantages. *Field Crop Abstracts* **32**: 1–10.

Synthèse

L’objectif de ce premier chapitre a consisté à **évaluer les approches de modélisation** utilisées pour estimer le partage du rayonnement dans les associations blé – pois. Ce travail a ainsi permis i) d’identifier une **approche pertinente** permettant de répondre aux objectifs de la thèse et ii) d’évaluer les **variations de structure de canopées d’associations céréales – légumineuses** ainsi que leurs **effets sur le partage du rayonnement**. Les résultats ont ainsi montré que la prise en compte explicite de l’architecture aérienne des plantes était nécessaire dans le but d’estimer le partage du rayonnement au sein de **couverts hétérogènes** (*e.g.* forte structuration verticale de la surface foliaire). Ce chapitre a ainsi permis d’établir que l’approche **plante virtuelle** était la plus adaptée au regard des objectifs fixés pour le travail de thèse. Une telle approche nécessite donc **d’accéder de façon explicite aux paramètres architecturaux** des modèles de représentation des plantes mais également de pouvoir **estimer leur impact sur l’interception du rayonnement** au sein de couvert pouvant présenter de fortes hétérogénéités.

Il s’agit donc maintenant de caractériser et modéliser la **morphogénèse** du pois et du blé afin de simuler le partage du rayonnement dans l’association et de comprendre les **le déterminisme architectural de son partage entre espèces associées**. Contrairement au blé, peu de travaux et d’outils sont disponibles quant à la modélisation de l’architecture aérienne du pois. La suite du travail de thèse est ainsi plus particulièrement focalisée sur la **morphogénèse du pois**.

Chapitre II

How does pea architecture influence light sharing in virtual wheat - pea mixtures? A simulation study based on pea genotypes with contrasting architectures.

Romain BARILLOT, Didier Combes, Valérie Chevalier, Christian Fournier, Abraham J. Escobar-Gutiérrez

Publié dans le journal AoB Plants

AoB PLANTS http://aobplants.oxfordjournals.org/

Open access – Research article

How does pea architecture influence light sharing in virtual wheat–pea mixtures? A simulation study based on pea genotypes with contrasting architectures

Romain Barillot[1], Didier Combes[2], Valérie Chevalier[1], Christian Fournier[3,4]
and Abraham J. Escobar-Gutiérrez[2]*

[1] LUNAM Université, Groupe Ecole Supérieure d'Agriculture, UPSP Laboratoire d'Ecophysiologie Végétale & Agroécologie, 55 rue Rabelais, BP 30748, F-49007 Angers cedex 01, France
[2] INRA, UR4 P3F, Equipe Ecophysiologie des plantes fourragères, Le Chêne - RD 150, BP 6, F-86600 Lusignan, France
[3] INRA, UMR 759 LEPSE, F-34060 Montpellier, France
[4] SupAgro, UMR 759 LEPSE, F-34060 Montpellier, France

Received: 21 June 2012; **Revised:** 5 September 2012; **Accepted:** 11 October 2012; **Published:** 24 October 2012

Citation details: Barillot R, Combes D, Chevalier V, Fournier C, Escobar-Gutiérrez AJ. 2012. How does pea architecture influence light sharing in virtual wheat–pea mixtures? A simulation study based on pea genotypes with contrasting architectures. *AoB PLANTS* **2012**: pls038; doi:10.1093/aobpla/pls038

Abstract

Background and aims Light interception is a key factor driving the functioning of wheat–pea intercrops. The sharing of light is related to the canopy structure, which results from the architectural parameters of the mixed species. In the present study, we characterized six contrasting pea genotypes and identified architectural parameters whose range of variability leads to various levels of light sharing within virtual wheat–pea mixtures.

Methodology Virtual plants were derived from magnetic digitizations performed during the growing cycle in a greenhouse experiment. Plant mock-ups were used as inputs of a radiative transfer model in order to estimate light interception in virtual wheat–pea mixtures. The turbid medium approach, extended to well-mixed canopies, was used as a framework for assessing the effects of leaf area index (LAI) and mean leaf inclination on light sharing.

Principal results Three groups of pea genotypes were distinguished: (i) early and leafy cultivars, (ii) late semi-leafless cultivars and (iii) low-development semi-leafless cultivars. Within open canopies, light sharing was well described by the turbid medium approach and was therefore determined by the architectural parameters that composed LAI and foliage inclination. When canopy closure started, the turbid medium approach was unable to properly infer light partitioning because of the vertical structure of the canopy. This was related to the architectural parameters that determine the height of pea genotypes. Light capture was therefore affected by the development of leaflets, number of branches and phytomers, as well as internode length.

Conclusions This study provides information on pea architecture and identifies parameters whose variability can be used to drive light sharing within wheat–pea mixtures. These results could be used to build up the architecture of pea ideotypes adapted to multi-specific stands towards light competition.

* Corresponding author's e-mail address: abraham.escobar@lusignan.inra.fr

Introduction

Cereal–legume intercropping systems are assumed to provide high and stabilized yields in terms of quantity and quality (Ofori and Stern 1987; Jensen 1996; Corre-Hellou *et al.* 2006), allow lower use of fertilizers and pesticides, and enhance biodiversity conservation (for a review see Malézieux *et al.* 2009). Intercropping benefits result from a trade-off between complementarity (e.g. separate root and canopy areas) and competition processes (for light, water and nutrients) that occur between the component crops. Among the contested resources, solar radiation, and in particular photosynthetically active radiation (PAR), is an important factor driving plant functioning as it provides the energy required for photosynthesis and thus for plant growth. Light capture also drives biological nitrogen fixation by legume species and therefore the autonomy of the intercropping system towards nitrogen resources. Finally, light determines the potential for crop productivity (Loomis and Williams 1963; Goudriaan 1982). Therefore, its sharing in multi-specific stands appeared to be a crucial issue for managing the balance between the component species as well as for determining the final yield of the mixture. It has been proposed that increasing the light interception efficiency (LIE) of intercropping systems could be achieved through: (i) maximizing total light interception by improving the spatial and temporal ground cover and (ii) adequately sharing light between component species by improving their spatial and temporal complementarity (Sinoquet and Caldwell 1995).

Total radiation interception, as well as its sharing among intercropped species, is highly related to the physical structure of the canopy (Ross 1981*b*; Sinoquet and Caldwell 1995), which emerges from the architecture of the individuals growing within the stand (Moulia *et al.* 1998). Individuals' architecture can be described as a collection of subunits called phytomers. After Godin (2000), such a description needs to include (i) an inventory of the plant components (decomposition information), (ii) the topological relationships between these components, and (iii) their geometry, given by the organ shape and spatial position (Godin 2000). Such a multiscale analysis of the canopy structure reveals the importance of plant architectural parameters as underpinning factors determining light interception and sharing within sole and mixed cropped systems.

Contrasting architectural parameters could result from: (i) the genotypic variability of a given species, (ii) the environmental conditions to which plants are exposed during their growth, and (iii) the genotype and environment interactions characterizing the phenotypic plasticity. Architectural plasticity of wheat (*Triticum aestivum* L.) has been described for various cultivars, sowing dates and row orientations, plant densities and nitrogen fertilization regimes (Evers *et al.* 2007; Baccar *et al.* 2011; Dornbusch *et al.* 2011). Plasticity of some architectural components of pea (*Pisum sativum* L.) has also been studied. For instance, Turc and Lecoeur (1997) found that leaf primordium initiation and leaf production of several pea cultivars were coordinated and stable in a large range of environmental conditions. Lateral branching of pea appeared to be dependent not only on environmental conditions such as low temperatures (Jeudy and Munier-Jolain 2005) but also on the genotype and its interactions with plant density (Spies *et al.* 2010). Further, the genetic determination of some architectural parameters of pea is now well documented (for a review see Huyghe 1998). Nevertheless, to our knowledge, the effects of the genetic variability of these architectural parameters on the level of competition for light within cereal–legume intercropping systems have not been reported. Such information would be useful for building up the architecture of pea ideotypes adapted to multi-specific stands.

Recently, virtual plant models have been used to study ideotype architectures in order to optimize light interception and photosynthesis in tomato (Sarlikioti *et al.* 2011) and rice (Zheng *et al.* 2008), and manage light sharing in an integrated legume–weed system (Cici *et al.* 2008). Although virtual plant models are able to take into account the multiscale aspect of plant functioning (stand, plant and organ levels), they have not been used to analyse the relationships between species architecture and light sharing within cereal–legume intercropping systems. The present study therefore focused on wheat–pea mixtures and in particular pea architecture, which has been little described. The aim of the present work was to identify the parameters of pea architecture whose genotypic variability leads to various levels of light sharing within wheat–pea canopies. To this end, we combined the virtual plant approach with an explicit description of the above-ground architecture of six pea genotypes. This allowed us to assess the effects of contrasting pea architectures on light sharing within mixtures.

Theory of light sharing in well-mixed canopies

In monocrop stands, light capture is well described by applying the Beer–Lambert law (Monsi and Saeki 1953) on homogeneous canopies. This approach is based on the assumption that the canopy can be described as a turbid medium where leaf area index (LAI) and mean leaf inclination are the main information needed. In our study, the turbid medium approach was used as a framework for assessing the effect of LAI and mean

leaf inclination on light sharing within a range of intercrop architectures. Indeed, some authors extended this approach to the case of well-mixed intercropping systems (Rimmington 1985; Sinoquet and Bonhomme 1991). Under such conditions, LIE of a species i in a mixture of N components is given by

$$\mathrm{LIE}_i = \frac{K_i \times \mathrm{LAI}_i}{\sum_{j=1}^{N} K_j \times \mathrm{LAI}_j}\left[1 - \exp^{\left(-\sum_{j=1}^{N} K_j \times \mathrm{LAI}_j\right)}\right] \quad (1)$$

where K_i and LAI_i are the extinction coefficient and leaf area index of species i. The extinction coefficients are derived from the mean leaf inclination of species (Sinoquet *et al.* 2000). Light sharing in the mixture of two species is therefore given by the ratio of the LIE of one species over the total light interception of the canopy. The contribution of species 1 to light capture of a bi-specific mixture is thus estimated by

$$\frac{\mathrm{LIE}_1}{\mathrm{LIE}_1 + \mathrm{LIE}_2} = \frac{(K_1 \times \mathrm{LAI}_1)/\varphi \times [1 - \mathrm{e}^{(-\varphi)}]}{(K_1 \times \mathrm{LAI}_1)/\varphi \times [1 - \mathrm{e}^{(-\varphi)}] + (K_2 \times \mathrm{LAI}_2)/\varphi \times [1 - \mathrm{e}^{(-\varphi)}]} \quad (2)$$

with $\varphi = K_1 \times \mathrm{LAI}_1 + K_2 \times \mathrm{LAI}_2$.

Simplifying,

$$\frac{\mathrm{LIE}_1}{\mathrm{LIE}_1 + \mathrm{LIE}_2} = \frac{K_1 \times \mathrm{LAI}_1}{\varphi} = \frac{K_1 \times \mathrm{LAI}_1}{K_1 \times \mathrm{LAI}_1 + K_2 \times \mathrm{LAI}_2} \quad (3)$$

Considering $K_1 = \alpha \times K_2$, we obtain

$$\frac{\mathrm{LIE}_1}{\mathrm{LIE}_1 + \mathrm{LIE}_2} = \frac{\alpha \times K_2 \times \mathrm{LAI}_1}{\alpha \times K_2 \times \mathrm{LAI}_1 + K_2 \times \mathrm{LAI}_2} = \frac{\mathrm{LAI}_1}{\mathrm{LAI}_1 + (\mathrm{LAI}_2/\alpha)} \quad (4)$$

Figure 1 shows the relative light interception by species 1 and 2 as a function of their contribution to the LAI of the mixture. For well-mixed canopies, theoretical isolines of light interception have been derived from equation (4) for different values of α, i.e. ratios of K_1/K_2. On the other hand, heterogeneous canopies would not follow these theoretical isolines, meaning that light sharing is not mainly determined by the species LAI and leaf inclination. Indeed, a component species can exhibit different height, leading to a vertical arrangement of the canopy. In this case, information on the vertical structure of the canopy is needed for estimating light sharing between component species (Sinoquet 1993; Barillot *et al.* 2011).

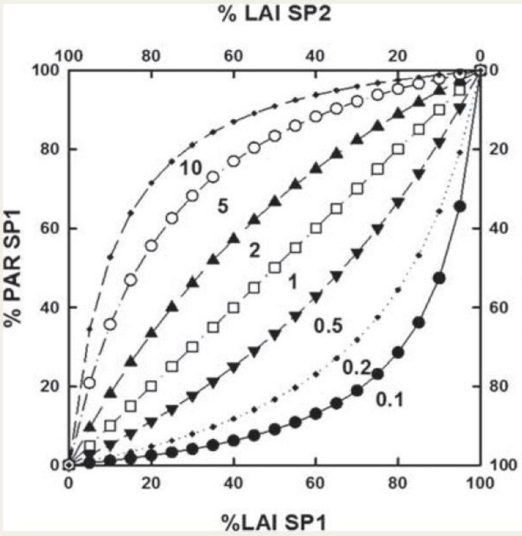

Fig. 1 Light sharing in a well-mixed mixture of two species (SP1 and SP2) as a function of their contribution to the total LAI. Theoretical isolines are shown for different ratios of the species extinction coefficients (K). $K_{\mathrm{SP1}}/K_{\mathrm{SP2}}$ ranged from 0.1 to 10.

Methods

Growing conditions and plant material

Six winter pea cultivars (*P. sativum*) were grown in 2 L individual plastic pots, spaced 10 cm apart, in a greenhouse from 24 March 2011 to 7 June 2011 in Angers, France (47°27′N, 00°32′W). Air temperature in the greenhouse ranged from 15 to 28 °C, water supply was adapted to maintain soil moisture content around 15 % (w/w). Individual pots were filled with soil containing 47 mg of $\mathrm{NO_3^-}$ $\mathrm{kg^{-1}}$. To ensure pea nodulation, each plant was inoculated with a solution of *Rhizobium leguminosarum* P221 at 2.2×10^9 bacteria $\mathrm{L^{-1}}$. Pea genotypes included four semi-leafless cultivars: Lucy, James, AOPH10 and 886/01 (HR type), and two leafy cultivars: China and US13 (Table 1). Eight plants of each pea cultivar were arranged according to a monofactorial experimental design in two randomized complete blocks, which were surrounded by non-measured plants in order to avoid border effects.

Three-dimensional digitizing of pea plants and virtual reconstructions

Pea cultivars were digitized twice a week during their growing cycle from 200 growing degree-days (DD) after emergence (base temperature 0 °C) until physiological maturity. Physiological maturity of pea ranged from

Table 1 Description of pea cultivars. Contribution of stipules, leaflets and stems to the maximum green area is also indicated for each pea cultivar.

Pea cultivar	Leaf type	hr/HR[a]	Last digitizing date (DD)	Organ contribution to the green area (%)		
				Stipules	Leaflets	Stems
China	Leafy	hr	1310	47 ± 2.8	45 ± 2.3	8 ± 0.9
US13	Leafy	hr	1445	46 ± 0.7	49 ± 0.9	5 ± 0.2
Lucy	Semi-leafless	hr	1565	91 ± 0.6	–	9 ± 0.6
James	Semi-leafless	hr	1445	89 ± 0.8	–	11 ± 0.8
AOPH10	Semi-leafless	hr	1630	91 ± 1.0	–	9 ± 1.0
886/01	Semi-leafless	HR	1890	91 ± 0.8	–	9 ± 0.8

[a] Pea cultivars of hr type are not sensitive to photoperiod, whereas cultivar 886/01 shows high response to photoperiod (HR type).

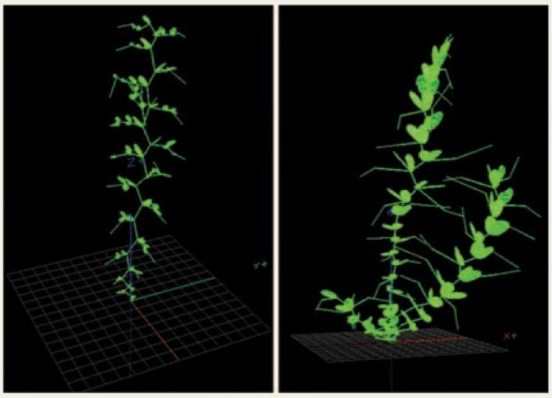

Fig. 2 Horizontal views of some reconstructed pea cultivars. Left: the semi-leafless cultivar 886/01; right: the leafy cultivar US13, both at 1000 DD.

1310 to 1890 DD (Table 1), which represented 21 dates of measurement for the latest cultivars. Details on the digitizing procedure and virtual plant reconstruction are given in Barillot *et al.* (2011). Briefly, magnetic digitizing was carried out by using a three-dimensional (3D) digitizer (3Space Fastrak, Polhemus Inc., Colchester, VT, USA). Spatial coordinates as well as each phytoelement orientation (apart from tendrils which were not digitized) were collected and encoded as Multiscale Tree Graphs. Data from digitizing were then imported into the Openalea platform (Pradal *et al.* 2008) where plant mock-ups were digitally reconstructed for each digitized plant (Fig. 2). Digitizing from 800 DD was done on phytomers located above the half-height of stems (for main stems and branches), assuming that by this time lower phytomers had completed their growth (Turc and Lecoeur 1997). Non-measured phytomers were reconstructed from their previous digitizing, thus reducing the duration of digitizing. Computations of LAI, height and architectural parameters of the pea genotypes were thus performed on the virtual mock-ups.

Calculation of light interception

Radiative model Light interception estimates are based on a nested radiosity model (Chelle and Andrieu 1998). Computations were performed considering only diffuse radiations according to the Uniform Overcast Sky radiation distribution (Moon and Spencer 1942). Diffuse radiations were approximated by a set of light sources on a sky vault discretized in 20 solid angle sectors using the spherical coordinates, including 5 zenith angles (18°, 36°, 54°, 72°, 90°) and 4 azimuths. Light interception was computed for each direction and then integrated over the sky vault by summing up the 20 directional values.

Estimation of light sharing within virtual wheat–pea mixtures Light sharing was computed for virtual wheat–pea mixtures at four digitization dates: 300, 600, 1240 and 1560 DD. Wheat (*T. aestivum*) mock-ups were obtained from a dynamic but non-plastic 3D architectural model of wheat development (Fournier *et al.* 2003). The data set was derived from an experiment of Bertheloot *et al.* (2009), where wheat plants (cultivar Caphorn) were grown in field conditions under low-nitrogen fertilization at a density of 250 plants m^{-2}. In the present study, wheat mock-ups were generated at the same stages of development as pea and then merged with pea reconstructions in the Openalea platform (Pradal *et al.* 2008). Inter-row spacing of virtual mixtures was 17 cm with a final density of 125 plants m^{-2} for wheat and 45 plants m^{-2}

for pea, i.e. 50 % of each crop optimal density used in local agricultural practices (Corre-Hellou *et al.* 2006). Species were mixed within each row.

Statistical analysis

Data analyses were performed by using exploratory data analysis and variance analysis. Pea cultivars were compared by using the Tukey's honestly significant difference (HSD) test. The significance threshold was fixed at the 0.05 probability level for all statistical tests. Statistical analyses were performed with SAS 9.2 (SAS Institute, Cary, NC, USA) and R (R Development Core Team 2011).

The variable phytomer appearance (defined by the number of phytomers visible, i.e. emergence of the stipules from the apex) was fitted with Schnute's non-linear model (Schnute 1981) using the least-square method. The model is written as

$$Y = \left[y_{\max}^{B} \times \frac{1 - e^{-A(t)}}{1 - e^{-A(t_{\max})}} \right]^{1/B} + \varepsilon_i \qquad (5)$$

where Y is the phytomer appearance variable; parameters A and B implicitly define the shape of the curve; $t_{\max}$ is the last value of the time (t) domain for which the model is fitted; and parameter $y_{\max}$ is the value of Y at $t_{\max}$. Parameters were optimized using the Levenberg–Marquardt iterative method with automatic computation of the analytical partial derivatives.

The first derivatives of Schnute adjustments were used in order to estimate the rates of phytomer appearance of the pea cultivars.

Results and discussion

Light sharing within wheat–pea mixtures

To dynamically analyse the effects of the architectural parameters of pea on light sharing in a mixture, we first assessed, for each contrasting genotype, the relationships between light interception and LAI, foliage inclination and plant height. These basic parameters contribute to plant architecture and thus to canopy structure (Sinoquet and Caldwell 1995). Details on wheat and pea mock-ups used for each simulation time are summarized in Table 2. Leaf area index of pea plants ranged from 0.06 m^2 m^{-2} for cultivar Lucy at 300 DD to 3.44 m^2 m^{-2} for 886/01 at 1560 DD. Foliage inclination of pea cultivars, ranging from 20.8° to 55°, was more planophile than that of wheat (64.5° on average throughout the growing cycle). At the first stage of development (300 DD), the height of wheat and pea was similar (11.3 cm for wheat and 13.2–17.5 cm for pea genotypes). In contrast, pea cultivars largely overtopped wheat plants from 600 DD. This was particularly the case for the cultivar China, which reached 127 cm at 1240 DD.

Effects of LAI and foliage inclination on light sharing

The relationships between species' relative contribution to light interception and LAI of virtual intercrops at four stages of development are shown in Fig. 3 (left column). Based on the observed foliage inclination, the ratio of the species extinction coefficient was computed in order to perform a theoretical estimation of light sharing for each simulation (dotted lines). These theoretical values of light sharing, based on the turbid medium approach, were thus estimated assuming that canopies were well-mixed. Contrasting

Table 2 **LAI, foliage inclination and plant height of wheat and pea mock-ups used to simulate light sharing in virtual mixtures.**

Species	Genotype	Growing degree-day (°C day)			
		300	600	1240	1560
Leaf area index (m^2 m^{-2})					
Pea	China	0.11	0.81	1.81	
Pea	US13	0.13	0.79	2.42	
Pea	Lucy	0.06	0.29	1.29	
Pea	James	0.08	0.34	1.12	
Pea	AOPH10	0.07	0.37	1.96	2.03
Pea	886/01	0.08	0.39	2.48	3.44
Wheat	Caphorn	0.13	0.83	1.00	0.46
Foliage inclination (°)					
Pea	China	20.8	30.2	40.9	
Pea	US13	32.3	32.9	46.6	
Pea	Lucy	44.5	43.3	48.7	
Pea	James	38.0	39.3	45.2	
Pea	AOPH10	37.8	38.7	49.7	49.8
Pea	886/01	41.7	38.6	51.1	55.0
Wheat	Caphorn	65.5	67.0	64.3	61.0
Plant height (cm)					
Pea	China	17.5	70.7	127.1	
Pea	US13	14.4	45.5	94.7	
Pea	Lucy	13.2	32.7	83.6	
Pea	James	13.8	36.1	81.3	
Pea	AOPH10	13.9	32.0	84.2	87.1
Pea	886/01	14.6	31.3	70.4	86.3
Wheat	Caphorn	11.3	16.0	65.2	69.1

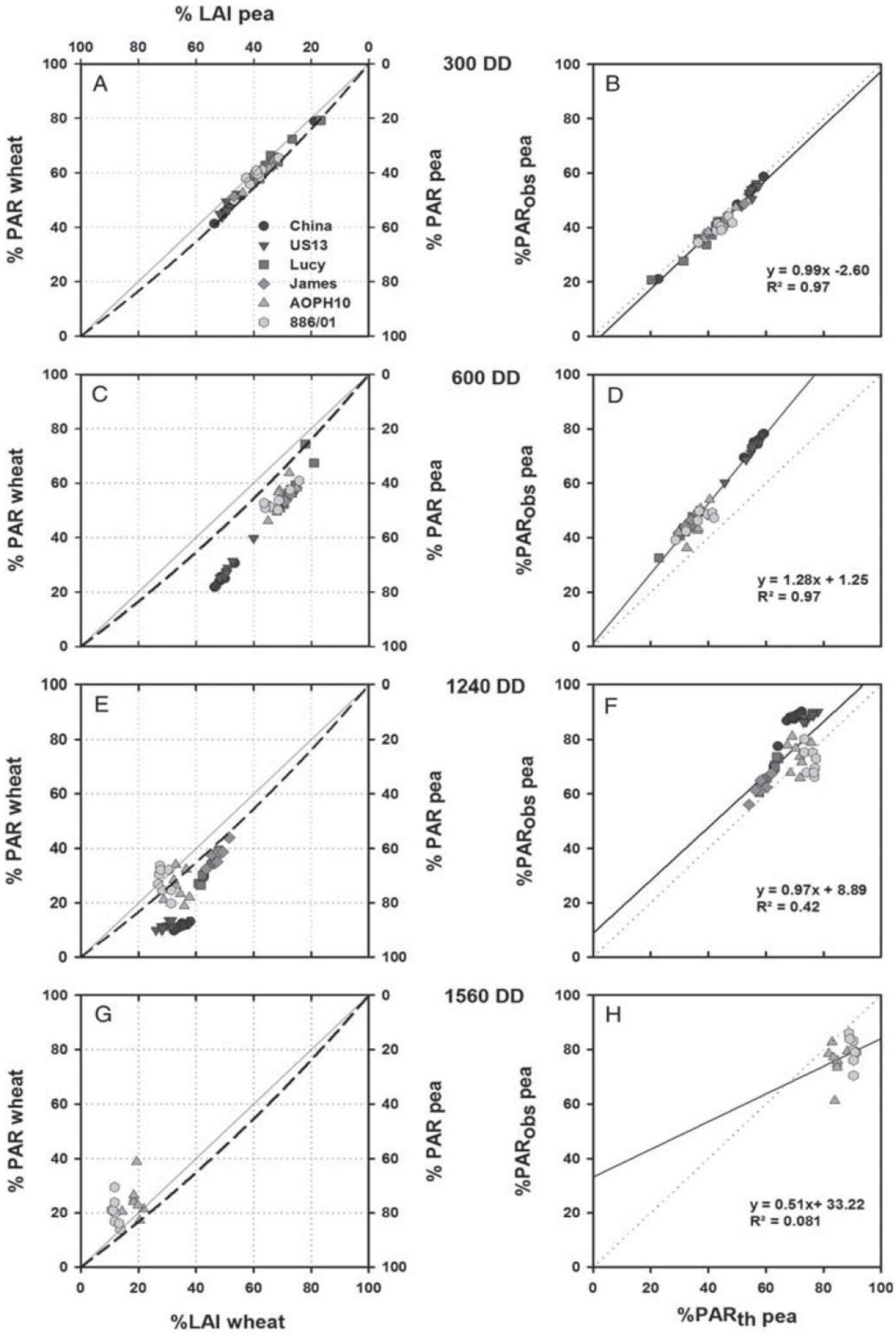

Fig. 3 Light sharing within virtual wheat–pea mixtures at 300, 600, 1240 and 1560 DD. Relative contributions of the species to the LAI of the mixture and to PAR interception are shown in (A), (C), (E) and (G). Theoretical isolines, based on the ratio of extinction coefficients of the species, are represented by dotted lines. Deviations between the estimated values of light interception of pea and the theoretical isoline are given in (B), (D), (F) and (H) where the equation and coefficient of determination R^2 of linear regressions are also shown. For each simulation date (300, 600, 1240 and 1887 DD), computations were performed on eight plants of each pea cultivar.

deviations were observed between computed and theoretical values of the species' relative contribution to light interception within the virtual mixtures (Fig. 3, right column). In the early stages of development (Fig. 3A and C), a wide range of relative LAI emerged from the variability in plant architecture between the studied genotypes. This variability in relative LAI resulted in an equivalent variability in LIE by each of the two species. At 300 DD (Fig. 3A), computed values of light sharing were close to the theoretical isoline estimated for well-mixed canopies (Fig. 3B, slope of the linear regression $= 0.99$, $R^2 = 0.97$). At this early stage of development (species LAI ranging from 0.06 to 0.13 $m^2\ m^{-2}$, Table 2), light sharing therefore appeared to be strongly dependent on the architectural parameters that contributed to the LAI and foliage inclination of each species. At 600 DD (Fig. 3C), pea genotypes appeared more efficient for light interception compared with the previous stage of development. This was particularly the case for the leafy cultivars China and US13, which exhibited similar amounts of LAI to wheat (0.81, 0.79 and 0.83 $m^2\ m^{-2}$, respectively, Table 2) and which captured 70–75 % of light intercepted by the mixture. Nevertheless, computations of light sharing strongly deviated from the theoretical isoline (Fig. 3D, slope of the linear regression $= 1.28$, $R^2 = 0.97$), meaning that light sharing was not only determined by the architectural parameters that contribute to the species LAI and foliage orientation.

After 1200 DD (Fig. 3E and F), LAI of the pea genotypes (1.12–3.44 $m^2\ m^{-2}$, Table 2) was higher than that of wheat (1.00–0.46 $m^2\ m^{-2}$, Table 2). Pea therefore captured >50 % of the radiation intercepted by the mixture. At 1240 DD (Fig. 3E), three groups of pea genotypes are distinguishable: (i) the cultivars Lucy and James, which were close to the theoretical isoline, (ii) 'AOPHA10' and '886/01' cultivars, vertically distributed around the isoline and (iii) the cultivars China and US13, exhibiting a strong efficiency for light capture. The two last groups, for which the contribution to total LAI exceeded 60 %, showed divergences between computed values of light sharing and the theoretical approach that assumes well-mixed canopies (Fig. 3F, slope of the linear regression $= 0.97$, $R^2 = 0.42$). Thus, at this late stage of development, the architectural parameters that determine the LAI and the foliage inclination of these cultivars do not only determine light sharing between the component species. Similar conclusions could be drawn for the simulations made at 1560 DD (Fig. 3G and H). Indeed, the two late semi-leafless cultivars, AOPH10 and 886/01, constituted 81 and 88 % of the whole LAI and intercepted 80 and 75 % of incident light, respectively. These two cultivars were less efficient at capturing light in regard to their relative contribution to the LAI of the mixture. This could be related to a combination of architectural parameters that lead to intra-specific foliage clumping (Nilson 1971) due to high values of LAI. Indeed at 1560 DD, cultivars AOPH10 and 886/01 exhibited an LAI of 2.03 and 3.44 $m^2\ m^{-2}$, respectively, whereas wheat LAI was 0.46 $m^2\ m^{-2}$.

The above results show that when canopy closure and species interactions begin, the level of light sharing was not only determined by the species LAI and foliage inclination as can be estimated for well-mixed canopies. Light sharing within such mixtures is therefore also related to architectural parameters that lead to heterogeneous canopies such as contrasted vertical profiles of leaf area or height between component species (Sinoquet and Caldwell 1995).

Effects of pea genotype height on light sharing

Deviations between computed values of light sharing and the theoretical approach, which assumes well-mixed canopies, were then studied in regard to the relative height of the component species (wheat/pea height, Fig. 4). As expected from the previous analysis, no clear relationship could be established between the species height ratio and the deviations of estimated values of light interception at 300 DD. On the other hand, these deviations appeared to be exponentially related to the species height for the simulations made at 600, 1240 and 1560 DD. Indeed, deviations between computed values of light interception and the theoretical approach were strongly related to the species relative height for wheat/pea ratios ranging from 1 to 2, whereas, for higher values, the effect of pea height on light sharing remained constant. These results are consistent with the study of Sinoquet and Caldwell (1995), who showed that the difference in light interception between two species in a mixture increased when the relative height deviates from the 1:1 line. The present results also demonstrate that this relationship is preserved for concomitant variations of plant LAI and height.

Characterization of the architectural parameters of pea genotypes

In the first step of this study, we assessed the impact of the pea genotypes on light sharing within virtual mixtures through basic descriptors, i.e. LAI, foliage inclination and plant height. The second step of this work then consisted in a characterization of the above-ground architecture of the pea genotypes in order to analyse the

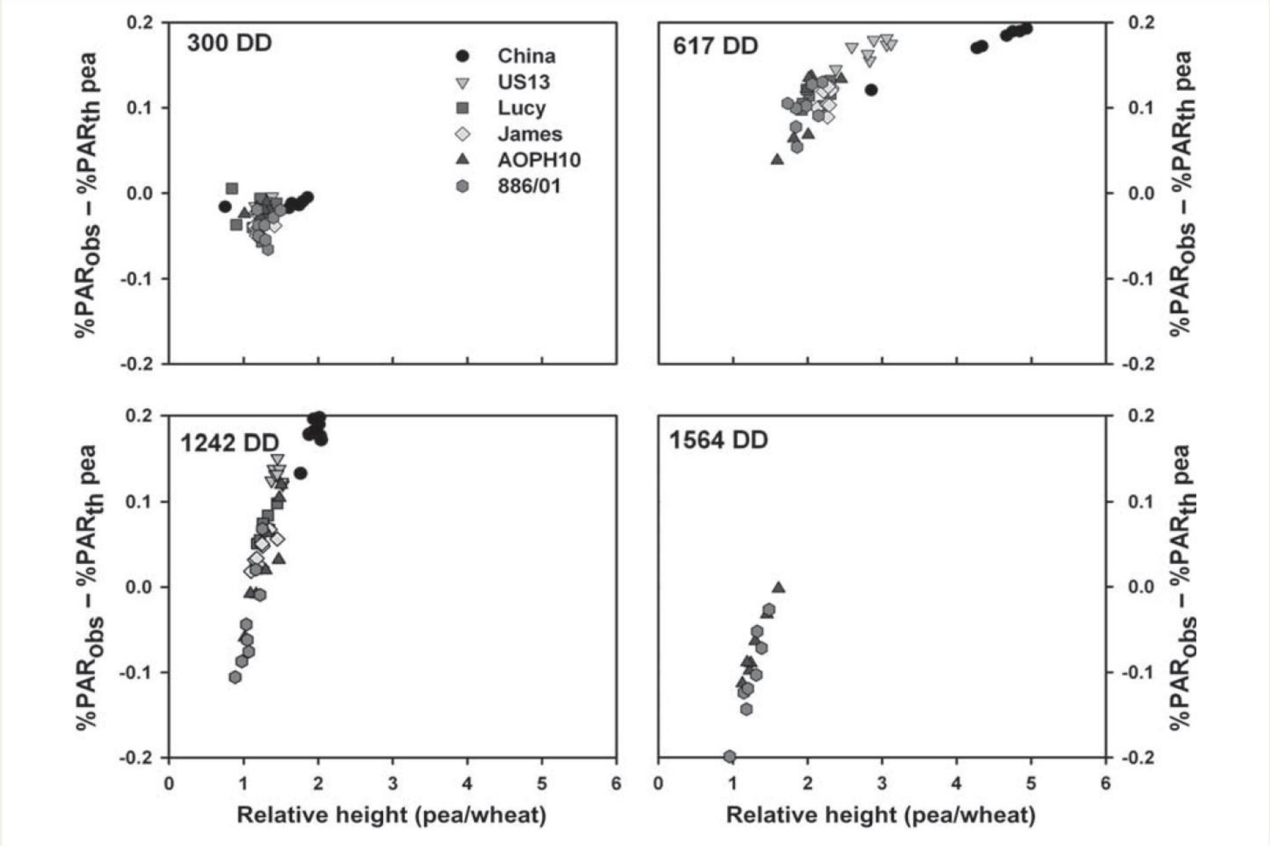

Fig. 4 **Relationship between the species height ratio and the deviations between computed and theoretical (based on the ratio of extinction coefficients of the species) values of light interception.**

contribution of the architectural parameters to light interception.

Branching The number of branches and the number of phytomers per branch produced by the pea cultivars are given in Table 3. In a few cases, cultivars China, US13 and Lucy developed one branch with 2.8–8.0 phytomers at their maximal development. Most of the plants belonging to cultivars 'James' and 'AOPH10' produced one branch early in their growing cycle (between 300 and 600 DD). However, branches developed by cultivar James did not develop beyond 6.0 (±2.16) phytomers, contrasting with cultivar AOPH10 (25.7 ± 1.5). Cultivar 886/01 was the most branching cultivar with one to three branches developed since 600 DD and composed of 12.4–23.5 phytomers. Branches were initiated from the basal part of the main stem (i.e. on the primordia of vestigial leaves) except for 'China' whose branches were mainly initiated between the 12th and 14th phytomer. Our results show that the pea genotypes exhibited different branching capacities, although lateral branches were less developed compared with field-grown spring (Jeudy and Munier-Jolain 2005; Spies *et al.* 2010) and winter cultivars (unpublished personal results). It has been well documented that branching is strongly determined by the environment. Winter cultivars generally produce a large number of lateral branches due to frost damage to the apex of the main stem that occurs during the growing cycle (Jeudy and Munier-Jolain 2005). In our study, the greenhouse growing conditions prevented frost damage to the apex so that its dominance on axillary buds was maintained (Cline 1991). Spies *et al.* (2010) also showed that basal branching in spring pea cultivars was dependent on the sowing density. Indeed, independently of the trophic aspects of light competition, plant density also modifies the quality of light within the canopy (Varlet-Grancher *et al.* 1993; Escobar-Gutiérrez *et al.* 2009) and in particular the

Table 3 Number of branches and number of phytomers per branch of pea cultivars at each simulation date. B1, B2 and B3 point out the chronological emission of branches. Mean values are given ± SD ($n = 8$ for each cultivar).

Growing degree-day	Pea cultivar	Range of the number of branches	Mean number of phytomers per branch		
			B1	B2	B3
300	China	0			
	US13	0			
	Lucy	0			
	James	[0–1]	3.0 ± 0 ($n = 5$)		
	AOPH10	[0–1]	3.0 ± 0 ($n = 4$)		
	886/01	0			
600	China	[0–1]	2.5 ± 0.5 ($n = 2$)		
	US13	0			
	Lucy	0			
	James	[0–1]	5.7 ± 2.0 ($n = 6$)		
	AOPH10	[0–2]	9.5 ± 0.5 ($n = 6$)	5.0 ± 0 ($n = 1$)	
	886/01	[0–2]	7.4 ± 1.9 ($n = 5$)	3.7 ± 0.7 ($n = 5$)	
1240	China	[0–1]	2.8 ± 0.4 ($n = 4$)		
	US13	[0–1]	8.0 ± 0 ($n = 1$)		
	Lucy	[0–1]	3.0 ± 0 ($n = 1$)		
	James	[0–1]	6.0 ± 2.16 ($n = 3$)		
	AOPH10	[0–2]	22.8 ± 1.3 ($n = 6$)	6.0 ± 0 ($n = 1$)	
	886/01	[1–3]	18.6 ± 4.1 ($n = 8$)	14.2 ± 2.0 ($n = 6$)	10.0 ± 2.3 ($n = 4$)
1560	AOPH10	[0–1]	25.7 ± 1.5 ($n = 6$)		
	886/01	[1–3]	23.5 ± 3.8 ($n = 8$)	16.9 ± 6.4 ($n = 7$)	12.4 ± 5.1 ($n = 5$)

red/far red ratio, which has been reported to control branching (Ballaré and Casal 2000). The branching ability of pea cultivars is therefore a plastic architectural parameter that strongly impacts light interception as the development of a new vegetative axis modifies the amount of foliar area as well as its spatial distribution.

Phytomer appearance Dynamics of phytomer appearance were measured on main stems, assuming that phyllochrons of branches were similar (Jeudy and Munier-Jolain 2005). Phytomer appearance on the main stems followed a contrasting range of sigmoid-type dynamics (Fig. 5) among the evaluated cultivars. These dynamics were fitted with the Schnute function (Table 4). The cultivar China reached its maximum number of phytomers (21, see Table 4) at 1080 DD, while cultivars 'US13', 'Lucy' and 'James' reached 25 phytomers at 1240 DD. Owing to a long period of phytomer production, cultivars 'AOPH10' and '886/01' reached 32 and 37 phytomers at 1445 and 1890 DD, respectively. Maximum rates of phytomer appearance were reached in the earlier stages of development (between 350 and 530 DD) and ranged from 0.025 to 0.029 phytomer DD^{-1} (Table 4). 'China' and 'James' were the earliest cultivars and reached their maximum rate of phytomer appearance at 350 and 360 DD, respectively. On the other hand, '886/01' was the latest cultivar and exhibited its highest rate of phytomer production at 530 DD. The kinetics of phytomer appearance are usually estimated by a mean value over the growing cycle (e.g. Turc and Lecoeur 1997; Bourion *et al.* 2002). However, our results show that pea phytomers are not produced at a constant rate. In this case, Schnute's non-linear regressions appeared to be well suited to estimate the rates of phytomer appearance. Rates of phytomer initiation (plastochron) and appearance (phyllochron) (Lyndon 1998) characterize the development of the vegetative axes (main stems and branches). Phytomer appearance is therefore a key parameter of plant architecture that determines (i) the dynamics of foliar development and (ii) the height reached by the vegetative axis (stack of phytomers), thus affecting the ability of a plant to capture light.

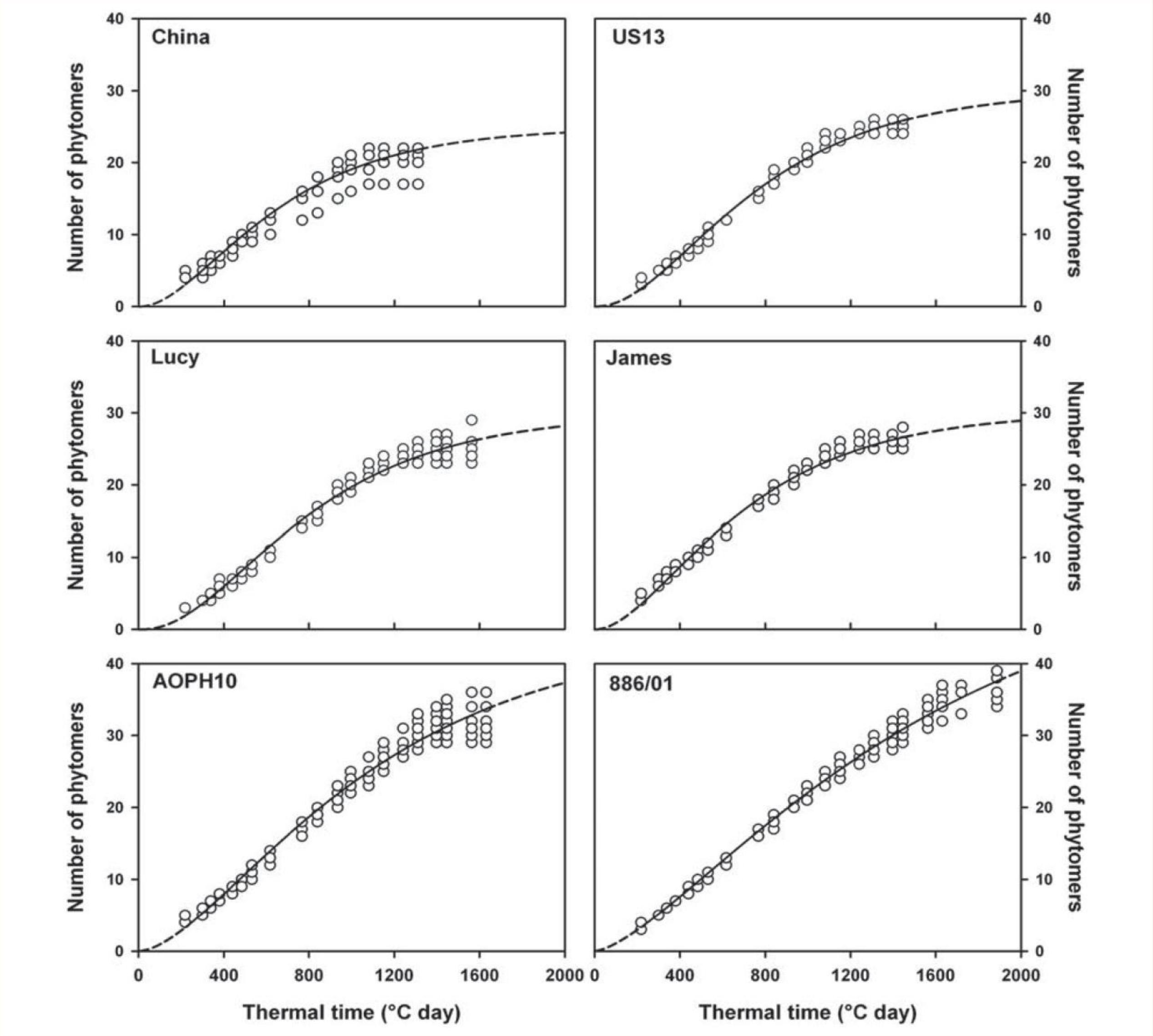

Fig. 5 **Phytomer appearance for the pea cultivars during the growing cycle.** Values are indicated for main stems only. The fitting of Schnute's functions is shown by a solid line or by a dotted line when extrapolated ($n = 8$ for each cultivar).

Organ final length and vertical distribution The contribution of stipules, leaflets and stems to the maximum green area reached by plants was also estimated for each cultivar (Table 1). Leaves (stipules and leaflets) accounted for >90 % of the green area whatever the cultivar. For leafy cultivars, this area was similarly composed of stipules and leaflets. The contribution of stems to the green area appeared to be constant whatever the genotype (8–11 %), except for the leafy cultivar US13 whose stems constitute 5 % of the cultivar green area.

The vertical distribution of the main vegetative organs is shown in Fig. 6. The vertical distribution of stipule final length did not appear to be dependent on the cultivar (Fig. 6A) but was reported to be rather sensitive to environmental factors such as water stress deficits (Lecoeur *et al.* 1995). The final length reached by stipules appeared to be dependent on their position along the stem as the distribution of stipule length followed triangular profiles as described by Lecoeur (2005). The longest stipules (50 mm) were located between the normalized phytomer numbers 0.6 and 0.8. For leafy

Table 4 Parameters ($A \times 10^{-3}$, B and y_{max}) of Schnute adjustments made on cultivars' kinetics of phytomer emission. Indicated values are the mean ± SD of eight individual adjustments made for each cultivar. Goodness of fit is also given by RMSE values. Cultivars with the same letter are not significantly different (Tukey's HSD test, $\alpha = 0.05$). First derivative of the adjustments provided the maximum rate of phytomer emission.

Parameter	Cultivar					
	China	**US13**	**Lucy**	**James**	**AOPH10**	**886/01**
Kinetics of phytomer emission (Schnute adjustments)						
A ($\times 10^{-3}$)	2.14 ± 0.34^{a}	1.89 ± 0.28^{a}	1.89 ± 0.34^{a}	1.94 ± 0.26^{a}	1.18 ± 0.22^{b}	0.80 ± 0.22^{b}
B	0.47 ± 0.08^{dc}	0.44 ± 0.05^{dc}	0.39 ± 0.05^{d}	0.49 ± 0.05^{bc}	0.57 ± 0.05^{ab}	0.65 ± 0.08^{a}
y_{max}	20.6 ± 1.6^{d}	24.6 ± 0.5^{c}	24.8 ± 1.1^{c}	25.6 ± 0.7^{c}	32.9 ± 2.1^{b}	37.6 ± 1.6^{a}
RMSE	0.69	0.72	0.75	0.70	0.81	0.47
Maximal rate of phytomer emission						
Time (DD)	350	440	490	360	480	530
V_{max} (phytomer °C day^{-1})	0.026	0.027	0.026	0.029	0.028	0.025

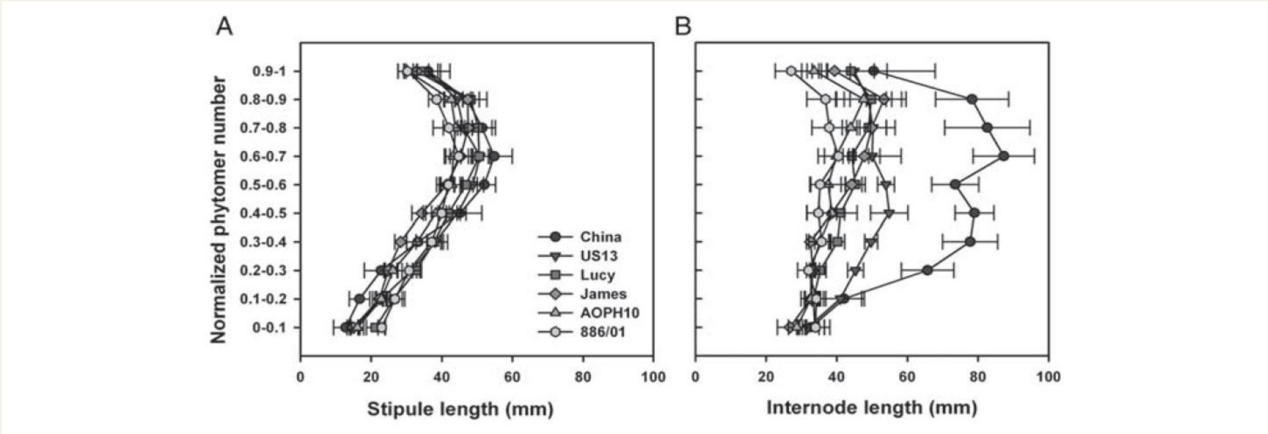

Fig. 6 Vertical distribution of stipule (A) and internode (B) length. Indicated values are the final lengths reached by organs as a function of the normalized phytomer number of the main stem ($n = 8$ for each pea cultivar).

cultivars China and US13, the vertical distribution of leaflet length was also dependent on their position on the stem (data not shown). Maximum values of leaflet length (45 mm) were found at the middle of the main stem. The spatial distribution and dimensions of the vegetative organs significantly affect the efficiency of light interception (Niinemets *et al.* 2004*a*, *b*; Pearcy *et al.* 2005). For pea plants, the size and localization of stipules and leaflets would indeed determine the amount of foliar area exposed to solar radiation.

Among the tested cultivars, the vertical distribution of internode length was nearly uniform (Fig. 6B), although maximum values tend to be reached on the upper part of the stem (between normalized phytomer numbers 0.5 and 0.8). Within this interval, the leafy cultivars displayed longer internodes than semi-leafless cultivars; this was particularly the case for 'China' whose internodes exceeded 75 mm in length. The cultivars AOPH10 and 886/01 developed the shortest internodes on average (37.0 and 35.0 mm, respectively). 'Lucy' and 'James' were intermediate cultivars with mean internode length reaching 41.5 and 40.0 mm, respectively. Internode lengths and their spatial distribution are also key parameters of pea architecture determining plant

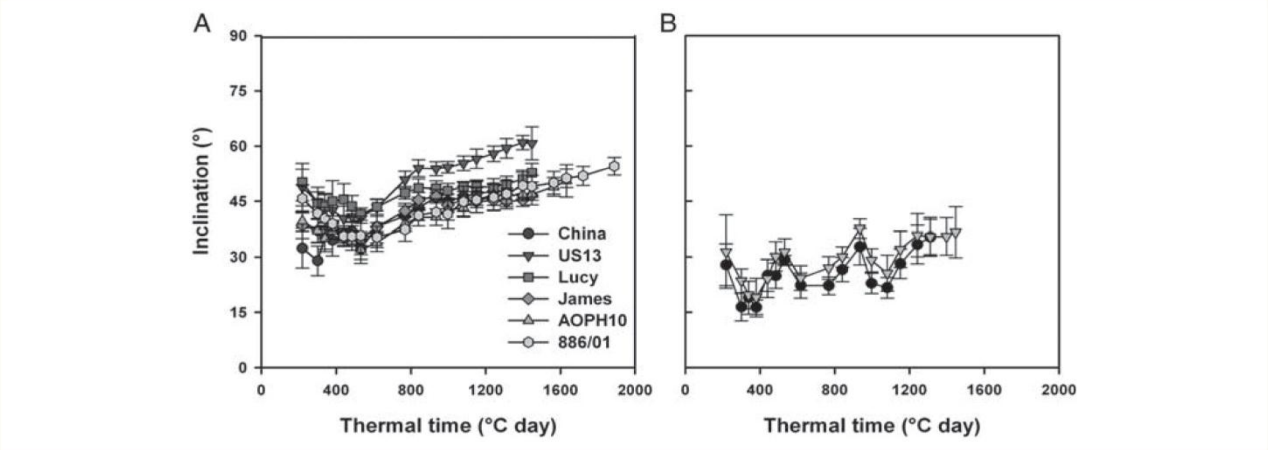

Fig. 7 Dynamics of stipule (A) and leaflet (B) inclination during the growing cycle. Values are indicated for main stems only ($n = 8$ for each pea cultivar).

height and leaf area density, and consequently the ability to capture light.

Stipule and leaflet inclination Inclination of stipules located on main stems ranged from 30 to 60° among cultivars but was not constant over time as all cultivars showed a slight increase in stipule inclination from 600 DD (Fig. 7A). At the end of the growing cycle, the inclination of stipules ranged from 45° to 55°, except for 'US13' which showed more erect stipules reaching 60°. Leaflets of the two leafy cultivars China and US13 were more planophile than stipules as their inclination ranged from 16° to 37° (Fig. 7B). These results on foliage inclination were consistent with previous studies conducted on legume species (Ross 1981*a*; Barillot *et al.* 2011). As mentioned before, leaf inclination has been described as an architectural parameter that contributes to the efficiency of plants in intercepting light (Sinoquet and Andrieu 1993).

Relationships between pea architecture and light sharing

Our results allowed us to distinguish three groups of development among the tested cultivars. The first group is composed of the leafy cultivars (China and US13) which exhibited a rapid vertical and leaf area growth. The second group is constituted by the late cultivars (AOPH10 and 886/10, late hr and HR-type, respectively) which also developed a large leaf area. The third group is composed of cultivars with low developmental rates, 'Lucy' and 'James', which displayed the smallest leaf area and height.

These contrasting pea architectures were then virtually mixed with wheat mock-ups obtained from data where wheat was grown under low nitrogen supply (Bertheloot *et al.* 2009). The level of available nitrogen is obviously a major factor impacting the species growth. However, increasing the nitrogen availability in a cereal–legume mixture enhances the dominance of the cereal species over the legume (e.g. Corre-Hellou *et al.* 2006; Naudin *et al.* 2010). Cereal–legume mixtures are therefore usually grown under low-nitrogen conditions that are close to the data from which the mock-ups were derived. Within open canopies, our results showed that light sharing was mainly related to the architectural parameters that composed the LAI and leaf inclination. Thus, the earliness and the development of leaflets exhibited by the leafy cultivars as well as a large number of phytomers and branches (late semi-leafless cultivars) led to strong competitive abilities for light capture. When canopy closure and competition between component species started, light sharing within the virtual mixtures also appeared to be strongly dependent on the species height ratio. The vertical dominance of pea was due to (i) the rapid development of long internodes for leafy cultivars and (ii) the stack of numerous phytomers on stems for late semi-leafless cultivars. In addition, the dominance of pea genotypes was reinforced by the planophile property of their leaves compared with wheat. However, as very few differences were observed between leaf inclinations of cultivars, this architectural parameter does not appear to be a major factor explaining the contrasting levels of light sharing observed in the different wheat–pea mixtures.

Conclusions and forward look

In the present study, the virtual plant approach was used as a means to provide a suitable framework for the assessment of the effects of the architectural parameters of pea on light sharing within wheat–pea mixture. Nevertheless, the present approach did not account for plant plasticity, i.e. above and below-ground feedbacks between the mixed species were not taken into account. Moreover, wheat and pea mock-ups were derived from data obtained in mono-specific conditions and pea plants were staked, although this can be representative of the field conditions as wheat plants generally support pea stems. However, these mock-ups were not aimed to be representative of the development of species grown in a field mixture. These virtual plant models were intended to generate a large range of physical structures reflecting contrasting canopies which can be found in multi-specific stands. Therefore, pea plants that exhibited contrasting architectures (stemming from the different cultivars and stages of development) were virtually mixed with a given wheat architecture in order to compare their efficiency for light interception in relation to their architectural features. The present study highlights levers of pea architecture that are determinant parameters driving light sharing. These parameters were mainly involved in the composition of the species LAI and height. Competitive pea ideotypes for light capture therefore exhibited (i) a large foliar area, through the presence of leaflets and/or the development of a larger number of branches and phytomers, and/or (ii) a vertical dominance due to the stack of numerous phytomers and the development of long internodes. To drive the interspecific competition, the developmental dynamics of these architectural parameters must also be taken into account in regard to the other components of the mixture. In addition, we identified contrasting architectural parameters among the tested genotypes, associated to variability in their earliness/lateness that would, in field conditions, lead to different levels of competition for light in the mixture. Further studies should be conducted on supplementary genotypes and growing conditions in order to reveal additional categories of architectural development and assess their effects on light sharing. At the present state-of-the-art, it is still complex to assess the optimal level of light sharing within intercropping systems. However, the present results could help to identify/design suitable cultivars/ideotypes for intercropping systems towards light sharing, in particular because of the genetic progress which has already identified several genes driving pea architecture.

Sources of funding

This research is supported by 'La Région Pays de la Loire', France through a Ph.D. fellowship to R.B. The research of D.C. and A.E.-G. is partially funded by 'La Région Poitou-Charentes', France.

Contributions by the authors

All the authors contributed to a similar extent overall.

Acknowledgements

We thank Sylvain Pineau and Pierre Huynh for their great technical assistance and Gaëtan Louarn for his comments on the manuscript. We also thank INRA-Agri-obtentions – URD78 (Orsonville, France) which provided 'US13', '886/01' and 'AOPH10' pea cultivars and INRA UMRLEG (Dijon, France) for 'China' cultivar.

Conflicts of interest statement

None declared.

Literature cited

Baccar R, **Fournier C**, **Dornbusch T**, **Andrieu B**, **Gouache D**, **Robert C**. **2011**. Modelling the effect of wheat canopy architecture as affected by sowing density on *Septoria tritici* epidemics using a coupled epidemic-virtual plant model. *Annals of Botany* **108**: 1179–1194.

Ballaré CL, **Casal JJ**. **2000**. Light signals perceived by crop and weed plants. *Field Crops Research* **67**: 149–160.

Barillot R, **Louarn G**, **Escobar-Gutiérrez AJ**, **Huynh P**, **Combes D**. **2011**. How good is the turbid medium-based approach for accounting for light partitioning in contrasted grass-legume intercropping systems? *Annals of Botany* **108**: 1013–1024.

Bertheloot J, **Andrieu B**, **Fournier C**, **Martre P**. **2009**. Modelling nitrogen distribution in virtual plants, as exemplified by wheat culm during grain filling. *Proceedings of the 2009 Plant Growth Modeling, Simulation, Visualization, and Applications*. Beijing, China: IEEE Computer Society.

Bourion V, **Fouilloux G**, **Le Signor C**, **Lejeune-Hénaut I**. **2002**. Genetic studies of selection criteria for productive and stable peas. *Euphytica* **127**: 261–273.

Chelle M, **Andrieu B**. **1998**. The nested radiosity model for the distribution of light within plant canopies. *Ecological Modelling* **111**: 75–91.

Cici SZ-H, **Adkins S**, **Hanan J**. **2008**. A canopy architectural model to study the competitive ability of chickpea with sowthistle. *Annals of Botany* **101**: 1311–1318.

Cline M. **1991**. Apical dominance. *The Botanical Review* **57**: 318–358.

Corre-Hellou G, **Fustec J**, **Crozat Y**. **2006**. Interspecific competition for soil N and its interaction with N_2 fixation, leaf expansion and crop growth in pea–barley intercrops. *Plant and Soil* **282**: 195–208.

Dornbusch T, **Baccar R**, **Watt J**, **Hillier J**, **Bertheloot J**, **Fournier C**, **Andrieu B**. **2011**. Plasticity of winter wheat modulated by sowing date, plant population density and nitrogen fertilisation: dimensions and size of leaf blades, sheaths and internodes in relation to their position on a stem. *Field Crops Research* **121**: 116–124.

Escobar-Gutiérrez AJ, **Combes D**, **Rakocevic M**, **de Berranger C**, **Eprinchard-Ciesla A**, **Sinoquet H**, **Varlet-Grancher C**. **2009**. Functional relationships to estimate morphogenetically active radiation (MAR) from PAR and solar broadband irradiance measurements: the case of a sorghum crop. *Agricultural and Forest Meteorology* **149**: 1244–1253.

Evers JB, **Vos J**, **Fournier C**, **Andrieu B**, **Chelle M**, **Struik PC**. **2007**. An architectural model of spring wheat: evaluation of the effects of population density and shading on model parameterization and performance. *Ecological Modelling* **200**: 308–320.

Fournier C, **Andrieu B**, **Ljutovac S**, **Saint-Jean S**. **2003**. ADEL-wheat: a 3D architectural model of wheat development. *Proceedings of the 2003 Plant Growth Modeling, Simulation, Visualization, and Applications*. Beijing, China: IEEE Computer Society, 54–63.

Godin C. **2000**. Representing and encoding plant architecture: a review. *Annals of Forest Science* **57**: 413–438.

Goudriaan J. **1982**. Potential production processes. In: Vries FWTP, Laar HH, eds. *Simulation of plant growth and crop production*. Wageningen: Centre for Agricultural Pub. and Documentation, 98–113.

Huyghe C. **1998**. Genetics and genetic modifications of plant architecture in grain legumes: a review. *Agronomie* **18**: 383–411.

Jensen ES. **1996**. Grain yield, symbiotic N_2 fixation and interspecific competition for inorganic N in pea-barley intercrops. *Plant and Soil* **182**: 25–38.

Jeudy C, **Munier-Jolain N**. **2005**. Developpement des ramifications. In: Munier-Jolain N, Biarnes V, Chaillet I, Lecoeur J, Jeuffroy M-H, eds. *Agrophysiologie du pois protéagineux*. Paris: Inra-Quae, 51–58.

Lecoeur J. **2005**. Developpement vegetatif. In: Munier-Jolain N, Biarnes V, Chaillet I, Lecoeur J, Jeuffroy M-H, eds. *Agrophysiologie du pois protéagineux*. Paris: Inra-Quae, 27–45.

Lecoeur J, **Wery J**, **Turc O**, **Tardieu F**. **1995**. Expansion of pea leaves subjected to short water deficit: cell number and cell size are sensitive to stress at different periods of leaf development. *Journal of Experimental Botany* **46**: 1093–1101.

Loomis RS, **Williams WA**. **1963**. Maximum crop productivity: an estimate. *Crop Science* **3**: 67–72.

Lyndon RF. **1998**. Partitioning the apex: the size of the apical meristem and the primordia. In: Lyndon RF, ed. *The shoot apical meristem: its growth and development*. Cambridge: Cambridge University Press, 171–193.

Malézieux E, **Crozat Y**, **Dupraz C**, **Laurans M**, **Makowski D**, **Ozier-Lafontaine H**, **Rapidel B**, **de Tourdonnet S**, **Valantin-Morison M**. **2009**. Mixing plant species in cropping systems: concepts, tools and models. A review. *Agronomy for Sustainable Development* **29**: 43–62.

Monsi M, **Saeki T**. **1953**. Über den Lichtfaktor in den Pflanzengesellschaften und seine Bedeutung für die Stoffproduktion. *Japanese Journal of Botany* **14**: 22–52.

Moon P, **Spencer DE**. **1942**. Illumination from a non-uniform sky. *Illuminating Engineering Society* **37**: 707–726.

Moulia B, **Edelin C**, **Jeuffroy MH**, **Allirand JM**, **Loup C**, **Chartier M**. **1998**. Premiers éléments d'analyse du développement architectural des herbacées cultivées. In: Maillard P, Bonhomme R, eds. *Fonctionnement des peuplements végétaux sous contraintes environnementales*. Paris, France: INRA Editions, 149–184.

Naudin C, **Corre-Hellou G**, **Pineau S**, **Crozat Y**, **Jeuffroy M-H**. **2010**. The effect of various dynamics of N availability on winter pea-wheat intercrops: Crop growth, N partitioning and symbiotic N_2 fixation. *Field Crops Research* **119**: 2–11.

Niinemets U, **Al Afas N**, **Cescatti A**, **Pellis A**, **Ceulemans R**. **2004*a***. Petiole length and biomass investment in support modify light-interception efficiency in dense poplar plantations. *Tree Physiology* **24**: 141–154.

Niinemets U, **Cescatti A**, **Christian R**. **2004*b***. Constraints on light interception efficiency due to shoot architecture in broad-leaved *Nothofagus* species. *Tree Physiology* **24**: 617–630.

Nilson T. **1971**. A theoretical analysis of the frequency of gaps in plant stands. *Agricultural Meteorology* **8**: 25–38.

Ofori F, **Stern WR**. **1987**. Cereal-legume intercropping systems. *Advances in Agronomy* **41**: 41–90.

Pearcy RW, **Muraoka H**, **Valladares F**. **2005**. Crown architecture in sun and shade environments: assessing function and trade-offs with a three-dimensional simulation model. *New Phytologist* **166**: 791–800.

Pradal C, **Dufour-Kowalski S**, **Boudon F**, **Fournier C**, **Godin C**. **2008**. OpenAlea: a visual programming and component-based software platform for plant modelling. *Functional Plant Biology* **35**: 751–760.

R Development Core Team. **2010**. R: A language and environment for statistical computing. R Foundation for Statistical Computing, Vienna, Austria. ISBN 3-900051-07-0; **http://www.R-project.org**.

Rimmington GM. **1985**. A test of a model for light interception by mixtures. *Australian Journal of Plant Physiology* **12**: 681–683.

Ross J. **1981*a***. Foliage area orientation in stands. In: Ross J, ed. *The radiation regime and architecture of plant stands*. The Hague, The Netherlands: W. Junk, 66–89.

Ross J. **1981*b***. Role of phytometric investigations in the studies of plant stand architecture and radiation regime. In: Ross J, ed. *The radiation regime and architecture of plant stands*. The Hague, The Netherlands: W. Junk, 9–11.

Sarlikioti V, **de Visser PHB**, **Buck-Sorlin GH**, **Marcelis LFM**. **2011**. How plant architecture affects light absorption and photosynthesis in tomato: towards an ideotype for plant architecture using a functional-structural plant model. *Annals of Botany* **108**: 1065–1073.

Schnute J. **1981**. A versatile growth model with statistically stable parameters. *Canadian Journal of Fisheries and Aquatic Sciences* **38**: 1128–1140.

Sinoquet H. **1993**. Modelling radiative transfer in heterogeneous canopies and intercropping systems. In: Varlet-Grancher C, Bonhomme R, Sinoquet H, eds. *Crop structure and light microclimate*. Paris: INRA Editions, 229–252.

Sinoquet H, **Andrieu B**. **1993**. The geometrical structure of plant canopy: characterization and direct measurement methods. In: Varlet-Grancher C, Bonhomme R, Sinoquet H, eds. *Crop structure and light microclimate*. Paris: INRA Editions, 131–158.

Sinoquet H, **Bonhomme R**. **1991**. A theoretical analysis of radiation interception in a two-species plant canopy. *Mathematical Biosciences* **105**: 23–45.

Sinoquet H, **Caldwell MM**. **1995**. Estimation of light capture and partitioning in intercropping systems. In: Sinoquet H, Cruz P, eds. *Ecophysiology of tropical intercropping*. Paris: INRA Editions, 79–97.

Sinoquet H, **Rakocevic M**, **Varlet-Grancher C**. **2000**. Comparison of models for daily light partitioning in multispecies canopies. *Agricultural and Forest Meteorology* **101**: 251–263.

Spies JM, **Warkentin T**, **Shirtliffe S**. **2010**. Basal branching in field pea cultivars and yield-density relationships. *Canadian Journal of Plant Science* **90**: 679–690.

Turc O, **Lecoeur J**. **1997**. Leaf primordium initiation and expanded leaf production are co-ordinated through similar response to air temperature in pea (*Pisum sativum* L.). *Annals of Botany* **80**: 265–273.

Varlet-Grancher C, **Moulia B**, **Sinoquet H**, **Russell G**. **1993**. Spectral modification of light within plant canopies – how to quantify its effects on the architecture of the plant stand. In: Varlet-Grancher C, Moulia B, Sinoquet H, eds. *Crop structure and light microclimate. Characterization and applications*. Versailles: INRA, 427–452.

Zheng B, **Shi L**, **Ma Y**, **Deng Q**, **Li B**, **Guo Y**. **2008**. Comparison of architecture among different cultivars of hybrid rice using a spatial light model based on 3-D digitising. *Functional Plant Biology* **35**: 900–910.

Synthèse

Ce second chapitre a permis i) de **caractériser la morphogénèse** et l'architecture aérienne du pois afin de, ii) développer un modèle de plante virtuelle statique permettant de **reconstruire numériquement** l'architecture du pois, iii) d'évaluer l'effet de la **variabilité de l'architecture** du pois issue de différents génotypes sur le partage de la lumière, et iv) **d'identifier des paramètres architecturaux** déterminant dans le partage du rayonnement au sein d'association blé - pois**.** Ce travail, réalisé sous certaines hypothèses (pois cultivés en plantes isolées sous serre, caractérisation de l'architecture par digitalisation à intervalles de temps déterminés, variabilité des maquettes de blé limitée…), met ainsi en évidence la nécessité de mettre en place un **simulateur** afin de modéliser **la dynamique de la morphogénèse aérienne du pois et du blé**. Pour ce dernier, un modèle architecturé est d'ores et déjà disponible dans la littérature (Fournier *et al.*, 2003). Un tel simulateur permettrait en effet de répondre aux objectifs fixés pour la thèse *i.e.* appréhender le déterminisme architectural du partage de la lumière dans les associations blé - pois.

Pour cela il est au préalable nécessaire de construire un modèle architecturé de la morphogénèse aérienne du pois. Le chapitre suivant est donc dédié à caractériser la morphogénèse aérienne de génotypes de pois cultivés en cultures pures ou en association avec du blé.

Chapitre III

Comparison of the morphogenesis of three genotypes of pea (*Pisum sativum)* grown in pure stands and wheat-based intercropping systems.

Romain BARILLOT, Didier COMBES, Sylvain PINEAU, Pierre HUYNH and Abraham J. ESCOBAR-GUTIÉRREZ

En révision dans le journal Agronomy for Sustainable Development

Title page

Type of article: research article

Title: **Comparison of the morphogenesis of three genotypes of pea (*Pisum sativum)* grown in pure stands and wheat-based intercropping systems.**

Author names and affiliations: Romain BARILLOT[1*], Didier COMBES[2], Sylvain PINEAU[1], Pierre HUYNH[1] and Abraham J. ESCOBAR-GUTIÉRREZ[2].

Adresses: [1]LUNAM Université, Groupe Ecole Supérieure d'Agriculture, UPSP Laboratoire d'Ecophysiologie Végétale & Agroécologie, 55 rue Rabelais, BP 30748, F-49007 Angers cedex 01, France.
[2]INRA, UR4 P3F, Equipe Ecophysiologie des plantes fourragères, Le Chêne - RD 150, BP 6, F-86600 Lusignan, France.

*** Corresponding author:** Romain BARILLOT
LUNAM Université, Groupe Ecole Supérieure d'Agriculture, UPSP Laboratoire d'Ecophysiologie Végétale & Agroécologie, 55 rue Rabelais, BP 30748, F-49007 Angers cedex 01, France.
Tel.: +33 24123 5555
r.barillot@groupe-esa.com

Keywords: morphogenesis, *Pisum sativum*, plant architecture, plasticity, *Triticum aestivum*, wheat-pea intercropping

ABSTRACT

Nowadays, there is an increasing interest in growing cereal-legume intercrops. The complex interactions that occurred within the canopy of a mixture are affected by the functional and structural characteristics of the component species. The morphogenetic rules that build up the species architecture are therefore of major interest as they determine the intensity of the inter-specific competition for resources. However, species morphogenesis has been mainly described in mono-specific growing conditions although plastic responses could occur when grown in multi-specific stands. The aim of the present study was therefore to characterize the variability of the morphogenesis of three contrasting pea cultivars grown either in pure stands or mixed with wheat. This was achieved through a field experiment where the development of the stands as well as the morphogenesis of the pea cultivars was measured both for sole crops and mixtures. The present results show that most of the assessed parameters of pea morphogenesis (phenology, branching, final number of vegetative organs and their kinetics of appearance) were mainly dependent on the considered genotype thus highlighting the importance of the choice of cultivars in intercropping systems. However, the plasticity of pea morphogenesis was low between sole and mixed stands except for plant height and branching of the late cultivar. The information provided in the present study at both stand and plant scale can therefore be used for the building and parameterization of structural-functional models that would allow to improve our understanding of the functioning of cereal–legume intercrops.

1 Introduction

In Europe, there is a strong need for growing legume species in order to reduce dependency on imported vegetable proteins (Duc *et al.*, 2010). Moreover, thanks to their ability to fix the atmospheric N_2, legume species can improve the sustainability of cropping systems by decreasing the use of nitrogen fertilizers and through a diversification of crop successions (Crews et Peoples, 2004, Duc *et al.*, 2010). Currently, pea (*Pisum sativum* L.) is the principle source of vegetable proteins in Europe although the potential productivity has not been reached , mainly due to a strong sensitivity to foliar diseases and lodging (Ney et Carrouée, 2005). The increasing interest in growing cereal - legume intercrops, such as wheat – pea mixtures, represents an alternative way to reintroduce pea crop in agrosystems. These mixtures are assumed to provide high and stable yields (Ofori et Stern, 1987, Jensen, 1996b, Corre-Hellou *et al.*, 2006). Such advantages result from a trade-off between complementary (*e.g.* separate root and canopy areas) and competition processes (for light, water, nitrogen and other nutrients) that occur between the component crops. These complex interactions depend on the pedo-climatic context, agricultural practices and also on the functional and structural characteristics of the component species (Corre-Hellou *et al.*, 2006, Launay *et al.*, 2009, Louarn *et al.*, 2010, Naudin *et al.*, 2010).

The latter point can be driven through the choice of cultivars to be mixed which therefore appears as a determinant parameter of i) the proportion of each component species at harvest and ii) the mixture productivity. Cultivars are usually discriminated according to their earliness, sensitivity to diseases or potential yield, but in the particular case of multi-specific stands, the above-ground architecture of the cultivar; given by the geometry, optical properties and topology of the phytoelements (Godin, 2000); should also be taken into account. Indeed, plant architecture defines the plant interface with the biotic (*e.g.* with *Mycosphaerella pinodes*, Béasse *et al.*, 2000, Le May *et al.*, 2009) and abiotic factors (*e.g.* light, Ross, 1981b, Varlet-Grancher *et al.*, 1993a). In the case of multi-specific stands, the complementarity between the architecture of the mixed species represents a crucial issue. For instance, the level of complementarity between the above ground architecture of the component species determines their respective ability to compete for light that in turn drives the production and allocation of biomass (Sinoquet et Caldwell, 1995). For pea, several genes involved in the set up of the above ground architecture have been identified (for a review see Huyghe, 1998). These studies have led to the breeding of several pea cultivars with contrasting architectures that therefore constitute as much as potential combinations for wheat – pea intercrops. Characterizing the morphogenesis; defined as the sequence of developmental and growth processes bringing to the acquisition of architecture; of these various pea genotypes is therefore of major interest for the improvement of the management of intercropped stands. Several parameters can be used to characterize pea architecture including those related to the leaf area and its spatial distribution which strongly determine plant ability to compete for light.

The amount and distribution of foliar area are related to the number of developed stems and the production of leaves that occurred during the initiation of a phytomer by the apex. A phytomer being defined as a basic unit repeated along the stem and including an internode, a node, a leaf and an axillary bud (Gray, 1849, White, 1979). The sharing of resources within multi-specific stands also depend on the respective height reached by the component species (Sinoquet et Caldwell, 1995, Schwinning et Weiner, 1998, Louarn *et al.*, 2010, Barillot *et al.*, 2011, Barillot *et al.*, 2012a). Although these architectural parameters are key factors of the mixture development, they have been mainly described in mono-specific growing conditions (for a review see Munier-Jolain *et al.*, 2005a). However, the morphogenesis of plant can exhibit strong plastic responses when facing environmental variations as it can occur between mono- and multi-specific stands.

The aim of the present study was therefore to characterize the variability of the morphogenesis of three contrasting pea cultivars grown either in pure stands or mixed with wheat. This was achieved through a field experiment where the growth and phenology of pea cultivars was measured regularly during their growing cycle. This study provides information at both stand and plant scale in order to improve our understanding of the functioning of cereal–legume intercrops.

2 Materials and methods

2.1 Plant material and growing conditions

A field experiment was carried out in 2010-2011 at Brain-sur-l’Authion, western France (47°26’N, 00°26’W) in a clay soil (51% clay, 26% silt and 23% sand). Daily mean air temperature, precipitations and Photosynthetically Active Radiation (PAR) were recorded by an automatic standard agro-meteorological station located close to the experimental field.

Winter wheat (*Triticum aestivum* L.) *cv.* Cézanne and three cultivars of winter field pea (*Pisum sativum* L.) *cv.* Lucy (hr type), AOPH10 (hr type) and 886/01 (HR type) were sown on 28th November 2010 in sole crops (SC) and intercrops (IC). Flowering of HR cultivars is sensitive to the photoperiod. Sowing density of SC was 250 plant m^{-2} for wheat. Optimal densities of pea cultivars were chosen in regard of their ability for lateral development and the risk of lodging. As a consequence, SC composed of pea cultivars Lucy and AOPH10 were sown at 80 plant m^{-2} whereas cultivar 886/01 was sown at 40 plant m^{-2}. Intercrops followed a substitutive design where the two species were mixed within the row. Wheat and pea crops grown in IC were sown at half of their respective density in pure stands. The experiment was arranged in a randomized complete block design with three replicates. The size of each plot was 1.2 x 10 m.

In all plots, pests and weeds control was carried out with pesticides. Stands of sole wheat were fertilized with 14 g N m^{-2} whereas pea SC and wheat – pea IC were not supplied with external nitrogen.

Table 1: Harvest time, expressed in growing degree day (DD) from emergence (base, 0°C), of species grown in sole crop (SC) and intercrops (IC).

Species	Genotype	Time of harvest in SC (DD)	Time of harvest in IC (DD)
Pea	Lucy	1900	2275
Pea	AOPH10	1985	2275
Pea	886/01	2130	2275
Wheat	Cézanne	2275	2275

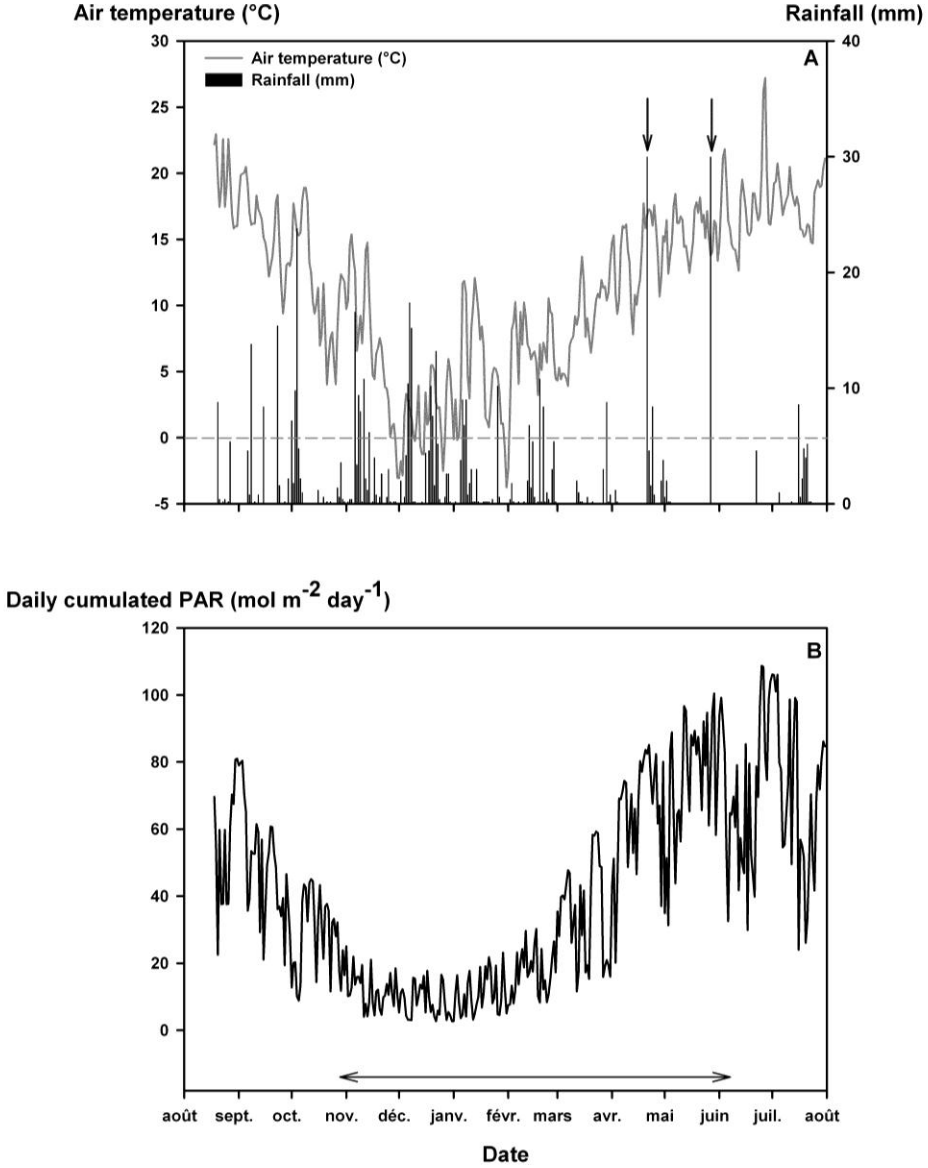

Figure 1: Meteorological conditions during the growing season 2010-2011 at Brain-sur-l'Authion, France. Daily mean air temperatures and rainfall are shown in A. Vertical arrows represent a water supply of 30mm by irrigation. Daily cumulated PAR (Photosynthetically Active Radiation) is shown in B. The horizontal arrow represent the growing period of pea and wheat stands.

2.2 Plant sampling and measurement of pea morphogenesis

The above ground biomass and maximal height of SC and IC stands were measured during the growing cycle at 645, 1525 Growing Degree Day (GDD) from emergence (base temperature 0°C) and at last, at crop maturity (Table 1). Samplings were carried out on 0.75 m^2. The morphogenesis of five pea plants per plot was characterized for each vegetative axis *i.e.* main stems and lateral branches. Measurements were performed for a single branch (randomly selected) at each nodal position of the main stem. Vegetative axes were grouped according to their topological order *i.e.* main stems were denoted axis-0, branches that emerged from the first phytomer (vestigial leaf) were referenced as axis-1 and so on.

For each order of axis, the kinetics of phytomer appearance (unfolding leaf visible to the naked eye) were measured and fitted with the Schnute's non-linear model (Schnute, 1981) using the least-square method. The model is written as:

$$Y = \left[{y_{max}}^{B} * \frac{1 - e^{-A(t)}}{1 - e^{-A(t_{max})}} \right]^{1/B} + \varepsilon_i$$

Where Y is the *number of visible phytomer* variable; estimated parameters were A and B which implicitly define the shape of the curve; t_{max} is the last value of the time (t) domain for which the model is fitted, corresponding to the end of the vegetative development of the stem; and parameter y_{max} is the value of Y at t_{max}. Parameters were optimised using the Levenberg-Marquardt iterative method with automatic computation of the analytical partial derivatives. The first derivatives of Schnute adjustments were also used in order to estimate the rates of phytomer emission of the pea cultivars.

2.3 Statistical analyses

Data analyses were performed by using analysis of variance (ANOVA). Effects of growing conditions and pea cultivars were assessed by using the Tukey's HSD test. The normal distribution of the residuals of Schnute's adjustments was tested using the Shapiro–Wilk test. Significance threshold was fixed at 0.05 probability level for all statistical tests. Statistical analyses were performed with R (R Development Core Team, 2011).

3 Results and discussion

Environmental conditions during crop growth are summarized in Figure 1. Daily average air temperature ranged from -4°C to 27°C on 31st January and 27th June respectively (Figure 1A). Irrigation supplied 30 mm of water on 21st April and 27th May 2011. Daily cumulated Photosynthetically Active Radiation (PAR), Figure 1B, ranged from 2.70 to 108.70 moles m^{-2} on 31st December 2010 and 25th June 2011 respectively.

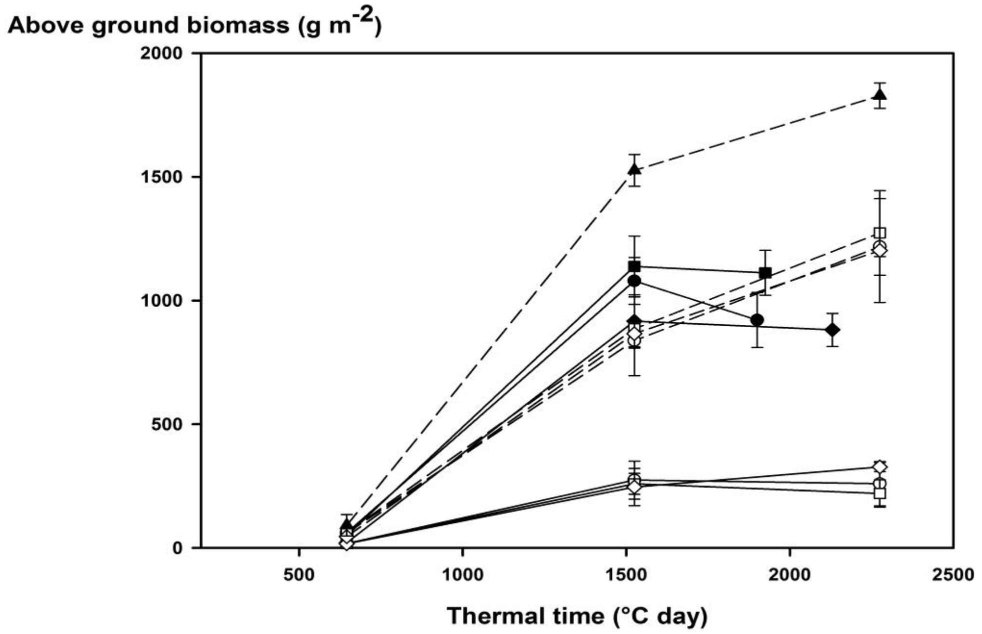

Figure 2: Accumulation of above ground biomass as a function of thermal time from emergence (base temperature = 0°C). Sole crops are shown in closed symbols and intercrops in open symbols. Pea cultivars are in solid lines: Lucy is denoted by circles (—●—, —○—) AOPH10 by squares (—■—, —□—), 886/01 by diamonds (—◆— ,—◇—). Wheat is in dotted lines with triangles (– ▲–) in sole crops, and with the corresponding pea cultivar symbol in intercrops (– ○– with 'Lucy', – □– with 'AOPH10' and – ◇– with '886/01).

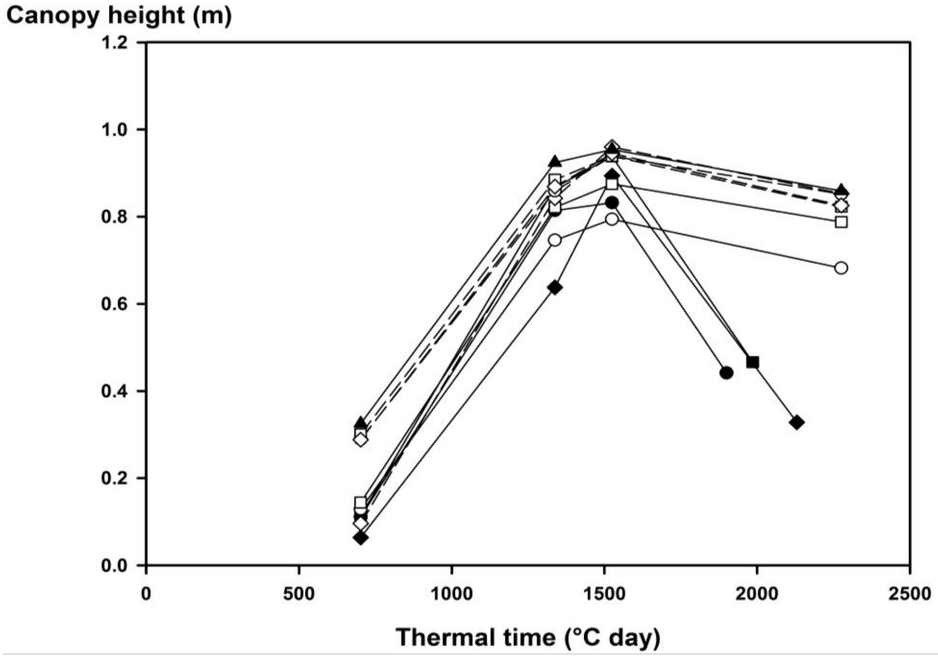

Figure 3: Observed height of canopies during the growing cycle. Sole crops are shown in closed symbols and intercrops in open symbols. Pea cultivars are in solid lines: Lucy is denoted by circles (—●—, —○—), AOPH10 by squares (—■— ,—□—), 886/01 by diamonds (—◆— ,—◇—).Wheat is in dotted lines with triangles (– ▲–) in sole crops, and with the corresponding pea cultivar symbol in intercrops (– ○– with 'Lucy', – □– with 'AOPH10' and – ◇– with '886/01).

3.1 Growth of sole and intercropped stands

3.1.1 Biomass accumulation

The above ground biomass of the species increased from 645 to 1525 GDD (Figure 2). Wheat SC showed the highest amount of biomass during the growing cycle and finally reached 1830 g m^{-2} of biomass. The above ground biomass accumulated by the three pea cultivars in SC ranged from 880 to 1275 g m^{-2}. '886/01' was the cultivar that exhibited the lowest biomass in SC throughout the growing cycle although this amount of biomass was obtained with 50 % less plants than the other cultivars. Indeed the cultivar 886/01 was sown at 40 and 20 plant m^{-2} in SC and IC respectively. The architectural analysis performed in the following sections of the paper will then provide information on how cultivar 886/01 balanced its lower initial density. Intercropped wheat (IC stands) accumulated in average 1230 g m^{-2} of biomass regardless of the component pea cultivar and therefore contributed to the main part of the mixture biomass (in average 3.75 times the biomass of pea). Indeed, pea grown in IC stands produced 220 to 325 g m^{-2} of biomass regardless of the cultivar. These results appeared to be representative of the development of sole and intercropped pea stands as the dynamics of biomass accumulation are closed to the results reported by Naudin *et al.* (2010) in wheat – pea mixtures with different cultivars grown in contrasting pedo-climatic conditions. Moreover, these authors as well as other studies (Jensen, 1996b, Corre-Hellou *et al.*, 2006) showed that the contribution of each component species to the biomass of the mixture was dependent on the amount of available nitrogen which enhances the growth of the cereal species. Supplementary studies should therefore be conducted in order to characterize the morphogenesis of wheat and pea grown in mixtures under contrasting levels of nitrogen fertilisation thus providing information on how nitrogen affects plant morphogenesis and by the way the interspecific competition.

The harvest of IC stands (Table 1) was performed at wheat maturity *i.e.* at 2275 GDD whereas the harvest of pea grown in SC occurred earlier (from 1900 to 2130 GDD) and was dependent on the cultivar. Indeed, the physiological maturity of pea varied among the cultivars according to their earliness which is assumed to be mainly driven by their sensitivity to the photoperiod that in particular involves the *Hr* gene (Murfet, 1973). Cultivars Lucy and AOPH10 are hr types and are thus unaffected by the day-length whereas cultivar 886/01, which is a HR type, needs a longer photoperiod to reach flowering. Cultivar 886/01 therefore reached its maturity later than hr cultivars as the photoperiod starts to increase from the months of February-March in Western Europe (Figure 1). The maturity of cultivar 886/01 and that of wheat was therefore reached in a similar period of time (2130 and 2275 GDD respectively). Within the framework of wheat – pea intercropping, HR pea therefore appeared as suitable cultivars allowing to the two component species to reach their physiological maturity simultaneously, whereas gaps of maturity as encountered with hr cultivars represent a strong practical constraint at harvest (Louarn *et al.*, 2010).

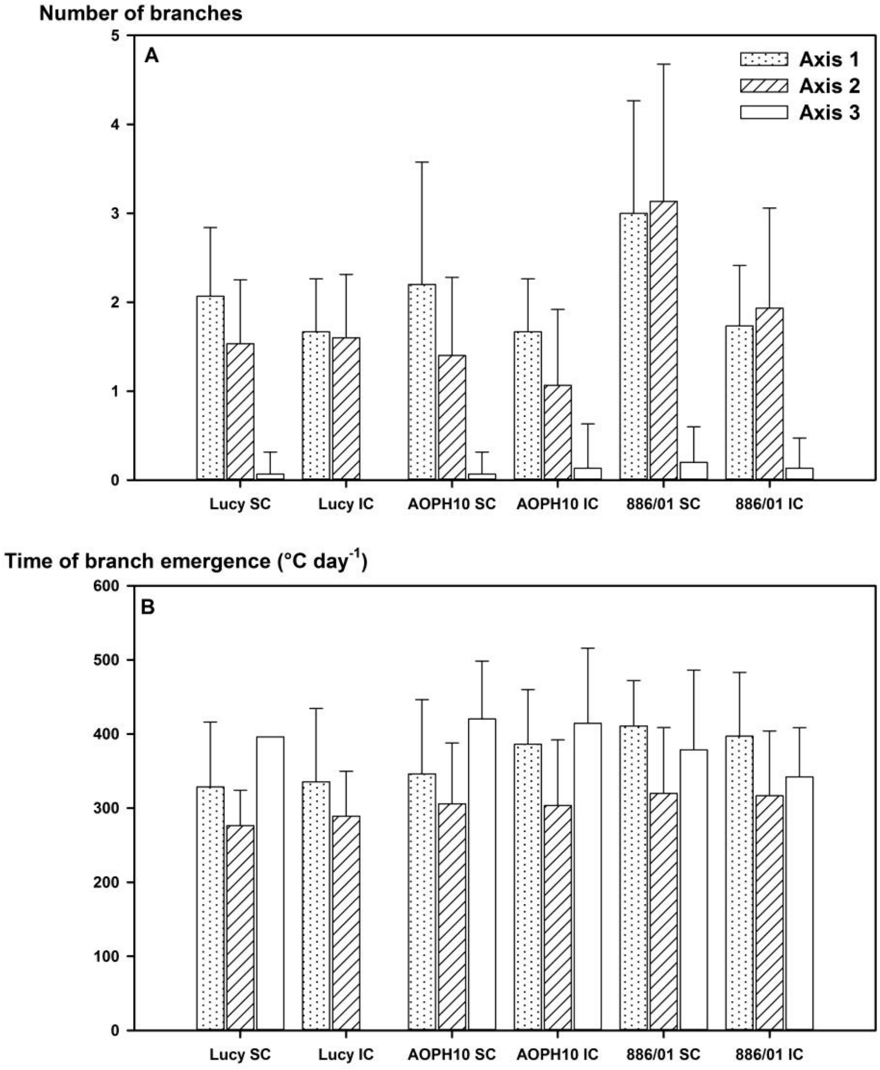

Figure 4: Lateral branching of pea cultivars (*n=15 plants for each condition*). A: number of lateral branches developed by the pea cultivars Lucy, AOPH10 and 886/01 grown in sole crops (SC) or in intercrops (IC).B: time of branching expressed in thermal time from crop emergence. Branches were distinguished according to their nodal position on the main stem. Axis-1: branches emerged at the first node, Axis-2: second node and Axis-3: third node.

3.1.2 Plant height

Wheat plants grown in SC and IC stands exhibited similar height along the developmental cycle and reached a maximum of 0.95 m (Figure 3). Wheat grown in IC was taller than pea from the early stages of development whatever the pea cultivar. The height reached by the pea cultivars appeared to be variable, depending on the cropping system (SC or IC stand). The canopy height of sole pea crops reached a maximum of 0.83 to 0.94 m for 'Lucy' and 'AOPH10' respectively. Height of sole pea finally decreased dramatically at the end of the growing cycle due to plant lodging. However, the height of pea cultivars grown in IC stands stayed higher than 0.70 m meaning that pea plants grown in IC were staked by wheat stems thus avoiding their lodging. The height reached by each species in the canopy is an important feature of the stand that affects and emerges from the competition processes occurring between plants. For instance, the species height ratio has been widely shown to affect light sharing in a mixture (*e.g.* Sinoquet et Caldwell, 1995, Louarn *et al.*, 2010, Barillot *et al.*, 2011, Barillot *et al.*, 2012a). Moreover, Corre-Hellou *et al.* (2011) reported that the high sensitivity of pea to lodging causes significant yield losses as well as an enhanced growth of weed. Intercropping cereals and legumes is therefore an interesting way to reintroduce legume species within European agrosystems while settling the problems encountered in pure stands.

3.2 Morphogenesis of the pea cultivars

3.2.1 Lateral branching of pea plants

The number of branches produced by individual pea plant as well as their nodal position is shown in Figure 4A. Cultivars Lucy and AOPH10 grown in SC developed in average 3 to 4 branches corresponding to axis-1 and -2. Cultivar 886/01 in SC was the most branching with about 6 branches per plant and developed a significantly higher number of branches from the second phytomer of the main stem (*p-value* < 0.001). For this latter cultivar, its ability to develop lateral branches appeared to balance its low sowing density (40 and 20 plant m^{-2} for SC and IC respectively). Indeed, although sown at half density, cultivar 886/01 accumulated a similar amount of biomass than the cultivars Lucy and AOPH10 (Figure 2). Most of lateral branches emerged from the first and second phytomer of the main stems (axis-1 and -2) whatever the cropping system (SC and IC) whereas very few branches (9 in all, regardless of the cultivar) were produced on the third phytomer. As reported by Jeudy and Munier-Jolain (2005) the position of branches on the stem is mainly determined by the hormonal balance as well as the light microclimate. It therefore appears that the physiological and environmental conditions were similar for pea grown in SC and IC.

Compared to SC conditions, cultivars Lucy and AOPH10 grown with wheat (IC stands) decreased their mean number of lateral branches by 11 and 22% respectively.

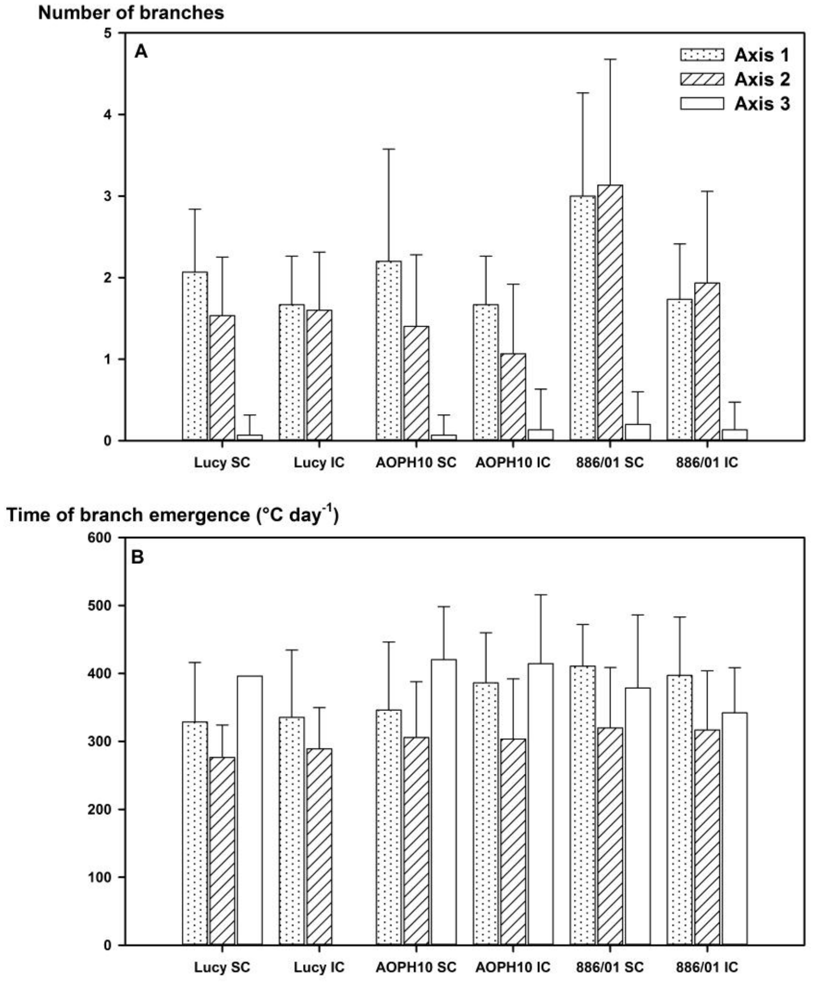

Figure 4 (Bis): Lateral branching of pea cultivars (*n=15 plants for each condition*). A: number of lateral branches developed by the pea cultivars Lucy, AOPH10 and 886/01 grown in sole crops (SC) or in intercrops (IC).B: time of branching expressed in thermal time from crop emergence. Branches were distinguished according to their nodal position on the main stem. Axis-1: branches emerged at the first node, Axis-2: second node and Axis-3: third node.

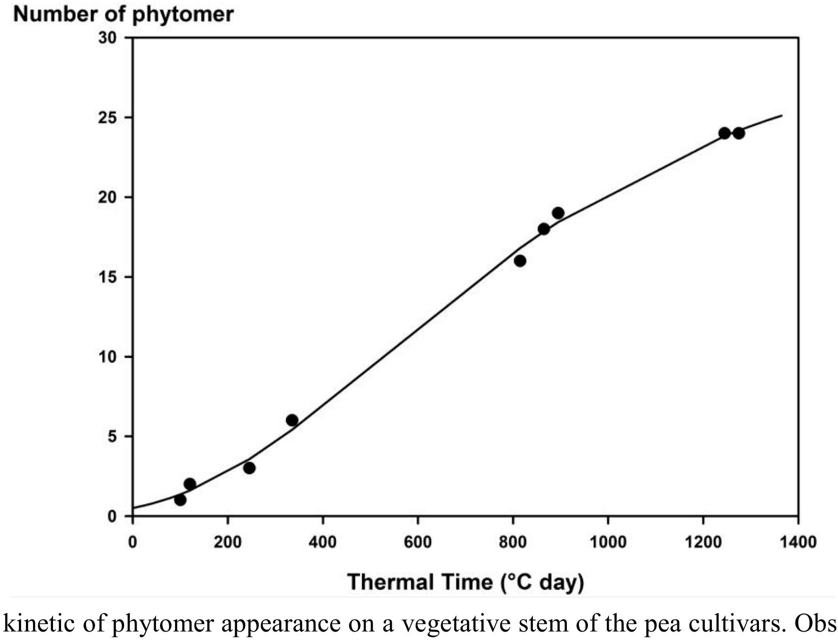

Figure 5: Typical kinetic of phytomer appearance on a vegetative stem of the pea cultivars. Observed values are in closed symbols. Non-linear adjustment (solid line) was performed using Schnute's equation.

For these cultivars, it was however not possible to detect significant differences in the number of branches produced between the two cropping systems, probably due to the high variability observed. The most important decrease was observed for cultivar 886/01 which produced 40% less branches whatever the considered axis in IC compared to SC stands (*p-value* < 0.01 and < 0.05 for axis-1 and axis-2 respectively). Branching has been shown to be dependent on the genotype, environmental factors such as low temperature (Jeudy et Munier-Jolain, 2005) and plant density (Spies *et al.*, 2010). In the present study, contrasting abilities for branching were indeed found between the two genotypes Lucy - AOPH10 and 886/01. Unlike cultivar 886/01 which was sensitive to the cropping system, the number of branches developed by the cultivars Lucy and AOPH10 was similar between plants grown in SC and IC meaning that other parameters were driving the production of branches. Some authors like Casal *et al.* (1986) and Ballaré and Casal (2000) showed that the tillering of several grass species is also affected by the quantity (PAR) and quality (Red/Far red ratio) of light perceived by the axillary buds. In the present study, we can therefore hypothesize that light quantity and quality were similar within Lucy SC – Lucy IC and AOPH10 SC – AOPH10 IC canopies. This means that the replacement of a "Lucy/AOPH10" plant (in SC) by a wheat plant (in IC) lead to similar modifications of the light microclimate. This may be the result of similar architectural patterns between the two mixed species in terms of leaf area, height, geometry and/or optical properties. On contrast, the number of branches was significantly reduced when cultivar 886/01 was grown in IC compared with SC. As this cultivar has a late development (HR type), we can hypothesize that at the beginning of branching, the wheat component was more developed (in IC) than a neighbour '886/01' pea plant would have been in SC, thus modifying the light perceived by axillary buds.

In average, lateral branches emerged between 275 and 420 GDD regardless of the cultivar and cropping system (Figure 4B). Branches developed on the second phytomer of the main stem (axis-2) appeared 70 GDD earlier than those located on the first node (axis-1). Indeed, in most cases, the first phytomer (carrying the first vestigial leaf) is located a few millimetres under the ground which may mechanically delay the emergence of branches, depending for instance on the sowing depth or soil structure which also affect the quantity of light perceived by the axillary bud (Jeudy et Munier-Jolain, 2005). Figure 4B also shows that cultivar Lucy developed its branches earlier than '886/01' (*p-value* < 0.01) while 'AOPH10' had an intermediary behaviour. There were however no significant differences in the time of branch emergence between SC and IC stands meaning that this parameter of pea morphogenesis is mainly dependent of the genotype.

3.2.2 Rate of phytomer appearance and final number of phytomers

The kinetic of phytomer appearance was assessed for main stems and a randomly selected branch at each nodal position. Phytomer appearance on the vegetative stems followed sigmoïd-type dynamics as illustrated in Figure 5.

Table 2: Parameters (A*10^{-3}, B and t_{max}) of Schnute adjustments made on the kinetics of phytomer appearance for each pea cultivars (Lucy, AOPH10, 866/01) grown in sole crops (SC) or in intercrops (IC). Schnute's adjustments were performed for each vegetative axis (0: main stem, 1: branch developed on the first node of the main stem, 2: second node, 3: third node). Indicated values are the mean ± SD. Goodness of fit is also given by RMSE values. (*n=15 plants for each cultivar and cropping system*)

Axis	**Parameter**	**Stand**					
		Lucy SC	**Lucy IC**	**AOPH10 SC**	**AOPH10 IC**	**886/01 SC**	**886/01 IC**
0	**A (*10^{-3})**	4.57 ± 3.35	5.10 ± 4.43	3.87 ± 4.03	4.95 ± 3.13	3.18 ± 2.20	4.11 ± 2.10
	B	0.25 ± 0.19	0.23 ± 0.19	0.28 ± 0.19	0.21 ± 0.17	0.29 ± 0.17	0.24 ± 0.18
	t_{max}	775 ± 368	679 ± 267	1015 ± 398	716 ± 292	711 ± 225	599 ± 111
1	**A (*10^{-3})**	2.42 ± 1.44	2.83 ± 0.96	4.24 ± 4.58	2.51 ± 2.07	2.24 ± 1.52	1.93 ± 1.78
	B	0.18 ± 0.12	0.13 ± 0.10	0.17 ± 0.22	0.24 ± 0.20	0.16 ± 0.13	0.25 ± 0.17
	t_{max}	1267 ± 205	1264 ± 120	1152 ± 327	1259 ± 240	1258 ± 170	1305 ± 190
2	**A (*10^{-3})**	2.27 ± 1.14	3.20 ± 0.86	2.35 ± 1.20	2.82 ± 0.98	1.06 ± 0.79	2.18 ± 1.27
	B	0.23 ± 0.17	0.13 ± 0.04	0.18 ± 0.08	0.18 ± 0.10	0.33 ± 0.11	0.22 ± 0.10
	t_{max}	1285 ± 154	1180 ± 194	1276 ± 224	1257 ± 182	1412 ± 163	1241 ± 243
3	**A (*10^{-3})**				6.06 ± 0	1.59 ± 0.09	
	B				0.002 ± 0	0.17 ± 0.04	
	t_{max}				890 ± 0	1293 ± 53	

Table 3: Rate of phytomer emission of each pea cultivars (Lucy, AOPH10, 866/01) grown in sole crops (SC) or in intercrops (IC). Maximum rate of phytomer emission (V_{max}, phytomer degree day^{-1}) and time at which it was reached (X_{Vmax}, GDD) are shown (mean ± SD).). *n=15 plants for each cultivar and cropping system.*

Axis	**Parameter**	**Stand**					
		Lucy SC	**Lucy IC**	**AOPH10 SC**	**AOPH10 IC**	**886/01 SC**	**886/01 IC**
0	**V_{max}**	0.02 ± 0.01	0.02 ± 0	0.04 ± 0.05	0.03 ± 0.01	0.03 ± 0.01	0.03 ± 0.01
	X_{Vmax}	694.08 ± 589.37	411.67 ± 57.33	715.67 ± 526.14	619.57 ± 563.70	699.67 ± 530.86	579.46 ± 407.62
1	**V_{max}**	0.03 ± 0	0.03 ± 0.01	0.07 ± 0.09	0.03 ± 0.01	0.05 ± 0.03	0.03 ± 0.01
	X_{Vmax}	937.67 ± 232.89	843.67 ± 136.16	1131.00 ± 402.00	955.44 ± 381.67	1204.33 ± 346.08	1183.22 ± 336.11
2	**V_{max}**	0.02 ± 0.01	0.03 ± 0	0.03 ± 0.01	0.02 ± 0.01	0.03 ± 0.01	0.03 ± 0
	X_{Vmax}	848.69 ± 345.23	692.25 ± 102.28	859.89 ± 137.23	677.67 ± 117.47	1294.08 ± 394.49	863.22 ± 203.89

These dynamics were fitted with Schnute's function (Table 2). The first three parameters of the Schnute's function, A, B and t_{max}, respectively ranged from 1.06 to 5.10 x 10^{-3}, 0.13 to 0.33 and 599 to 1305 GDD. The shape parameters A and B of the Schnute's functions fitted on axis-2 of cultivar 886/01 appeared to be significantly different between 'Lucy' and 'AOPH10' (*p-value* < 0.05) whatever the considered stand. Moreover, parameter A of cultivar Lucy and 886/01 was statistically higher for the main stems compared to branches (*p-value* < 0.05 and < 0.01 respectively). For most of the plants, the duration of phytomer emission (parameter t_{max}, expressed from stem emergence) appeared to be dependent neither on the cultivar nor on the cropping system. Parameter t_{max} of the main stems of 'AOPH10' appeared to be higher than the other cultivars (*p-value* < 0.05), this was in particular the case in IC stands. Moreover, parameter t_{max} of main stems was significantly lower than for branches whatever the cultivar (*p-value* < 0.001).

The first derivative of the Schnute adjustments (Table 3) allowed to assess the maximum rate of phytomer appearance (V_{max}) as well as the time at which it was reached (X_{vmax}). The maximum rate of phytomer appearance ranged from 0.02 to 0.07 phytomer degree day^{-1}. Due to the high variability observed no significant differences were found among the cultivars and cropping systems. The maximum rate of phytomer appearance was reached between 410 and 1300 GDD from stem emergence. Parameter X_{vmax} of main stems was similar for all cultivars whatever their cropping system. Moreover, cultivar 886/01 reached its V_{max} statistically later than the other cultivars, in particular for axis-2 (*p-value* < 0.001). To conclude, few statistical differences were found between the parameters belonging to the different genotypes and cropping systems. Moreover, these parameters cannot be directly related to a biological meaning, in particular parameter A and B. Nevertheless, these results mean that the kinetics of phytomer production can be analysed or modelled by using Schnute's functions with similar parameters for the three pea cultivars and whether they are grown in sole stands or mixed with wheat (except for y_{max} which will be discussed below). Turc and Lecoeur (1997) also reported similar rates of leaf primordium initiation and emergence for contrasting plant growth rates, cultivars and sowing densities in spring pea cultivars. These parameters were however well correlated with cumulated degree days.

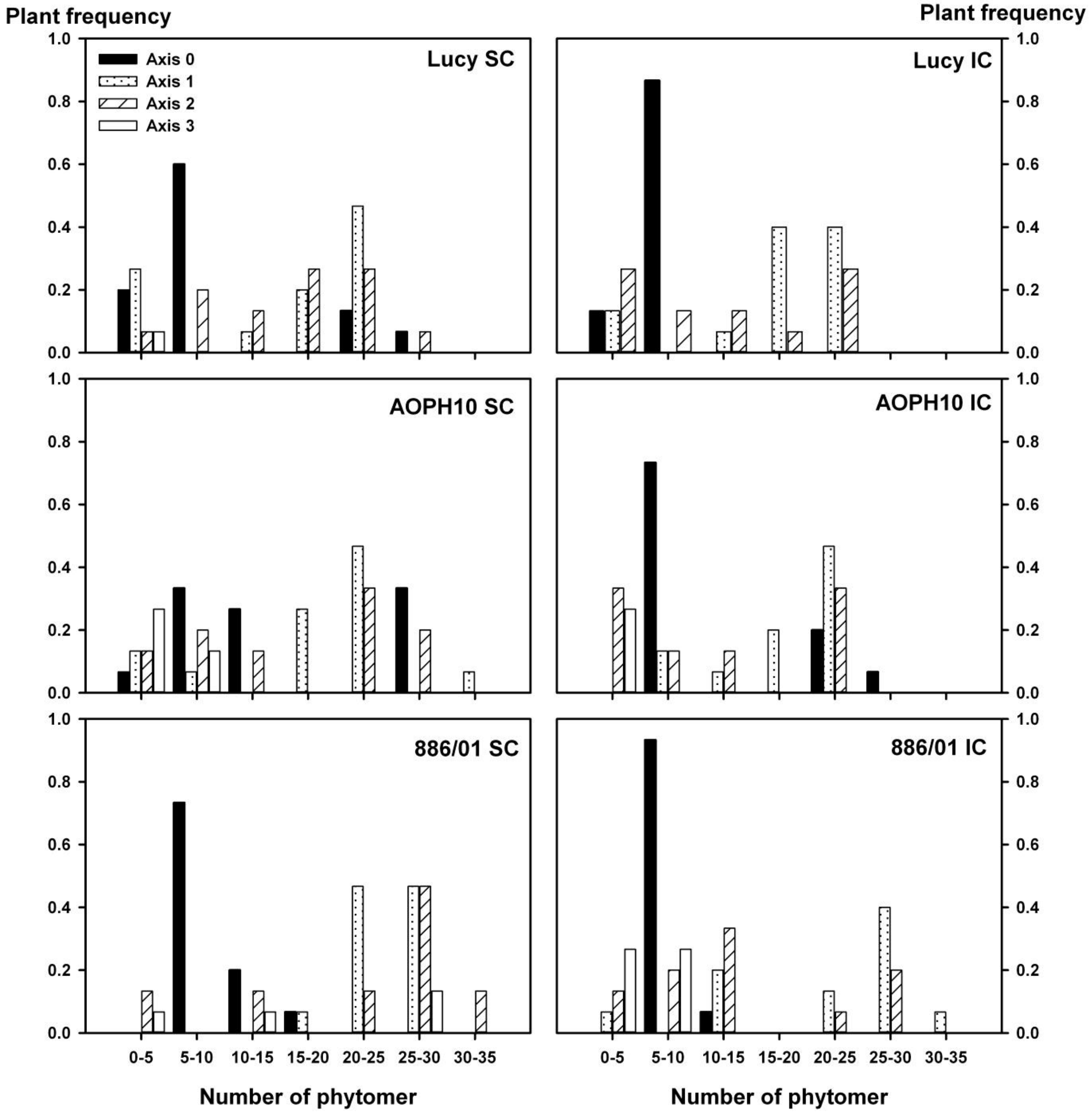

Figure 6: Plant frequency according to their final number of phytomers. Results are shown for the pea cultivars Lucy, AOPH10 and 886/01 grown in sole crops (SC) or in intercrops (IC), *n=15 plants for each condition*. Main stems are denoted Axis-0 and branches were distinguished according to their nodal position on the main stem. Axis-1: branches developed at the first node, Axis-2: second node and Axis-3: third node.

The last parameter of the Schnute adjustments to be analysed is the final number of phytomer (y_{max}). Pea cultivars grown in the different cropping systems reached a various number of phytomers, ranging from 1 to 31 (Figure 6). More than 20% of the overall branches developed by pea plants stopped their growth early with few phytomers (between 1 to 5 phytomers). This was in particular the case for main stems. Indeed, more than 70% of the main stems of cultivars Lucy and 886/01 grown in SC and IC stopped their growth with less than 10 phytomers. These results show that the canopy of the three pea cultivars was mainly composed of branches. As reported by Jeudy and Munier-Jolain (2005), the development of branches is increased in winter pea cultivars because of the frost damage experienced by the apex of the main stem that occurred under low temperatures. Such conditions were indeed encountered during the first months of the growing cycle (December-February, Figure 1) and the emergence of lateral branches started at the beginning of February (275 GDD, Figure 4). As a consequence, stems with more than 15 phytomers were mainly branches developed on the first and second phytomer of main stems (Figure 6). This behaviour was however significantly different in the case of cultivar AOPH10 (*p-value* < 0.01) for which 30% of the main stems produced more than 20 phytomers. Branches of cultivar 886/01 developed more phytomers than ‘Lucy’ and ‘AOPH10’ whatever the cropping systems, this was in particular the case for those located at the first phytomer of the main stem (*p-value* < 0.01). Finally, the final number of phytomers reached on vegetative axes appeared to be dependent on the genotype. In contrast, the number of initiated phytomers was similar whether pea plants were grown on pure stands or mixed with wheat.

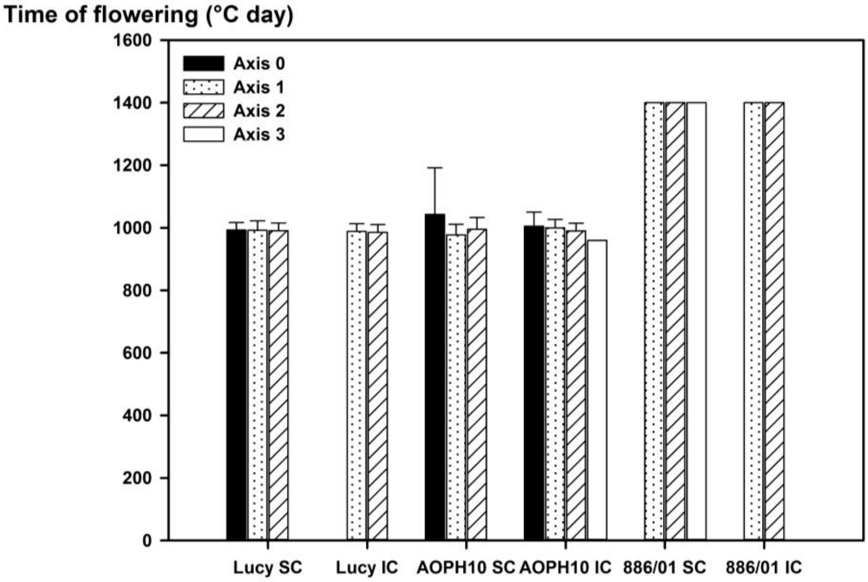

Figure 7: Emergence time of the first flower of pea cultivars of the pea cultivars Lucy, AOPH10 and 886/01 grown in sole crops (SC) or in intercrops (IC). Main stems are denoted Axis-0 and branches were distinguished according to their nodal position on the main stem. Axis-1: branches developed at the first node, Axis-2: second node and Axis-3: third node. (*n=15 plants for each condition)*.

3.2.3 Beginning of the reproductive stages: flowering

The reproductive development of pea cultivars was characterized by measuring the nodal position of the first flower as well as its emergence time. The beginning of flowering occurred between 950 and 1400 GDD for AOPH10 IC and 886/01 in SC and IC respectively (Figure 7). For each pea cultivar and cropping system, vegetative axes (main stems and branches) exhibited their first flowers at similar times. As reported by Jeuffroy and Sebillotte (1997), we also found similar time of flowering between main stems and basal branches although they were emitted later. Flowering of cultivar 886/01 occurred significantly later (1400 GDD) compared to 'Lucy' and 'AOPH10' (*p-value* < 0.001). Flowering is a crucial stage of the growing cycle that has been widely studied and used in order to model the growth of pea. For instance, Truong and Duthion (1993) showed that the time of flowering is a function of the leaf appearance rate and the position of the node bearing the first flower.

The position of the first flower (Figure 8) was located between the 9th and the 28th phytomer among the different plots. Branches emitted from the first and second phytomer (axis-1 and -2) of the cultivar 886/01 developed their first flowers at higher phytomer positions than the other cultivars (*p-value* < 0.001). As it was the case for the time of flowering, the nodal position of the first flower was similar between plants grown in pure or mixed stands whatever the cultivar. Some authors also reported that for a given genotype, the position of the first flowering node was constant over various conditions (Roche *et al.*, 1998, Munier-Jolain *et al.*, 2005b). However, we found that the first flowering node varied both among the genotypes and the position of branches on the main stem. Although numerous branches were produced by the pea cultivars, the analysis of the number of phytomers emitted by these vegetative axes reveals that few of them were fully developed and had reached flowering (from 55 to 100%).

4 Conclusion

To our knowledge, the present study is the first that compares the morphogenesis of pea grown in sole stands and in a mixture with wheat. This characterization was conducted at the stand scale but also at plant scale in order to assess the plasticity of the morphogenesis of the pea cultivars. On the one hand, the present results show that most of the assessed parameters of pea morphogenesis (phenology, branching, final number of vegetative organs and their kinetics of appearance) were mainly dependent on the considered genotype. This emphasizes the importance of the choice of cultivars in particular for intercropping systems as it determines the level of competition and complementarity between the component species. We can however hypothesize that, in our growing conditions, the growth habits of each of the pea cultivars did not lead to contrasting levels of competition when mixed with wheat.

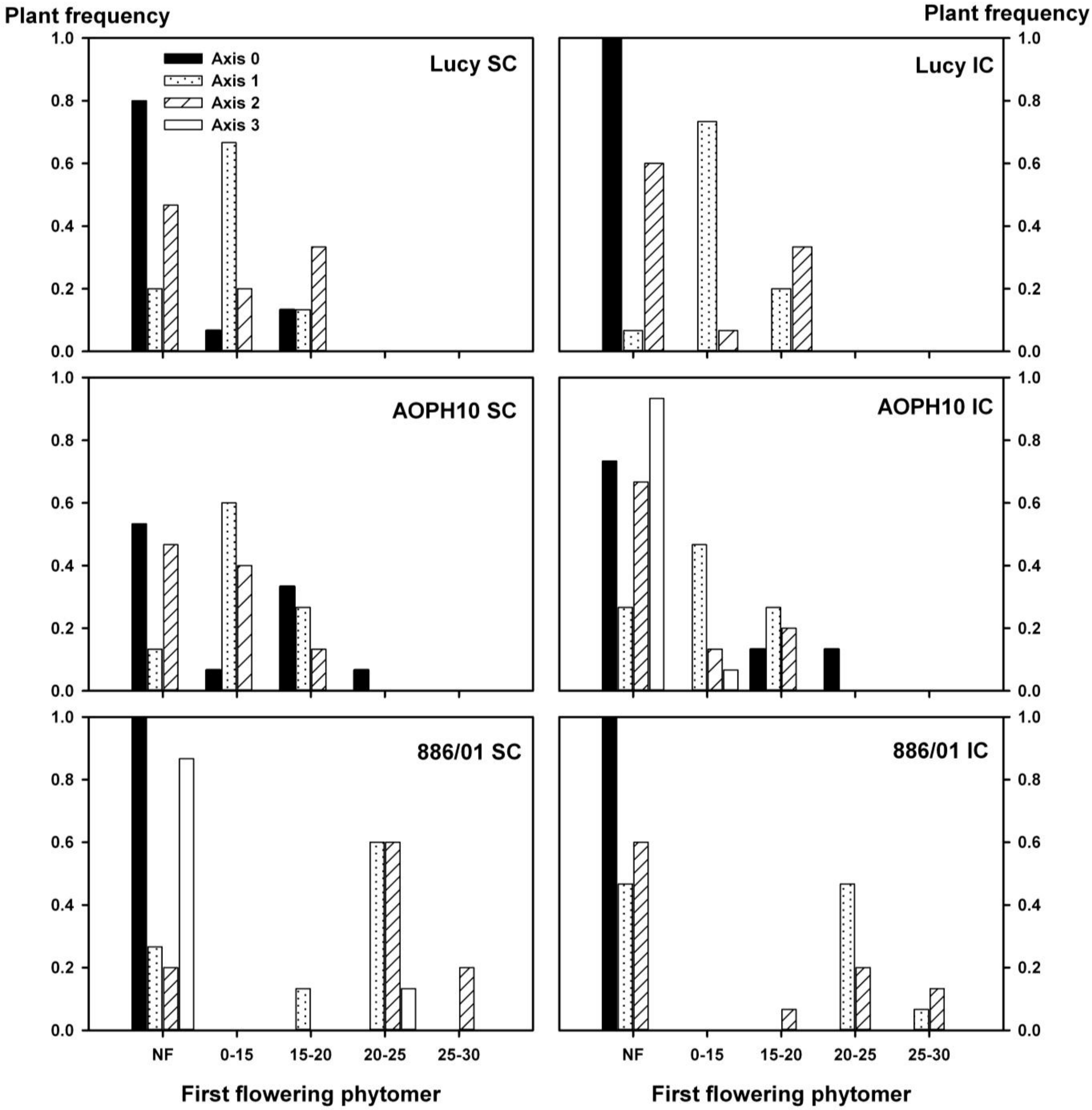

Figure 8: Plant frequency according to the first flowering node of the stems (NF: non-flowered). Results are shown for the pea cultivars Lucy, AOPH10 and 886/01 grown in sole crops (SC) or in intercrops (IC), *n=15 plants for each condition*. Main stems are denoted Axis-0 and branches were distinguished according to their nodal position on the main stem. Axis-1: branches developed at the first node, Axis-2: second node and Axis-3: third node.

Indeed, the component species of each mixture exhibited similar accumulation of biomass whatever the pea cultivar. On the other hand, the plasticity of pea morphogenesis was low between sole and mixed stands except for plant height and branching of the late cultivar 886/01. We can thus hypothesize that i) the morphogenesis of pea is mainly determined by the genotype and is therefore not very plastic and/or ii) the architecture of pea and wheat are quite similar so that the environmental conditions perceived by plants in the canopy (phylloclimate, Chelle, 2005) are similar between sole pea crops and wheat – pea mixtures. Functional – structural models (Vos *et al.*, 2010, DeJong *et al.*, 2011), are able to take into account the explicit architecture of plants and its interactions with physiological processes and environmental conditions. Such models therefore constitute suitable tools for assessing these hypotheses and can in particular be used to characterize the microclimate perceived by plants located in mono- and multi-specific stands. The information provided in the present study on the plasticity of pea morphogenesis can therefore be used for the building and parameterization of such models.

5 References

Ballaré CL, Casal JJ. 2000. Light signals perceived by crop and weed plants. *Field Crops Research,* **67**: 149-160.

Barillot R, Combes D, Chevalier V, Fournier C, Escobar-Gutiérrez AJ. 2012. How does pea architecture influence light sharing in virtual wheat - pea mixtures? A simulation study based on pea genotypes with contrasting architectures. *AoB PLANTS*: Accepted.

Barillot R, Louarn G, Escobar-Gutiérrez AJ, Huynh P, Combes D. 2011. How good is the turbid medium-based approach for accounting for light partitioning in contrasted grass-legume intercropping systems? *Annals of Botany,* **108**: 1013-1024.

Béasse C, Ney B, Tivoli B. 2000. A simple model of pea (*Pisum sativum*) growth affected by Mycosphaerella pinodes. *Plant Pathology,* **49**: 187-200.

Casal JJ, Sanchez RA, Deregibus VA. 1986. The effect of plant density on tillering: The involvement of R/FR ratio and the proportion of radiation intercepted per plant. *Environmental and Experimental Botany,* **26**: 365-371.

Chelle M. 2005. Phylloclimate or the climate perceived by individual plant organs: What is it? How to model it? What for? *New Phytologist,* **166**: 781-790.

Corre-Hellou G, Dibet A, Hauggaard-Nielsen H, Crozat Y, Gooding M, Ambus P, Dahlmann C, von Fragstein P, Pristeri A, Monti M, Jensen ES. 2011. The competitive ability of pea–barley intercrops against weeds and the interactions with crop productivity and soil N availability. *Field Crops Research,* **122**: 264-272.

Corre-Hellou G, Fustec J, Crozat Y. 2006. Interspecific competition for soil N and its interaction with N_2 fixation, leaf expansion and crop growth in pea–barley intercrops. *Plant and Soil,* **282**: 195-208.

Crews TE, Peoples MB. 2004. Legume versus fertilizer sources of nitrogen: ecological tradeoffs and human needs. *Agriculture, Ecosystems & Environment,* **102**: 279-297.

DeJong TM, Da Silva D, Vos J, Escobar-Gutiérrez AJ. 2011. Using functional–structural plant models to study, understand and integrate plant development and ecophysiology. *Annals Of Botany,* **108**: 987-989.

Duc G, Mignolet C, Carrouée B, Huyghe C. 2010. Importance économique passée et présente des légumineuses : Rôle historique dans les assolements et les facteurs d'évolution. *Innovations Agronomiques,* **11**: 1-24.

Godin C. 2000. Representing and encoding plant architecture: A review. *Annals of Forest Science,* **57**: 413-438.

Gray A. 1849. On the composition of the plant by phytons, and some applications of phyllotaxis. In 438-444.

Huyghe C. 1998. Genetics and genetic modifications of plant architecture in grain legumes: a review. *Agronomie,* **18**: 383-411.

Jensen ES. 1996. Grain yield, symbiotic N2 fixation and interspecific competition for inorganic N in pea-barley intercrops. *Plant and Soil,* **182**: 25-38.

Jeudy C, Munier-Jolain N. 2005. Developpement des ramifications. In: Munier-Jolain N, Biarnes V, Chaillet I, Lecoeur J, Jeuffroy M-H eds. *Agrophysiologie du pois protéagineux.* Paris, Inra-Quae.

Jeuffroy MH, Sebillotte M. 1997. The end of flowering in pea: influence of plant nitrogen nutrition. *European Journal of Agronomy,* **6**: 15-24.

Launay M, Brisson N, Satger S, Hauggaard-Nielsen H, Corre-Hellou G, Kasynova E, Ruske R, Jensen ES, Gooding MJ. 2009. Exploring options for managing strategies for pea-barley intercropping using a modeling approach. *European Journal Of Agronomy,* **31**: 85-98.

Le May C, Ney B, Lemarchand E, Schoeny A, Tivoli B. 2009. Effect of pea plant architecture on spatiotemporal epidemic development of ascochyta blight (*Mycosphaerella pinodes*) in the field. *Plant Pathology,* **58**: 332-343.

Louarn G, Corre-Hellou G, Fustec J, Lô-Pelzer E, Julier B, Litrico I, Hinsinger P, Lecomte C. 2010. Déterminants écologiques et physiologiques de la productivité et de la stabilité des associations graminées-légumineuses. *Innovations Agronomiques,* **11**: 79-99.

Munier-Jolain N, Biarnès V, Chaillet I, Lecoeur J, Jeuffroy M-H, Carrouée B, Crozat Y, Guilioni L, Lejeune I, Tivoli B. 2005a. *Agrophysiologie du pois protéagineux.* INRA: Paris, FRANCE.

Munier-Jolain N, Turc O, Ney B. 2005b. Développement reproducteur. In: Munier-Jolain N, Biarnes V, Chaillet I, Lecoeur J, Jeuffroy M-H eds. *Agrophysiologie du pois protéagineux.* Paris, Inra-Quae.

Murfet IC. 1973. Flowering in *Pisum*. Hr, a gene for high response to photoperiod. *Heredity,* **31**: 157-164.

Naudin C, Corre-Hellou G, Pineau S, Crozat Y, Jeuffroy M-H. 2010. The effect of various dynamics of N availability on winter pea-wheat intercrops: Crop growth, N partitioning and symbiotic N2 fixation. *Field Crops Research,* **119**: 2-11.

Ney B, Carrouée B. 2005. Préface. In: Munier-Jolain N, Biarnes V, Chaillet I, Lecoeur J, Jeuffroy M-H eds. *Agrophysiologie du pois protéagineux.* Paris, Inra-Quae.

Ofori F, Stern WR. 1987. Cereal-legume intercropping systems. *Advances in agronomy,* **41**: 41-90.

Roche R, Jeuffroy M-H, Ney B. 1998. A Model to Simulate the Final Number of Reproductive Nodes in Pea (*Pisum sativum* L.). *Annals of Botany,* **81**: 545-555.

Ross J. 1981. Role of phytometric investigations in the studies of plant stand architecture and radiation regime. In: Ross J ed. *The radiation regime and architecture of plant stands.* The Hague, The Netherlands, Junk, W.

Schnute J. 1981. A Versatile Growth Model with Statistically Stable Parameters. *Canadian Journal of Fisheries and Aquatic Sciences,* **38**: 1128-1140.

Schwinning S, Weiner J. 1998. Mechanisms determining the degree of size asymmetry in competition among plants. *Oecologia,* **113**: 447-455.

Sinoquet H, Caldwell MM. 1995. Estimation of light capture and partitioning in intercropping systems. In: Sinoquet H, Cruz P eds. *Ecophysiology of tropical intercropping.* Paris, INRA Editions.

Spies JM, Warkentin T, Shirtliffe S. 2010. Basal branching in field pea cultivars and yield-density relationships. *Canadian Journal of Plant Science,* **90**: 679-690.

Truong HH, Duthion C. 1993. Time of Flowering of Pea (*Pisum sativum* L.) as a Function of Leaf Appearance Rate and Node of First Flower. *Annals Of Botany,* **72**: 133-142.

Turc O, Lecoeur J. 1997. Leaf Primordium Initiation and Expanded Leaf Production are Co-ordinated through Similar Response to Air Temperature in Pea (*Pisum sativum* L.). *Annals of Botany,* **80**: 265-273.

Varlet - Grancher C, Bonhomme R, Sinoquet H. 1993. *Crop structure and light microclimate.* Paris.

Vos J, Evers JB, Buck-Sorlin GH, Andrieu B, Chelle M, de Visser PHB. 2010. Functional-structural plant modelling: a new versatile tool in crop science. *Journal of Experimental Botany,* **61**: 2101-2115.

White J. 1979. The Plant as a Metapopulation. *Annual Review of Ecology and Systematics,* **10**: 109-145.

Synthèse

L'objectif du troisième chapitre a consisté à i) collecter des données sur la **morphogénèse aérienne de différents génotypes de pois** en conditions non contrôlées (expérimentation au champ), et ii) à évaluer la **plasticité** de ces génotypes de pois entre des conditions de culture pure et d'association avec du blé. Les résultats ont révélé une variabilité génotypique importante en termes de précocité, développement de ramifications et phytomères. En revanche, il semble que les règles de morphogénèse du pois puissent être en grande partie transposables entre conditions de culture pure et d'association. Toutefois, un paramètre majeur se distingue entre ces deux types de couvert : la hauteur atteinte par le pois (forte verse en culture pure).

Le chapitre suivant est dédié à la **construction d'un modèle architecturé de pois.** Dans cette optique la quantification des processus morphogénétiques du pois consiste donc en une étape primordiale. Ces résultats permettront également d'alimenter le modèle avec des informations issues de génotypes différents, rendant ainsi compte de la variabilité génotypique de l'architecture aérienne du pois.

Chapitre IV

L-Pea: a 3D architectural model of pea development for assessing the effects of architectural parameters on light partitioning within wheat - pea mixtures.

Romain BARILLOT, Christian FOURNIER, Pierre HUYNH, Abraham J. ESCOBAR-GUTIÉRREZ and Didier COMBES

Ce chapitre fera l'objet de la soumission de deux articles scientifiques : l'un dédié à la présentation du modèle architecturé de pois, et l'autre destiné aux travaux relatifs à la réponse du partage de la lumière en fonction de l'architecture des plantes.

Type of article: research article

Title: **L-Pea: a 3D architectural model of pea development for assessing the effects of architectural parameters on light partitioning within wheat - pea mixtures.**

Author names and affiliations: Romain BARILLOT[1*], Christian FOURNIER[2,3], Pierre HUYNH[1], Abraham J. ESCOBAR-GUTIÉRREZ[4] and Didier COMBES[4*].

Addresses: [1]LUNAM Université, Groupe Ecole Supérieure d'Agriculture, UPSP Laboratoire d'Ecophysiologie Végétale & Agroécologie, 55 rue Rabelais, BP 30748, F-49007 Angers cedex 01, France.
[2]INRA, UMR 759 LEPSE, F-34060 Montpellier, France
[3]SupAgro, UMR 759 LEPSE, F-34060 Montpellier, France
[4]INRA, UR4 P3F, Equipe Ecophysiologie des plantes fourragères, Le Chêne - RD 150, BP 6, F-86600 Lusignan, France.

***Corresponding authors:**
Romain BARILLOT
Tel.: +33 24123 5555; r.barillot@groupe-esa.com
Didier COMBES
Tel.: +33 54955 6091; didier.combes@lusignan.inra.fr

Keywords: architectural parameters, *Pisum sativum*, plant architecture, *Triticum aestivum*, virtual plant model, wheat-pea intercropping

ABSTRACT

Light partitioning within wheat-pea mixtures is a determinant factor for the proportion of the component species in the stand and their potential productivity. The interception of light by wheat and pea is highly related to their above-ground architecture. However, the relationships between the architectural parameters of the component species and light partitioning have been little studied. Such an analysis requires the development of architectural plant models as they provide an explicit description of the physical structure of plants. Unlike for pea, there is already a dynamic and non-plastic model of wheat architecture available in the literature (Adel-Wheat).

The aim of the present study was therefore twofold. First, we developed a dynamic and architectural model of pea morphogenesis, hereafter called L-Pea. In a second step, a virtual mixture of wheat and pea was built up in order to assess the effects of architectural variations on light partitioning within virtual wheat – pea mixtures. To this end, architectural parameters of both models were modified in order to quantify their impact on light partitioning throughout the growing cycle of the mixture.

L-Pea model was implemented in the L-Py and Openalea platforms using the L-systems formalism and Python language. The model accounts for the aerial morphogenesis of pea through a *vegetative* and *growth* module. Based on results obtained in field conditions, the first module describes the initiation of stems, branches as well as the organs which compose the phytomers. The second module is devoted to simulate the growth of the vegetative organs which were initiated in the vegetative module. The kinetic of organ elongation (stipules, internodes, petioles) is assumed to follow the non-linear β growth function. Parameters of the β function were derived from a specific experiment carried out in controlled conditions.

A tripartite simulator was then built up from L-Pea, ADEL-Wheat and CARIBU, a radiative transfer model. The architectural parameters of both models, selected as a function of their contribution to the Leaf Area Index (LAI), height and geometry, were then modified in order to generate contrasting architectures of wheat and pea.

By scaling-down our analysis at plant scale, we showed that architectural parameters can significantly affect light partitioning. In particular, the number of branches and the internode length appeared as crucial factors that determine the ability of the component species to compete for light. The present results also show that the architectural parameters have contrasting effects on light partitioning depending on the considered species and stage of development. The present study provides information for building up the architecture of ideotypes suited to multi-specific stands.

1 Introduction

The overall interception of radiation by vegetal stands and its partitioning among intercropped species are highly related to the physical structure of the canopy (Ross, 1981b, Sinoquet et Caldwell, 1995, Barillot *et al.*, 2012a) emerging from the architecture of the individuals growing within the stand (Moulia *et al.*, 1998). Plant architecture is defined as the resultant of i) the inventory of the plant components (decomposition information), ii) the topological relations between these components, and iii) their geometry, given by the organ shape, orientation and spatial position (Godin, 2000). Such a multiscale description of the canopy structure reveals the importance of the architectural parameters as underpinning factors that determine light partitioning within mixed cropped systems.

Contrasting architectures among plants emerge from their genetic variability and phenotypic plasticity, the latter resulting from the environmental conditions and the gene - environment interactions. In the case of wheat – pea mixtures, Barillot *et al.* (2012b) reported that contrasting architectures of pea (*Pisum sativum* L.); in terms of height, kinetics of development and final number of branches and phytomers; mainly arose from the genotypic variability rather than from plasticity between sole and intercrop conditions. Moreover, this variability in the architectural parameters of pea showed to significantly affect light partitioning of virtual wheat – pea mixtures (Barillot *et al.*, 2012a). Regarding wheat (*Triticum aestivum* L.), the variability of its architecture has been described for various cultivars, sowing dates and row orientation, plant density, and nitrogen fertilization regime (Evers *et al.*, 2007, Baccar *et al.*, 2011, Dornbusch *et al.*, 2011). Nevertheless, the effects of contrasting architectural patterns of both wheat and pea on the level of competition for light within mixtures have not been studied. The present work focused on the architectural parameters that composed the Leaf Area Index (LAI), height and geometry of plant, three variables which are known to affect light capture (*e.g.* Sinoquet et Caldwell, 1995, Barillot *et al.*, 2011, Bertheloot *et al.*, 2011, Barillot *et al.*, 2012a).

In the present state of our knowledge, and due to experimental and cost constraints, light partitioning within wheat – pea mixtures cannot be assessed directly by radiation sensors (Sonohat *et al.*, 2002). The only current and feasible alternative is the modelling approach which involves various concepts and formalisms. For instance, Corre-Hellou *et al.* (2009) adapted the crop model STICS (Brisson *et al.*, 2009) in order to simulate nitrogen accumulation and crop growth in pea – barley intercrops based on the turbid medium paradigm. Other approaches, such as the Functional – Structural Plant Models (FSPMs, Vos *et al.*, 2010, DeJong *et al.*, 2011), have been proved to be well suited for studying light partitioning within contrasting canopies (Barillot *et al.*, 2011). FSPMs allow to take into account the explicit architecture of plants and its dynamical interactions with physiological processes and environmental conditions. As a consequence, these models can be considered as pertinent frameworks for assessing the effects of architectural parameters on light partitioning among the component species of intercropping systems.

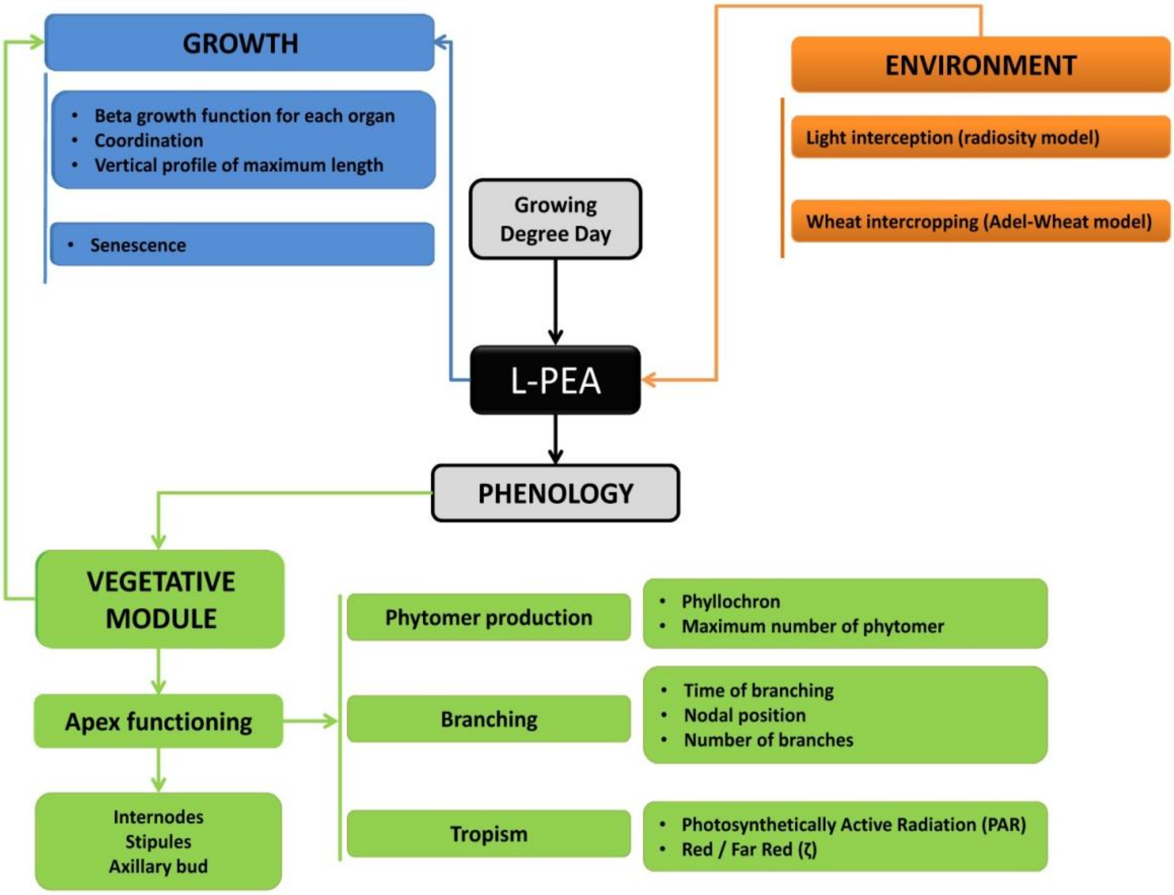

Figure 1: Conceptual representation of L-pea model

A dynamic and 3D architectural model of wheat development (Adel-Wheat) has already been proposed by Fournier *et al.* (2003). In previous studies, we built up virtual plants of pea based on digitizations performed at particular stages of development (Barillot *et al.*, 2011, Barillot *et al.*, 2012a). However, to our knowledge, an equivalent model for pea has not been developed up to now.

The aim of the present study is twofold. First, we developed a dynamic and architectural model of pea development, hereafter called L-Pea. This model is mainly based on the results described in Barillot *et al.* (2012b). In a second step, L-Pea and Adel-Wheat models were coupled in order to assess the effects of architectural variations on light partitioning within virtual wheat – pea mixtures. To this end, architectural parameters of both models were modified in order to quantify their impact on light partitioning throughout the growing cycle of the mixture. Architectural parameters were chosen as a function of their contribution to the Leaf Area Index (LAI), height and geometry of plant.

2 Model description

2.1 Functional aspects of plant morphogenesis

In the present model, the development of pea architecture is modelled as a function of the growing degree day (GDD) cumulated since sowing (base temperature = 0°C). L-pea model is based on thermal time, as heat units have shown to be relevant references when dealing with plant development including pea. Indeed, Turc and Lecoeur (1997) showed that the rates of primordium initiation and production of expanded leaves in pea presented similar responses to air temperature. At each time step of the model, the increment of thermal time can be constant or provided by the meteorological data recorded during an experiment. This option thus allows to model the development of pea architecture as a function of meteorological variations. Thermal time is thus driving the phenology of pea which is first described in a *vegetative module* (Figure 1). The elongation and coordination of the organs generated by the *vegetative module* are then handled by a *growth module*. L-Pea model is also coupled with an *environment module* that enables to compute light interception at each thermal time step. The model is designed to generate stands of user-defined size given by the length and width of the plot, inter-row length and plant density. The stand can be set to be mono- or multi-varietal provided that the input parameters for each cultivar and their proportion in the stand are defined. We also implemented an optional rule which allow to account for the variability measured on a given parameter (*e.g.* phyllochron, number of branches…). The variability results from a selection made on a Gaussian distribution given by the mean value and standard deviation of the parameter.

The structure of L-pea model is based on the concept of plant modularity in order to represent their morphogenesis. Indeed, the development of the above ground architecture of plant can be described as a collection of basic units repeated along the stems.

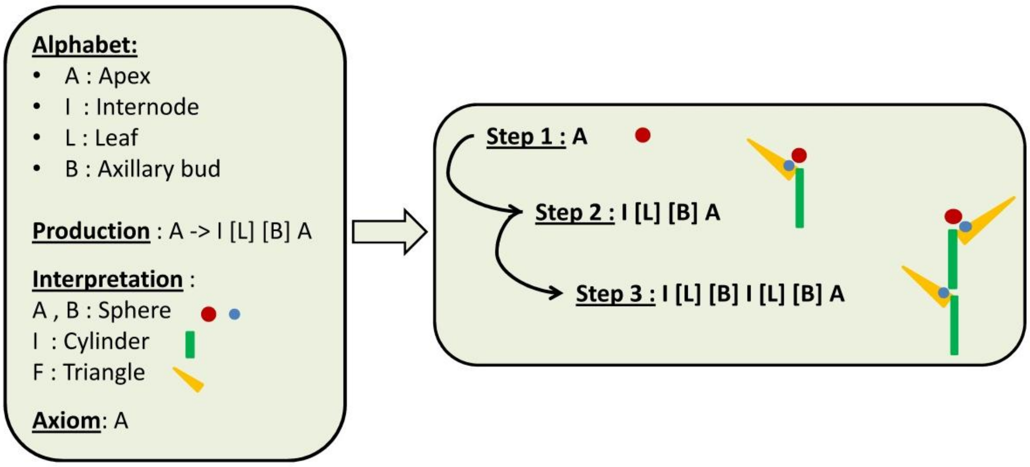

Figure 2: simplified representation of the L-system functioning

These units are called *phytomers* and include an internode, a node, a leaf and an axillary bud (Gray, 1849, White, 1979). The initiation of these phytomers results from the functioning of the shoot apical meristem located at the extremity of the stems. This process is repeated throughout the growing cycle in a more or less regular way thus defining the plastochron (Lyndon, 1998).

2.2 Tools and theoretical concepts of L-systems

The iterative functioning of plants described above constitutes a key paradigm of the architectural plant models such as the Lindenmayer systems (Lindenmayer, 1968). The model of pea development proposed in the present article was developed on the L-Py platform (Boudon *et al.*, 2012) where the L-system formalism (Lindenmayer, 1968, Prusinkiewicz et Lindenmayer, 1990) is coupled with an open source and dynamic programming language called Python. The principle of the L-system consists in describing the plant architecture as a network of elementary subunits called modules which *in fine* represent [virtual] organs (Fournier *et al.*, 2007). This network of modules is assimilated to a string of characters using the L-system formalism. The dynamic of plant morphogenesis is then handled by the central concept of the L-system which consists in the rewriting of the string of characters (Prusinkiewicz et Lindenmayer, 1990, Verdenal, 2009). In the end, a L-system is a mathematical object constituted by i) an alphabet of the different modules, ii) an axiom describing the initial state of the system and iii) production rules which specify the procedure of rewriting. Moreover, specific characters allow to account for a part of the architecture topology, in particular like square brackets (“[“, “]”) used for specifying branches. Finally, the rules for the geometrical interpretation of the string are embedded in the L-systems in order to provide a graphical representation of the plant architecture which is generated as a *mock-up*.

For illustration, a simplified example of L-system is shown in Figure 2 where the apex (*A*) gives rise (→) to an internode (*I*), a leaf (*L*), an axillary bud (*B*) and an on-going apex (*A*). The production rules enable the rewriting of the string of character at steps *2* and *3* while the interpretation rules provide a graphic representation of the L-system.

2.3 Vegetative module

The vegetative module mainly accounts for the production of phytomers by the stems. The ability of pea to produce lateral branches as well as their spatial orientation are also handled by the model. The input parameters used in this module are detailed in Table 1.

Table 1: Parameters of the model

Module	Function	Parameters	Unit	Value	Source
Vegetative	Phyllochron	*phyll**	phytomer°C day^{-1}	0.017 ± 0.003 **Can be adapted to the stem order*	Barillot *et al*. (2012b)
		phyto_max	phytomer	Function of the stem order	Barillot *et al*. (2012b)
	Branching	*nb_branch*	branch	Function of the nodal position	Barillot *et al*. (2012b)
		bud_break	C day	Function of the nodal position	Barillot *et al*. (2012b)
	Tropism	*e*	µmol m^{-2} s^{-1}	$0.05 + 0.2(1 - PAR) + 0.25(1.15 - R/FR)$	Gautier *et al.* (2000)
Growth	Organ length	L_{final}	mm	Function of the organ + nodal position	Fitted to data (Table 2)
		t_{base}	C day	Function of the organ	Fitted to data (Table 2)
		t_{max}	C day	Function of the organ	Fitted to data (Table 2)
		t_{end}	C day	Function of the organ	Fitted to data (Table 2)
	Stipule width	*k*	mm	0.57	Fitted to data
	Senescence	*lifespan*	C day	480	Adapted from Lecoeur (2005)
Light	Red/Far Red (ζ)	*a*	unitless	3.09	Escobar *et al.* (2009)
		b	unitless	1.59	Escobar *et al.* (2009)
		c	unitless	0	Escobar *et al.* (2009)
		d	unitless	1.12	Escobar *et al.* (2009)
		x1	unitless	0	Escobar *et al.* (2009)
		x2	unitless	2	Escobar *et al.* (2009)

2.3.1 Phyllochron

In L-Pea model, the development of stems has been implemented as a function of the rate of phytomer appearance (phyllochron). At each time step, the optimal number of phytomers (N_{phyto}) of plant p and stem s is estimated as a linear function of the thermal time:

$$Nphyto_{p,s} = \min(phyll_{p,s} * GDD,\ phyto\_max_{p,s}) \qquad \text{Equation 1}$$

where N_{phyto} is the optimal *number of phytomer* at a given thermal time (*GDD*, Growing Degree Day); parameter *phyll* is the rate of phytomer appearance (phytomer C° day^{-1}); *GDD* is the thermal time from emergence and *phyto_max* is the maximum number of phytomers. Parameters *phyll* and *phyto_max* are input parameters of the model which can be specified for each plant (*p*) and stem (s) *i.e.* main stems and each order of lateral branches. At each time step, the model assesses if the current number of phytomers on a given stem is lower than N_{phyto}. If this condition is satisfied, then the apex initiates the production of one or more phytomer(s).

The initiation of a phytomer by the apex (*A*) is then associated to the production (→) of the vegetative organs following the rule:
A (stateA) → I(stateI)[S(stateS)][S(stateS)] [P(stateP)] [B(stateB)] A(stateA)

where *I* refers to an internode, *S* to the two stipules (left and right), *P* to a petiole and *B* to an axillary bud. The arguments in brackets are objects, in the computer science meaning, which bear the state of each organ *e.g.* identification information (the cultivar, plant, stem order and phytomer to which they belong), their age, length or the amount of intercepted light.

2.3.2 Branching

Branching is also handled by the model through two main input parameters (Table 1) which are i) the number of axillary buds (B) located at each nodal position (*nb_branch*) and ii) the time of bud break (*bud_break*). To be precise, axillary buds should be rather called "active buds" as they do not represent the actual number of buds on a nodal position but only the buds which actually lead to the development of a branch. These "axillary buds" are then set inactive until bud break after which they initiate the development of a lateral branch by following the functioning of main stems. This is achieved by turning an inactive module *B* in *A*:

B(stateB) → A(stateA)

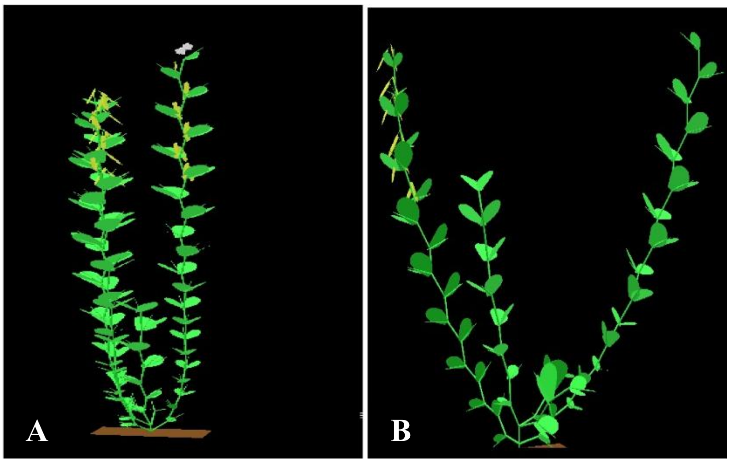

Figure 3: Stem tropism. A: only 10% of light is reaching the apex whereas on B, 90 % of the area of the apex is illuminated thus leading to contrasting orientation of stems

2.3.3 Stem tropism

The spatial orientation of stems is described through a curvature function. Instead of fixing the curvature, the orientation of stems was implemented using a tropism model (Prusinkiewicz et Lindenmayer, 1990) which consecutively reorientates the internode segments according to:

$$\varphi = e\left|\vec{H} * \vec{T}\right| \qquad \text{Equation 2}$$

where φ is the angle between two consecutives internode segments, $\vec{H}$ the orientation of a segment before turning, $\vec{T}$ the tropism direction and *e* an elasticity coefficient that controls the magnitude of the tropism. As proposed by Gautier *et al.* (2000) for another legume species (clover), $\vec{T}$ was orientated upwards. The coefficient *e* is then estimated as a linear function of the Photosynthetically Active Radiation (PAR) and Red/Far Red ratio (R/FR) which are perceived on the stem extremity *i.e.* by the apex:

$$e = 0.05 + 0.2(1 - PAR) + 0.25(1.15 - R/FR) \qquad \text{Equation 3 (Gautier et al., 2000)}$$

In a dense canopy, where the competition for light is high, there is i) a low amount of PAR reaching the apex and ii) a low R/FR ratio due to a strong absorption of the Red wavelengths by the neighbouring leaves (Smith, 1982). As a result, the elasticity coefficient *e* is high and thus the stems are reorientated towards the vertical direction (Figure 3A). In contrast, within open canopies, the apex perceived a large amount of PAR with a high R/FR ratio. In that case, the stems grow more laterally and thus occupy a larger space (Figure 3B).

2.4 Growth module

The growth module accounts for the kinetics of organ elongation as well as their final length. Leaves are also submitted to the senescence process. Details on the parameters used are given in (Table 1).

2.4.1 Organ growth kinetics

The growth of the main aerial vegetative organs *i.e.* internodes, leaves (stipules in the case of semi-leafless cultivars) and petioles is assumed to follow a β growth function (Yin *et al.*, 2003):

$$L = \begin{cases} L_{final}\left(1 + \dfrac{t_{end} - t}{t_{end} - t_{max}}\right)\left(\dfrac{t - t_{base}}{t_{end} - t_{base}}\right)^{\frac{t_{end}-t_{base}}{t_{end}-t_{max}}} & \text{, for } t < t_{end} \\ L_{final} & \text{, for } t \geq t_{end} \end{cases} \qquad \text{Equation 4}$$

where L_{final} (mm) is the final organ length, *t* (°C day) the age of the organ, t_{base} the beginning of organ growth (°C day), t_{max} (°C day) the time at which the maximum rate of organ elongation is reached and t_{end} (°C day) the duration of organ elongation.

Moreover, the parameter t_{base} enables to account for the coordination between the organs that belong to the same phytomer by specifying the beginning of their growth from the initiation of the phytomer. The final length reached by organs (L_{final}) is implemented in the model as a function of the phytomer rank.

2.4.2 Senescence

In L-pea model, shoot senescence only concerns leaves (stipules) and is implemented following the concept of leaf lifespan. Values of leaf lifespan were derived from Lecoeur (2005). Leaves are thus removed through senescence once their lifetime has elapsed (Table 1).

2.5 Geometrical interpretation of the model

Rules for the geometrical interpretation are implemented in the model in order to allow the virtual reconstruction of each organ. Internodes and petioles were associated to generalized cylinders. Stipules were reconstructed from a library of about 200 geometrical objects stemming from photographs used to extract the stipule shape. At each time step of the model, the geometrical objects are resized according to the organ length which is calculated from Equation 4. The parameters required for this equation are directly obtained from the modules (objects) associated to each organ at the time of their production by the apex (L-system rule described in the *phyllochron* subsection). Finally, the width of stipules ($W_{stipule}$) is derived from allometric rules:

$$W_{\text{stipule}} = k * L_{\text{stipule}} \qquad \text{Equation 5}$$

where k is the allometric coefficient and $L_{stipule}$ is stipule length.

3 Material and methods

Initial values of the input parameters required by L-Pea model were obtained in two separate experiments during which the morphogenesis and growth of pea were characterized.

3.1 Phenology and architecture

Most of the data used in the vegetative module of L-Pea model (Table 1) was obtained from a field experiment conducted in 2010-2011 at Brain-sur-l'Authion, Western France (47°26'N, 00°26'W). Details on the experiment and methodology are given in Barillot *et al.* (2012b). Briefly, this study provides information on the morphogenesis of three pea cultivars (Lucy, AOPH10 and 886/01) grown either in sole crop or in mixture with wheat. In the present study, L-Pea model was parameterized with the measurements performed on cultivar Lucy grown in mixture with wheat.

For each plant, the number of visible phytomers (unfolding leaf) was recorded for each vegetative axis (main stems and branches) throughout the growing cycle.

Table 2: Parameters of the β growth function fitted to the growth of the vegetative organ of pea. Parameters have been normalized by the time of emergence of the first organ (t_{base} of stipules).

	Vegetative organ		
β growth parameters (°C day)*	Internode	Petiole	Stipule
t_{base}	34.88	18.38	0
t_{max}	87.71	112.80	71.28
t_{end}	171.51	171.04	197.66

* *Last parameter of the β function (L_{final}) is described in* Figure 5.

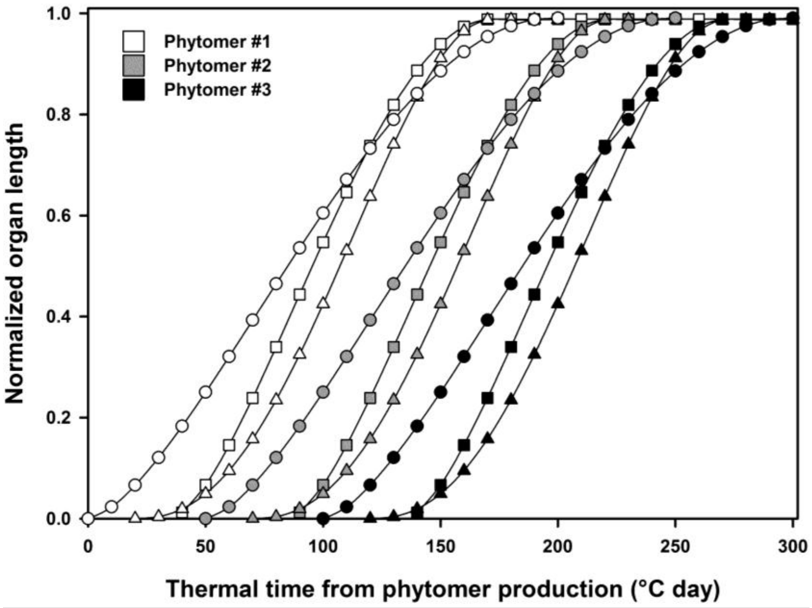

Figure 4: Normalized elongation of vegetative organs as a function of thermal time. The simultaneous growth of stipules (circles), internodes (squares) and petioles (triangles) are shown for three consecutive phytomers. Kinetics were obtained from the adjustments of the β function on measurements of organ elongation (parameters are available in Table 2).

The delay between two successive visible leaves was thus defining the phyllochron. This result was then used for estimating the parameter *phyll* used in the vegetative module (Equation 1). The final number of phytomers (*phyto_max*) was also measured from this experiment and parameterized for main stems and lateral branches. Measurements carried out in Barillot *et al.* (2012b) were finally used to implement the number of branches produced at each nodal position (*nb_branch*) as well as their time of emergence (*bud_break)*.

3.2 Growth of the vegetative organs

The growth of the vegetative organs of cultivar Lucy was assessed in a specific experiment carried out in a growth cabinet in 2012 in Angers, France (47°27’N, 00°32’W). Seeds of cultivar Lucy were sown in 2L individual plastic pots filled with soil. In order to ensure pea nodulation, each plant was inoculated with a solution of *Rhizobium leguminosarum* P221 at 2.2×10^9 bacteria L^{-1}. Pea plants were then moved to a growth cabinet with 80% relative humidity and watered when necessary. Plants were grown under 250 $\mu mol\ m^{-2}\ s^{-1}$ of PAR with a 16 h photoperiod provided by metal halide lamps (HQI 400 W, Osram, France). The temperature in the growth cabinet was maintained at 22°C and 18°C for day and night respectively.

Measurements of internode, stipule and petiole length were performed daily on 10 plants from their emergence to the end of their vegetative growth (in average 1100 GDD). Kinetics of organ elongation (normalized by their final length) were then individually fitted with a non-linear function inspired from the β integral (Equation 4) using GraphPad Prism (GraphPad Software, La Jolla California USA). This experiment was also carried out on a leafy cultivar (US13), in order to characterize the growth of leaflets. These results are however not included in the present study.

Normalized parameters of the β function adjustments (Equation 4) are detailed in Table 2 for each vegetative organ, thus characterizing their coordination. The results of the experiment showed that the development of phytomers was initiated by the emergence of stipules ($t_{base} = 0$ °C day) which started to grow earlier than petioles and internodes (Table 2). Indeed petioles and internodes initiated their growth 18.38 and 34.88 GDD after the stipules respectively. These results also show that about three phytomers were growing simultaneously on the stems (Figure 4).

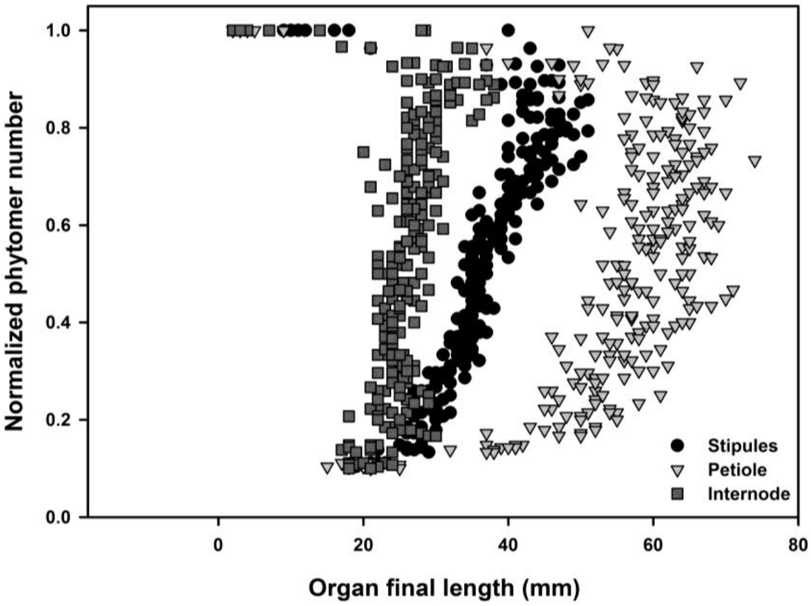

Figure 5: final length of vegetative organs as a function of the phytomer rank

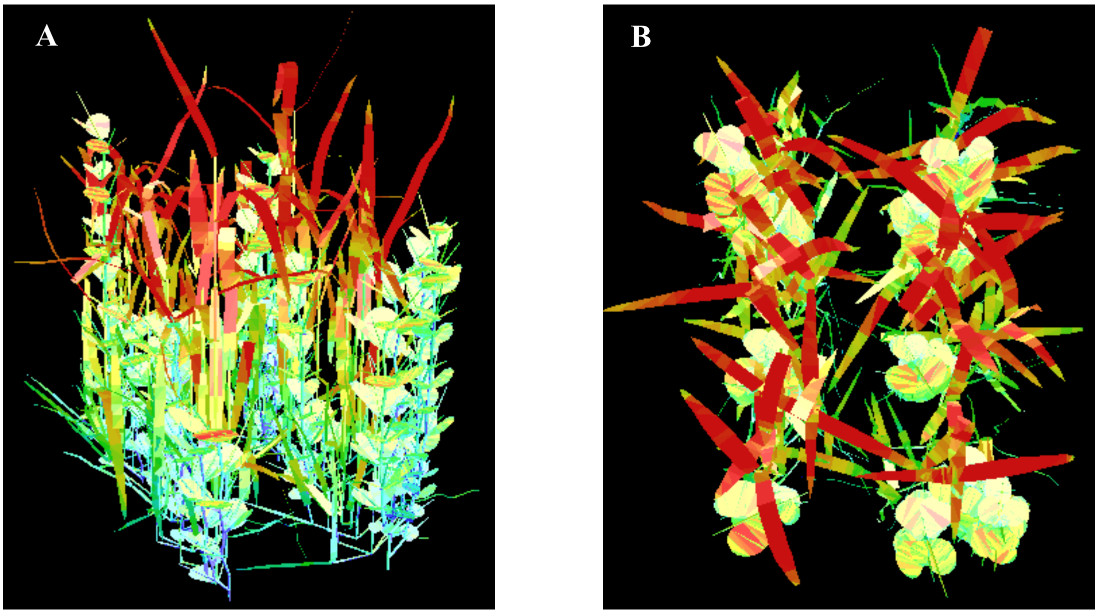

Figure 6: Illustrations of a virtual wheat – pea mixture in a horizontal (A) and vertical (B) view. The gradient of colour is a function of the light intercepted by organs (from blue to red).

The final length reached by organs (L_{final}) is shown in Figure 5 as a function of the phytomer rank. The vertical distribution of the final length of stipules and petioles showed a triangular profile with maximum values (51 and 74 mm respectively) reached in the upper part of the stem. In average, the final length of internodes reached 25.5 mm and was more uniformly distributed compared to petioles and stipules.

Finally, the results obtained on stipule growth were used to estimate the allometric relation between their length and width (parameter k, Equation 5). The relation was performed on all stipules whatever their developmental stage:
where $W_{stipule}$ and $L_{stipule}$ are the width and length of the stipule respectively.

$$W_{\text{stipule}} = 0.57 * L_{\text{stipule}}, \ (\mathrm{R}^2 = 0.95) \qquad \text{Equation 6}$$

4 Modelling light partitioning within wheat – pea mixtures

4.1 ADEL-Wheat model

Virtual wheat plants were obtained from a dynamic and 3D architectural model of wheat development which does not account for the phenotypic plasticity (Fournier *et al.*, 2003). This model is available on the Openalea platform (Pradal *et al.*, 2008). The dataset was derived from an experiment carried out by Bertheloot *et al.* (2009) where wheat (cultivar Caphorn) was grown in field conditions under low nitrogen fertilization at a density of 250 plants m^{-2}.

According to the literature (*e.g.* Corre-Hellou *et al.*, 2006, Naudin *et al.*, 2010), increasing the nitrogen availability in a cereal - legume mixture enhances the dominance of the cereal species over the legume. In order to have a substantial proportion of pea at harvest, wheat – pea mixtures are usually grown under low nitrogen conditions. The input parameters of both ADEL-Wheat and L-Pea models which were used to build up the virtual mixtures are thus closed to the agronomic practices encountered in Western Europe.

4.2 Virtual wheat – pea mixtures: coupling L-Pea with ADEL-Wheat model

L-pea model was then implemented into the Openalea platform in order to generate the virtual wheat – pea mixtures (Figure 6). Wheat and pea mock-ups were merged in scene graphs using the PlantGL graphic library (Pradal *et al.*, 2009). Simulations were processed from 0 to 2000 GDD with a time step of 50 GDD. Inter-row space of mixtures was 0.17 m with a final density of 125 plants m^{-2} for wheat and 45 plants m^{-2} for pea *i.e.* 50 % of the optimal density of each crop as encountered in agricultural practices in Western Europe (Corre-Hellou *et al.*, 2006). The component species were mixed within each row in virtual mixtures of 0.14 m^2 (18 and 6 plants of wheat and pea respectively).

Table 3: Architectural parameters selected for modifying the species LAI, height and geometry.

	Variable		
Species	LAI	Height	Geometry
Wheat	Tillering	Internode length	-
Pea	Branching	Internode length	Leaf inclination

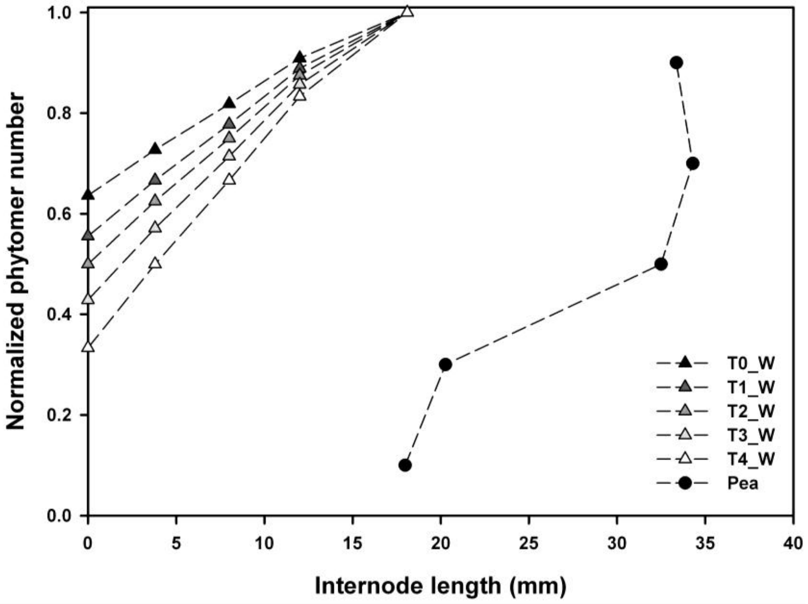

Figure 7: Vertical profile of the final length of internodes of wheat and pea as used in the reference simulation. Internode length of wheat is defined for main stem (T0) and four tillers (T1 to T4).

4.3 Light partitioning within virtual wheat – pea mixtures

Virtual wheat – pea mixtures were coupled with a radiative transfer model that allows to estimate the dynamic of PAR partitioning at each step of the growing cycle. Calculation of light interception was provided by the nested radiosity model *Caribu* developed by Chelle and Andrieu (1998). Computations were performed considering only diffuse radiations according to the Uniform OverCast (UOC) sky radiation distribution (Moon et Spencer, 1942). Diffuse radiations were approximated by a set of light sources on a sky vault discretized in 20 solid angle sectors using the spherical coordinates, including 5 zenith angles (18, 36, 54, 72, 90 degrees) and 4 azimuths. Light interception was computed for each direction and then integrated over the sky vault by summing up the weighted values coming from the 20 directions. The R/FR ratio needed for the calculation of the tropism of pea stems (Equation 3) was estimated using the functional relations between the photon flux coming from the Morphogenetically Active Radiation (MAR) and the transmitted PAR as proposed by Escobar-Gutiérrez *et al.* (2009):

$$R/_{FR} = \left[c^b + (d^b - c^b) * \frac{1 - e^{-a(PAR-x1)}}{1 - e^{-a(x2-x1)}}\right]^{1/b} \qquad \text{Equation 7}$$

where parameters a and b implicitly define the shape of the curve; $x1$ and $x2$ are respectively the minimum and maximum values of *PAR* for which the model is fitted and parameters c and d are the values of the R/FR ratio at $x1$ and $x2$ respectively (see Table 1).

4.4 Building contrasting wheat and pea architectures

The architectural parameters of both models were modified in order to quantify their impact on light partitioning throughout the growing cycle of the mixture. Architectural parameters were selected as a function of their contribution to the Leaf Area Index (LAI), plant height and geometry (Table 3).

The architectural parameters of both models were first set so that there is the slightest possible difference of LAI and height dynamics between wheat and pea. This first simulation is hereafter called *reference simulation* (Figure 7 and Table 4). All simulations were carried out by modifying one parameter at a time, which represents a total of 21 simulations (Table 4). To this end, both L-pea and ADEL-Wheat models were modified so that the random selections made on the parameters of the models were identical among the successive simulations. Different plants of pea and wheat were therefore selected in order to constitute the mixture and were then reproduced at each successive simulation, the only difference being the tested architectural parameter.

Variations by 25 and 50 % of the architectural parameters were then applied on the basis of the reference simulation. Variations of LAI were obtained by increasing and decreasing the lateral development of wheat and pea (tillering and branching respectively). Similar modifications of the final length of internodes were performed in order to affect plant height.

Table 4: Variations of the input parameters of ADEL-Wheat and L-Pea models used in the experimental design.

	Wheat		Pea		
Variation	Tillering	Internode length (mm)	Branching	Internode length (mm)	Leaf inclination (°)
+ 50 %	+	=	=	=	=
	=	+	=	=	=
	=	=	+	=	=
	=	=	=	+	=
	=	=	=	=	+
+ 25 %	+	=	=	=	=
	=	+	=	=	=
	=	=	+	=	=
	=	=	=	+	=
	=	=	=	=	+
Reference	4	See Figure 7	4	See Figure 7	45
- 50 %	-	=	=	=	=
	=	-	=	=	=
	=	=	-	=	=
	=	=	=	-	=
	=	=	=	=	-
- 25 %	-	=	=	=	=
	=	-	=	=	=
	=	=	-	=	=
	=	=	=	-	=
	=	=	=	=	-

In previous studies (Barillot *et al.*, 2011, Barillot *et al.*, 2012a), leaf inclination was suspected to have minor effects on light partitioning within virtual wheat – pea mixtures compared to the species LAI and height. In order to validate this assumption, light partitioning was also estimated within mixtures where leaf inclination of pea was increased or decreased by 25 and 50 %.

The effects of each architectural parameter (*simul*) on plant LAI, height, geometry and later on light partitioning were compared to the reference simulation (*Ref*) by calculating the relative variations:

$$Relative\ variation = (Ref - Simul)/Ref \qquad \text{Equation 8}$$

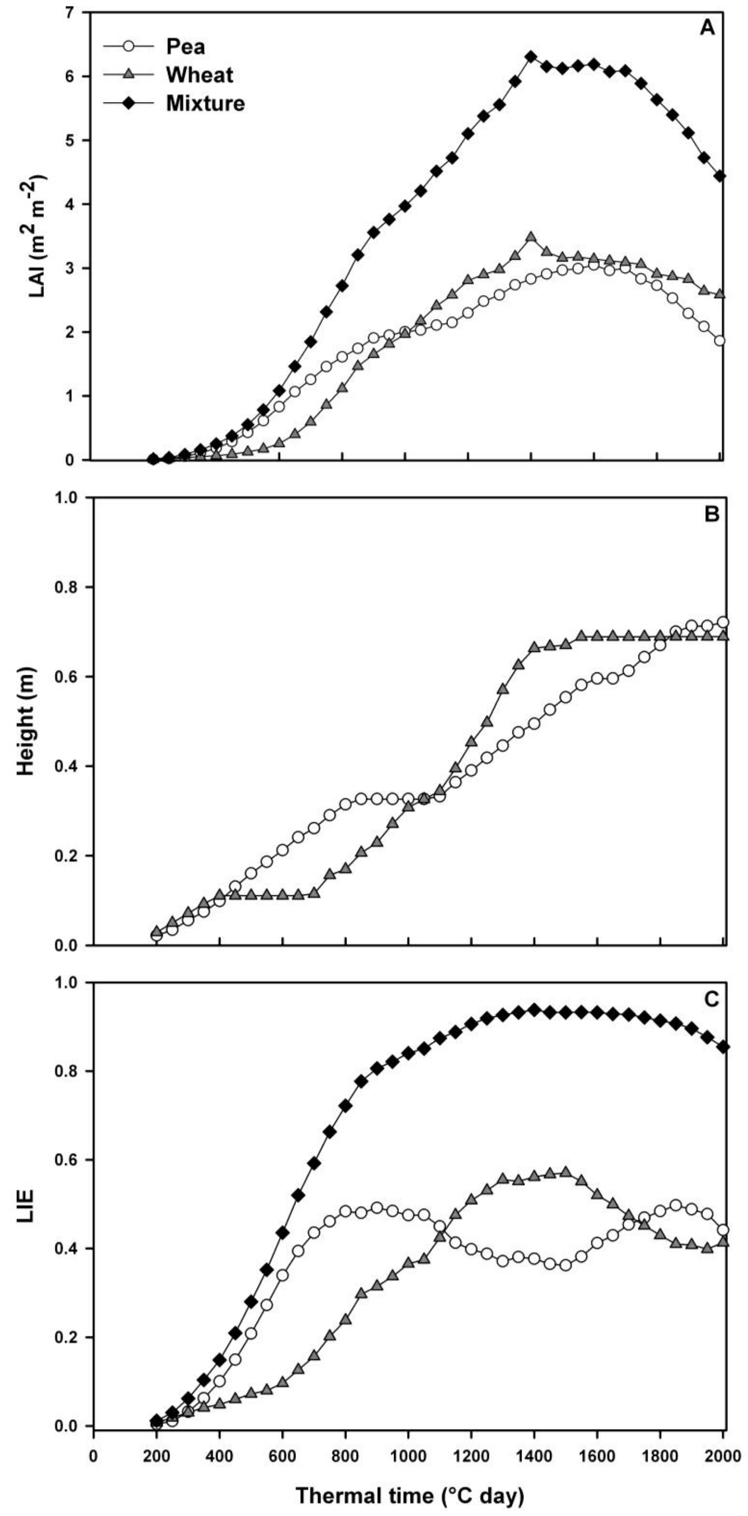

Figure 8: Dynamics of LAI (A), plant height (B) and Light Interception Efficiency (LIE, C) of the reference simulation as a function of thermal time. The dynamics are shown for the overall mixture as well as for the component species (pea and wheat).

5 Effects of species architecture on light partitioning

5.1 Reference simulation

Dynamics of the species LAI, height and light interception for the reference simulation are shown in Figure 8. The development of the LAI of both mixture and component species (Figure 8A) followed typical sigmoidal kinetics (*e.g.* Corre-Hellou *et al.*, 2009) from 200 to 2000 GDD after sowing. The mixture reached a maximum of 6.30 $m^2 m^{-2}$ of LAI at 1400 GDD. After 1700 GDD, the senescence of wheat and pea leaves gave rise to a decrease in the mixture LAI up to 4.45 $m^2 m^{-2}$ at 2000 GDD. As expected, the contributions of both component species to the LAI of the mixture were similar throughout the growing cycle. Indeed, the LAI developed by pea was slightly higher than that of wheat in the early stages of development and the dominance of wheat in terms of LAI did not exceed 0.66 $m^2 m^{-2}$ between 1000 and 2000 GDD.

The vertical dominance of the species (Figure 8B) followed similar dynamics as those observed for LAI. Indeed, pea was taller than wheat from 400 to1000 GDD although its height remained constant at 0.33 m from 800 GDD. This steady state is explained by i) the death of the main stem which frequently occurs in winter pea cultivars (Barillot *et al.*, 2012b) thus causing the cessation of vertical growth and ii) the growth delay of branches which overtopped the main stems from 1100 GDD. The development of branches therefore led to the resumption of the vertical growth of pea up to 0.70 m. The height of wheat also remained 0.11 m from 400 to700 GDD *i.e.* during the tillering stage. Then, the elongation of internodes was responsible for the linear vertical growth of wheat up to a maximum of 0.70 m at 1400 GDD. As a consequence, wheat was the tallest of the two species from 1100 to 1800 GDD.

Light Interception Efficiency (LIE) of the mixture rapidly increased from 200 to 1000 GDD (Figure 8C). After 1200 GDD, the LIE of the canopy was stabilized and intercepted more than 90 % of the incident light. As a consequence of a combined dominance on wheat in terms of LAI and height, pea captured in average 62 % of the light intercepted by the overall mixture up to 1100 GDD. Then, wheat exhibited a vertical dominance over pea up to 1700 GDD (Figure 8B). As a result, the contribution of wheat to the interception of light by the mixture was in average 57 % during this period of time.

5.2 Variations of LAI and height in response to the architectural alterations

5.2.1 LAI

The modifications made on the architectural parameters of both pea and wheat resulted in contrasting LAI compared to the reference simulation. Figure 9 shows the relative variations in the LAI of pea and wheat.

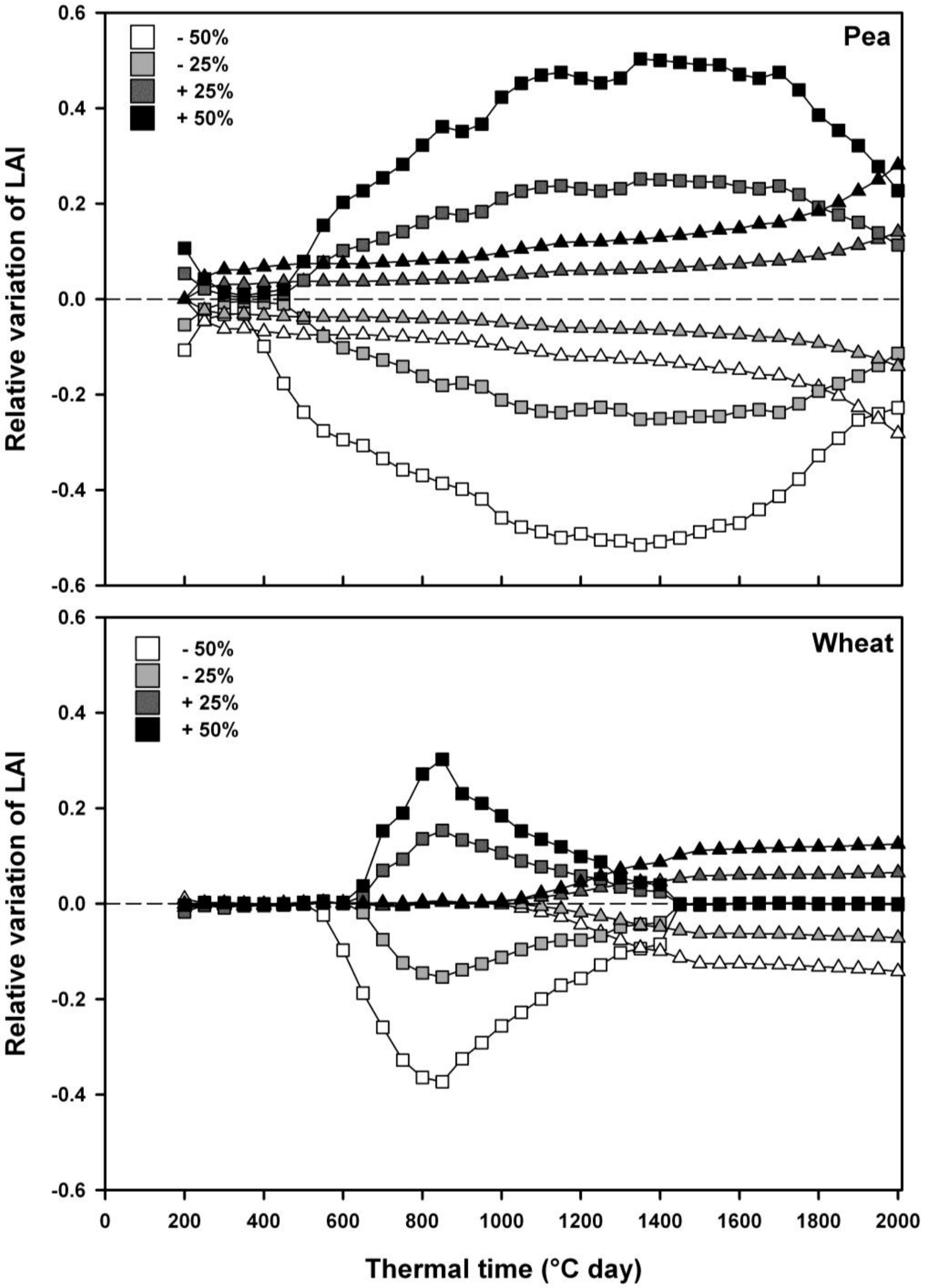

Figure 9: Relative variations in pea (up) and wheat (down) LAI estimated from the reference simulation. The variations were obtained through a modification of i) the number of branches or tillers (squares) and ii) internode length (triangles). The gradient of colours indicates the amplitude of the modifications applied on the architectural parameters.

The modifications related to the number of branches of pea dramatically affected the LAI from the early stages of development (400-500 GDD). Moreover, similar absolute variations in LAI were observed after an increase or a decrease of the number of branches. As expected, the highest variations of LAI were observed when the number of branches was increased or decreased by 50 % (+0.50 and – 0.52 respectively). In a lesser extent, Figure 9 also reveals that the modifications of the final length of internodes affected the LAI of pea. This effect was particularly marked during the latest stages of the growing cycle, mainly due to the foliar senescence which decreased the contribution of leaf to the LAI. Indeed, the relative variation in LAI reached at most ± 0.28 at 2000 GDD consecutively to an increase or a decrease of the internode length by 50 %. This emphasises that variations of internode length can significantly affect the LAI of pea, although the effects are lower than those resulting from the modifications of the number of branches. Barillot *et al.* (2012a) also reported that the internodes can constitute up to 10 % of the green area of pea.

The architectural modifications made on wheat also led to strong relative variations in LAI although the amplitude was lower than for pea (Figure 9). Moreover, changes in the number of tillers started to alter the LAI of wheat from 600-650 GDD. Maximum relative variations of 0.30 and -0.37 in wheat LAI were observed at 850 GDD and respectively resulted from an increase and a decrease of the tillers by 50%. The relative variations in LAI rapidly decreased from 900 GDD for wheat plants altered in the number of tillers. From 1450 GDD, these plants even reached the same levels of LAI as those of the reference simulation. This was the result of the foliar senescence that occurred on each stem of wheat. As mentioned for pea, modifications of internode length also affected the relative variations in wheat LAI mainly from 1000 GDD. Indeed, altering the final length of internodes by -50 or +50 % led to maximum relative variations of -0.14 and 0.13 respectively.

5.2.2 Height

As expected, modifications of internode length induced strong variations of plant height for both pea and wheat species (Figure 10). Similar absolute variations in pea and wheat height were observed after an increase or a reduction of the internode length.

Modifications of the final internode length of pea resulted in strong variations of height throughout the growing cycle. Maximum relative variations were observed at 1800 GDD (0.47) and 1850 GDD (– 0.47) consecutively to an increase and decrease by 50 % of the internode length respectively. The number of branches did not affect pea height, except when branches were reduced by 50 %. Indeed, pea plants were temporarily shorter than those of the reference simulation from 1150 to 1600 GDD. This was related to the removal of the earlier branches that constitute the top of the canopy at 1000 GDD (Figure 8).

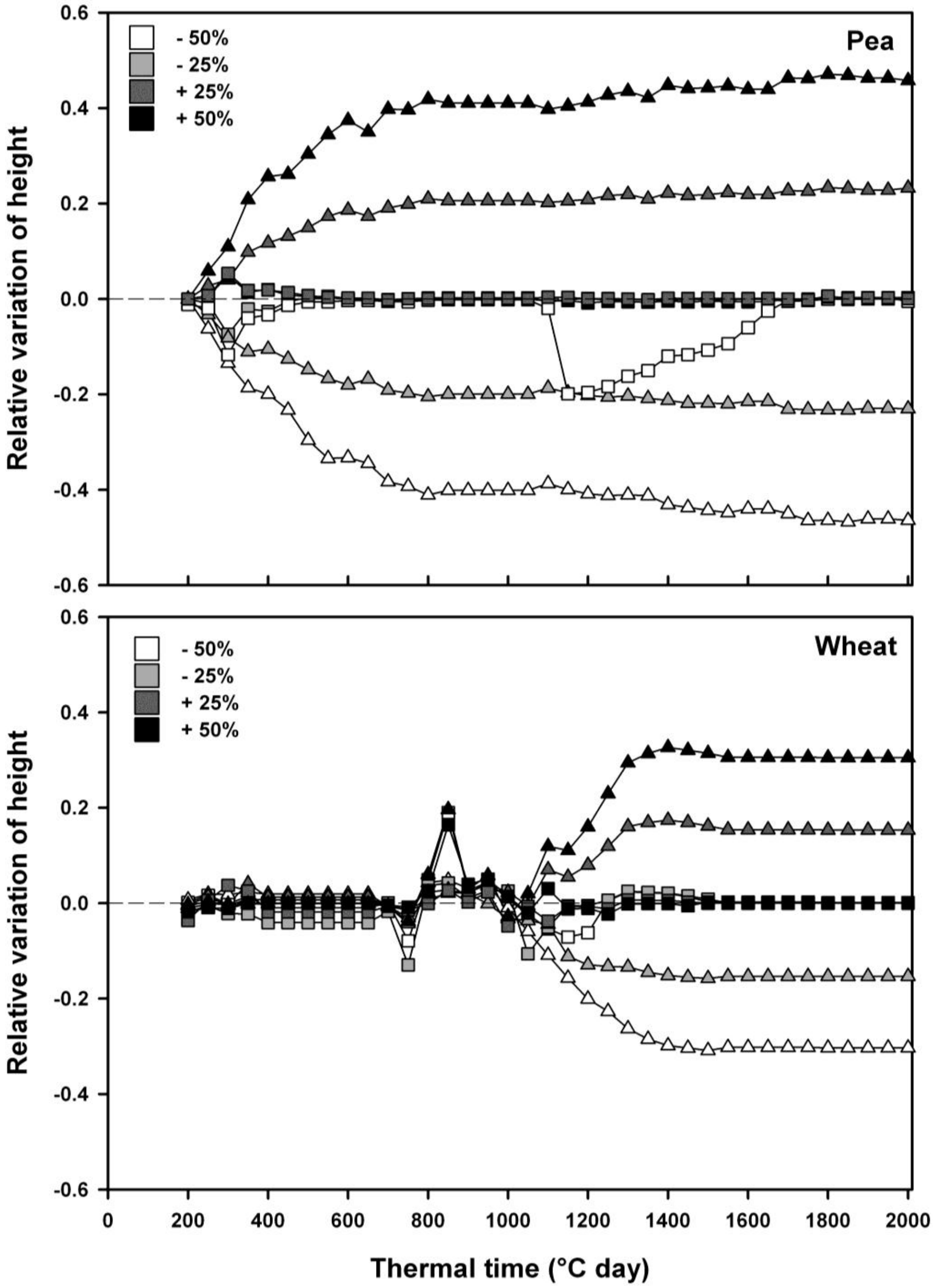

Figure 10: Relative variations in pea (up) and wheat (down) height estimated from the reference simulation. The variations were obtained through a modification of i) the number of branches or tillers (squares) and ii) internode length (triangles). The gradient of colours indicates the amplitude of the modifications applied on the architectural parameters.

Then, due to the growth of the following branches, pea plants reached a similar height to those of the reference simulation (relative variation was close to zero from 1700 GDD).

For wheat, the effects of internode length on plant height were observed later than for pea (1100 GDD). This was related to the elongation of wheat internodes which started from 1000 GDD. Maximum relative variations were observed at 1400 GDD (0.33) and 1500 GDD (-0.31) consecutively to an increase and decrease by 50 % of the internode length respectively. The modifications performed on the number of tillers did not cause any significant variation in plant height.

5.3 Effects of the architectural modifications on light partitioning

Scaling-down to the architectural parameters allowed us to directly assess their effects on light partitioning. The architectural modifications applied on branching, internode length and leaf inclination had contrasting effects on light partitioning among wheat and pea (Figure 11). Interestingly, the modifications carried out on the architectural parameters led to asymmetric responses of light partitioning whereas they symmetrically affected the LAI and plant height (Figure 9 and Figure 10). Indeed, Figure 11 shows that increasing or reducing the value of the architectural parameters (branching, height, and leaf inclination) did not result in similar absolute variations of light partitioning but rather defined asymmetric responses.

5.3.1 *Branching*

Alterations of the ability for lateral development (production of branches and tillers) conducted to higher variations of light partitioning when they were carried out on pea. This was in particular the case when the number of branches was reduced. These architectural modifications decreased dramatically the proportion of light intercepted by pea from the early stages of development (500 GDD). In that case, the light captured by pea continued to decline throughout the growing cycle and was minimal between 1000 and 1500 GDD *i.e.* during the period of time when wheat was the dominant species in terms of LAI (Figure 8A). Therefore, a reduction in the branches of pea by 25 and 50 % respectively caused a maximum loss of light interception of 17 and 53 % at 1250 GDD (Figure 11, right column). In contrast, increasing the number of branches resulted in lower variations of light partitioning than those caused by the reduction of branches. Moreover, a similar gain of light capture was observed consecutively to an increase of branches by 25 or 50 %, both led to a maximum gain of light capture by 20 % at 1400 GDD. Although the branches of pea were increased in these simulations, it did not appear to be sufficient to balance the domination of wheat in light capture at this stage of development, as wheat still intercepted 54 % of the light cptured by the overall mixture.

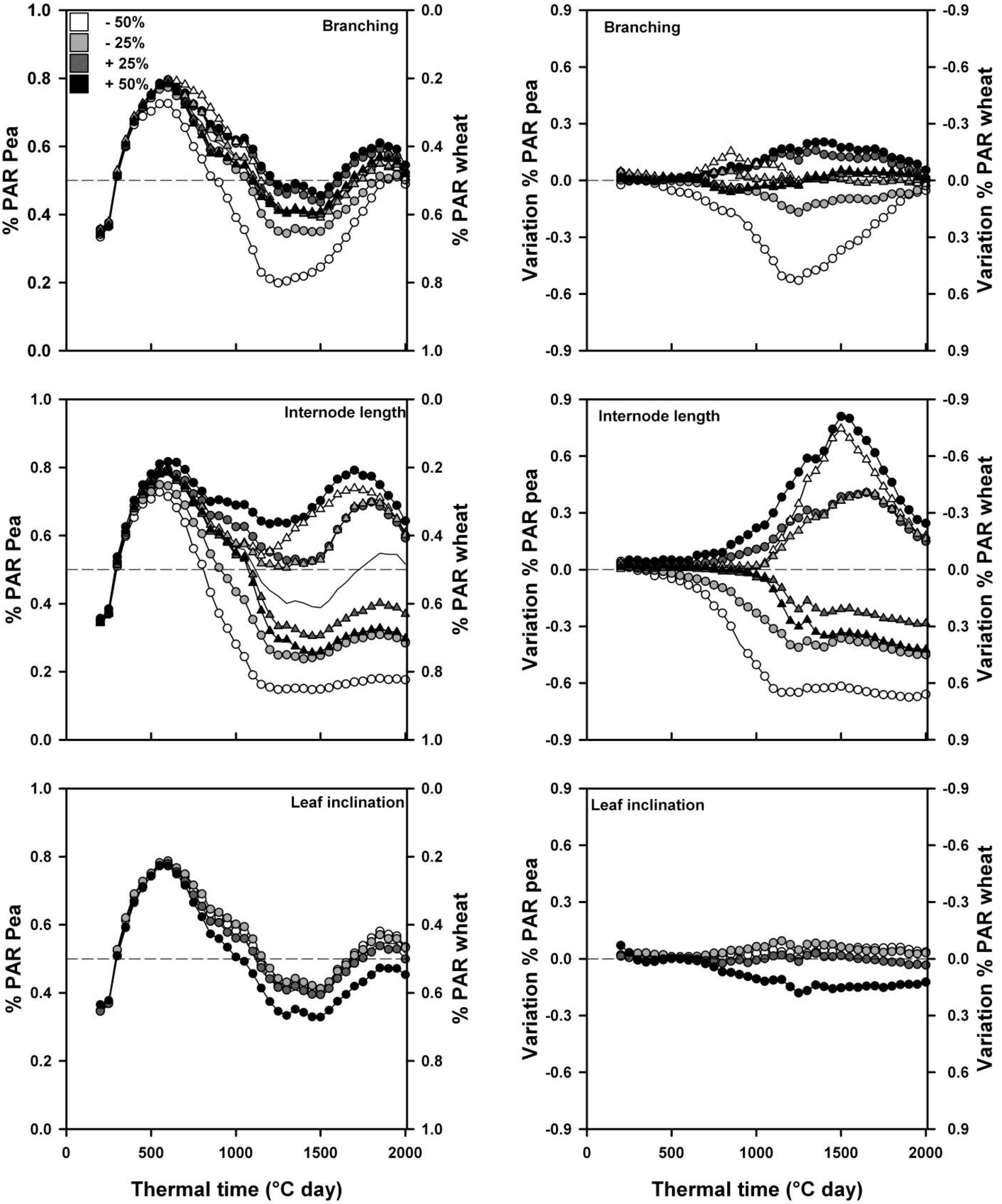

Figure 11: Dynamics (left) and relative variations (right, estimated from the reference simulation) of light partitioning (%PAR) among pea and wheat. Values of light partitioning are complementary between pea and wheat and those of relative variations are opposite. The number of branches, internode length and leaf inclination (only for pea) were altered for both pea (circles) and wheat (triangles) following the gradient of colours.

Compared to the modifications of branches in pea, the number of tillers of wheat led to slight relative variations of light partitioning (at most 15 %). The variations of wheat LAI that were observed in Figure 9 (30-35 %) had therefore little effects on light partitioning meaning that other determinant parameters were involved.

5.3.2 *Internode length*

Modifications of internode length appeared to have the most dramatic effects on light partitioning compared to branching (at most a gain in light capture of 81 % and a loss of 65 %). For both pea and wheat, longer internodes resulted in a strong increase of light interception compared to the reference simulation. These effects were observed from 500 GDD for pea and 1000 GDD for wheat (beginning of internode elongation of wheat). A strong asymmetry was found in the variations of light partitioning between plants subjected to an increase of their internode length and those whose internodes were reduced, especially from 1500 GDD. From this stage of development, the effects of internode length which had led to a gain of light interception by pea (longer internodes for pea and shorter for wheat) started to decline up to 2000 GDD, whereas those which enhanced light interception of wheat were maintained.

Increasing the internode length of pea or reducing those of wheat led to the highest variations of light capture. Figure 9 also shows that similar variations of light partitioning could result from an increase of the internode length of pea or an equivalent reduction of wheat internodes. For instance, at 1500 GDD, pea increased its capture of light by i) 81 % with 50 percent longer internodes and ii) 75 % when wheat internodes were shortened by 50 %. In contrast, increasing the internode length of wheat did not bring a similar gain of light interception as an equivalent reduction of pea internodes. Wheat was the most dominant species for light capture when internodes of pea were shortened by 25 and 50 % (respectively up to 76 and 85 % of light captured by wheat). Increasing internode length of wheat by 50 % resulted in a similar gain in light interception than decreasing those of pea by 25 %.

5.3.3 *Leaf inclination of pea*

Alterations of the inclination of pea leaves clearly had minor effects on light partitioning compared to those applied on branching and internode length. Nevertheless, increasing leaf inclination by 50 %, *i.e.* leaves become more erected, appeared to affect light partitioning as it decreased light capture of pea by 18 % at most.

5.4 Light partitioning as a function of the ratios of the species LAI and height

The results described above have shown the dynamic of light partitioning in response to contrasting plant architectures. As illustrated in Figure 9 and Figure 10, the architectural alterations induced a large range of variation of the component species LAI and height.

Table 5: Particular stages of the development of wheat and pea

Growing Degree Day	**Species**	
	Wheat	**Pea**
500	4 unfolded leaves	4 unfolded leaves
850	End of tillering	End of branching Branch elongation
1000	Beginning of stem elongation	Branch elongation
1500	Beginning of flowering	Flowering
2000	Grain filling - maturity	Maturity

The following section is thus aimed to analyse the relationships between light partitioning and the variations of both ratios of species LAI and height. To this end, five particular stages of development were selected (Table 5). The first dates represent the vegetative stages of the two species and their lateral development (branching, tillering). Then phases of vertical elongation were selected as well as the flowering period of wheat and pea. Relationships between light partitioning and the species LAI and height were finally studied in the last stages of development (2000 GDD). For each of these stages of development, Figure 12 shows the relation between light partitioning and i) the ratio of LAI_{pea} / LAI_{wheat} and ii) the ratio of $Height_{pea}$ / $Height_{wheat}$.

At 500 GDD, the architectural modifications which were performed mainly affected pea height (Figure 9 and Figure 10). Therefore, the ratio of the component species LAI did not show strong variations in response to the architectural modifications (except when the number of branches was reduced by 50 %). The ratio of LAI stayed in favour of pea (3.31 ± 0.37) which intercepted 75 % of the light captured by the overall mixture. In contrast, variations of internode length of pea led to different height ratios ranging from 1 to 1.92. Light partitioning appeared to be linearly correlated to the height ratio from this early stage of development. Indeed, short internodes of pea favoured the capture of light by wheat whereas increasing internode length reinforced the dominance of pea (up to 78 % of light interception). In spite of the modification of internode length, pea stayed the dominant species, mainly due to its larger LAI compared to wheat.

At 850 GDD, wheat and pea developed contrasting levels of LAI in response to the architectural variations and were exhibiting equivalent ratios of height to those described at 500 GDD (Figure 12). This resulted in strong variations of light partitioning as pea intercepted from 51 to 71 % of the light captured by the mixture. At 850 GDD, the component species had completed their lateral development, so any modification in the number of branches or tillers affected the balance of LAI between wheat and pea. Whether the architectural variations were applied on pea or wheat, the ratios of LAI were similar, although they are obviously affected in opposite ways. As shown at 500 GDD, light partitioning was also affected by the height ratio between the component species. As wheat had not started to elongate, the modifications of internode length applied on wheat did not modify its height and had therefore no effect on light partitioning.

The relation between light partitioning and the ratio of LAI appeared to be no longer linear at 1000 GDD (Figure 12). On the one hand, decreasing the number of branches or tillers by 50 % affected the ratio of LAI (0.55 and 1.37 respectively) which strongly impacted light partitioning (39 % of light captured by pea in the first case against 61 % in the last one). On the other hand, increasing the number of branches and tillers still modified the ratio of LAI but it only resulted in slight variations of light partitioning. The sharing of light among the component species was however linearly related to the variations of the height ratio which originated from the modifications of the internode length of pea.

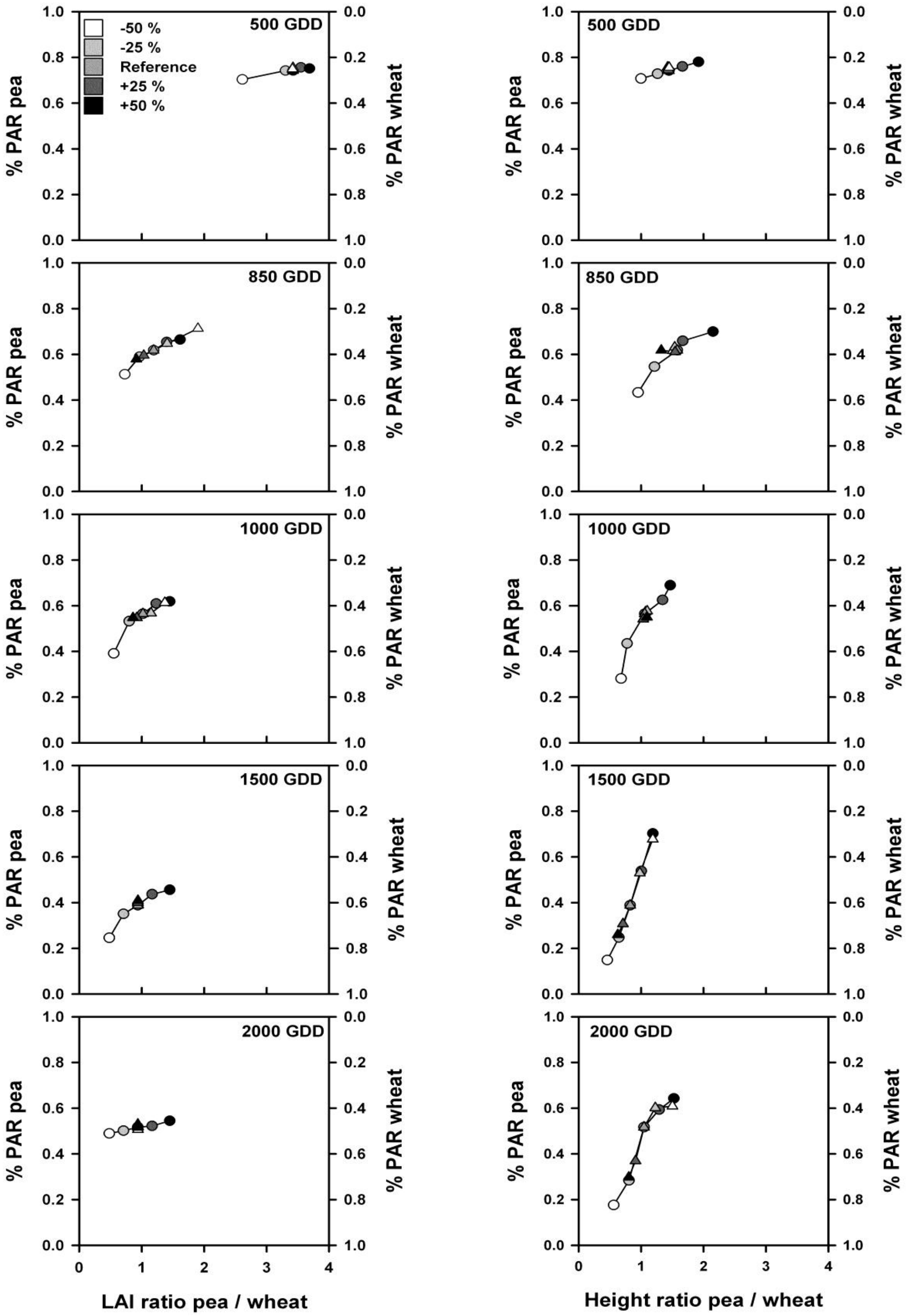

Figure 12: relation between light partitioning (%PAR) and the species ratios of LAI (left) and height (right) at five particular stages of development. Variations of the ratios of LAI and height resulted from architectural alterations applied on pea (circles) and wheat (triangles) following the gradient of colours.

Indeed, pea intercepted from 28 to 69 % of the incident light when its internodes were modified by ±50 %.

During flowering (1500 GDD), a non-linear relationship was also observed between the ratio of LAI and light partitioning among wheat and pea (Figure 12). This was in particular the case for the modifications applied on the number of branches developed by pea. The ratio of LAI between the component species remained constant whatever the initial number of tillers developed by wheat, mainly due to foliar senescence. However, the beginning of internode elongation of wheat generated contrasting vertical dominance with pea (height ratio ranged from 0.63 to 1.20). At this developmental stage, the modifications applied on internode length led to similar variations of the height ratio and light partitioning whatever they were made on pea or wheat. The height ratio strongly affected light partitioning which ranged from 15 to 70 % of the light captured by pea.

The effect of the variations of the species LAI on light partitioning continued to decline at maturity (2000 GDD, Figure 12). The ratio of LAI ranged from 0.48 to 1.45 but only increased light interception of pea by 10 %. Variations of the height ratio at this stage of development were similar to those observed at 1500 GDD. These variations ranged from 0.56 (after decreasing the internode length of pea by 50 %) to 1.52 (after increasing the internode length of pea by 50 % or when wheat internodes were reduced by 50 %). However, the relation with light partitioning also appeared to become non-linear, in particular for the strongest alterations of internode length (± 50 %)

6 Discussion

Light partitioning in multi-specific stands is a crucial issue for managing the balance between the component species as well as determining the final yield of the mixture (Ofori et Stern, 1987, Keating et Carberry, 1993, Sinoquet et Caldwell, 1995, Malézieux *et al.*, 2009, Louarn *et al.*, 2010). The present study was therefore directed at assessing the effects of architectural parameters on light partitioning within wheat – pea mixtures. This was achieved by using the approach of Functional Structural Plant Models (FSPM) that allows to take into account the explicit architecture of plants in relation with their functioning and environment (for a review see DeJong *et al.*, 2011), light in the present study. Such an approach also presents the advantage to provide direct access to the architectural parameters identified for modification. Indeed, statistical models providing a simplified description of the canopy (*e.g.* the turbid medium approach, Rimmington, 1985, Faurie *et al.*, 1996, Lantinga *et al.*, 1999, Sinoquet *et al.*, 2000, Tsubo et Walker, 2002) would have only allowed to assess the effects of integrated parameters *i.e.* LAI and plant geometry and in some cases the LAI distribution and plant height . Therefore these statistical models cannot be used to infer the response of light partitioning to the variation of architectural parameters described at plant scale.

Moreover, FSPMs have been shown to be more suitable tools for estimating light interception in heterogeneous canopies compared to the turbid medium approach that uses the Beer-Lambert-law (Sonohat *et al.*, 2002, Combes *et al.*, 2008, Barillot *et al.*, 2011). Heterogeneous stands can result from non-random dispersion of foliage or canopies with a strong vertical structure. Such conditions can be encountered in multi-specific stands or after architectural modifications, such as those performed in the present study. FSPMs could also be used for further analysis of plant growth in complex conditions that are not accessible to conventional experimentation. Virtual plant models generally required numerous input parameters that in particular implied measurements of plant geometry using the 3D digitizing for instance (Moulia et Sinoquet, 1993). Such models also conducted to longer computation times than simplified approaches. However, in order to tackle such limitations, Louarn *et al.* (2012) proposed an intermediate approach based on simple envelope reconstructions of plants and which can infer light partitioning in mixtures, provided that height and vertical leaf area distribution gradients are characterised.

6.1 L-pea model

The present study has therefore required to develop an architectural and dynamic model of the aerial development of pea, a 3D model of wheat being already available in the literature (Fournier *et al.*, 2003). L-pea model accounts for the vegetative development of pea mainly based on data derived from an experiment carried out in wheat – pea mixtures (Barillot *et al.*, 2012b). The growth of the vegetative organs was characterized from a specific experiment conducted in controlled conditions. As shown in a previous study (Barillot *et al.*, 2012b), pea exhibited low plasticity of its morphogenesis under different growing conditions. We therefore assumed that the characterization of the organ growth in controlled conditions did not affect the underlying hypothesis of the model. Moreover, L-Pea model was used in a comparative study for the assessment of the architectural parameter effects on light partitioning.

The present model was developed using a deterministic approach which was considered to be efficient for assessing the effects of architectural parameters on light partitioning. Indeed, architectural modifications performed with a more mechanistic model, which for instance account for feedbacks between plant growth and its environment, can result in smoothed responses of light interception because of the compensation processes occurring in plants. Such responses, which can result from self-regulated processes (Verdenal *et al.*, 2008), would have made it difficult to assess the effects of individual architectural parameters on light capture. Nevertheless, the tropism of stems, implemented as a function of the quantity and quality of light, is a part of the model that accounts for plant responses to their environment.

Compared to a fixed curvature of stems, we assumed that accounting for stem tropism provides better perspectives for the model in particular for studying the effects of the sowing density which is known to affect branching (Casal *et al.*, 1986, Spies *et al.*, 2010) As mentioned earlier, the response of the stem to light environment was implemented in L-Pea model using the study of Gautier *et al.* (2000) on clover. Supplementary experiments should therefore be conducted in order to characterize the tropism of pea stems (*e.g.* location of the site of perception, duration of the signal necessary to induce a photomorphogenetic response, *etc.*). Although not used in the present study, L-pea model can also handle the intra-specific variability of pea provided that the average value and standard deviation of the parameters are given. As a consequence, virtual stands generated by the model are not composed of a repetition of a mean plant but rather reflect the variability of the studied population. Depending on the user aim, L-pea model can also operate in a more mechanistic approach for studying the functioning of pea (*e.g.* photosynthesis) in relation with its physical structure and environment. This can be easily achieved as parameters and functions of the model are accessible and can be modified in order to implement new functions or input data. The object-oriented development of the model also provides an efficient tool for taking into account the feedbacks between plant growth and environment. Indeed, each organ carries information on its own state (age, position, length, light captured…) which therefore enables to regulate the organ growth according to the amount of intercepted light or other environmental factors *e.g.* Tardieu *et al.* (1999) for a model of leaf expansion.

6.2 Architecture and light partitioning

The present study provides novel information on the sensitivity of light partitioning to the architecture of the component species by scaling-down our analysis to plant scale. This characterization was also conducted throughout the growing cycle of the mixture which allows to dynamically assess the effects of the architectural parameters on light partitioning. Some previous studies were also aimed to analyse the relationships between light partitioning and the simplified or explicit architecture of component species (Sinoquet et Caldwell, 1995, Louarn *et al.*, 2012). However, these studies focused on integrated parameters (height, LAI, geometry) which do not allow to discriminate the effect of explicit architectural parameters defined at plant scale. For instance, internode length affects both plant LAI and height. In a similar way, LAI can be affected by several architectural parameters (*e.g.* branching or leaf length). In contrast with previous studies, the results shown in the present work were not obtained by modifying one architectural parameter while maintaining the others constant throughout the growing cycle. The alterations were made on a single architectural parameter at a time, but the other parameters of the model were still following their dynamic, as specified by the hypotheses of the model.

The effects of single-parameter on plant architecture and light partitioning were then compared to a reference simulation designed to provide equivalent dynamics of LAI and height between pea and wheat. This reference simulation therefore constituted a theoretical case that does not necessarily reflect the behaviour of wheat – pea mixtures grown in field conditions.

As reported in several studies (Sinoquet et Caldwell, 1995, Barillot *et al.*, 2011, Barillot *et al.*, 2012a, Louarn *et al.*, 2012), the present results also confirmed that light partitioning is highly related to the ratio of the component species LAI and height. However, this relation appeared to be dependent on the considered species (wheat or pea) and was not constant throughout the growing cycle. Light partitioning in the early stages of development was strongly related to the contribution of the component species to the LAI of the mixture. Species with high ability for branching therefore exhibited high competitiveness for light capture. As the mixture was growing, the component species started to interact and the inter-specific competition [for light] began thus enhancing the importance of the species height. Moreover, when the species started their vertical growth (internode elongation), the relation between light partitioning and the ratio of the component species LAI became no longer linear. These non-linear relationships reveal that the architectural variations that affected the LAI of developed plants had lower effects on the partitioning of light than in the earlier stages of development and was rather related to the height ratio. In the late stages of the growing cycle, the height reached by each species of the mixture strongly determined their ability to capture light. These results are consistent with a previous study carried out on virtual wheat – pea mixtures derived from the digitization of several pea cultivars grown in greenhouse conditions (Barillot *et al.*, 2012a).

The present study also showed that leaf inclination could affect light partitioning but in a lower extent than alterations of branching or internode length. These results therefore strengthen the hypothesis risen in previous studies on digitized wheat – pea mixtures (Barillot *et al.*, 2011, Barillot *et al.*, 2012a). However, Sarlikioti *et al.* (2011b) reported that leaf inclination in tomato impacted the distribution of light interception rather than its total light interception. As shown by Barillot *et al.* (2012a) for pea, the present study illustrated that LAI and plant height are strongly related to the number of lateral branches and internode length respectively. The number of branches (for pea) or tillers (for wheat) was a determinant parameter of the species LAI from their emergence to the beginning of foliar senescence. The latter appeared to significantly decrease the LAI of the component species in particular for wheat. As a consequence, alterations of the number of tillers had lower effects on light partitioning than those performed on the number of branches of pea. Moreover, light partitioning was found to be highly sensitive to the internode length of the component species. This was in particular the case for pea as the alterations of internode length resulted in a large range of light partitioning levels which may lead to asymmetric competition for light (Schwinning et Weiner, 1998, Louarn *et al.*, 2010).

Although they were significant, the effects of wheat internode length on light capture were less marked. Internode elongation of wheat started later than for pea thus leading to lower competitiveness for light capture. Cici *et al.* (2008) also reported that in chickpea, changes in the internode length did not lead to the highest competitiveness against sowthistle compared to phyllochron variations. On contrast, Lemerle *et al.* (2001) reviewed that wheat plants with longer internodes would have an enhanced competitive ability for light capture against weeds. It therefore appears that the assessment of the effects of an architectural parameter (*e.g.* branching, internode length or leaf inclination) on light partitioning must be carried out in regard of i) the whole plant structure (*i.e.* the other architectural parameters), as well as ii) the component species morphogenesis. Indeed, determinant parameters that are known to affect the interception of light in pure stands (*e.g.* number of tillers or internode length) do not necessarily have the same quantitative effects in multi-specific stands, depending on the behaviour of the component species.

The present results show that branching and internode length have contrasting effects on LAI and plant height depending on the species and stage of development. Similar conclusions have therefore been observed on the way that these two architectural parameters affected light partitioning. Generally, the modifications performed on the architecture of pea caused higher variations of light partitioning than those applied on wheat. Supplementary simulations should therefore be conducted in order to assess the effects of other architectural parameters of wheat *e.g.* leaf and sheath length which would also affect the LAI and plant height. Moreover, the modifications performed on branching and internode length resulted in symmetric absolute variations of LAI and height respectively. However, they triggered asymmetric variations of light partitioning meaning that i) other ranges of variation of the architectural parameters should be tested in order to better explore the responses of light partitioning and ii) interactions with other parameters should be taken into account *e.g.* leaf area distribution and clumping (Ross, 1981c, Lantinga *et al.*, 1999).

7 Conclusion

The present study provides quantitative information on the effects of LAI and plant height on light partitioning within wheat – pea mixtures. By scaling-down our analysis at plant scale, we showed that branches as well as internode length are crucial architectural parameters that determine the ability of the component species to compete for light. These two architectural traits therefore appeared as important levers for driving competition for light within wheat – pea mixtures. To this aim, we should consider and take advantage of the studies that have already been done by geneticists and breeders on such architectural traits (*e.g.* for pea, Arumingtyas *et al.*, 1992, Kusnadi *et al.*, 1992). Further simulations should however be conducted in order to assess the effects of other architectural parameters on light partitioning such as leaf size, rate of senescence or the dynamic of morphogenesis.

Increasing the number of parameters would then require to perform a sensitivity analysis that enables to hierarchize the parameters while accounting for their interactions.

The present study required to develop a 3D and dynamic architectural model of pea which is, to our knowledge, the first available one in the literature. This has led to the construction of a complex modelling framework integrating the architectural models of pea and wheat as well as a light model based on the radiosity approach. Further works on L-Pea model could also be conducted in order to implement the reproductive stages of pea (Truong et Duthion, 1993, Roche *et al.*, 1998) as well as the development of the root system which is also an important parameter of the component species competitiveness for the capture of water and nitrogen (*e.g.* Ozier-Lafontaine *et al.*, 1998, Corre-Hellou *et al.*, 2006). Such a framework could also be used to assess the functioning of wheat – pea mixtures in regard with the dispersion of diseases as epidemiological models are available for wheat and pea grown in pure stands (*e.g.* Le May *et al.*, 2005, Robert *et al.*, 2008). This virtual environment therefore appeared to be suitable for building-up the architecture of ideotypes suited to multi-specific stands.

8 Literature cited

Arumingtyas EL, Floyd RS, Gregory MJ, Murfet IC. 1992. Branching in *Pisum*: inheritance and allelism tests with 17 *ramosus* mutants. *Pisum Genetics,* **24**: 17-31.

Baccar R, Fournier C, Dornbusch T, Andrieu B, Gouache D, Robert C. 2011. Modelling the effect of wheat canopy architecture as affected by sowing density on *Septoria tritici* epidemics using a coupled epidemic-virtual plant model. *Annals of Botany,* **108**: 1179-1194.

Barillot R, Combes D, Chevalier V, Fournier C, Escobar-Gutiérrez AJ. 2012a. How does pea architecture influence light sharing in virtual wheat - pea mixtures? A simulation study based on pea genotypes with contrasting architectures. *AoB PLANTS*: Accepted.

Barillot R, Combes D, Pineau S, Huynh P, Escobar-Gutiérrez AJ. 2012b. Comparison of the morphogenesis of three genotypes of pea (*Pisum sativum*) grown in pure stands and wheat-based intercropping systems. *Agronomy for Sustainable Development*: UNDER REVIEW.

Barillot R, Louarn G, Escobar-Gutiérrez AJ, Huynh P, Combes D. 2011. How good is the turbid medium-based approach for accounting for light partitioning in contrasted grass-legume intercropping systems? *Annals of Botany,* **108**: 1013-1024.

Bertheloot J, Andrieu B, Fournier C, Martre P. 2009. Modelling Nitrogen Distribution in Virtual Plants, as Exemplified by Wheat Culm During Grain Filling. . *Proceedings of the 2009 Plant Growth Modeling, Simulation, Visualization, and Applications.* Beijing, China, IEEE Computer Society.

Bertheloot J, Cournède P-H, Andrieu B. 2011. NEMA, a functional–structural model of nitrogen economy within wheat culms after flowering. I. Model description. *Annals of Botany,* **108**: 1085-1096.

Boudon F, Pradal C, Cokelaer T, Prusinkiewicz P, Godin C. 2012. L-Py: an L-System simulation framework for modeling plant development based on a dynamic language. *Frontiers in Plant Science,* **3**.

Brisson N, Launay M, Mary B, Beaudoin N. 2009. *Conceptual basis, formalisations and* *parameterization of the STICS crop model.* Collection “Update Science and Technologies”: Versailles.

Chelle M, Andrieu B. 1998. The nested radiosity model for the distribution of light within plant canopies. *Ecological Modelling,* **111**: 75-91.

Cici SZ-H, Adkins S, Hanan J. 2008. A Canopy Architectural Model to Study the Competitive Ability of Chickpea with Sowthistle. *Annals of Botany,* **101**: 1311-1318.

Combes D, Chelle M, Sinoquet H, Varlet-Grancher C. 2008. Evaluation of a turbid medium model to simulate light interception by walnut trees (hybrid NG38 x RA and *Juglans regia*) and sorghum canopies (*Sorghum bicolor*) at three spatial scales. *Functional Plant Biology,* **35**: 823-836.

Corre-Hellou G, Faure M, Launay M, Brisson N, Crozat Y. 2009. Adaptation of the STICS intercrop model to simulate crop growth and N accumulation in pea–barley intercrops. *Field Crops Research,* **113**: 72-81.

Corre-Hellou G, Fustec J, Crozat Y. 2006. Interspecific competition for soil N and its interaction with N_2 fixation, leaf expansion and crop growth in pea–barley intercrops. *Plant and Soil,* **282**: 195-208.

DeJong TM, Da Silva D, Vos J, Escobar-Gutiérrez AJ. 2011. Using functional–structural plant models to study, understand and integrate plant development and ecophysiology. *Annals Of Botany,* **108**: 987-989.

Dornbusch T, Baccar R, Watt J, Hillier J, Bertheloot J, Fournier C, Andrieu B. 2011. Plasticity of winter wheat modulated by sowing date, plant population density and nitrogen fertilisation: Dimensions and size of leaf blades, sheaths and internodes in relation to their position on a stem. *Field Crops Research,* **121**: 116-124.

Escobar-Gutiérrez AJ, Combes D, Rakocevic M, de Berranger C, Eprinchard-Ciesla A, Sinoquet H, Varlet-Grancher C. 2009. Functional relationships to estimate Morphogenetically Active Radiation (MAR) from PAR and solar broadband irradiance measurements: The case of a sorghum crop. *Agricultural and Forest Meteorology,* **149**: 1244-1253.

Evers JB, Vos J, Fournier C, Andrieu B, Chelle M, Struik PC. 2007. An architectural model of spring wheat: Evaluation of the effects of population density and shading on model parameterization and performance. *Ecological Modelling,* **200**: 308-320.

Faurie O, Soussana JF, Sinoquet H. 1996. Radiation interception, partitioning and use in grass -clover mixtures. *Annals of Botany,* **77**: 35-46.

Fournier C, Andrieu B, Buck-Sorlin G, Evers JB, Drouet JL, Escobar-Gutiérrez AJ, Vos J. 2007. Functional-structural modelling of Gramineae. In: Vos J, Marcelis LFM, de Visser PHB, Struik PC, Evers JB eds. *Functional-Structural Plant Modelling in Crop Production.* Springer.

Fournier C, Andrieu B, Ljutovac S, Saint-Jean S. 2003. ADEL-wheat: A 3D architectural model of wheat development. *Proceedings of the 2003 Plant Growth Modeling, Simulation, Visualization, and Applications.* Beijing, China, IEEE Computer Society.

Gautier H, Mech R, Prusinkiewicz P, Varlet-Grancher C. 2000. 3D Architectural Modelling of Aerial Photomorphogenesis in White Clover (*Trifolium repens* L.) using L-systems. *Ann Bot,* **85**: 359-370.

Godin C. 2000. Representing and encoding plant architecture: A review. *Annals of Forest Science,* **57**: 413-438.

Gray A. 1849. On the composition of the plant by phytons, and some applications of phyllotaxis. In 438-444.

Keating BA, Carberry PS. 1993. Resource capture and use in intercropping: solar radiation. *Field Crops Research,* **34**: 273-301.

Kusnadi J, Gregory M, Murfet IC, Ross JJ, Bourne F. 1992. Internode length in *Pisum*: phenotypic characterisation and genetic identity of the short internode mutant Wt11242. *Pisum Genetics,* **24**: 64-74.

Lantinga EA, Nassiri M, Kropff MJ. 1999. Modelling and measuring vertical light absorption within grass-clover mixtures. *Agricultural and Forest Meteorology,* **96**: 71-83.

Le May C, Schoeny A, Tivoli B, Ney B. 2005. Improvement and validation of a pea crop growth model to simulate the growth of cultivars infected with Ascochyta blight (*Mycosphaerella pinodes*). *European Journal of Plant Pathology,* **112**: 1-12.

Lecoeur J. 2005. Developpement vegetatif. In: Munier-Jolain N, Biarnes V, Chaillet I, Lecoeur J, Jeuffroy M-H eds. *Agrophysiologie du pois protéagineux.* Paris, Inra-Quae.

Lemerle D, Gill GS, Murphy CE, Walker SR, Cousens RD, Mokhtari S, Peltzer SJ, Coleman R, Luckett DJ. 2001. Genetic improvement and agronomy for enhanced wheat competitiveness with weeds. *Australian Journal of Agricultural Research,* **52**: 527-548.

Lindenmayer A. 1968. Mathematical models for cellular interactions in development I. Filaments with one-sided inputs. *Journal of Theoretical Biology,* **18**: 280-299.

Louarn G, Corre-Hellou G, Fustec J, Lô-Pelzer E, Julier B, Litrico I, Hinsinger P, Lecomte C. 2010. Déterminants écologiques et physiologiques de la productivité et de la stabilité des associations graminées-légumineuses. *Innovations Agronomiques,* **11**: 79-99.

Louarn G, Da Silva D, Godin C, Combes D. 2012. Simple envelope-based reconstruction methods can infer light partitioning among individual plants in sparse and dense herbaceous canopies. *Agricultural and Forest Meteorology,* **166–167**: 98-112.

Lyndon RF. 1998. Partitioning the apex: the size of the apical meristem and the primordia. In: Lyndon RF ed. *The shoot apical meristem: its growth and development.* Cambridge university press.

Malézieux E, Crozat Y, Dupraz C, Laurans M, Makowski D, Ozier-Lafontaine H, Rapidel B, de Tourdonnet S, Valantin-Morison M. 2009. Mixing plant species in cropping systems: concepts, tools and models. A review. *Agron. Sustain. Dev.,* **29**: 43-62.

Moon P, Spencer DE. 1942. Illumination from a non-uniform sky. *Illuminating Engineering Society* **37**: 707-726.

Moulia B, Edelin C, Jeuffroy MH, Allirand JM, Loup C, Chartier M. 1998. Premiers éléments d'analyse du développement architectural des herbacées cultivées. In: Maillard P, Bonhomme R eds. *Fonctionnement des peuplements végétaux sous contraintes environnementales.* Paris, France, INRA editions.

Moulia B, Sinoquet H. 1993. Three-dimensional digitizing systems for plant canopy geometrical structure: a review. In: Varlet - Grancher C, Bonhomme R, Sinoquet H eds. *Crop structure and light microclimate.* Paris, INRA editions.

Naudin C, Corre-Hellou G, Pineau S, Crozat Y, Jeuffroy M-H. 2010. The effect of various dynamics of N availability on winter pea-wheat intercrops: Crop growth, N partitioning and symbiotic N2 fixation. *Field Crops Research,* **119**: 2-11.

Ofori F, Stern WR. 1987. Cereal-legume intercropping systems. *Advances in agronomy,* **41**: 41-90.

Ozier-Lafontaine H, Lafolie F, Bruckler L, Tournebize R, Mollier A. 1998. Modelling competition for water in intercrops: theory and comparison with field experiments.

Plant and Soil, **204**: 183-201.

Pradal C, Boudon F, Nouguier C, Chopard J, Godin C. 2009. PlantGL: A Python-based geometric library for 3D plant modelling at different scales. *Graphical Models,* **71**: 1-21.

Pradal C, Dufour-Kowalski S, Boudon F, Fournier C, Godin C. 2008. OpenAlea: a visual programming and component-based software platform for plant modelling. *Functional Plant Biology,* **35**: 751-760.

Prusinkiewicz P, Lindenmayer A. 1990. *The algorithmic beauty of plants.* Springer-Verlag: New-York.

Rimmington GM. 1985. A test of a model for light interception by mixtures. *Australian Journal of Plant Physiology,* **12**: 681-683.

Robert C, Fournier C, Andrieu B, Ney B. 2008. Coupling a 3D virtual wheat (*Triticum aestivum*) plant model with a *Septoria tritici* epidemic model (Septo3D): a new approach to investigate plant–pathogen interactions linked to canopy architecture. *Functional Plant Biology,* **35**: 997-1013.

Roche R, Jeuffroy M-H, Ney B. 1998. A Model to Simulate the Final Number of Reproductive Nodes in Pea (*Pisum sativum* L.). *Annals of Botany,* **81**: 545-555.

Ross J. 1981a. Role of phytometric investigations in the studies of plant stand architecture and radiation regime. In: Ross J ed. *The radiation regime and architecture of plant stands.* The Hague, The Netherlands, Junk, W.

Ross J. 1981b. Spatial distribution of phytoelements in stands. In: Ross J ed. *The radiation regime and architecture of plant stands.* The Hague, The Netherlands, Junk, W.

Sarlikioti V, de Visser PHB, Marcelis LFM. 2011. Exploring the spatial distribution of light interception and photosynthesis of canopies by means of a functional-structural plant model. *Annals Of Botany,* **107**: 875-883.

Schwinning S, Weiner J. 1998. Mechanisms determining the degree of size asymmetry in competition among plants. *Oecologia,* **113**: 447-455.

Sinoquet H, Caldwell MM. 1995. Estimation of light capture and partitioning in intercropping systems. In: Sinoquet H, Cruz P eds. *Ecophysiology of tropical intercropping.* Paris, INRA Editions.

Sinoquet H, Rakocevic M, Varlet-Grancher C. 2000. Comparison of models for daily light partitioning in multispecies canopies. *Agricultural and Forest Meteorology,* **101**: 251-263.

Smith H. 1982. Light quality, photoperception, and plant strategy. *Annual Review of Plant Physiology,* **33**: 481-518.

Sonohat G, Sinoquet H, Varlet-Grancher C, Rakocevic M, Jacquet A, Simon JC, Adam B. 2002. Leaf dispersion and light partitioning in three-dimensionally digitized tall fescue-white clover mixtures. *Plant, Cell and Environment,* **25**: 529-538.

Tardieu F, Granier C, Muller B. 1999. Modelling leaf expansion in a fluctuating environment: are changes in specific leaf area a consequence of changes in expansion rate? *New Phytologist,* **143**: 33-43.

Truong HH, Duthion C. 1993. Time of Flowering of Pea (*Pisum sativum* L.) as a Function of Leaf Appearance Rate and Node of First Flower. *Annals Of Botany,* **72**: 133-142.

Tsubo M, Walker S. 2002. A model of radiation interception and use by a maize-bean intercrop canopy. *Agricultural and Forest Meteorology,* **110**: 203-215.

Turc O, Lecoeur J. 1997. Leaf Primordium Initiation and Expanded Leaf Production are Co-ordinated through Similar Response to Air Temperature in Pea (*Pisum sativum* L.). *Annals of Botany,* **80**: 265-273.

Verdenal A. 2009. *De la simulation de la morphogénèse de l'appareil aérien du ray-grass anglais (Lolium perenne L.).*

Exploration d'un schéma cybernétique inspiré du concept d'auto-organisation et applications., UNIVERSITE DE POITIERS, Poitiers.

Verdenal A, Combes D, Escobar-Gutiérrez AJ. 2008. A study of ryegrass architecture as a self-regulated system, using functional-structural plant modelling. *Functional Plant Biology,* **35**: 911-924.

Vos J, Evers JB, Buck-Sorlin GH, Andrieu B, Chelle M, de Visser PHB. 2010. Functional-structural plant modelling: a new versatile tool in crop science. *Journal of Experimental Botany,* **61**: 2101-2115.

White J. 1979. The Plant as a Metapopulation. *Annual Review of Ecology and Systematics,* **10**: 109-145.

Yin X, Goudriaan J, Lantinga EA, Vos J, Spiertz HJ. 2003. A Flexible Sigmoid Function of Determinate Growth. *Annals of Botany,* **91**: 361-371.

Synthèse

Ce quatrième chapitre a été dédié à la construction d'un **modèle architecturé de pois, L-Pea,** intégrant i) les conclusions issues du premier chapitre, ii) l'approche de modélisation développée au cours des 2ème et 3ème chapitres et iii) les résultats sur la morphogénèse aérienne du pois issus des données présentées lors du 3ème chapitre. Sur la base des conclusions issues du second chapitre, nous avons poursuivi l'analyse du **déterminisme architectural du partage de la lumière** dans les associations blé – pois. L'architecture des plantes virtuelles de blé et de pois a ainsi été modifiée au niveau de paramètres impactant le LAI, la hauteur et les propriétés géométriques, permettant ainsi de quantifier l'impact de ces paramètres sur l'interception du rayonnement de chacune des espèces. Ces travaux ont montré que des paramètres architecturaux définis à l'échelle de la plante (*e.g.* ramifications, entrenœuds…) sont des éléments déterminants de la capacité des plantes à intercepter le rayonnement dans une association blé - pois. L'originalité de cette étude a également résidé dans l'analyse dynamique de l'effet de ces paramètres architecturaux sur le partage du rayonnement, fournissant ainsi des éléments de réflexion sur la conception d'idéotypes adaptés aux cultures multispécifiques.

Discussion générale et perspectives

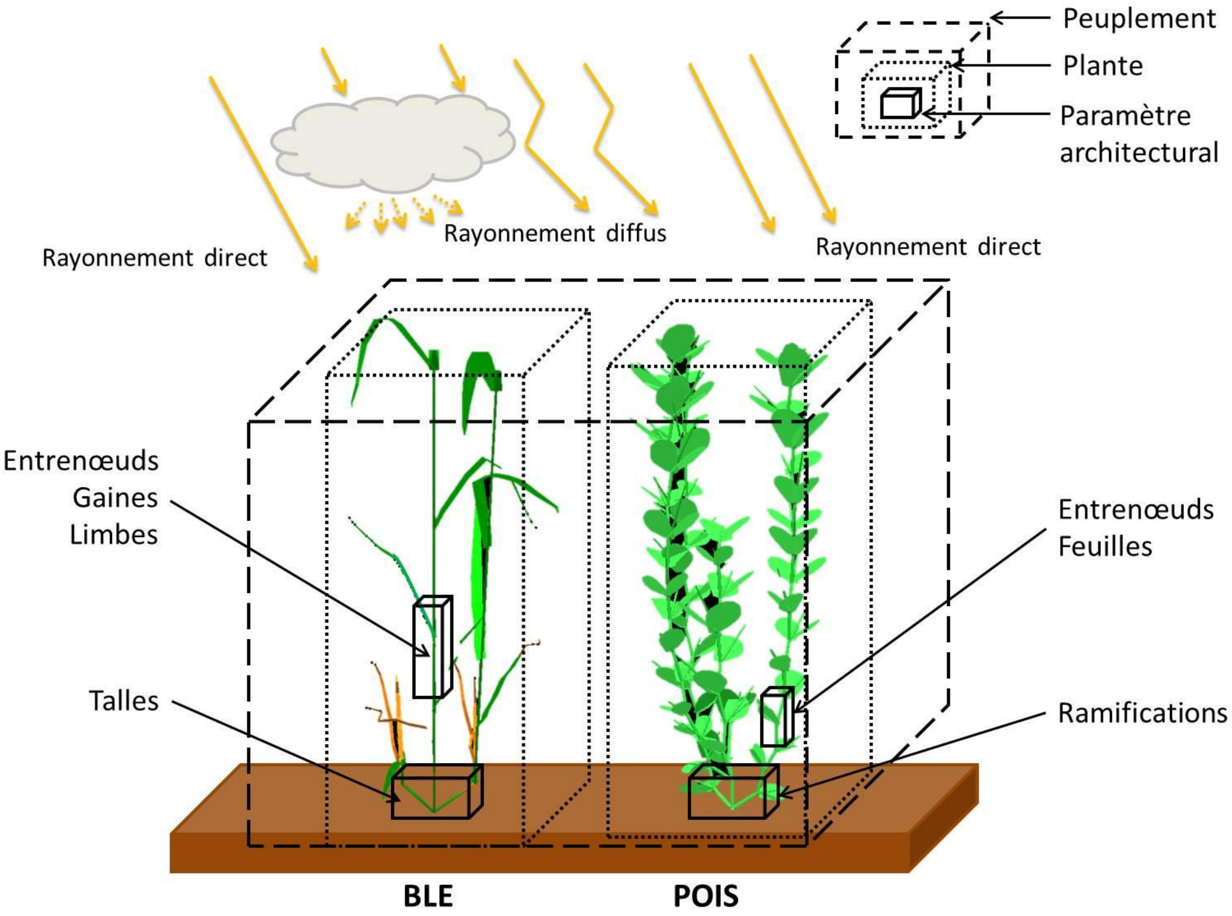

Figure 1 : Analyse multi-échelle du partage de la lumière dans les associations blé-pois. L'interception du rayonnement réalisée au niveau du peuplement ainsi que son partage entre espèce sont liés à la structure physique des individus du couvert. Des paramètres architecturaux définis à l'échelle de la plante (ramifications, entrenœuds…) sont donc des paramètres déterminant du partage du rayonnement entre espèce, affectant ainsi directement la productivité de l'association.

Les objectifs du travail de thèse entrepris ici se proposaient de contribuer i) à l'analyse du déterminisme architectural dans le partage de la lumière dans les associations blé – pois et ii) au développement d'un simulateur de la morphogénèse aérienne des plantes capable de répondre à ces objectifs. Le travail de modélisation réalisé au cours de la thèse a été ainsi principalement destiné à mettre en place un modèle architecturé de l'appareil aérien du pois, afin de recréer une association virtuelle blé - pois [après couplage à un modèle de blé, (Fournier *et al.*, 2003)] permettant d'estimer le partage du rayonnement.

1 Synthèse des principaux résultats

Par ailleurs, les résultats présentés dans ce document se proposent de contribuer à la caractérisation i) de la **morphogénèse aérienne du pois dans plusieurs conditions de culture** (serre, conditions non-contrôlées, plantes individuelles ou en culture pure ou associée avec du blé) ainsi que ii) de la **structure physique de la canopée des associations blé - pois**.

Ce dernier point a notamment révélé une **forte variabilité de la structure de la canopée** (plus ou moins homogène) constituée par les associations céréales – légumineuses (Barillot *et al.*, 2011). Ces résultats apportent des informations utiles dans les processus de décision concernant le **choix des approches de modélisation** du partage de la lumière dans les associations céréales - légumineuses.

Nous avons ainsi considéré **l'approche plante virtuelle comme étant la plus pertinente** dans la perspective d'analyser les modalités du partage du rayonnement dans l'association blé - pois. A cet effet, il a été nécessaire de construire des **modèles architecturés** des plantes, qu'ils soient statiques (issus de la digitalisation du pois et du blé) ou dynamiques (L-Pea pour le pois). L'originalité du travail de thèse réside donc dans :

- Le développement d'un **modèle 3D de la morphogénèse aérienne du pois**, qui est à notre connaissance le premier disponible dans la littérature.
- La construction d'un **simulateur intégrant trois modèles** : pois, blé et rayonnement.

Ces étapes ont permis d'apporter des éléments de réponse à des problématiques d'ordre écophysiologique, agronomique telles que :

- L'étude de la **dynamique** du **partage du rayonnement** en fonction de **paramètres architecturaux** définis à **l'échelle de la plante**.

Nous avons ainsi montré, à travers une analyse multi-échelle Figure 1, que certains composants de l'architecture aérienne des plantes (*e.g.* longueurs des entrenœuds, nombre de ramifications) **impactent significativement** la quantité de lumière interceptée par chacune des espèces du couvert.

Ces paramètres architecturaux ont révélé une **forte variabilité génotypique** chez le pois. De plus, l'impact de variations des paramètres architecturaux du pois et du blé sur le partage du rayonnement s'est avéré comme étant fonction du **stade de développement** des plantes, de **l'espèce concernée**, et des autres composants architecturaux au sein non seulement d'une **même plante** mais également entre **plante voisines**. Dans la perspective du pilotage du fonctionnement de couverts plurispécifiques, ces résultats permettent d'identifier des **leviers** capables d'affecter le partage du rayonnement. Ainsi, les travaux décrits dans cette thèse fournissent des éléments de réflexion quant à la **sélection** de **génotypes/idéotypes** adaptés aux associations de cultures ***via* l'intégration de critères morphologiques déterminant pour le partage du rayonnement**. Par ailleurs, les paramètres architecturaux identifiés ont notamment fait l'étude de travaux relevant du domaine de la génétique, et sont donc pour la plupart accessibles aux sélectionneurs variétaux (*e.g.* pour le pois, voir la revue de Huyghe, 1998).

2 Le modèle ou un modèle ?

Tout au long de ce document, nous avons mentionné de manière univoque les termes de *modèle*, de *simulateur*. Or, derrière ces notions de modélisation se cachent une grande diversité d'approches, de formalismes et de formes (graphiques, analytiques, informatiques…). A mon sens, un modèle est une **représentation plus ou moins simplifiée de la réalité, destinée à reproduire un phénomène dans le but de l'appréhender**. Un modèle est donc issu de la simplification, de l'abstraction d'un phénomène, il est donc *de facto* soumis à la **subjectivité** de son concepteur/utilisateur. Ainsi, il s'agit de bien distinguer les propriétés du modèle de celles de la réalité. Ces éléments font ressortir que le choix des formes, paradigmes et formalismes d'un modèle doit résulter **des objectifs qui lui sont assignés**. En conséquence, l'objectif ultime n'est pas nécessairement d'aboutir à l'intégration de l'ensemble des processus liés à l'objet d'étude dans le modèle.

La démarche de modélisation résulte donc d'une réflexion scientifique, issue de l'observation de faits concrets, puis de **l'abstraction de mécanismes sous-jacents** dans l'objectif de comprendre, transposer, prédire ou encore faire émerger des propriétés relatives au fonctionnement de l'objet d'étude. Ainsi, la conception de modèle se rapproche des étapes de la formation de l'esprit scientifique tel qu'il est défini par Bachelard (2004) :

Dans sa formation individuelle, un esprit scientifique passerait donc par les trois états suivants […] :

1) *L'état concret où l'esprit s'amuse des premières images du phénomène […].*
2) *L'état concret-abstrait où l'esprit adjoint à l'expérience physique des schémas géométriques et s'appuie sur une philosophie de simplicité […].*
3) *L'état abstrait où l'esprit entreprend des informations volontairement soustraites à l'espace réel, […], en polémique ouverte avec la réalité première […].*

Ces travaux de thèse ont conduit au développement *d'un* modèle, et non *du modèle*, de morphogénèse aérienne du pois (**L-Pea**). Ce modèle a été construit avec la perspective d'appréhender les relations entre architectures des plantes et partage de la lumière dans les associations blé - pois. L-Pea est donc un modèle à **dominante déterministe** et dont l'algorithmique est basée sur la **description modulaire des plantes** (Prusinkiewicz et Lindenmayer, 1990), permettant donc d'évaluer l'effet **intrinsèque** de paramètres architecturaux sur le partage du rayonnement. Le simulateur « tripartite » (blé-pois-rayonnement) mis en place au cours de cette thèse a donc constitué un outil **heuristique** permettant d'évaluer des **hypothèses inaccessibles à l'expérimentation** physique, pour des raisons techniques et/ou de temps.

3 Perspectives

Le simulateur développé au cours de cette thèse constitue principalement une **première approche** permettant d'initier d'autres travaux de recherche. A ce titre, le modèle L-Pea ainsi que le simulateur de l'association blé - pois sont librement accessibles à la communauté scientifique *via* le site web https://gforge.inria.fr/projects/openalea/. A ce titre, le code du modèle du modèle L-Pea est disponible en Annexe de ce document. Concernant les travaux présentés dans ce travail de thèse, il convient par la suite d'évaluer les résultats obtenus en environnement virtuel, par la mise en place d'expérimentations *physiques* impliquant des associations blé - pois en conditions non contrôlées, et destinées à confirmer l'effet des paramètres architecturaux sur le partage du rayonnement dans le couvert. Toutefois, les résultats issus de ces simulations ont tout de même corroborés les conclusions avancées au cours du 2ème chapitre. De plus, il apparait nécessaire d'étudier d'autres paramètres architecturaux que ceux étudiés et notamment ceux en lien avec l'aspect dynamique de la morphogénèse. Ces analyses plus avancées des relations entre architecture des plantes et partage du rayonnement devront notamment s'attacher à caractériser l'agrégation foliaire (*clumping* en anglais). En effet, ce paramètre est un indicateur de l'efficience d'interception du couvert et de la complémentarité de la distribution spatiale du feuillage des espèces associées (Ross, 1981c, Sonohat *et al.*, 2002).

Par ailleurs, la thèse s'est focalisée sur les modalités architecturales *i.e.* physiques du *partage* de la lumière dans les associations, et non sur la *compétition* interspécifique pour cette ressource. Nous avons tenu à faire la distinction entre ces deux termes puisque la notion de **compétition** aurait nécessité de caractériser les **réponses structurales** et/ou **fonctionnelles** des plantes, induites par des modifications de l'accès à la ressource lumineuse consécutives au développement de chaque espèce.

A ce titre, le développement du simulateur de l'association blé - pois pourra notamment être poursuivi par l'intégration de fonctions permettant de tenir compte des effets de la compétition pour la lumière sur :

- Le **fonctionnement photosynthétique** des plantes. Cet aspect peut intégrer tout ou partie du processus photosynthétique *i.e.* assimilation du carbone, accumulation de biomasse et son allocation entre organes puits et source. Cet aspect **trophique** apparait ainsi déterminant dans la perspective d'améliorer notre compréhension des processus pilotant la proportion et de la productivité de chaque espèce dans les associations.
- La **photomorphogénèse** des plantes. En effet, comme nous l'avons mentionné en introduction de ce document, le développement des plantes modifie le microclimat et notamment la qualité de la lumière entendue par sa composition spectrale. Les réponses photomorphogénétiques (indépendantes de la photosynthèse) sont impliquées dans de nombreux processus de développement des plantes *e.g.* germination des graines, phototropisme, ontogénèse, floraison, horloge circadienne, sénescence…(Casal et Alvarez, 1988, VarletGrancher *et al.*, 1993, Rousseaux *et al.*, 1996, Ballare et Casal, 2000, Christie et Briggs, 2001). Ainsi, la vitesse d'allongement foliaire de certaines graminées semble sensible à la quantité d'énergie reçue dans le domaine du bleu (Gautier et Varlet-Grancher, 1996) concomitantes à des modifications de l'état stomatique et hydrique de la plante (Barillot *et al.*, 2010). Le recours au modèle de radiosité Caribu (Chelle et Andrieu, 1998), couplé aux architectures du pois et du blé fournit ici un cadre conceptuel pertinent pour étudier/intégrer la photomorphogénèse des plantes *via* par exemple, la réalisation de cartographie spatiale de la qualité du rayonnement dans le couvert.

L'algorithmique, ainsi que les formalismes employés pour développer le modèle L-Pea (programmation orientée-objet, L-System, modularité), constituent donc des atouts dans la perspective d'intégrer les réponses et rétroactions de la morphogénèse des plantes telles que citées ci-dessus. De plus, la capacité du modèle L-Pea à i) tenir compte de la variabilité observée sur un paramètre morphogénétique (voir chapitre 4), ii) à intégrer dans le peuplement différents génotypes de pois avec, iii) des proportions différentes de chaque espèce, constitue un cadre d'analyse performant, permettant d'étudier l'effet de la variabilité génétique et de différentes pratiques culturales sur le développement de l'association.

A plus long terme, la modélisation du fonctionnement des associations nécessitera également l'intégration des processus d'acquisition de l'ensemble des ressources du milieu, et notamment des **ressources azotées** qui constituent un point clé de l'équilibre et de la stabilité des associations. Cette étape devra ainsi tenir compte de la morphogénèse de l'appareil racinaire des espèces et du fonctionnement symbiotique de la légumineuse. La prise en compte des facteurs biotiques semble également être une perspective d'utilisation du modèle.

De tels travaux permettraient d'étudier la dispersion des maladies dans les couverts plurispécifiques. De plus, des modèles épidémiologiques prenant en compte l'architecture des plantes sont disponibles dans la littérature *e.g.* Le May *et al.* (2009) pour l'ascochytose du pois, et Robert *et al.* (2008) et Baccar *et al.* (2011) pour la septoriose du blé.

4 Conclusion

Le choix de la formulation des associations blé – pois ou plus généralement céréales – légumineuses est une problématique complexe devant intégrer les ressources et caractéristiques pédoclimatiques du milieu, le choix des espèces et variétés, ou encore la fertilisation azotée (Louarn *et al.*, 2010). Le choix des espèces et variétés, c'est-à-dire de leur caractéristiques fonctionnelles et structurales, constitue un des leviers importants de l'équilibre des espèces dans le couvert ainsi que de sa productivité.

Nous avons montré, par simulation, que l'architecture des plantes était un paramètre déterminant du fonctionnement des associations à travers ses effets sur le partage du rayonnement entre espèces. Les résultats présentés dans ce document apportent également des éléments de réflexion dans la construction d'idéotypes architecturaux destinés à piloter le partage de la lumière.

Ce point soulève toutefois la question complexe et non-intuitive du partage *optimal* dans les associations de cultures (50-50, 70-30… ?). À mon sens, aucune réponse absolue et définitive ne peut être formulée ici, tant elle dépend de nombreux paramètres tels que les objectifs de production ou encore le rôle de la légumineuse dans le couvert (production de graines, fourrage, plante de service). Louarn *et al.* (2010) apportent également des éléments de réponse sur ces notions d'équilibre dynamique entre espèces associées :

> *Les bases écologiques et physiologiques des interactions entre espèces […] permettent de dégager certaines règles d'assemblage [e.g.] le maximum de production est atteint en choisissant les espèces maximisant l'interception et l'utilisation des ressources dans l'espace et dans le temps.*

L'enjeu pour la recherche est donc aujourd'hui d'apporter des éléments tangibles (création variétale, indicateurs de fonctionnement des plantes, aide à la décision…) pour la conception et la gestion de systèmes de cultures, tels que les associations céréales – légumineuses, qui puissent répondre aux attentes socio-économiques et écologiques actuelles (*cf.* introduction générale).

Par cette thèse, je me propose ainsi de contribuer à la démarche de réflexion et de conception portée sur ces agrosystèmes performants et durables.

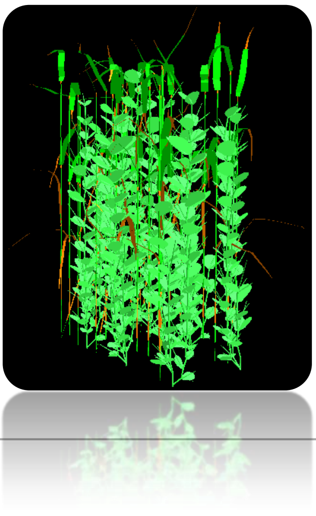

Références bibliographiques

Adam B, Donès N, Sinoquet H. 2002. VegeSTAR - software to compute light interception and canopy photosynthesis from images of 3D digitised plants. 3.0 ed. Clermont-Ferrand, UMR PIAF INRA-UBP.

Andrieu B. 2005. Approche plante virtuelle pour la modélisation des plantes et peuplements cultives.

Anil, Park, Phipps, Miller. 1998. Temperate intercropping of cereals for forage: a review of the potential for growth and utilization with particular reference to the UK. *Grass & Forage Science,* **53**: 301-317.

Arumingtyas EL, Floyd RS, Gregory MJ, Murfet IC. 1992. Branching in *Pisum*: inheritance and allelism tests with 17 *ramosus* mutants. *Pisum Genetics,* **24**: 17-31.

Awal MA, Koshi H, Ikeda T. 2006. Radiation interception and use by maize/peanut intercrop canopy. *Agricultural and Forest Meteorology,* **139**: 74-83.

Baccar R, Fournier C, Dornbusch T, Andrieu B, Gouache D, Robert C. 2011. Modelling the effect of wheat canopy architecture as affected by sowing density on *Septoria tritici* epidemics using a coupled epidemic-virtual plant model. *Annals of Botany,* **108**: 1179-1194.

Bachelard G. 2004. *La formation de l'esprit scientifique.* Vrin: Paris, France.

Ballare CL, Casal JJ. 2000. Light signals perceived by crop and weed plants. *Field Crops Research,* **67**: 149-160.

Ballaré CL, Casal JJ. 2000. Light signals perceived by crop and weed plants. *Field Crops Research,* **67**: 149-160.

Barillot R, Combes D, Chevalier V, Fournier C, Escobar-Gutiérrez AJ. 2012a. How does pea architecture influence light sharing in virtual wheat - pea mixtures? A simulation study based on pea genotypes with contrasting architectures. *AoB PLANTS*: Accepted.

Barillot R, Combes D, Pineau S, Huynh P, Escobar-Gutiérrez AJ. 2012b. Comparison of the morphogenesis of three genotypes of pea (*Pisum sativum*) grown in pure stands and wheat-based intercropping systems. *Agronomy for Sustainable Development*: UNDER REVIEW.

Barillot R, Frak E, Combes D, Durand J-L, Escobar-Gutiérrez AJ. 2010. What determines the complex kinetics of stomatal conductance under blueless PAR in *Festuca arundinacea*? Subsequent effects on leaf transpiration. *Journal of Experimental Botany,* **61**: 2795-2806.

Barillot R, Louarn G, Escobar-Gutiérrez AJ, Huynh P, Combes D. 2011. How good is the turbid medium-based approach for accounting for light partitioning in contrasted grass-legume intercropping systems? *Annals of Botany,* **108**: 1013-1024.

Béasse C, Ney B, Tivoli B. 2000. A simple model of pea (*Pisum sativum*) growth affected by Mycosphaerella pinodes. *Plant Pathology,* **49**: 187-200.

Bertheloot J, Andrieu B, Fournier C, Martre P. 2009. Modelling Nitrogen Distribution in Virtual Plants, as Exemplified by Wheat Culm During Grain Filling. . *Proceedings of the 2009 Plant Growth Modeling, Simulation, Visualization, and Applications.* Beijing, China, IEEE Computer Society.

Bertheloot J, Cournède P-H, Andrieu B. 2011. NEMA, a functional–structural model of nitrogen economy within wheat culms after flowering. I. Model description. *Annals of Botany,* **108**: 1085-1096.

Boudon F, Pradal C, Cokelaer T, Prusinkiewicz P, Godin C. 2012. L-Py: an L-System simulation framework for modeling plant development based on a dynamic language. *Frontiers in Plant Science,* **3**.

Bourion V, Fouilloux G, Le Signor C, Lejeune-Hénaut I. 2002. Genetic studies of selection criteria for productive and stable peas. *Euphytica,* **127**: 261-273.

Bournérias M, Bock C. 2006. *Le génie des végétaux.* Belin. Pour la science: Paris, France.

Boyeldieu J. 1991. *Produire des grains oléagineux et protéagineux.* Lavoisier Tec&Doc: Paris, France.

Brisson N, Gate P, Gouache D, Charmet G, Oury F-X, Huard F. 2010. Why are wheat yields stagnating in Europe? A comprehensive data analysis for France. *Field Crops Research,* **119**: 201-212.

Brisson N, Launay M, Mary B, Beaudoin N. 2009. *Conceptual basis, formalisations and parameterization of the STICS crop model.* Collection “Update Science and Technologies”: Versailles.

Bruno JF, Stachowicz JJ, Bertness MD. 2003. Inclusion of facilitation into ecological theory. *Trends in Ecology & Evolution,* **18**: 119-125.

Casal JJ, Alvarez MA. 1988. Blue-Light Effects On The Growth Of *Lolium-Multiflorum* Lam. Leaves Under Natural Radiation. *New Phytologist,* **109**: 41-45.

Casal JJ, Sanchez RA, Deregibus VA. 1986. The effect of plant density on tillering: The involvement of R/FR ratio and the proportion of radiation intercepted per plant. *Environmental and Experimental Botany,* **26**: 365-371.

Chelle M. 2005. Phylloclimate or the climate perceived by individual plant organs: What is it? How to model it? What for? *New Phytologist,* **166**: 781-790.

Chelle M, Andrieu B. 1998. The nested radiosity model for the distribution of light within plant canopies. *Ecological Modelling,* **111**: 75-91.

Chevassus-au-Louis B, Ferone G, Griffon M, Kahn A, Pisani E. 2009. *Les défis de l'agricultures mondiale au XXI siècle.* Angers, France.

Christie JM, Briggs WR. 2001. Blue light sensing in higher plants. *Journal Of Biological Chemistry,* **276**: 11457-11460.

Cici SZ-H, Adkins S, Hanan J. 2008. A Canopy Architectural Model to Study the Competitive Ability of Chickpea with Sowthistle. *Annals of Botany,* **101**: 1311-1318.

Cline M. 1991. Apical dominance. *The Botanical Review,* **57**: 318-358.

Combes D, Chelle M, Sinoquet H, Varlet-Grancher C. 2008. Evaluation of a turbid medium model to simulate light interception by walnut trees (hybrid NG38 x RA and *Juglans regia*) and sorghum canopies (*Sorghum bicolor*) at three spatial scales. *Functional Plant Biology,* **35**: 823-836.

Corre-Hellou G, Dibet A, Hauggaard-Nielsen H, Crozat Y, Gooding M, Ambus P, Dahlmann C, von Fragstein P, Pristeri A, Monti M, Jensen ES. 2011. The competitive ability of pea–barley intercrops against weeds and the interactions with crop productivity and soil N availability. *Field Crops Research,* **122**: 264-272.

Corre-Hellou G, Faure M, Launay M, Brisson N, Crozat Y. 2009. Adaptation of the STICS intercrop model to simulate crop growth and N accumulation in pea–barley intercrops. *Field Crops Research,* **113**: 72-81.

Corre-Hellou G, Fustec J, Crozat Y. 2006. Interspecific competition for soil N and its interaction with N_2 fixation, leaf expansion and crop growth in pea–barley intercrops. *Plant and Soil,* **282**: 195-208.

Crews TE, Peoples MB. 2004. Legume versus fertilizer sources of nitrogen: ecological tradeoffs and human needs. *Agriculture, Ecosystems & Environment,* **102**: 279-297.

DeJong TM, Da Silva D, Vos J, Escobar-Gutiérrez AJ. 2011. Using functional–structural plant models to study, understand and integrate plant development and ecophysiology. *Annals Of Botany,* **108**: 987-989.

Dornbusch T, Baccar R, Watt J, Hillier J, Bertheloot J, Fournier C, Andrieu B. 2011. Plasticity of winter wheat modulated by sowing date, plant population density and nitrogen fertilisation: Dimensions and size of leaf blades, sheaths and internodes in relation to their position on a stem. *Field Crops Research,* **121**: 116-124.

Duc G, Mignolet C, Carrouée B, Huyghe C. 2010. Importance économique passée et présente des légumineuses : Rôle historique dans les assolements et les facteurs d'évolution. *Innovations Agronomiques,* **11**: 1-24.

Escobar-Gutiérrez AJ, Combes D, Rakocevic M, de Berranger C, Eprinchard-Ciesla A, Sinoquet H, Varlet-Grancher C. 2009. Functional relationships to estimate Morphogenetically Active Radiation (MAR) from PAR and solar broadband irradiance measurements: The case of a sorghum crop. *Agricultural and Forest Meteorology,* **149**: 1244-1253.

Evers JB, Vos J, Fournier C, Andrieu B, Chelle M, Struik PC. 2007. An architectural model of spring wheat: Evaluation of the effects of population density and shading on model parameterization and performance. *Ecological Modelling,* **200**: 308-320.

Faurie O, Soussana JF, Sinoquet H. 1996. Radiation interception, partitioning and use in grass -clover mixtures. *Annals of Botany,* **77**: 35-46.

Fournier C, Andrieu B. 1998. A 3D Architectural and Process-based Model of Maize Development. *Annals Of Botany,* **81**: 233-250.

Fournier C, Andrieu B, Buck-Sorlin G, Evers JB, Drouet JL, Escobar-Gutiérrez AJ, Vos J. 2007. Functional-structural modelling of Gramineae. In: Vos J, Marcelis LFM, de Visser PHB, Struik PC, Evers JB eds. *Functional-Structural Plant Modelling in Crop Production.* Springer.

Fournier C, Andrieu B, Ljutovac S, Saint-Jean S. 2003. ADEL-wheat: A 3D architectural model of wheat development. *Proceedings of the 2003 Plant Growth Modeling, Simulation, Visualization, and Applications.* Beijing, China, IEEE Computer Society.

Fujita K, Ofosu-Budu KG, Ogata S. 1992. Biological nitrogen fixation in mixed legume-cereal cropping systems. *Plant And Soil,* **141**: 155-175.

Fustec J, Lesuffleur F, Mahieu S, Cliquet J-B. 2010. Nitrogen rhizodeposition of legumes. A review. *Agron. Sustain. Dev.,* **30**: 57-66.

Gate P. 1995. *Ecophysiologie du blé.* Lavoisier.

Gaucherel C, Boudon F, Houet T, Castets M, Godin C. 2012. Understanding Patchy Landscape Dynamics: Towards a Landscape Language. *PLoS ONE,* **7**: e46064.

Gautier H, Mech R, Prusinkiewicz P, Varlet-Grancher C. 2000. 3D Architectural Modelling of Aerial Photomorphogenesis in White Clover (*Trifolium repens* L.) using L-systems. *Ann Bot,* **85**: 359-370.

Gautier H, Varlet-Grancher C. 1996. Regulation of leaf growth of grass by blue light. *Physiologia Plantarum,* **98**: 424-430.

Ghaley B, Hauggaard-Nielsen H, Høgh-Jensen H, Jensen E. 2005. Intercropping of Wheat and Pea as Influenced by Nitrogen Fertilization. *Nutrient Cycling In Agroecosystems,* **73**: 201-212.

Giller KE, Beare MH, Lavelle P, Izac AMN, Swift MJ. 1997. Agricultural intensification, soil biodiversity and agroecosystem function. *Applied Soil Ecology,* **6**: 3-16.

Godin C. 2000. Representing and encoding plant architecture: A review. *Annals of Forest Science,* **57**: 413-438.

Godin C, Caraglio Y. 1998. A Multiscale Model of Plant Topological Structures. *Journal of Theoretical Biology,* **191**: 1-46.

Godin C, Sinoquet H. 2005. Functional-structural plant modelling. *New Phytologist,* **166**: 705-708.

Goudriaan J. 1982. Potential production processes. In: Vries FWTP, Laar HH eds. *Simulation of plant growth and crop production.* Wageningen, Centre for Agricultural Pub. and Documentation.

Gray A. 1849. On the composition of the plant by phytons, and some applications of phyllotaxis. In 438-444.

Griffon M. 1999. Développement durable et agriculture : la révolution doublement verte. *Cahiers Agricultures* **8**: 259-267.

Guichard L. 2009. Réduire les intrants azotés : intérêt des associations céréale-légumineuse. *Service Presse INRA.* Versailles-Grignon.

Hallé F, Oldeman RAA, Tomlinson PB. 1978. *Tropical trees and forests. An architectural analysis.* Springer-Verlag: Berlin.

Hauggaard-Nielsen H, Ambus P, Jensen ES. 2001. Interspecific competition, N use and interference with weeds in pea-barley intercropping. *Field Crops Research,* **70**: 101-109.

Haynes RJ. 1980. Competitive aspects of the grass-legume association. In: Brady NC ed. *Advances in agronomy.* Academic Press.

Huyghe C. 1998. Genetics and genetic modifications of plant architecture in grain legumes: a review. *Agronomie,* **18**: 383-411.

Huyghe C, Litrico I. 2008. Analyse de la relation entre la diversité spécifique des prairies et leur valeur agronomique (bibliographie). *Fourrages,* **194**: 147-160.

ITAB. 2011. La culture des associations céréales/protéagineux en AB.

Jensen ES. 1996a. Compared cycling in a soil-plant system of pea and barley residue nitrogen. *Plant And Soil,* **182**: 13-23.

Jensen ES. 1996b. Grain yield, symbiotic N2 fixation and interspecific competition for inorganic N in pea-barley intercrops. *Plant and Soil,* **182**: 25-38.

Jeudy C, Munier-Jolain N. 2005. Developpement des ramifications. In: Munier-Jolain N, Biarnes V, Chaillet I, Lecoeur J, Jeuffroy M-H eds. *Agrophysiologie du pois protéagineux.* Paris, Inra-Quae.

Jeuffroy MH, Sebillotte M. 1997. The end of flowering in pea: influence of plant nitrogen nutrition. *European Journal of Agronomy,* **6**: 15-24.

Keating BA, Carberry PS. 1993. Resource capture and use in intercropping: solar radiation. *Field Crops Research,* **34**: 273-301.

Kusnadi J, Gregory M, Murfet IC, Ross JJ, Bourne F. 1992. Internode length in *Pisum*: phenotypic characterisation and genetic identity of the short internode mutant Wt11242. *Pisum Genetics,* **24**: 64-74.

Lamanda N, Dauzat J, Jourdan C, Martin P, Malézieux E. 2008. Using 3D architectural models to assess light availability and root bulkiness in coconut agroforestry systems. *Agroforestry Systems,* **72**: 63-74.

Lantinga EA, Nassiri M, Kropff MJ. 1999. Modelling and measuring vertical light absorption within grass-clover mixtures. *Agricultural and Forest Meteorology,* **96**: 71-83.

Launay M, Brisson N, Satger S, Hauggaard-Nielsen H, Corre-Hellou G, Kasynova E, Ruske R, Jensen ES, Gooding MJ. 2009. Exploring options for managing strategies for pea-barley intercropping using a modeling approach. *European Journal Of Agronomy,* **31**: 85-98.

Le May C, Ney B, Lemarchand E, Schoeny A, Tivoli B. 2009. Effect of pea plant architecture on spatiotemporal epidemic development of ascochyta blight (*Mycosphaerella pinodes*) in the field. *Plant Pathology,* **58**: 332-343.

Le May C, Schoeny A, Tivoli B, Ney B. 2005. Improvement and validation of a pea crop growth model to simulate the growth of cultivars infected with Ascochyta blight (*Mycosphaerella pinodes*). *European Journal of Plant Pathology,* **112**: 1-12.

Le Roux X, Barbault R, Baudry J, Burel F, Doussan I, Garnier E, Herzog F, Lavorel S, Lifran R, Roger-Estrade J, Sarthou JP, Trommetter M. 2008. Agriculture et biodiversité. Valoriser les synergies. Expertise scientifique collective, synthèse du rapport. France, INRA.

Lecoeur J. 2005. Developpement vegetatif. In: Munier-Jolain N, Biarnes V, Chaillet I, Lecoeur J, Jeuffroy M-H eds. *Agrophysiologie du pois protéagineux.* Paris, Inra-Quae.

Lecoeur J, Wery J, Turc O, Tardieu F. 1995. Expansion of pea leaves subjected to short water deficit: cell number and cell size are sensitive to stress at different periods of leaf development. *Journal of Experimental Botany,* **46**: 1093-1101.

Lemerle D, Gill GS, Murphy CE, Walker SR, Cousens RD, Mokhtari S, Peltzer SJ, Coleman R, Luckett DJ. 2001. Genetic improvement and agronomy for enhanced wheat competitiveness with weeds. *Australian Journal of Agricultural Research,* **52**: 527-548.

Lindenmayer A. 1968. Mathematical models for cellular interactions in development I. Filaments with one-sided inputs. *Journal of Theoretical Biology,* **18**: 280-299.

Loomis RS, Williams WA. 1963. Maximum crop productivity: an estimate. *Crop Science,* **3**: 67-72.

Louarn G, Corre-Hellou G, Fustec J, Lô-Pelzer E, Julier B, Litrico I, Hinsinger P, Lecomte C. 2010. Déterminants écologiques et physiologiques de la productivité et de la stabilité des associations graminées-légumineuses. *Innovations Agronomiques,* **11**: 79-99.

Louarn G, Da Silva D, Godin C, Combes D. 2012. Simple envelope-based reconstruction methods can infer light partitioning among individual plants in sparse and dense herbaceous canopies. *Agricultural and Forest Meteorology,* **166–167**: 98-112.

Lyndon RF. 1998. Partitioning the apex: the size of the apical meristem and the primordia. In: Lyndon RF ed. *The shoot apical meristem: its growth and development.* Cambridge university press.

Malézieux E, Crozat Y, Dupraz C, Laurans M, Makowski D, Ozier-Lafontaine H, Rapidel B, de Tourdonnet S, Valantin-Morison M. 2009. Mixing plant species in cropping systems: concepts, tools and models. A review. *Agron. Sustain. Dev.,* **29**: 43-62.

Monsi M, Saeki T. 1953. Über den Lichtfaktor in den Pflanzengesellschaften und seine Bedeutung für die Stoffproduktion. *Japanese Journal of Botany,* **14**: 22-52.

Moon P, Spencer DE. 1942. Illumination from a non-uniform sky. *Illuminating Engineering Society* **37**: 707-726.

Moore KJ, Moser LE. 1995. Quantifying Developmental Morphology of Perennial Grasses. *Crop Sci.,* **35**: 37-43.

Moulia B, Edelin C, Jeuffroy MH, Allirand JM, Loup C, Chartier M. 1998. Premiers éléments d'analyse du développement architectural des herbacées cultivées. In: Maillard P, Bonhomme R eds. *Fonctionnement des peuplements végétaux sous contraintes environnementales.* Paris, France, INRA editions.

Moulia B, Sinoquet H. 1993. Three-dimensional digitizing systems for plant canopy geometrical structure: a review. In: Varlet - Grancher C, Bonhomme R, Sinoquet H eds. *Crop structure and light microclimate.* Paris, INRA editions.

Munier-Jolain N, Biarnès V, Chaillet I, Lecoeur J, Jeuffroy M-H, Carrouée B, Crozat Y, Guilioni L, Lejeune I, Tivoli B. 2005a. *Agrophysiologie du pois protéagineux.* INRA: Paris, FRANCE.

Munier-Jolain N, Turc O, Ney B. 2005b. Développement reproducteur. In: Munier-Jolain N, Biarnes V, Chaillet I, Lecoeur J, Jeuffroy M-H eds. *Agrophysiologie du pois* *protéagineux*. Paris, Inra-Quae.

Murfet IC. 1973. Flowering in *Pisum*. Hr, a gene for high response to photoperiod. *Heredity,* **31**: 157-164.

Naudin C. 2009. *Nutrition azotée des associations Pois-Blé d'hiver (Pisum sativum L. – Triticum aestivum L.) : Analyse, modélisation et propositions de stratégies de gestion*, Angers.

Naudin C, Corre-Hellou G, Pineau S, Crozat Y, Jeuffroy M-H. 2010. The effect of various dynamics of N availability on winter pea-wheat intercrops: Crop growth, N partitioning and symbiotic N2 fixation. *Field Crops Research,* **119**: 2-11.

Ney B, Carrouée B. 2005. Préface. In: Munier-Jolain N, Biarnes V, Chaillet I, Lecoeur J, Jeuffroy M-H eds. *Agrophysiologie du pois protéagineux.* Paris, Inra-Quae.

Niinemets U, Al Afas N, Cescatti A, Pellis A, Ceulemans R. 2004a. Petiole length and biomass investment in support modify light-interception efficiency in dense poplar plantations. *Tree Physiology,* **24**: 141-154.

Niinemets U, Cescatti A, Christian R. 2004b. Constraints on light interception efficiency due to shoot architecture in broad-leaved Nothofagus species. *Tree Physiology,* **24**: 617-630.

Nilson T. 1971. A theoretical analysis of the frequency of gaps in plant stands. *Agricultural Meteorology,* **8**: 25-38.

Ofori F, Stern WR. 1987. Cereal-legume intercropping systems. *Advances in agronomy,* **41**: 41-90.

Ozier-Lafontaine H, Lafolie F, Bruckler L, Tournebize R, Mollier A. 1998. Modelling competition for water in intercrops: theory and comparison with field experiments. *Plant and Soil,* **204**: 183-201.

Parmentier B. 2007. *Nourrir l'humanité, les grands problèmes de l'agriculture mondiale au XXIe siècle.* Paris, France.

Pearcy RW, Muraoka H, Valladares F. 2005. Crown architecture in sun and shade environments: assessing function and trade-offs with a three-dimensional simulation model. *New Phytologist,* **166**: 791-800.

Pisani E, Lebiez M. 2007. *Une politique mondiale pour nourrir le monde.* Springer: Paris, France.

Pradal C, Boudon F, Nouguier C, Chopard J, Godin C. 2009. PlantGL: A Python-based geometric library for 3D plant modelling at different scales. *Graphical Models,* **71**: 1-21.

Pradal C, Dufour-Kowalski S, Boudon F, Fournier C, Godin C. 2008. OpenAlea: a visual programming and component-based software platform for plant modelling. *Functional Plant Biology,* **35**: 751-760.

Prusinkiewicz P. 2004a. Art and science for life: Designing and growing virtual plants with L-systems. *Nursery Crops Development, Evaluation, Production And Use*: 15-28.

Prusinkiewicz P. 2004b. Modeling plant growth and development. *Current Opinion in Plant Biology,* **7**: 79-83.

Prusinkiewicz P, Lindenmayer A. 1990. *The algorithmic beauty of plants.* Springer-Verlag: New-York.

Reinhardt D, Kuhlemeier C. 2002. Plant architecture. *EMBO Rep,* **3**: 846-851.

Rimmington GM. 1985. A test of a model for light interception by mixtures. *Australian Journal of Plant Physiology,* **12**: 681-683.

Robert C, Fournier C, Andrieu B, Ney B. 2008. Coupling a 3D virtual wheat (*Triticum aestivum*) plant model with a *Septoria tritici* epidemic model (Septo3D): a new approach to investigate plant–pathogen interactions linked to canopy architecture. *Functional Plant Biology,* **35**: 997-1013.

Roche R, Jeuffroy M-H, Ney B. 1998. A Model to Simulate the Final Number of Reproductive Nodes in Pea (*Pisum sativum* L.). *Annals of Botany,* **81**: 545-555.

Ross J. 1981a. Foliage area orientation in stands. In: Ross J ed. *The radiation regime and architecture of plant stands.* The Hague, The Netherlands, Junk, W.

Ross J. 1981b. Role of phytometric investigations in the studies of plant stand architecture and radiation regime. In: Ross J ed. *The radiation regime and architecture of plant stands.* The Hague, The Netherlands, Junk, W.

Ross J. 1981c. Spatial distribution of phytoelements in stands. In: Ross J ed. *The radiation regime and architecture of plant stands.* The Hague, The Netherlands, Junk, W.

Rousseaux MC, Hall AJ, Sanchez RA. 1996. Far-red enrichment and photosynthetically active radiation level influence leaf senescence in field-grown sunflower. *Physiologia Plantarum,* **96**: 217-224.

Sarlikioti V, de Visser PHB, Buck-Sorlin GH, Marcelis LFM. 2011a. How plant architecture affects light absorption and photosynthesis in tomato: towards an ideotype for plant architecture using a functional-structural plant model. *Annals of Botany,* **108**: 1065-1073.

Sarlikioti V, de Visser PHB, Marcelis LFM. 2011b. Exploring the spatial distribution of light interception and photosynthesis of canopies by means of a functional-structural plant model. *Annals Of Botany,* **107**: 875-883.

Schnute J. 1981. A Versatile Growth Model with Statistically Stable Parameters. *Canadian Journal of Fisheries and Aquatic Sciences,* **38**: 1128-1140.

Schwinning S, Weiner J. 1998. Mechanisms determining the degree of size asymmetry in competition among plants. *Oecologia,* **113**: 447-455.

Sinoquet H. 1993. Modelling radiative transfer in heterogeneous canopies and intercropping systems. In: Varlet - Grancher C, Bonhomme R, Sinoquet H eds. *Crop structure and light microclimate.* Paris, INRA editions.

Sinoquet H, Andrieu B. 1993. The geometrical structure of plant canopy: characterization and direct measurement methods In: Varlet - Grancher C, Bonhomme R, Sinoquet H eds. *Crop structure and light microclimate.* Paris, INRA editions.

Sinoquet H, Bonhomme R. 1991. A theoretical analysis of radiation interception in a two-species plant canopy. *Mathematical Biosciences,* **105**: 23-45.

Sinoquet H, Caldwell MM. 1995. Estimation of light capture and partitioning in intercropping systems. In: Sinoquet H, Cruz P eds. *Ecophysiology of tropical intercropping.* Paris, INRA Editions.

Sinoquet H, Cruz P. 1995. *Ecophysiology of tropical intercropping.* INRA Editions: Paris, France.

Sinoquet H, Moulia B, Gastal F, Bonhomme R, Varlet -Grancher C. 1990. Modeling the radiative balance of the components of a well-mixed canopy: application to a white clover-tall fescue mixture. *Acta Oecologica-International Journal of Ecology,* **11**: 469-486.

Sinoquet H, Rakocevic M, Varlet-Grancher C. 2000. Comparison of models for daily light partitioning in multispecies canopies. *Agricultural and Forest Meteorology,* **101**: 251-263.

Smith H. 1982. Light quality, photoperception, and plant strategy. *Annual Review of Plant Physiology,* **33**: 481-518.

Sonohat G, Sinoquet H, Varlet-Grancher C, Rakocevic M, Jacquet A, Simon JC, Adam B. 2002. Leaf dispersion and light partitioning in three-dimensionally digitized tall fescue-white clover mixtures. *Plant, Cell and Environment,* **25**: 529-538.

Spies JM, Warkentin T, Shirtliffe S. 2010. Basal branching in field pea cultivars and yield-density relationships. *Canadian Journal of Plant Science,* **90**: 679-690.

Tardieu F, Granier C, Muller B. 1999. Modelling leaf expansion in a fluctuating environment: are changes in specific leaf area a consequence of changes in expansion rate? *New Phytologist,* **143**: 33-43.

Tilman D, Cassman KG, Matson PA, Naylor R, Polasky S. 2002. Agricultural sustainability and intensive production practices. *Nature,* **418**: 671-677.

Trenbath BR. 1993. Intercropping for the management of pests and diseases. *Field Crops Research,* **34**: 381-405.

Truong HH, Duthion C. 1993. Time of Flowering of Pea (*Pisum sativum* L.) as a Function of Leaf Appearance Rate and Node of First Flower. *Annals Of Botany,* **72**: 133-142.

Tsubo M, Walker S. 2002. A model of radiation interception and use by a maize-bean intercrop canopy. *Agricultural and Forest Meteorology,* **110**: 203-215.

Tsubo M, Walker S, Ogindo HO. 2005. A simulation model of cereal-legume intercropping systems for semi-arid regions: I. Model development. *Field Crops Research,* **93**: 10-22.

Turc O, Lecoeur J. 1997. Leaf Primordium Initiation and Expanded Leaf Production are Co-ordinated through Similar Response to Air Temperature in Pea (*Pisum sativum* L.). *Annals of Botany,* **80**: 265-273.

Vandermeer J. 1989. *The ecology of intercropping.* Cambridge University Press: Cambridge, UK.

Varlet-Grancher C, Bonhomme R, Sinoquet H. 1993a. *Crop structure and light microclimate.* Paris.

Varlet-Grancher C, Moulia B, Sinoquet H, Russell G. 1993b. Spectral Modification Of Light Within Plant Canopies - How To Quantify Its Effects On The Architecture Of The Plant Stand. In: Varlet-Grancher C, Moulia B, Sinoquet H eds. *Crop Structure And Light Microclimate. Characterization and applications.* Versailles, INRA.

VarletGrancher C, Moulia B, Sinoquet H, Russel G. 1993. Crop structure and light microclimate: characterization and applications. *Crop structure and light microclimate: characterization and applications.*

Verdenal A. 2009. *De la simulation de la morphogénèse de l'appareil aérien du ray-grass anglais (Lolium perenne L.).*

Exploration d'un schéma cybernétique inspiré du concept d'auto-organisation et applications., UNIVERSITE DE POITIERS, Poitiers.

Verdenal A, Combes D, Escobar-Gutiérrez AJ. 2008. A study of ryegrass architecture as a self-regulated system, using functional-structural plant modelling. *Functional Plant Biology,* **35**: 911-924.

Vos J, Evers JB, Buck-Sorlin GH, Andrieu B, Chelle M, de Visser PHB. 2010. Functional-structural plant modelling: a new versatile tool in crop science. *Journal of Experimental Botany,* **61**: 2101-2115.

White J. 1979. The Plant as a Metapopulation. *Annual Review of Ecology and Systematics,* **10**: 109-145.

Willey RW. 1979. Intercropping-its importance and research needs. Part 1. Competition and yield advantages. *Field Crop Abstracts,* **32**: 1-10.

Yin X, Goudriaan J, Lantinga EA, Vos J, Spiertz HJ. 2003. A Flexible Sigmoid Function of Determinate Growth. *Annals of Botany,* **91**: 361-371.

Zheng B, Shi L, Ma Y, Deng Q, Li B, Guo Y. 2008. Comparison of architecture among different cultivars of hybrid rice using a spatial light model based on 3-D digitising. *Functional Plant Biology,* **35**: 900-910.

Annexes

Le code informatique du modèle simulant l’architecture aérienne du pois (L-Pea) développé au cours de cette thèse, est présenté en annexe de ce document. Le modèle est composé de trois principaux modules correspondant à des fichiers séparés :

- Tout d’abord le fichier lpea.lpy qui contient le cœur du programme *i.e.* les différentes fonctions et classes, ainsi que les règles de production et d’interprétation du L-System.
- Un fichier de paramètre : lpy.cfg. Ce fichier contient l’ensemble des paramètres requis pour utiliser le modèle. Ces paramètres sont accessibles et modifiables de façon indépendante du code principal, facilitant ainsi l’utilisation du modèle. Les paramètres peuvent également être spécifiés pour plusieurs génotypes.
- Et enfin le fichier PeaConfig.py. Ce dernier fichier permet de lire les paramètres renseignés dans lpy.cfg et de les compiler dans un dictionnaire qui est injecté dans le code principal.

1 Code principal : lpea.lpy

```
import time
from random import randint, seed, random, gauss, sample
from math import exp, log
from copy import deepcopy
from openalea.plantgl.all import Sphere

# Personal libraries
from agronomicplot_IC import *
from share_time_lpy import *
from PeaConfig import *

params = PeaConfig() # Loads parameters of pea cultivars
share_time_lpy.time_DD = None
######## Classes and Functions #########
seed()
t0 = time.time()

def StartEach():
    if share_time_lpy.time_DD == None: # Stand generation
      useGroup(1)
      share_time_lpy.time_DD = 0
    else:
      useGroup(2)
      share_time_lpy.time_DD += params.dt
def End():
  global t0
  print 'Time', time.time()-t0
```

```
#def EndEach (lstring) :
  #print lstring

def calc_phyllo(cv,axis):
  # Phyllochrone
  mu,SD_a,ymax,SD_ymax = (i for i in params.pheno['phyll'][cv][axis])
  phyllo = (gauss(mu,SD_a) if eval(params.var) == True else mu)
  phyto_max = max(1,(abs(int(gauss(ymax,SD_ymax) if eval(params.var) ==
True else ymax))))
  return phyllo,phyto_max

def optimal_phyto (stateA):
  # Computes the optimal number of phytomer as a linear function of DD
  opt_phyto = min(stateA.phyllo * stateA.t,stateA.phyto[1])
  return opt_phyto

def calc_age_phyto (n, opt_phyto, stateA):
  # Computes age of phytomers that must be created and returns a list
  apex_age = stateA.t
  phyllo = stateA.phyllo
  l_age =[]
  for pid in range (opt_phyto-n+1, opt_phyto+1):
    age = apex_age - (pid / phyllo)
    l_age.append(age)
  return l_age

class Organ_base:
  # Basic properties of organs
  def __init__(self,age, name, cv, plt, axis, curr_phyto,max_phyto,
level=0):
    self.t = age
    self.name = name
    self.cv = cv
    self.plt = plt
    self.axis = axis
    self.phyto = [i for i in (curr_phyto,max_phyto)] # [current phyto id,
final number of phyto]
    self.level = level
    self.par = 0
    if name in ('A','E','I','S','Lft','P'):
      (self.organA, self.organE,
self.organPhyto)[{'A':0,'E':1,'I':2,'S':2, 'Lft':2,'P':2}[name]]()

  def organA(self):
    # Set reproductive nodes
    flower_params =
params.pheno['time_flower'][self.cv][int(float(self.axis))]
    if len(flower_params) !=0:
      mu = flower_params[0]
```

```
      SD = flower_params[1]
      self.phyto_flower = int((gauss(mu,SD) if eval(params.var) == True
else mu))
    else:
      self.phyto_flower = ""

  def organE(self):
    # Set maximal length of scales
    L_max = params.growth['L_max'][self.cv]
    mu = L_max[self.name][self.phyto[0]-1][0]
    SD = L_max[self.name][self.phyto[0]-1][1]
    self.Lmax = abs((gauss(mu,SD) if eval(params.var) == True else mu)) #
Abs to avoid negative length
    def organPhyto(self):
    # Set organ growth rules and maximal length (according to their
relative position on vertical axis)
    params_beta = params.growth['beta'][self.cv][self.name]
    self.Tb = float(params_beta[0])
    self.Tmax = float(params_beta[1])
    self.Tend = float(params_beta[2])
    # L_max
    rel_phyto = (float(self.phyto[0]) / float(self.phyto[1]))*10 # *10 in
order to avoid a decimals
    i = int((rel_phyto-rel_phyto%2)/2 + ((rel_phyto%2) >0) - 1) # Index
of the list used to select the class of relative phytomere
    if self.name not in ('Lft','P'):
      mu = params.growth['L_max'][self.cv][self.name][i][0]
      SD = params.growth['L_max'][self.cv][self.name][i][1]
      self.Lmax = (gauss(mu,SD) if eval(params.var) == True else mu)
    else : # Lft and Petiole have levels
      mu = params.growth['L_max'][self.cv][self.name][self.level-1][i][0]
      SD = params.growth['L_max'][self.cv][self.name][self.level-1][i][1]
      self.Lmax = (gauss(mu,SD) if eval(params.var) == True else mu)

class phyto(Organ_base):
  # Creates phyto objects
  def __init__(self,age,name,stateA,level=0):
    Organ_base.__init__(self, age, name, stateA.cv, stateA.plt,
stateA.axis, stateA.phyto[0],stateA.phyto[1],level) # Inheritance of the
organ base class
    if name in ('I','S','Lft'):
      (self.organI, self.organS,
self.organLft)[{'I':0,'S':1,'Lft':2}[name]](stateA)

  def organI (self, stateA): # Internode
    self.orient = randint(0,20) # Stem twist
    self.tropism = tropism(stateA.cv, stateA.par) # PAR is fix in Lpy
whereas caribu is used in Openalea
```

```
  def organS (self, stateA): # Stipules
    self.LR = 0 # Marker for left or right stipule
    self.orient = 50

  def organLft (self, stateA): # Leaflets
    self.orient = -90
class branch(Organ_base):
  # Creates branch objects
  def __init__(self, age, name, stateA,bid):
    Organ_base.__init__(self, age, name, stateA.cv, stateA.plt,
stateA.axis, stateA.phyto[0],stateA.phyto[1]) # Inheritance of the organ
base class
    self.orient = randint(0,360) # Random azimuth of emergence
    self.order = stateA.phyto[0] # Node supporting the branch
    self.id = bid # Branch id in case of multiple braanches
    # Defines time of branch break
    emerg = params.branch['emerg'][stateA.cv][self.order-1][bid-1] #
Selects mean and SD of a given branch emergence
    mu = emerg[0]
    SD = emerg[1]
    self.bbreak = (gauss(mu,SD) if eval(params.var) == True else mu)
    self.activity = True

def nb_branch(cv,ind_phyto):
  # Computes the number of branches to be emitted
  # TODO : PRENDRE EN COMPTE LES PROBA DE RAMIFS SECONDAIRES
  if eval(params.var) == True:
    branches = 0
    proba_b = random() + .0000001 # Avoid probability 0
    curr_branchfreq = params.branch['branchfreq'][cv][ind_phyto] # Loads
branching cumulated frequences of a given node
    for i in range(1,len(curr_branchfreq)):
        if proba_b >=  curr_branchfreq[i-1] and proba_b <
curr_branchfreq[i] :
          branches = i-1
          break
    branches = int(round(branches + (branches * params.mult_branch)))
  else:
    branches = params.branch['Nodes_mean'][cv][ind_phyto]
  return branches

def nb_org_comp(phyto,cv):
  # Number of leaflet by phytomer
    rel_phyto = (float(phyto[0]) / float(phyto[1]))*10 # *10 in order to
avoid a decimals
    i = int((rel_phyto-rel_phyto%2)/2 + ((rel_phyto%2) >0) - 1)# Index of
the list used to select the class of relative phytomere
    org_comp = params.growth['org_comp'][cv][i]
    return org_comp
```

```
def color(t):
  # To use for senescence
  return 1
#  if t<600:
#    return 1
#  elif 600<=t<1500:
#    return 2
#  else:
#    return 3

def growth_function (state):
  # Beta function for organ growth
  if state.name in ('I','S','P'):
    L = abs(state.Lmax*(1+(max(0,(state.Tend-state.t))/(state.Tend-
state.Tmax)))*(min(1,(state.t-state.Tb)/(state.Tend-
state.Tb))**((state.Tend-state.Tb)/(state.Tend-state.Tmax))))
  else :
    L = state.Lmax*exp(-exp(1.5-0.04*state.t))
  scale_fact = params.scale_fact # Factor of conversion  (if scale_fact =
1, unit = mm)
  L = (L + 0.1) * scale_fact # Increment of 0.1 in order to avoid very
small objects
  return L

def tropism (cv, PAR):
  # Orients stems according to the PAR and R/FR ratio perceived by the
apex
  PAR = 0.2
  fonct_rel = params.fonct_rel[cv]
  x1,x2,a,b,c,d = (i for i in fonct_rel)
  zeta = pow(pow(c,b) + (pow(d,b) - pow(c,b)) * ((1-exp(-a*(PAR -
x1)))/(1-exp(-a*(x2 - x1)))),(1/b)) # R/FR ratio computed from fonctional
relationships with PAR
  elasticity = 0.05 + 0.2 * (1-PAR) + 0.25 * (1.15 - zeta) # Capacity of
the stem to follow a tropism (vertical vector by default)
  return elasticity

# Stand generation (units : meter)
lengthp = .1
widthp = .1
sowing_density = 90
plant_density = 90
inter_row = 0.17
stand = params.stand
nb_plant,position,intra_row =
agronomicplot_IC(lengthp,widthp,sowing_density,plant_density,inter_row,st
and)
# Multicultivar stands
nb_cv = len(params.cultivar)
```

```
pop = []
for cv in range(nb_cv):
  pop += [ cv for i in range(params.cultivar[cv][1]*10)] # Population of
1000 individus
pop = sample(pop,nb_plant)

############# AXIOM ##########################

Axiom:  Sd(pop) Soil (lengthp, widthp) Label

derivation length: 2 + 1

############# PRODUCTION #####################

production:

group 1:
Sd(pop): # Stand generation
  for i in xrange(len(pop)):
    cv = params.cultivar[pop[i]][0] # Gets cultivars name through their
index
    phyllo, phyto_max = calc_phyllo(cv, 0) # Phyllochrone rules
    stateA = Organ_base(0,'A',cv, i+1, 0, 0, phyto_max)
    stateA.phyllo = phyllo
    x,y,z=  position[i][0],position[i][1],position[i][2]
    nproduce  [@M(x,y,z) A(stateA)]
endgroup

group 2: # Pea development
A(stateA): # Apex
  DD = share_time_lpy.time_DD
  stateA.t += params.dt

  # Compares actual and potential number of phytomers
  curr_phyto = stateA.phyto[0]
  opt_phyto = optimal_phyto (stateA)
  diff_phyto = opt_phyto - curr_phyto
  if diff_phyto >=1: # Must create one or more phytomers
    l_age = calc_age_phyto (int(diff_phyto), int(opt_phyto), stateA) #
Computes age of the phytomers that are going to be created
    for i in range(0,len(l_age)): # Loop for each phytomers
      stateA.phyto[0] += 1

      if stateA.axis == 0 and stateA.phyto[0] <=2: # First two scales
        stateE = Organ_base(l_age[i], 'E', stateA.cv, stateA.plt,
stateA.axis, stateA.phyto[0],stateA.phyto[1])
        nproduce E(stateE)
      else : # True phytomers
        # Internode
```

```
        stateI = phyto(l_age[i],'I', stateA)

        # Stipules
        stateSL = phyto(l_age[i],'S', stateA)
        stateSR = deepcopy(stateSL) # Right stipule
        stateSR.LR =1
        stateSR.orient = 130

        nproduce I(stateI)[S(stateSL)][S(stateSR)]

        # Leafy cultivars
        if params.geom['leaflet'].has_key(stateA.cv) and stateA.phyto[0]
> 2: # Computes leafet number for true phytomers
          # Number of leaflet levels
          org_comp = nb_org_comp(stateA.phyto,stateA.cv)
          for org in range(org_comp):
            #Petiole
            stateP = phyto(l_age[i],'P', stateA,org+1)
            # Leaflets
            stateLftL = phyto(l_age[i],'Lft', stateA,org+1) # Left
leaflet
            stateLftR = deepcopy(stateLftL) # Right leaflet
            stateLftR.orient = 90

            nproduce [P(stateP)[Lft(stateLftL)][Lft(stateLftR)]
          for org in range (org_comp):
            nproduce ]

        # Semi leafless cultivars
        else:
          # Petiole
          stateP = phyto(l_age[i],'P', stateA,1)
          nproduce [P(stateP)]

      # Branching module
      if stateA.phyto[0] <= params.branch['max_node'] and stateA.axis ==
0 : # Branching nodes id
        nb_branches = nb_branch(stateA.cv, stateA.phyto[0] -1) # -1 as
the list begins at 0 in create_ramif
        # Appends the returned number of axillary buds
        for j in range (1,nb_branches+1):
          stateB = branch(l_age[i],'B',stateA,j)
          nproduce [B(stateB)]
      # Reproductive stages
      if stateA.phyto[0] >= stateA.phyto_flower:
        statePd1 = Organ_base(l_age[i], 'Pd', stateA.cv, stateA.plt,
stateA.axis, stateA.phyto[0],stateA.phyto[1])
        statePd2 = Organ_base(l_age[i], 'Pd', stateA.cv, stateA.plt,
stateA.axis, stateA.phyto[0],stateA.phyto[1])
```

```
    statePd1.Lmax = 35
    statePd2.Lmax = 15
    statePd1.orient = [180,20]
    statePd2.orient = [180,60]
    stateF = Organ_base(l_age[i], 'F', stateA.cv, stateA.plt,
stateA.axis, stateA.phyto[0],stateA.phyto[1])
    stateF.Lmax = 15
    nproduce [Pd(statePd1)[F(stateF)] [Pd(statePd2)[F(stateF)]]]

  # Last produce : last phyto which supports the apex
  if stateA.phyto[0] < stateA.phyto[1]:
   produce A(stateA)
  # Apex death
  else:
   pass
 # No phytomer production
 else:
  produce A(stateA)

B(stateB): # Branch
 DD = share_time_lpy.time_DD
 stateB.t += params.dt

 if stateB.bbreak <= DD and stateB.activity == True: # Branch start
  b_axis = str(stateB.order) + '.' + str(stateB.id)
  phyllo, phyto_max = calc_phyllo(stateB.cv, stateB.order)  #
Phyllochrones rules of the branch
  stateA = Organ_base(params.dt,'A',stateB.cv, stateB.plt, b_axis, 0,
phyto_max) # Creates a new apex
  stateA.phyllo = phyllo
  stateB.activity = False # Turn off bud activity
  produce B(stateB) A(stateA)
 else:
  produce B(stateB)

E(stateE): # Scale
 stateE.t += params.dt
 produce E(stateE)

I(stateI): # Internode
 stateI.t += params.dt
 produce I(stateI)
S(stateS): # Stipule:
  stateS.t += params.dt
  produce S(stateS)

Lft(stateLft): # Leaflet
 stateLft.t += params.dt
 produce Lft(stateLft)
```

```
P(stateP):# Petiole
  stateP.t += params.dt
  produce P(stateP)

F(stateF): # Fleur
  stateF.t += params.dt
  if stateF.t < float(params.pheno['time_pods'][stateF.cv]):
    produce F(stateF)
  else: # Flower to pod
    statePod = Organ_base (0,'Pod', stateF.cv, stateF.plt, stateF.axis,
stateF.phyto[0], stateF.phyto[1])
    statePod.Lmax = 45
    produce Pod(statePod)

Pd(statePd): # Pedoncule floral
  statePd.t += params.dt
  produce Pd(statePd)

Pod(statePod): # Pod
  statePod.t += params.dt
  produce Pod(statePod)

endgroup

############# INTERPRETATION ####################

interpretation:

maximum depth : 2

Trop(e):
  produce @Ts(e)

A(stateA): # Apex
  diam = 1.5 * params.scale_fact
  s=Sphere(diam,4,4)
  produce SetColor(6)@g(s,1)
Soil (lengthp,widthp):
  # Units : mm
  l = lengthp*1000
  w = widthp*1000
  soil_size = Scaled(Vector3(l,w,0),params.sol[0].geometry)
  produce SetColor(4)@M(0,0,0)@g(soil_size)

Label:
  txt = '  Thermal Time: ' + str(share_time_lpy.time_DD) + ' Degree day'
  produce SetColor(0)@M(0,0,0)@L(txt)

B(stateB): # Branch
```

```
  # B represented as a small cylinder that orients branches
  branchtaxy = stateB.orient
  diam = params.growth['diam'][stateB.cv] * params.scale_fact
  produce SetColor(0)/(branchtaxy) +(70) F(0.10,diam)

E(stateE): # Scale
  length = growth_function(stateE)
  diam = params.growth['diam'][stateE.cv] * params.scale_fact
  produce SetColor(color(stateE.t)) F(length,diam)

I(stateI): # Internode
  if stateI.t >=stateI.Tb : # Coordination rule
    length = growth_function (stateI)
    nodetaxyI = stateI.orient
    e = stateI.tropism
    diam = params.growth['diam'][stateI.cv] * params.scale_fact

    if stateI.phyto[0] == 1: # Orient first phyto
      produce SetColor(color(stateI.t)) @Gc Trop(e) / (nodetaxyI) + (15)
F(length,diam) @Ge
    elif stateI.phyto[0]%2==0: # even id phyto
      produce SetColor(color(stateI.t)) @Gc Trop(e) / (nodetaxyI) - (30)
F(length,diam) @Ge
    else: # odd id phyto
      produce SetColor(color(stateI.t)) @Gc Trop(e) / (nodetaxyI) + (30)
F(length,diam) @Ge

S(stateS): # Stipule
  if stateS.t >=stateS.Tb and stateS.t <=
params.pheno['senes'][stateS.cv]: # Coordination rule  + senescence
    length = growth_function (stateS)
    orient = stateS.orient
    incl = params.geom['incl'][stateS.cv]
    geom =
(params.geom['sl'][stateS.cv],params.geom['sr'][stateS.cv])[stateS.LR ==
1]
    if stateS.phyto[0]%2==0: # even id phyto
      produce SetColor(color(stateS.t)) /(orient) &(incl) @g(geom,length)
    else:# odd id phyto
      produce SetColor(color(stateS.t)) \(orient) &(incl) @g(geom,length)

Lft(stateLft): # Leaflet
  if stateLft.t <= params.pheno['senes'][stateLft.cv]: # Coordination
rule + senescence
    length = growth_function (stateLft)
    orient = stateLft.orient
    geom = params.geom['leaflet'][stateLft.cv]
    produce SetColor(color(stateLft.t)) +(orient) /(90) @g(geom,length)
```

```
P(stateP): # Petiole
  if stateP.t >=stateP.Tb and stateP.t <=
params.pheno['senes'][stateP.cv]: # Coordination rule + senescence
    length = growth_function (stateP)
    c=Cylinder (0.5,length)
    #@g(c)f(length)
    diam = 0.5 * params.scale_fact
    if stateP.level ==1 and stateP.phyto[0]%2==0:# even id phyto
      produce SetColor(color(stateP.t)) /(90) ^(60) F(length,diam)
    elif stateP.level ==1 and stateP.phyto[0]%2!=0:# odd id phyto
      produce SetColor(color(stateP.t)) \(90) ^(60) F(length,diam)
    else: # Secondary petiole
      produce SetColor(color(stateP.t)) ^(40) F(length,diam)

F(stateF):# Fleur
  length = growth_function (stateF)
  flower = params.geom['flower'][stateF.cv]
  produce SetColor(0) @g(flower,length)

Pd(statePd):# Pedoncule floral
  length = growth_function (statePd)
  diam = 0.3 * params.scale_fact
  c=Cylinder (diam,length)
  orient1 = statePd.orient[0]
  orient2 = statePd.orient[1]
  if statePd.phyto[0]%2==0:# even id phyto
    produce SetColor(color(statePd.t)) /(orient1) ^(orient2)
@g(c)f(length)
  else :# odd id phyto
    produce SetColor(color(statePd.t)) \(orient1) ^(orient2)
@g(c)f(length)
Pod(statePod):
    pod = params.geom['pod'][statePod.cv]
    length = growth_function (statePod)
    produce SetColor(3)^(40) @g(pod[0].geometry,length)
endlsystem
```

2 Paramètres du modèle : lpea.cfg

```
# Config file containing the parameters for running L-Pea with multiple
cultivars
# Each specific section must be repeated for each cultivar

[GLOBAL]
# Set global variables
# L1 : increment of time used in L-Pea (in Degree Day)
# L2 : Tuples of [cultivar, proportion in the stand]
# L3 : optional : geom object used for soil representation
# L4 : Scale factor for plant size (default = 1 -> unit = mm)
```

```
# L5 : Type of stand: SC or IC. SC = Sole crop, IC = Intercrop and thus a
gap is added between plants in order to place the component species
dt = 50
Cultivar = [['Lucy',100]] #,['US',50]]
geom_sol=sol.geom
scale_fact = 0.1
stand = IC
mult_branch = 0
var = False

### GEOM SECTION ###
# One line for each geom
# Provide a leaflet geom ('geom_Lft') for leafy cultivars
# Last line : mean inclination of stipule (degree)
[Lucy_GEOM]
geomsti_L=01-01-L.geom
geomsti_R=01-01-R.geom
geom_flower=corpisum2.geom
geom_pod=goussepisum.geom
incl=45.

### PHENOLOGIE ###
[Lucy_Phyllochrone]
# Analytical description of phytomer emission by apex
# L1 : [Mean slope of linear regression, SD, Mean max_phyto(including
scales), SD] for each axis
phyll =
[[0.0165,0.00148,9.0667,1.569],[0.0183,0.0027,19.3333,2.2998],[0.0171,0.0
036,14.7692,6.75]]

[Lucy_Reproductive_stages]
# L1 : Mean and SD of the first phytomer with flowers for each axis (in
Degree Day)
# L2 : Time for a flower to turn on a pod (in Degree Day)
Flowers = [[],[14, 2],[16, 0.7]]
Pods = 400
[Lucy_Senescence]
# Lifespan of stipules and petioles (DD)
senes = 540

### BRANCHES ###
[Lucy_Ramification]
# L1 : [cumulated frequences to develop 0, 1, 2, 3 ... branches,
separated with commas] for each node of a given axis
# (must start with the frequence of plants that won't develop any
branches at node 0)
# L2 : tuples of mean and SD of emergence grouped by node and branch
number
Nodes = [[0,0.4,0.93,1.0],[0.13,0.2,1.0]]
```

```
Nodes_mean = [2,2]
Emerg = [[[388.05,49.30], [482.14,49.30],[482.14,49.30]],[[295.27,72.05],
[374.43,72.05]]]

### GROWTH ###
[Lucy_Diameters]
# Unit : mm
Internode = 1.5

[Lucy_Growth]
# Line 1 : list of organs
# Lines 2,3,4 : Parameters of normalized beta function (Tb,Tmax,Tend)
Organ = I,S,P
I = 34.88,87.71,171.51
S = 0,71.28,197.66
P = 18.38,112.80,171.04

[Lucy_Lmax]
# First line : list of organs (unit = mm)
# For E : [[mean value scale1,SD scale1], [mean value scale2,SD scale2]]
# Following organs : [mean value,SD] for each class of relative phytomere
(0 to 1, step =0.2)
Organ = E,I,S,P
E = [[4.4,5.16],[19,4.19]]
I = [[21.98,3.55],[24.26,1.98],[25.49,2.02],[27.29,2.25],[27.36,9.27]]
S = [[25.,3.52],[31.56,2.63],[36.02,1.65],[42.53,3.65],[39.,11.72]]
P = [[[35.23,11.55],[53.48,4.64],[60.02,4.81],[62.30,4.52],[49.23,21.]]]

### PHOTOMORPHOGENESIS ###
[Lucy_Photomorpho]
# First line : paramters of the functional relations used to estimate
zeta from PAR (Escobar et al, 2009)
fonct_rel = [0,2,3.09,1.59,0,1.12]


################################# GENOTYPE 2 ############################
########################################################################

### GEOM SECTION ###
# One line for each geom
# Provide a leaflet geom ('geom_Lft') for leafy cultivars
[US_GEOM]
geomsti_L=01-01-L.geom
geomsti_R=01-01-R.geom
geom_Lft=folpisum2.bgeom
geom_flower=corpisum2.geom
geom_pod=goussepisum.geom
```

```
### PHENOLOGIE ###
[US_Phyllochrone]
# Analytical description of phytomer emission by apex
# L1 : [Mean slope of linear regression, SD, Mean max_phyto(including scales), SD] for each axis
phyll = [[0.0165,0.00148,9.0667,1.569],[0.0183,0.0027,19.3333,2.2998],[0.0171,0.0036,14.7692,6.75]]

[US_Reproductive_stages]
# L1 : Mean and SD of the first phytomere with flowers for each axis (in Degree Day)
# L2 : Time for a flower to turn on a pod (in Degree Day)
Flowers = [[],[14, 2],[16, 0.7]]
Pods = 400

[US_Senescence]
# Lifespan of stipules and petioles (DD)
senes = 1000
### BRANCHES ###
[US_Ramification]
# L1 : [cumulated frequences to develop 0, 1, 2, 3 ... branches, separated with commas] for each node of a given axis
# (must start with the frequence of plants that won't develop any branches at node 0)
# L2 : tuples of mean and SD of emergence grouped by node and branch number
Nodes = [[0,0.4,0.93,1.0],[0.13,0.2,1.0]]
Emerg = [[[388.05,49.30], [482.14,49.30],[482.14,49.30]],[[295.27,72.05],[374.43,72.05]]]

### GROWTH ###
[US_Diameters]
# Unit : mm
Internode = 1.5
[US_Growth]
# Line 1 : list of organs
# Lines 2,3,4 : Parameters of normalized beta function (Tb,Tmax,Tend)
Organ = I,S,P,Lft
I = 34.59,65.90,172.05
S = 0.05,65.9,186.82
P = 15.43,104.12,166.44
Lft = 0,65.90,215.65

[US_Lmax]
# First line : list of organs (unit = mm)
# For E : [[mean value scale1,SD scale1], [mean value scale2,SD scale2]]
# Following organs : [mean value,SD] for each class of relative phytomere (0 to 1, step =0.2)
```

```
Organ = E,I,S,P,Lft
E = [[4.4,5.16],[19,4.19]]
I = [[19.27,4.56],[25.12,2.72],[31.12,4.27],[35.97,2.37],[28.04,9.64]]
S = [[15.92,3.65],[25.81,2.73],[35.22,4.52],[44.22,2.06],[32.93,11.04]]
Lft =
[[[24.03,3.18],[28.06,2.78],[32.25,3.34],[37.53,1.91],[20.64,10.31]],[[],
[],[22.89,1.98],[27.39,1.54],[15.83,7.30]],[[],[],[],[22.68,1.51],[13.80,
6.09]]]
P =
[[[15.95,4.79],[31.90,5.38],[45.69,4.73],[46.66,3.46],[29.61,14.43]],[[],
[],[33.76,3.03],[31.21,3.90],[18.74,7.76]],[[],[],[],[27.23,2.76],[18.31,
9.15]]]

### PHOTOMORPHOGENESIS ###
[US_Photomorpho]
# First line : paramters of the functional relations used to estimate
zeta from PAR (Escobar et al, 2009)
fonct_rel = [0,2,3.09,1.59,0,1.12]
```

3 Chargement des paramètres : PeaConfig.py

```
import os, sys
from ConfigParser import ConfigParser
from openalea.plantgl.all import
Scene,Scaled,AxisRotated,Cylinder,Vector3

class PeaConfig:
  '''
  Authors : R.Barillot and P.Huynh - 2012
  Description : - Loads the pea growth parameters from file
L_pea_params.cfg
                - Parameters are stored in an object for each cultivar
  '''
  def __init__(self):

    # Software environment
    from openalea.core.pkgmanager import PackageManager
    _pm = PackageManager()
    _pkgs = _pm.get_packages()

    if len(_pkgs)==0: # In L-py
      _path = os.getcwd()
    else: # In Visualea
      _pkg = _pm.get('intercropping.l-py')
      _path = _pkg.path
      sys.path.append(_path)
    _path_geom = _path + '\\Geom'

    _cfg = ConfigParser()
```

```
    _cfg.read(_path + '\\' + 'L_pea_params.cfg')

    ###### Global variables ######
    self.dt = _cfg.getfloat('GLOBAL', 'dt') # Time increment
    self.sol = Scene(_path_geom + '\\' + _cfg.get('GLOBAL','geom_sol')) #
Soil
    self.scale_fact = _cfg.getfloat('GLOBAL', 'scale_fact') # Scale
factor for plant size
    self.stand = _cfg.get('GLOBAL', 'stand')
    self.mult_branch = _cfg.getfloat('GLOBAL', 'mult_branch')
    self.var = _cfg.get('GLOBAL', 'var')

    # Initiates the object as a multiple dictionnary
    self.cultivar = eval(_cfg.get('GLOBAL', 'Cultivar'))
    self.geom = {'sl' :{}, 'sr' : {}, 'leaflet' : {}, 'flower' : {},
'pod' : {}, 'incl' : {}}
    self.pheno = {'phyll' : {}, 'time_flower' : {}, 'time_pods' : {},
'senes' : {}}
    self.branch = {'branchfreq' : {}, 'emerg' : {}, 'Nodes_mean' : {}}
    self.growth = {'diam' : {}, 'beta' : {}, 'L_max' : {}, 'org_comp':{}}
    self.fonct_rel = {}

    for cvl in self.cultivar:
      cv = cvl[0]
      ###### GEOM ######
      sec_name = cv + '_GEOM'
      # Stipules
      sl = Scene(_path_geom + '\\' + _cfg.get(sec_name,'geomsti_L'))
      sr = Scene(_path_geom + '\\' + _cfg.get(sec_name,'geomsti_R'))
      sl = Scaled((1,0.57,1),sl[0].geometry) # allometry
      sr = Scaled((1,0.57,1),sr[0].geometry)
      self.geom['sl'][cv] = sl
      self.geom['sr'][cv] = sr
      self.geom['incl'][cv]= _cfg.getfloat(sec_name, 'incl')
      # Leaflets
      if _cfg.has_option(sec_name,'geom_Lft'):
        leaflet = Scene(_path_geom + '\\' +
_cfg.get(sec_name,'geom_Lft'))
        self.geom['leaflet'][cv] =
Scaled((0.5347,1,1),leaflet[0].geometry)

      # Flowers
      flower = Scene(_path_geom + '\\' +
_cfg.get(sec_name,'geom_flower'))
      flower = AxisRotated((1,0,0),-1.57,flower[0].geometry)
      flower = AxisRotated((0,0,1),-1.57,flower)
      self.geom['flower'][cv] = flower
      # Pods
      pod = Scene(_path_geom + '\\' + _cfg.get(sec_name,'geom_pod'))
```

```
      self.geom['pod'][cv] = pod

      ###### PHENOLOGIE ######
      # Phyllochrone
      sec_name = cv + '_Phyllochrone'
      self.pheno['phyll'][cv] = eval(_cfg.get(sec_name,'phyll'))
      # Reproductive stages
      sec_name = cv + '_Reproductive_stages'
      self.pheno['time_flower'][cv] = eval(_cfg.get(sec_name, 'Flowers'))
# Flowering time
      self.pheno['time_pods'][cv] = _cfg.getfloat(sec_name, 'Pods') #
Time between flowering and pod emergence
      # Senescence
      sec_name = cv + '_Senescence'
      self.pheno['senes'][cv] = _cfg.getfloat(sec_name, 'senes')

      ###### BRANCHING ######
      sec_name = cv + '_Ramification'
      self.branch['branchfreq'][cv] = eval(_cfg.get(sec_name,'Nodes'))
      self.branch['max_node'] = len(self.branch['branchfreq'][cv])
      for i in range(self.branch['max_node']):
        self.branch['branchfreq'][cv][i].insert(0,0.0) # Branching
probabilities
      self.branch['emerg'][cv] = eval(_cfg.get(sec_name,'Emerg')) # time
of branches emergence
      self.branch['Nodes_mean'][cv] =
eval(_cfg.get(sec_name,'Nodes_mean')) # mean time of branches emergence

      ###### GROWTH ######
      # Diameter
      sec_name = cv + '_Diameters'
      self.growth['diam'][cv] = _cfg.getfloat(sec_name, 'Internode')

      # Coordination and organ growth
      sec_name = cv + '_Growth'
      organ = _cfg.get(sec_name,'Organ').split(',')
      self.growth['beta'][cv] = {}
      for org in organ:
        self.growth['beta'][cv][org] = [float(v) for v in
_cfg.get(sec_name,org).split(',')] # Parameters of beta functions

      # Maximal length
      sec_name = cv + '_Lmax'
      organ = _cfg.get(sec_name,'Organ').split(',')
      self.growth['L_max'][cv] = {}
      self.growth['org_comp'][cv] = {}
      __dict = {'Lft':[],'P':[]}
      for org in organ:
        self.growth['L_max'][cv][org] = eval(_cfg.get(sec_name,org))
```

```
    g = eval(_cfg.get(sec_name,org))
    # Number of petiole and leaflet levels for each class of relative
phytomere (0 to 1, step =0.2)
    if org in ('P', 'Lft'):
      __dict[org] = [0]* len(g[0])
      for i in range(len(g)):
        for j in range(len(g[i])):
          __dict[org][j]+= (g[i][j]!=[])
   if 'Lft' in organ : # Leafy cultivar
     assert __dict['Lft'] == __dict['P'], 'Warning: different levels
between petioles and leaflets'
     self.growth['org_comp'][cv] = __dict['Lft']
     del(__dict)

   ###### PHOTOMORPHOGENESIS ######
   sec_name = cv + '_Photomorpho'
   self.fonct_rel[cv] = eval(_cfg.get(sec_name,'fonct_rel'))
```

l'université nantes angers le mans
PÔLE DE RECHERCHE ET D'ENSEIGNEMENT SUPÉRIEUR

université angers

Thèse de Doctorat

Romain Barillot

Modélisation du partage de la lumière dans les associations de cultures blé - pois (*Triticum aestivum* L. - *Pisum sativum* L.).

Une approche de type plante virtuelle.

Résumé

Les associations de cultures céréales-légumineuses participent au développement d'agrosystèmes performants et durables. La proportion de chaque espèce dans le couvert ainsi que leur productivité sont cependant fortement dépendantes de l'équilibre entre compétition et complémentarité interspécifique. Le partage de la lumière entre la céréale et la légumineuse est donc déterminant dans le fonctionnement des associations. La structuration physique de la canopée, qui conditionne l'interception du rayonnement lumineux, résulte de la mise en place de l'architecture aérienne des individus composant le peuplement. Afin d'appréhender les relations entre architecture et partage du rayonnement dans les associations blé–pois (*Triticum aestivum* L.-*Pisum sativum* L.), un modèle 3D de la morphogénèse aérienne du pois, baptisé L-Pea, a été développé sur la base de l'approche plante virtuelle. Des expérimentations ont été conduites afin i) de caractériser la morphogénèse de génotypes de pois contrastés cultivés sous différentes conditions (serre/champ, pur/associé), et ii) de modéliser l'architecture aérienne du pois. Un simulateur tripartite, intégrant les modèles L-Pea, ADEL-Blé (modèle architecturé de blé) ainsi que CARIBU (modèle de transferts radiatifs), a ensuite été construit afin de créer une association virtuelle. Cette approche de type plante virtuelle s'est révélée pertinente dans l'optique d'étudier le déterminisme architectural du partage de la lumière dans les associations blé–pois. Ce simulateur a par ailleurs montré que des paramètres architecturaux (*e.g.* ramifications, entrenœuds) peuvent affecter de manière significative et dynamique le partage de la lumière et donc le développement de l'association. Cette thèse se propose i) de démontrer la pertinence de l'approche plante virtuelle pour appréhender le partage du rayonnement dans les associations et ii) de contribuer à la sélection/construction de variétés/idéotypes adaptés aux couverts plurispécifiques.

Mots clés : architecture des plantes, association céréales-légumineuses, modélisation, morphogénèse, partage de la lumière, *Pisum sativum* L., plante virtuelle, *Triticum aestivum* L.

Abstract

Cereal-legume intercropping systems are assumed to provide efficient and sustainable agrosystems. However, the proportion of each species in the stand, as well as their productivity, are highly related to the trade-off between the interspecific competition and their complementarity. Light partitioning between the cereal and the legume is therefore a determinant of the mixture functioning. The physical structure of the canopy, which drives light interception, emerges from the above-ground architecture of the individuals growing within the stand. In order to assess the relationships between plant architecture and light partitioning in wheat-pea mixtures (*Triticum aestivum* L.-*Pisum sativum* L), a 3D model of the above-ground morphogenesis of pea, so called L-Pea, was built up based on the virtual plant approach. Experiments were conducted in order to i) characterize the morphogenesis of contrasting pea genotypes grown under different conditions (greenhouse/field, pure/mixture), and ii) to model the above-ground architecture of pea. A tripartite simulator, integrating the L-Pea model, ADEL-Wheat an (architectural model of wheat) and CARIBU (a radiative transfer model), was then built up in order to study the architectural determinism of light partitioning in wheat-pea mixtures. This simulator furthermore demonstrates that architectural parameters (*e.g.* branches, internodes) are able to significantly and dynamically affect light partitioning and thus the mixture development. The present thesis contributes i) to demonstrate the pertinence of the virtual plant approach for accounting of light partitioning in mixtures and ii) to the selection/building of cultivars/ideotypes suited for multispecific stands.

Key Words: cereal-legume intercropping, light partitioning, modelling, morphogenesis, *Pisum sativum* L., plant architecture, *Triticum aestivum* L., virtual plant.